

A KNOWLEDGE-BASED DESIGN FRAMEWORK FOR AIRPLANE
CONCEPTUAL AND PRELIMINARY DESIGN

By

Wilhelmus A.J Anemaat

M.S., Delft University of Technology

Submitted to the Department of Aerospace Engineering and the
Faculty of the Graduate School of the University of Kansas
In partial fulfillment of the requirements for the degree of
Doctor of Philosophy

Dr. Richard A. Hale
Committee Chairman

Dr. Jan Roskam
Committee Member

Dr. C. Edward Lan
Committee Member

Dr. David R. Downing
Committee Member

Dr. Arvin Agah
Committee Member

Date defended: April 6, 2007

The Dissertation Committee for Wilhelmus A.J. Anemaat certifies
that this is the approved version of the following dissertation:

A KNOWLEDGE-BASED DESIGN FRAMEWORK FOR AIRPLANE
CONCEPTUAL AND PRELIMINARY DESIGN

Committee:

Dr. Richard A. Hale
Committee Chairman

Dr. Jan Roskam
Committee Member

Dr. C. Edward Lan
Committee Member

Dr. David R. Downing
Committee Member

Dr. Arvin Agah
Committee Member

Date approved _____

Abstract

The goal of work described herein is to develop the second generation of Advanced Aircraft Analysis (AAA) into an object-oriented structure which can be used in different environments. One such environment is the third generation of AAA with its own user interface, the other environment with the same AAA methods (i.e. the knowledge) is the AAA-AML program. AAA-AML automates the initial airplane design process using current AAA methods in combination with AMRaven methodologies for dependency tracking and knowledge management, using the TechnoSoft Adaptive Modeling Language (AML).

This will lead to the following benefits:

- *Reduced design time:* computer aided design methods can reduce design and development time and replace tedious hand calculations.
- *Better product through improved design:* more alternative designs can be evaluated in the same time span, which can lead to improved quality.
- *Reduced design cost:* due to less training and less calculation errors substantial savings in design time and related cost can be obtained.
- *Improved Efficiency:* the design engineer can avoid technically correct but irrelevant calculations on incomplete or out of sync information, particularly if the process enables robust geometry earlier.

Although numerous advancements in knowledge based design have been developed for detailed design, currently no such integrated knowledge based conceptual and preliminary airplane design system exists.

The third generation AAA methods are tested over a ten year period on many different airplane designs. Using AAA methods will demonstrate significant time savings. The AAA-AML system will be exercised and tested using 27 existing airplanes ranging from single engine propeller, business jets, airliners, UAV's to fighters. Data for the varied sizing methods will be compared with AAA results, to validate these methods. One new design, a Light Sport Aircraft (LSA), will be developed as an exercise to use the tool for designing a new airplane.

Using these tools will show an improvement in efficiency over using separate programs due to the automatic recalculation with any change of input data. The direct visual feedback of 3D geometry in the AAA-AML, will lead to quicker resolving of problems as opposed to conventional methods.

Table of Contents

Title Page	i
Acceptance Page	ii
Abstract	iii
List of Figures	ix
List of Tables	xv
List of Symbols	xvi
1 Introduction.....	1
2 Airplane Design Systems and Overview of Past Work	4
2.1 Design Systems	5
2.1.1 CDS: Configuration Development System	5
2.1.2 Paper Airplane	5
2.1.3 ACSYNT: Aircraft Synthesis	6
2.1.4 ADAS: Aircraft Design and Analysis System	6
2.1.5 RDS.....	7
2.1.6 Advanced Aircraft Analysis: First Generation	7
2.1.7 Advanced Aircraft Analysis: Second Generation	9
2.1.8 General Aviation Computer Aided Design: G.A.-CAD	14
2.2 Knowledge-based Design Systems	24
2.2.1 The University of Texas.....	24
2.2.2 Delft University of Technology	24
2.2.3 NASA Langley Research Center	25
3 Development Approach and Architecture	27
3.1 Object-Oriented Programming.....	27
3.2 Knowledge-Based Design.....	30
3.2.1 Common Computational Model	30
3.2.2 Model Abstraction, Fidelity and Object Aspects	31
4 Adaptive Modeling Language (AML) and AMRaven.....	33
4.1 AML: Adaptive Modeling Language.....	33
4.2 AMRaven.....	37
5 Airplane Design Process in AAA and AAA-AML.....	40
5.1 Preliminary Design Steps.....	42

5.1.1	Mission Specification.....	43
5.1.2	Preliminary Sizing and Sensitivity Studies.....	43
5.1.3	Preliminary Configuration Layout and Propulsion System Integration ...	46
5.1.4	Class I Analysis, Configuration Design and Configuration Comparison .	46
5.1.5	Class II Analysis and Configuration Refinement	47
5.2	Class I and Class II Design and Analysis Methods	48
6	Theoretical Background of Implemented Methods	50
6.1	Class I Sizing Methods	50
6.1.1	Weight Sizing.....	50
6.1.1.1	Mission Profile.....	51
6.1.1.2	Take-off Weight.....	53
6.1.1.3	Mission Profile Fuel Fraction	58
6.1.1.3.1	Climb Fuel Fraction	58
6.1.1.3.2	Cruise Fuel Fraction.....	59
6.1.1.3.3	Loiter Fuel Fraction	59
6.1.1.3.4	Turn Fuel Fraction	60
6.1.1.4	Regression Coefficients	61
6.1.1.5	Sensitivity	61
6.1.2	Estimation of Class I Drag Polars.....	67
6.1.3	Performance Sizing.....	69
6.1.3.1	Sizing to Stall Speed Requirements.....	70
6.1.3.2	Sizing to Take-off Distance Requirements	72
6.1.3.2.1	Sizing to FAR 23, JAR 23 and VLA Take-off Distance Requirements	74
6.1.3.2.2	Sizing to FAR 25 Take-off Distance Requirements	75
6.1.3.2.3	Sizing to Military Take-off Distance Requirements.....	75
6.1.3.2.3.1	Land Based Airplanes	75
6.1.3.2.3.2	Carrier Based Airplanes.....	77
6.1.3.2.4	Climb Sizing	77
6.1.3.2.4.1	Sizing to FAR 23, JAR 23, and VLA Climb requirements	78
6.1.3.2.4.2	Sizing to FAR 25 Climb requirements.....	88
6.1.3.2.4.3	Sizing to Military Climb requirements	97
6.1.3.2.5	Sizing to Maximum Cruise Speed Requirements	108
6.1.3.2.6	Sizing to Maneuvering Requirements.....	109

6.1.3.2.7	Sizing to Landing Distance Requirements.....	111
6.1.3.2.7.1	Land based Airplanes.....	112
6.1.3.2.7.2	Carrier based Airplanes.....	113
6.2	Airplane and Wing Maximum Lift.....	114
6.2.1	Airfoil Maximum Lift Coefficient.....	114
6.2.2	Wing Maximum Lift Coefficient.....	115
6.3	Flap Sizing.....	117
6.3.1	Plain Flap.....	120
6.3.2	Split Flap.....	122
6.3.3	Single Slotted Flap.....	123
6.3.4	Type I Double Slotted Flap.....	124
6.3.5	Type II Double Slotted Flap.....	127
6.3.6	Fowler Flap.....	130
6.3.7	Triple Slotted Flap.....	131
6.3.8	Lift Distribution.....	132
6.4	Class I Weights.....	137
6.5	Class I Center of Gravity.....	142
6.6	Class I Moments of Inertia.....	142
6.7	Class I Stability: Volume Methods.....	145
6.8	Geometry.....	148
6.8.1	Lifting Surfaces.....	148
6.8.1.1	Straight Tapered.....	148
6.8.1.2	Cranked Surfaces.....	153
6.8.2	Volume Coefficient.....	157
6.8.3	Fuel Volume.....	159
6.8.4	Bodies.....	160
6.9	Class II Analysis Methods.....	164
6.9.1	Class II Drag.....	164
6.9.1.1	Tailboom Drag.....	165
6.9.1.2	Trim Drag.....	165
6.9.1.3	Miscellaneous Drag.....	167
6.9.1.4	Total Drag.....	168
6.9.2	Class II Weights.....	169
6.10	Atmospheric Properties.....	171

6.10.1	Temperature in Standard Atmosphere	172
6.10.2	Pressure in Standard Atmosphere	174
6.10.3	Density in Standard Atmosphere	175
6.10.4	Speed of Sound in Standard Atmosphere	176
6.10.5	Kinematic Viscosity in Standard Atmosphere	176
7	Implementation and Testing of AAA and AAA-AML	177
7.1	Advanced Aircraft Analysis	177
7.1.1	Structure of the Software	178
7.1.1.1	Windows and Command Bars	178
7.1.1.1.1	Application Windows	180
7.1.1.1.2	Input/Output Windows	183
7.1.1.1.3	Input/Output Window Command Bar	189
7.1.1.1.4	Plot Windows	191
7.1.1.1.5	Plot Window Command Bar	193
7.1.1.2	Toolbars	195
7.1.1.2.1	Main Toolbar	195
7.1.1.2.2	The File Toolbar	203
7.1.1.2.3	Configuration Setup Toolbar	204
7.1.1.2.4	Certification Toolbar	205
7.1.1.2.5	System Setup Toolbar	206
7.1.2	Objects in AAA	208
7.1.3	AAA and Airplane Design	211
7.2	Advanced Aircraft Analysis Methods Implemented in AML	214
7.2.1	Implementation	214
7.2.2	Testing	218
7.2.2.1	Light Sport Aircraft Requirements	221
7.2.2.2	Starting AAA-AML	223
7.2.2.2.1	Vehicle Certification	225
7.2.2.2.2	Vehicle Configuration	227
7.2.2.2.3	Engine Model	229
7.2.2.3	Weight Sizing	230
7.2.2.3.1	Primary Mission	230
7.2.2.3.2	Regression	235
7.2.2.3.3	Weight Sizing	236

7.2.2.4	Class I Drag.....	239
7.2.2.5	Performance Sizing.....	243
7.2.2.6	Aerodynamics	247
7.2.2.6.1	Wing Maximum Lift.....	247
7.2.2.6.2	Flap Sizing	248
7.2.2.6.3	Wing Lift Distribution	250
7.2.2.7	Volume Methods.....	251
7.2.2.8	Class I Weight and Balance	252
7.2.2.8.1	Weight Fractions.....	252
7.2.2.8.2	Weight and Balance	255
7.2.2.8.3	Class I Moments of Inertia.....	256
7.2.2.9	Class II Weights.....	258
7.2.2.10	Class II Drag	258
7.2.2.11	Geometry and Configuration Layout.....	258
7.2.3	Feedback on Use of AAA-AML for Design.....	263
8	Conclusions and Recommendations	264
9	References.....	267
Appendix A.	Airplane Mission Specifications	A-1
A.1	Mission Specification for a Twin Engine Propeller Driven Airplane.....	A-1
A.2	Mission Specification for a Jet Transport	A-2
A.3	Mission Specification for a Fighter.....	A-3
Appendix B.	Advanced Aircraft Analysis 3.1 Module Description	B-1
B.1	Weight Module.....	B-1
B.2	Aerodynamics Module	B-5
B.3	Performance Module	B-12
B.4	Geometry Module	B-14
B.5	Propulsion Module	B-16
B.6	Stability & Control Module.....	B-17
B.7	Dynamics Module	B-21
B.8	Loads Module.....	B-24
B.9	Structures Module	B-26
B.10	Cost Analysis Module	B-27
Appendix C.	Theory and history of CAD and Computer Graphics.....	C-1

Appendix D. Theory and History of Airplane Design Tools and Systems.....	D-1
Appendix E. Description of Functions and Procedures in Dynamic Link Libraries .	E-1
E.1 AeroCoef.dll	E-4
E.2 DragCoefficient.dll.....	E-36
E.3 WeightSizing.dll.....	E-64
E.4 Atmosphere.dll	E-65
E.5 FuselageDrag.dll.....	E-68
E.6 WeightII.dll	E-76
E.7 GroundEffects.dll	E-77
E.8 BetaDot.dll.....	E-81
E.9 LatDirStabFigures.dll	E-83
E.10 HingeMoment.dll.....	E-89
Appendix F. Least-Squares Method to Digitize Figures	F-1

List of Figures

Figure 2.1 AAA(X-Client) in the X-Window System	11
Figure 2.2 AAA Second Generation User Interface	13
Figure 2.3 G.A.-CAD User Interface.....	16
Figure 2.4 Input/Output Window for Class I Clean Airplane Drag Polar	17
Figure 2.5 Input/Output Parameter Element.....	17
Figure 2.6 G.A.-CAD Class I Clean Airplane Drag Polar Help System	18
Figure 2.7 G.A.-CAD Graphical Help System	19
Figure 2.8 G.A.-CAD Window with Main Menu Buttons	20
Figure 2.9 G.A.-CAD Graphical Help Window	21
Figure 2.10 Class I Drag Polar Plot	21
Figure 2.11 Input/Output Window for Class II Wing Drag.....	22
Figure 2.12 Flight Condition Dialog.....	23
Figure 4.1 Products Decomposed into Decreasing Abstractions while Enforcing Dependencies (Ref. 61).....	35
Figure 4.2 AMRaven Pod Editor User Interface (Ref. 67, Courtesy TechnoSoft).....	38
Figure 4.3 AMRaven Airliner Geometry (Ref. 67, Courtesy TechnoSoft)	39
Figure 4.4 AMRaven Airliner Substructure (Ref. 67, Courtesy TechnoSoft)	39
Figure 5.1 Preliminary Design Process.....	40
Figure 5.2 Preliminary Design Process Detailed Steps	41
Figure 5.3 Class I Sizing Flow Chart.....	45
Figure 5.4 Class I Weights and Stability Sizing Flow Chart	47
Figure 6.1 Take-off Distance Definition.....	73
Figure 6.2 Landing Distance Definition	112
Figure 6.3 Flapped Area Definition	118
Figure 6.4 Plain Flap.....	120
Figure 6.5 Split Flap	122
Figure 6.6 Single Slotted Flap	124
Figure 6.7 Type I Double Slotted Flap	125
Figure 6.8 Type II Double Slotted Flap	127
Figure 6.9 Fowler Flap.....	130

Figure 6.10 Triple Slotted Flap.....	131
Figure 6.11 Definition of Coordinates.....	146
Figure 6.12 Lifting Surface Parameters.....	148
Figure 6.13 Sweep Angle Definition.....	151
Figure 6.14 Cranked Surfaces Definition.....	153
Figure 6.15 Cross-section Definition.....	161
Figure 6.16 Atmospheric Properties in British Units.....	172
Figure 7.1 The AAA Main Window.....	179
Figure 7.2 Input/Output Window.....	184
Figure 7.3 Input/Output Elements.....	185
Figure 7.4 Work Pad Window.....	187
Figure 7.5 Combo Box Element.....	188
Figure 7.6 Input/Output Window Command Bar Buttons.....	189
Figure 7.7 Plot Window.....	191
Figure 7.8 Change Axis Dialog.....	193
Figure 7.9 Plot Window Command Bar Buttons.....	194
Figure 7.10 Main Toolbar.....	195
Figure 7.11 Flight Condition Dialog Box (Both Pages).....	197
Figure 7.12 Recalculate Dialog.....	201
Figure 7.13 The Print Dialog.....	202
Figure 7.14 File Toolbar.....	203
Figure 7.15 Configuration Setup Toolbar.....	204
Figure 7.16 Certification Toolbar.....	206
Figure 7.17 System Setup Toolbar.....	207
Figure 7.18 Input/Output Window Object Structure.....	208
Figure 7.19 Airplane Configuration Object Structure.....	210
Figure 7.20 Forward and Aft Center of Gravity Limits.....	213
Figure 7.21 Model Tree in AML.....	216
Figure 7.22 Primary Mission in AML.....	217
Figure 7.23 Tandem Seater LSA.....	221
Figure 7.24 Mission Profile of the Tandem Seater LSA.....	222
Figure 7.25 Airplane Design and Analysis Class Name.....	223
Figure 7.26 Airplane Design and Analysis Design Environment.....	224
Figure 7.27 Airplane Design and Analysis Design Model Tree.....	225

Figure 7.28 Airplane Design and Analysis Design Model Tree.....	226
Figure 7.29 Vehicle Configuration Model Tree	228
Figure 7.30 Engine Model	229
Figure 7.31 Segment Menu.....	230
Figure 7.32 Mission Segment Definition.....	231
Figure 7.33 Mission Segments Expanded.....	233
Figure 7.34 Climb Segment Input Data	234
Figure 7.35 Climb Segment Output Data	234
Figure 7.36 Weight Regression Coefficients	236
Figure 7.37 Weight Sizing: Input.....	236
Figure 7.38 Weight Sizing: Output.....	237
Figure 7.39 Weight Sizing: Mission Profile Table	238
Figure 7.40 Weight Iteration.....	238
Figure 7.41 Take-off Weight Sensitivity	239
Figure 7.42 Input for Class I Drag Polar.....	239
Figure 7.43 Input for Clean Class I Drag Polar	240
Figure 7.44 Output for Clean Class I Drag Polar.....	241
Figure 7.45 Drag Polar.....	242
Figure 7.46 Take-off Performance Input	244
Figure 7.47 Climb Performance Input	244
Figure 7.48 Cruise Performance Input.....	245
Figure 7.49 Landing Performance Input.....	245
Figure 7.50 Stall Performance Input.....	246
Figure 7.51 Performance Sizing Plot.....	246
Figure 7.52 Airfoil Maximum Lift Coefficient.....	248
Figure 7.53 Flap Maximum Lift Input.....	249
Figure 7.54 Flap Maximum Lift Output	249
Figure 7.55 Wing Lift Distribution Input Data.....	250
Figure 7.56 Wing Lift Distribution.....	251
Figure 7.57 Horizontal Tail Volume Method Output	252
Figure 7.58 Weight Fractions	253
Figure 7.59 Average Weight Fractions.....	254
Figure 7.60 Average Weights	254
Figure 7.61 Empty Weight Component C.G.	255

Figure 7.62 Empty Weight C.G.	256
Figure 7.63 Radius of Gyration	257
Figure 7.64 Moments of Inertia	257
Figure 7.65 AAA-AML Wing Geometry Input	259
Figure 7.66 AAA-AML Wing Geometry	259
Figure 7.67 AML Wing Editor	260
Figure 7.68 Fuselage Geometry Definition	261
Figure 7.69 Fuselage-Wing Geometry.....	262
Figure 7.70 LSA 3D Geometry.....	262

List of Tables

Table 6-1 Component Weights	141
Table 7-1 Application Modules of the Program	181
Table 7-2 Application Modules of the Program Continued.....	182
Table 7-3 Input/Output Window Command Bar Functions	190
Table 7-4 Plot Window Command Bar Buttons	194
Table 7-5 Toolbar Buttons	196
Table 7-6 File Management Toolbar Buttons	204
Table 7-7 Configuration Setup Toolbar Buttons	205
Table 7-8 Certification Toolbar Buttons.....	206
Table 7-9 System Setup Toolbar Buttons	207
Table 7-10 Weight Data for Sport Planes and Experimental Airplanes	235

List of Symbols

Symbol	Description	Unit
A	Regression Coefficient A	-
A	Intermediate Parameter	-
a	Regression Coefficient a to Estimate Parasite Area from Wetted Area	-
AR_c	Canard Aspect Ratio	-
AR_h	Horizontal Tail Aspect Ratio	-
AR_v	Vertical Tail Aspect Ratio	-
AR_{vee}	V-Tail Aspect Ratio	-
AR_{vf}	Ventral Fin Aspect Ratio	-
AR_w	Wing Aspect Ratio	-
B	Regression Coefficient B	-
B	Intermediate Calculation Parameter	-
b	Regression Coefficient b to Estimate Parasite Area from Wetted Area	-
b	Span	ft
b_c	Canard Span	ft
$B_{CD1misc\alpha}$	Coefficient 1 for a Generic Drag Polar (function of angle of attack)	-
$B_{CD2misc\alpha}$	Coefficient 2 for a Generic Miscellaneous Drag Polar (function of angle of attack)	-
$B_{CD3misc\alpha}$	Coefficient 3 for a Generic Miscellaneous Drag Polar (function of angle of attack)	-
$B_{CD4misc\alpha}$	Coefficient 4 for a Generic Miscellaneous Drag Polar (function of angle of attack)	-
$B_{CD5misc\alpha}$	Coefficient 5 for a Generic Miscellaneous Drag Polar (function of angle of attack)	-
B_{DP}	B of Drag Polar	-
$B_{DP_{clean}}$	B of Drag Polar in Clean Configuration	-
B_{DPL_down}	B of Drag Polar in Landing Configuration with Gear Down	-
B_{DPL_up}	B of Drag Polar in Landing Configuration with Gear Up	-

Symbol	Description	Unit
B_{DPOEI}	B of Drag Polar with One Engine Inoperative	-
$B_{DP_{TO_down}}$	B of Drag Polar in Takeoff Configuration with Gear Down	-
$B_{DP_{TO_up}}$	B of Drag Polar in Takeoff Configuration with Gear Up	-
b_h	Horizontal Tail Span	ft
b_v	Vertical Tail Span	ft
b_{vee}	V-Tail span	ft
b_{vf}	Ventral Fin Span	ft
b_w	Wing Span	ft
BFL	Balanced (Critical) Field Length	ft
BPR	Engine Bypass Ratio	-
C	Intermediate Calculation Parameter	-
c	Regression Coefficient c to Estimate Wetted Area from Take-off Weight	-
C'	Chord	ft
c_1/c_w	Forward Flap Chord to Wing Chord Ratio	-
c_2/c_w	Aft Flap Chord to Wing Chord Ratio	-
\bar{c}_c	Canard Mean Geometric Chord	ft
C_D	Airplane Drag Coefficient	-
C_{D1}	Airplane Steady State Drag Coefficient	-
$C_{D_{canopy}}$	Canopy Drag Coefficient	-
$C_{D_{cv}}$	Airplane Drag-coefficient-due-to-canardvator-deflection	-
C_{D_e}	Airplane Drag-coefficient-due-to-elevator-deflection	-
$C_{D_{el}}$	Airplane Drag-coefficient-due-to-elevon-deflection	-
$C_{D_{fixed}}$	Fixed Landing Gear Drag Coefficient	-
$C_{D_{flap}}$	Trailing Edge Flap Drag Coefficient	-
$C_{D_{gap_a}}$	Drag Coefficient due to Gaps caused by Retracted Ailerons	-
$C_{D_{gap_{cv}}}$	Drag Coefficient due to Gaps caused by Retracted Canardvators	-
$C_{D_{gap_e}}$	Drag Coefficient due to Gaps caused by Retracted Elevators	-
$C_{D_{gap_{flap}}}$	Drag Coefficient due to Gaps caused by Retracted Flaps	-

Symbol	Description	Unit
$C_{D_{gear}}$	Landing Gear Drag Coefficient	-
$C_{D_{inl_{ext}}}$	Inlet Extra Drag Coefficient	-
$C_{D_{kf}}$	Leading Edge Krueger Flap Drag Coefficient	-
$C_{D_{L_c}}$	Canard Drag Coefficient due to Lift	-
$C_{D_{L_{float}}}$	Float Drag Coefficient due to Lift	-
$C_{D_{L_f}}$	Fuselage Drag Coefficient due to Lift	-
$C_{D_{L_h}}$	Horizontal Tail Drag Coefficient due to Lift	-
$C_{D_{L_{vee}}}$	V-Tail Drag Coefficient due to Sideforce and Lift	-
$C_{D_{L_v}}$	Vertical Tail Drag Coefficient due to Sideforce	-
$C_{D_{L_w}}$	Wing Drag Coefficient due to Lift	-
$C_{D_{misc}}$	Miscellaneous Drag Coefficient	-
C_{D_n}	Nacelle Drag Coefficient Including Interference	-
$C_{D_{n_{isolated}}}$	Isolated Nacelle Drag Coefficient	-
$C_{D_{nf}}$	Leading Edge Nose Flap Drag Coefficient	-
C_{D_o}	Airplane Class I Zero-lift Drag Coefficient	-
C_{D_o}	Zero-lift Drag Coefficient for a Generic Drag Polar	-
$C_{D_{o_c}}$	Canard Zero-lift Drag Coefficient	-
$C_{D_{o_{clean}}}$	Airplane Zero-lift Drag Coefficient with Gears and Flaps Retracted	-
$C_{D_{o_{clean,M}}}$	Airplane Zero-lift Drag Coefficient Corrected for Mach Effects with Gears and Flaps Retracted	-
$C_{D_{oL_{down}}}$	Airplane Zero-lift Drag Coefficient at Landing with Gear Down	-
$C_{D_{oL_{up}}}$	Airplane Zero-lift Drag Coefficient at Landing with Gear Up	-
$C_{D_{oOEI}}$	Airplane Zero-lift Drag Coefficient with One Engine Inoperative	-
$C_{D_{oTO_{down}}}$	Airplane Zero-lift Drag Coefficient at Take-off with Gear Down	-
$C_{D_{oTO_{up}}}$	Airplane Zero-lift Drag Coefficient at Take-off with Gear Up	-

Symbol	Description	Unit
$C_{D_{oflap}}$	Flap Profile and Interference Drag Coefficient	-
$C_{D_{ofloat}}$	Float Zero-lift Drag Coefficient	-
$C_{D_{ofloat(vol)}}$	Float Zero-lift Drag Coefficient based on Volume to the Power 2/3	-
$C_{D_{of}}$	Fuselage Zero-lift Drag Coefficient	-
$C_{D_{oh}}$	Horizontal Tail Zero-lift Drag Coefficient	-
$C_{D_{omisc\ \alpha}}$	Zero-angle-of -attack Drag Coefficient for a Generic Miscellaneous Drag Polar	-
$C_{D_{ov}}$	Vertical Tail Zero-sideforce Drag Coefficient	-
$C_{D_{ovee}}$	V-Tail Zero-lift Drag Coefficient	-
$C_{D_{ow}}$	Wing Zero-lift Drag Coefficient	-
$C_{D_{prop}}$	Stopped Propeller Drag Coefficient	-
$C_{D_{py}}$	Pylon Drag Coefficient	-
$C_{D_{retract}}$	Retractable Landing Gear Drag Coefficient	-
$C_{D_{rudder}}$	Airplane Drag-coefficient-due-to-rudder-deflection	-
$C_{D_{rv}}$	Airplane Drag-coefficient-due-to-ruddervator-deflection	-
$C_{D_{slat}}$	Leading Edge Slat Drag Coefficient	-
$C_{D_{sb}}$	Speed Brake Drag Coefficient	-
$C_{D_{sp}}$	Spoiler Drag Coefficient	-
$C_{D_{store}}$	Store(s) Drag Coefficient	-
$C_{D_{tb}}$	Tailboom Drag Coefficient	-
$C_{D_{trim}}$	Trim Drag Coefficient	-
$C_{D_{wm}}$	Windmilling Engine Drag Coefficient	-
$C_{D_{ws}}$	Windshield Drag Coefficient	-
$C_{D_{gapkf}}$	Drag Coefficient due to Gaps caused by Retracted Krueger Flaps	-
$C_{D_{gapr}}$	Drag Coefficient due to Gaps caused by Retracted Rudder	-
$C_{D_{gapvee}}$	Drag Coefficient due to Gaps caused by Retracted Ruddervators	-
$C_{D_{gapslat}}$	Drag Coefficient due to Gaps caused by Retracted Slats	-

Symbol	Description	Unit
c_f / c_w	Flap Chord Ratio	-
CGR	Climb Gradient	rad
$CGR_{25.121_{ER}}$	FAR 25.121 (One Engine Inoperative) En-route Segment Climb Gradient	rad
$CGR_{25.119}$	FAR 25.119 (All Engines Operative) Climb Gradient at Landing Condition	rad
$CGR_{23.65}$	FAR 23.65 (All Engines Operative) Climb Gradient	rad
$CGR_{23.65_T}$	FAR 23.65 (All Engines Operative) Climb Gradient for Turbine Aircraft	rad
$CGR_{23.67}$	FAR 23.67 (One Engine Inoperative) Climb Gradient for Turbine Aircraft	rad
$CGR_{23.67_{OSA}}$	FAR 23.67 (One Engine Inoperative) Climb Gradient for Turbine Aircraft at Altitude	rad
$CGR_{23.77}$	FAR 23.77 (All Engines Operative) Climb Gradient	rad
$CGR_{25.121_L}$	FAR 25.121 (One Engine Inoperative) Climb Gradient at Landing Condition	rad
$CGR_{25.111}$	FAR 25.111 (One Engine Inoperative) Climb Gradient	rad
$CGR_{25.121_{SS}}$	FAR 25.121 (One Engine Inoperative) Second Segment Climb Gradient	rad
CGR_L	Climb Gradient for Landing Climb at 50 ft (15.24 m) Obstacle	rad
CGR_{TO50}	Climb Gradient for Take-off Gear Up at 50 ft (15.24 m) Obstacle	rad
CGR_{TO}	Climb Gradient for Take-off Climb Gear Down	rad
$CGR_{25.121_T}$	FAR 25.121 (One Engine Inoperative) Transition Segment Climb Gradient	rad
c_h	Horizontal Tail Chord Length	ft
\bar{c}_h	Horizontal Tail Mean Geometric Chord	ft
c_j	Engine Specific Fuel Consumption	lb/hr/lb
C_L	Airplane Lift Coefficient	-
C_L^3 / C_D^2	Lift-to-drag Parameter	-
C_L / C_D	Lift-to-drag Ratio	-
$C_L^{0.5} / C_D$	Lift-to-drag Parameter	-
C_{L1}	Airplane Steady State Lift Coefficient	-
$C_{L_{c_{max clean}}}$	Airplane Maximum Lift Coefficient due to Canard without Flap Effects	-

Symbol	Description	Unit
C_{L_h}	Horizontal Tail Lift Coefficient	-
$C_{L_{max}}$	Airplane Maximum Lift Coefficient Including Flap Effects	-
$C_{L_{max_{clean}}}$	Airplane Maximum Lift Coefficient without Flap Effects	-
$C_{L_{max_A}}$	Airplane Maximum Lift Coefficient at Approach	-
$C_{L_{max_{c_{clean}}}}$	Canard Maximum Lift Coefficient without Flap Effects	-
$c_{l_{max_{rc}}}$	Canard Root Section Maximum Lift Coefficient	-
$c_{l_{max_{tc}}}$	Canard Tip Section Maximum Lift Coefficient	-
$C_{L_{max_{h_{clean}}}}$	Airplane Maximum Lift Coefficient due to Horizontal Tail without Flap Effects	-
$c_{l_{max_{rh}}}$	Horizontal Tail Root Section Maximum Lift Coefficient	-
$c_{l_{max_{th}}}$	Horizontal Tail Tip Section Maximum Lift Coefficient	-
$C_{L_{max_L}}$	Airplane Maximum Lift Coefficient at Landing	-
$c_{l_{max_{rv}}}$	Vertical Tail Root Section Maximum Lift Coefficient	-
$c_{l_{max_{rvee}}}$	V-Tail Root Section Maximum Lift Coefficient	-
$c_{l_{max_{rw}}}$	Wing Root Section Maximum Lift Coefficient	-
$C_{L_{max_S}}$	Airplane Maximum Lift Coefficient for that Flight Condition at which the Stall Speed is Evaluated	-
$C_{L_{max_S_{cln}}}$	Airplane Maximum Lift Coefficient for the Clean Configuration	-
$C_{L_{max_{TO}}}$	Airplane Maximum Lift Coefficient at Take-off	-
$c_{l_{max_{tv}}}$	Vertical Tail Tip Section Maximum Lift Coefficient	-
$c_{l_{max_{tvee}}}$	V-Tail Tip Section Maximum Lift Coefficient	-
$c_{l_{max_{tw}}}$	Wing Tip Section Maximum Lift Coefficient	-
$C_{L_{max_{v_{clean}}}}$	Vertical Tail Maximum Lift Coefficient without Flap Effects	-
$C_{L_{max_w}}$	Airplane Maximum Lift Coefficient due to Wing including Flap Effects	-

Symbol	Description	Unit
$C_{L_{\max_w clean}}$	Airplane Maximum Lift Coefficient due to Wing without Flap Effects	-
$C_{L_{vee}}$	V-Tail Lift Coefficient	-
C_{L_w}	Wing Lift Coefficient with Flap Effects	-
$C_{L_w clean}$	Wing Lift Coefficient without Flap Effects	-
$C_{L_w cln p.off}$	Wing Lift Coefficient without Flap Effects, without Power Effects	-
$C_{L_w \max}$	Wing Maximum Lift Coefficient including Flap Effects	-
$C_{L_w \max clean}$	Wing Maximum Lift Coefficient without Flap Effects	-
$C_{L_{wf}}$	Wing-fuselage Lift Coefficient with Flap Effects	-
$C_{L_{wf clean}}$	Wing-fuselage Lift Coefficient without Flap Effects	-
$c_{l_{\alpha_w} @ M=0}$	Wing Airfoil Lift Curve Slope at Wing Mean Geometric Chord at $M = 0$ and $Re = 9 \times 10^6$	rad^{-1}
$c_{l_{\alpha_{rw}}}$	Wing Root Airfoil Lift Curve Slope at $M = 0$	rad^{-1}
$c_{l_{\alpha_{tw}}}$	Wing Tip Airfoil Lift Curve Slope at $M = 0$	rad^{-1}
$c_{l_{\delta f}}$	Section-lift-coefficient-due-to-flap-deflection Derivative	rad^{-1}
C_{m_1}	Airplane Steady State Pitching Moment Coefficient	-
c_p	Engine Specific Fuel Consumption	lb/hr/hp
c_r	Panel Root Chord	ft
c_{rc}	Canard Root Chord Length	ft
c_{rh}	Horizontal Tail Root Chord Length	ft
c_{rv}	Vertical Tail Root Chord	ft
c_{tc}	Canard Tip Chord	ft
c_t	Panel Tip Chord	ft
c_{th}	Horizontal Tail Tip Chord	ft
c_v	Vertical Tail Chord Length	ft
c_{vee}	V-Tail Chord Length	ft
\bar{c}_{vee}	V-Tail Mean Geometric Chord	ft
\bar{c}_v	Vertical Tail Mean Geometric Chord	ft
c_{tv}	Vertical Tail Tip Chord	ft

Symbol	Description	Unit
c_w	Wing Chord Length	ft
c_{wf_w}	Wing Chord at Wing-fuselage Intersection	ft
\bar{c}_w	Wing Mean Geometric Chord	ft
c_{r_w}	Wing Root Chord	ft
c_{t_w}	Wing Tip Chord	ft
D	Diameter	ft
D	Drag	lb
d	Regression Coefficient d to Estimate Wetted Area from Take-off Weight	-
E	Endurance of the Flight Segment	hr
\bar{E}	Endurance Parameter	-
e	Oswald Efficiency Factor	-
e_c	Canard Oswald Efficiency Factor	-
e_{clean}	Oswald Efficiency Factor in the Clean Configuration	-
e_h	Horizontal Tail Oswald Efficiency Factor	-
e_L	Landing Oswald Efficiency Factor	-
e_{OEI}	One Engine Inoperative Oswald Efficiency Factor	-
e_{TO}	Take-off Oswald Efficiency Factor	-
f	Equivalent Parasite Area Based on Wetted Area	-
f_{couple}	Coupling Factor due to Horizontal Tail or Canard Moment Arm	-
F_{Cr}	Ratio of the Cruise Thrust (or Power) to that at Take-off 0 ft ISA	-
F_{engine}	Engine Parameter depending on Number of Engines	-
F_F	Factor accounting for volume loss due to fuel expansion and volume of structure	-
$F_{F\ expansion}$	Factor to account for Fuel Expansion inside the Fuel Tank	-
F_M	Ratio of Maneuver Thrust (or Power) to that at Take-off 0 ft ISA	-
$F_{MaxCont}$	Ratio of Maximum Continuous Thrust (or Power) to that at Take-off 0 ft ISA	-
$F_{OSA5000}$	Ratio of Max Continuous Thrust (or Power) at Altitude, OSA to that at Take-off 0ft ISA	-
F_{TO}	Ratio of Take-off Thrust (or Power) to that at Take-off 0 ft ISA	-

Symbol	Description	Unit
F_W	Average Component Group Weight to Gross Weight Ratio	-
F_{WE}	Average Empty Weight to Gross Weight Ratio	-
F_{Wemp}	Average Empennage Group Weight to Gross Weight Ratio	-
F_{Wf}	Average Fuselage Group Weight to Gross Weight Ratio	-
F_{Wfix}	Average Fixed Equipment Weight to Gross Weight Ratio	-
F_{Wgear}	Average Landing Gear Group Weight to Gross Weight Ratio	-
F_{Wgross}	Average Gross Weight to Take-off Weight Ratio	-
F_{Wn}	Average Nacelle Group Weight to Gross Weight Ratio	-
F_{Wpp}	Average Powerplant Weight to Gross Weight Ratio	-
$F_{Wstructure}$	Average Structure Weight to Gross Weight Ratio	-
F_{Ww}	Average Wing Group Weight to Gross Weight Ratio	-
F_1	Factor Used in Landing Performance	-
F_{5000}	Ratio of Thrust (or Power) at 5000 ft (1524 m) to that at Take-off 0ft ISA	-
F_{8sec}	Ratio of the Thrust (or Power) After 8 Seconds to that at Take-off 0ft ISA	-
g	Gravitational Acceleration	ft/s ²
h	Change of Altitude in the Flight Segment	ft
h_{abs}	Absolute Ceiling to Size the Airplane for Time to Climb	ft
h_{obs}	Obstacle Height	ft
h_{Clend}	Altitude at End of Climb	ft
I_{power}	Power Index	hp ^{1/3} /ft ^{2/3}
I_{xxB}	Airplane Moment of Inertia about the X-body Axis	slugs/ft ³
I_{xxB}	Component Product of Inertia about the X-body Axis about its own C.G. Location	slugs/ft ³
I_{xzB}	Airplane Product of Inertia about XZ-body Axes	slugs/ft ³
I_{xzB}	Component Product of Inertia about the XZ-body Axis about its own C.G. Location	slugs/ft ³
I_{yyB}	Airplane Moment of Inertia about the Y-body Axis	slugs/ft ³
I_{yyB}	Component Product of Inertia about the Y-body Axis about its own C.G. Location	slugs/ft ³

Symbol	Description	Unit
I_{zzB}	Airplane Moment of Inertia about the Z-body Axis	slugs/ft ³
I_{zzB}	Component Product of Inertia about the Z-body Axis about its own C.G. Location	slugs/ft ³
K_{trim}	Flap Trim Factor	-
K'	Plain Flap Effectiveness Factor	-
k_{λ_c}	Taper Ratio Correction Factor for Canard Maximum Lift	-
k_{λ_h}	Taper Ratio Correction Factor for Horizontal Tail Maximum Lift	-
k_{λ_v}	Taper Ratio Correction Factor for Vertical Tail Maximum Lift	-
$k_{\lambda_{vee}}$	Taper Ratio Correction Factor for V-Tail Maximum Lift	-
k_{λ_w}	Taper Ratio Correction Factor for Wing Maximum Lift	-
L	Airplane Total Length	ft
l_c	X-distance Between the Canard and Wing Mean Geometric Chord Quarter Chord Points	ft
l_h	X-distance Between the Horizontal Tail and Wing Mean Geometric Chord Quarter Chord Points	ft
L	Lift	lb
L	Length	ft
L/D	Lift-to-drag Ratio During the Flight Segment	
l_{vee}	X-distance Between the V-tail and Wing Mean Geometric Chord Quarter Chord Points	ft
$l_{ac_{vee}}$	Distance between X-coordinate of V-Tail Aerodynamic Center and X-coordinate of Wing Aerodynamic Center in Stability Axes	ft
l_v	X-distance Between the Vertical Tail and Wing Mean Geometric Chord Quarter Chord Points	ft
l_v	Distance between X-coordinate of Vertical Tail Aerodynamic Center and X-coordinate of Wing Aerodynamic Center in Stability Axes	ft
M	Mach Number	-
M_{ff}	Mission Fuel Fraction	-
M_{ff}	Fuel Fraction of the Flight Segment	-
$M_{F_{res}}$	Reserve Fuel Fraction	-
M_{tfo}	Trapped Fuel and Oil Weight As Fraction of Take-off	-

Symbol	Description	Unit
	Weight	
M_1	Steady State Mach Number	-
N	Number	-
N	Revolutions per minute	rpm
n	Load Factor	-
N_{crew}	Number of Crew Members Required for the Airplane	-
N_{panel_h}	Number of Half Horizontal Tail Panels	-
$N_{panel_{vee}}$	Number of Half V-Tail Panels	-
N_{panel_v}	Number of Half Vertical Tail Panels	-
N_{panel_w}	Number of Half Wing Panels	-
P	Power	hp
$P_{SpExPwr}$	Specific Excess Power	hp
\bar{q}	Dynamic Pressure Ratio for Atmospheric Properties Calculation	lb/ ft ²
\bar{q}_1	Dynamic Pressure in Steady State	lb/ ft ²
R	Range of the Flight Segment	ft
Re	Reynolds Number	-
R_{turn}	Radius of Turn	ft
R_x	Radius of Gyration	ft
R_y	Radius of Gyration	ft
R_z	Radius of Gyration	ft
\bar{R}	Range Parameter	-
\bar{R}_x	Average Non-dimensional Radius of Gyration	-
\bar{R}_y	Average Non-dimensional Radius of Gyration	-
\bar{R}_z	Average Non-dimensional Radius of Gyration	-
RC	Rate of Climb	ft/min
RC	Airplane Rate of Climb During the Flight Segment	ft/min
$RC_{23.65}$	FAR 23.65 (All Engines Operative) Rate of Climb	ft/min
$RC_{5000_{OSA}}$	FAR 23.77 (All Engines Operative) Rate of Climb at Altitude	ft/min
S_c	Canard Area	ft ²
S_{FL}	Landing Field Length	ft
S_h	Horizontal Tail Area	ft ²
S_L	Landing Distance	ft
S_{LG}	Landing Ground Run to Zero Speed	ft

Symbol	Description	Unit
S_{TO}	Take-off Field Length	ft
S_{TOFL}	Take-off Field Length	ft
S_{TOG}	Take-off Ground Run	ft
S_v	Vertical Tail Area	ft ²
S_{vee}	V-Tail Unfolded Area	ft ²
S_{vf}	Ventral Fin Area	ft ²
S_w	Wing Area	ft ²
S_{wf} / S_w	Flapped Wing Area to Wing Area Ratio	-
S_{wf}	Flapped Wing Area	ft ²
S_{wet}	Airplane Wetted Area	ft ²
S_{wet}	Wetted Area	ft ²
T	Thrust	lb
t	Parameter along a curve	-
t/c	Thickness Ratio	%
$(t/c)_{r_w}$	Wing Root Thickness Ratio	%
$(t/c)_{t_w}$	Wing Tip Thickness Ratio	%
$(T/W)_{TO}$	Thrust Loading at Take-off Weight	-
T_{avail}	Available Installed Thrust	lb
TOP_{23}	FAR 23 Take-Off Parameter	-
T_{TO}	Total Take-off Thrust	lb
U_1	Steady State Flight Speed	kts
V	Speed for Atmosphere Properties Calculation	kts
V	Velocity	kts
V	Horizontal Velocity	kts
\bar{V}_c	Canard Volume Coefficient	-
\bar{V}_{c_g}	Canard Volume Coefficient based on Geometry (Quarter Chord Canard to Quarter Chord Wing)	-
V_{cat}	Expected Catapult End Speed	kts
V_{Cl}	Flight Speed During Climb	kts
V_{F_w}	Wing fuel volume	ft ³
\bar{V}_h	Horizontal Tail Volume Coefficient	-
\bar{V}_{h_g}	Horizontal Tail Volume Coefficient based on Geometry (Quarter Chord Tail to Quarter Chord Wing)	-
V_S	Stall Speed or the Minimum Speed	kts

Symbol	Description	Unit
V_S	Airplane Stall Speed	kts
\bar{V}_v	Vertical Tail Volume Coefficient	-
\bar{V}_{vee}	V-Tail Volume Coefficient	-
\bar{V}_{vg}	Vertical Tail Volume Coefficient based on Geometry (Quarter Chord Tail to Quarter Chord Wing)	-
\bar{V}_{veeg}	V-Tail Volume Coefficient based on Geometry (Quarter Chord Tail to Quarter Chord Wing)	-
V_{wod}	Wind Speed Over Deck for Carrier Based Airplanes	kts
$(W/P)_{TO}$	Power Loading at Take-off	-
W/S	Wing Loading	-
$(W/S)_{TO}$	Take-off Wing Loading	-
$W_{baggage}$	Baggage Weight	lb
W_{Cl}	Airplane Climb Weight	lb
W_{crew}	Crew Weight	lb
W_{Cr}	Airplane Cruise Weight	lb
W_E	Class I Airplane Empty Weight	lb
W_E	Class II Airplane Empty Weight	lb
W_{emp}	Class I Empennage Weight	lb
W_{eng}	Class I Engine Weight	lb
W_f	Class I Fuselage Weight	lb
W_f	Fuselage Weight	lb
W_F	Class I Mission Fuel Weight	lb
W_F	Class II Mission Fuel Weight	lb
W_{Fbegin}	Fuel Weight at the Beginning of the Flight Segment	lb
W_{FCr}	Weight of Fuel Used During the Cruise	lb
W_{Fmax}	Maximum Fuel Weight in the Fuel Tank at Any Point of the Mission	lb
W_{Fmax_w}	Maximum Fuel Weight Limited by the Fuel Tank Volume	lb
$W_{Frefuel}$	Total Refueled Fuel Weight	lb
$W_{Frefuel}$	Refueled Fuel Weight for the Flight Segment	lb
W_{Fres}	Class I Reserve Fuel Weight	lb
W_{Fres}	Class II Reserve Fuel Weight	lb
W_{Fused}	Class I Weight of Fuel Used in the Mission (without	lb

Symbol	Description	Unit
	Reserves)	
W_{Fused}	Class II Weight of Fuel Used in the Mission (without Reserves)	lb
W_{fix}	Class II Fixed Equipment Weight	lb
W_{fix}	Class I Fixed Equipment Weight	lb
W_{gear}	Gear Weight	lb
W_{gear}	Class I Landing Gear Weight	lb
W_{gross}	Take-off Gross Weight	lb
W_L	Airplane Landing Weight	lb
W_L/W_{TO}	Landing Weight to Take-off Weight Ratio	-
W_M	Airplane Maneuver Weight	lb
W_{man}/W_{TO}	Maneuvering Weight to Take-off Weight Ratio	-
W_n	Nacelle Weight	lb
W_n	Class I Nacelle Weight	lb
W_p	Propulsion System Weight	lb
W_{PL}	Payload Weight	lb
W_{PLexp}	Total Expended Payload Weight	lb
W_{PLexp}	Expended Payload Weight of the Flight Segment	lb
W_{pp}	Class I Powerplant Weight	lb
W_{pp}	Class II Powerplant Weight	lb
W_{prop}	Propeller Weight	lb
W_{prop}	Class I Propeller Weight	lb
W_S	Weight at which stall is evaluated	lb
W_S/W_{TO}	Stall Weight to Take-off Weight Ratio	lb
$W_{structure}$	Class I Airplane Structural Weight	lb
$W_{structure}$	Class II Airplane Structure Weight	lb
W_{tfo}	Class I Trapped Fuel and Oil Weight	lb
W_{tfo}	Class II Trapped Fuel and Oil Weight	lb
W_{TO}	Class I Airplane Take-off Weight	lb
W_{TOII}	Class II Airplane Take-off Weight	lb
W_w	Wing Weight	lb
W_w	Class I Wing Weight	lb
X	X-coordinate of Each Component	ft

Symbol	Description	Unit
X	X-coordinate in inches (mm) in the Weight and Balance Axes	ft
x	X-location of the Cross-section with respect to Component Apex (Nose)	ft
x	X-location of Fuselage Station Measured from the Fuselage Nose	ft
X_{ac_c}	X-coordinate of Canard Aerodynamic Center	ft
X_{ac_h}	X-coordinate of Horizontal Tail Aerodynamic Center	ft
X_{ac_v}	X-coordinate of Vertical Tail Aerodynamic Center	ft
$X_{ac_{vee}}$	X-coordinate of V-Tail Aerodynamic Center	ft
$X_{ac_{vf}}$	X-coordinate of Ventral Fin Aerodynamic Center	ft
X_{ac_w}	X-coordinate of Wing Aerodynamic Center	ft
$X_{ac_{wf}}$	X-coordinate of Wing-fuselage Aerodynamic Center	ft
X_{apex_c}	X-coordinate of Canard Apex	ft
X_{apex_f}	X-coordinate of Fuselage Nose	ft
X_{apex_h}	X-coordinate of Horizontal Tail Apex	ft
X_{apex_v}	X-coordinate of Vertical Tail Apex	ft
$X_{apex_{vee}}$	X-coordinate of V-Tail Apex	ft
X_{apex_w}	X-coordinate of Wing Apex	ft
X_{cg}	X-coordinate of Component Center of Gravity	ft
x_{mgc_c}	X-location of the Canard Mean Geometric Chord Leading Edge Relative to the Canard Apex	ft
x_{mgc_h}	X-location of Horizontal Tail Mean Geometric Chord Leading Edge Relative to the Horizontal Tail Apex	ft
x_{mgc_v}	X-location of the Vertical Tail Mean Geometric Chord Leading Edge Relative to the Vertical Tail Apex	ft
$x_{mgc_{vee}}$	X-Location of V-Tail Mean Geometric Chord Leading Edge Relative to the V-Tail Apex	ft
$x_{mgc_{vf}}$	X-location of the Ventral Fin Mean Geometric Chord Leading Edge Relative to the Ventral Fin Apex	ft
x_{mgc_w}	X-location of Wing Mean Geometric Chord Leading Edge Relative to the Wing Apex	ft
X_{nose_n}	X-coordinate of Nacelle Nose	ft
X_r	Chordwise X-coordinate of the Panel Root Chord Leading	ft

Symbol	Description	Unit
	Edge	
X_t	Chordwise X-coordinate of the Panel Tip Chord Leading Edge	ft
y	Parameter	ft
Y	Y-coordinate of Each Component	ft
y_{mgc_c}	Y-distance between the Canard Apex and the Canard Mean Geometric Chord	ft
Y_{cg}	Y-coordinate of Component Center of Gravity	ft
Y_{cg}	Y-coordinate of Component Center of Gravity	ft
Y	Cross-section Y-coordinate	ft
y_1	Y-location of the Cross-section Upper Section Point 1 with respect to Component Apex (Nose)	ft
y_{12}	Y-location of the Cross-section Upper Section Control Point with respect to Component Apex (Nose)	ft
y_2	Y-location of the Cross-section Point 2 with respect to Component Apex (Nose)	ft
y_{23}	Y-location of the Cross-section Lower Section Control Point with respect to Component Apex (Nose)	ft
y_3	Y-location of the Cross-section Lower Section Point 3 with respect to Component Apex (Nose)	ft
y_{mgc_h}	Y-distance between the Horizontal Tail Apex and the Horizontal Tail Mean Geometric Chord	ft
Y_{nose_n}	Y-coordinate of Nacelle Nose	ft
Y_r	Spanwise Y-coordinate of the Panel Root Chord	ft
Y	Spanwise Coordinate Measured from Fuselage Centerline	ft
$y_{mgc_{vee}}$	Y-distance between the V-tail Apex and the V-Tail Mean Geometric Chord	ft
$Y_{c_r/4_v}$	Y-coordinate of Vertical Tail Root Quarter Chord Point	ft
$Y_{c_t/4_v}$	Y-coordinate of Vertical Tail Tip Quarter Chord Point	ft
y_{mgc_w}	Y-distance between the Wing Apex and the Wing Mean Geometric Chord	ft
Y	Y-coordinate	ft
Y_{cg}	Y-coordinate of Airplane Center of Gravity	ft
Z	Z-coordinate of Each Component	ft
Z	Spanwise Coordinate	ft

Symbol	Description	Unit
Z_{apex_f}	Z-coordinate of Fuselage Nose	ft
Z_{apex_v}	Z-coordinate of Vertical Tail Apex	ft
Z_{cg}	Z-coordinate of Component Center of Gravity	ft
Z_{cg}	Z-coordinate of Airplane Center of Gravity	ft
z_{mgc_v}	Z-distance between Vertical Tail Apex and Vertical Tail Mean Geometric Chord	ft
$z_{mgc_{vf}}$	Z-distance between Ventral Fin Apex and Ventral Fin Mean Geometric Chord	ft
Z_r	Z-coordinate of Panel Root Chord Leading Edge	ft
z_1	Z-location of the Cross-section Upper Section Point 1 with respect to Component Apex (Nose)	ft
z_{12}	Z-location of the Cross-section Upper Section Control Point with respect to Component Apex (Nose)	ft
z_2	Z-location of the Cross-section Point 2 with respect to Component Apex (Nose)	ft
z_{23}	Z-location of the Cross-section Lower Section Control Point with respect to Component Apex (Nose)	ft
z_3	Z-location of the Cross-section Lower Section Point 3 with respect to Component Apex (Nose)	ft

Greek Symbols

Symbol	Description	Unit
α	Airplane Angle of Attack	deg
α_o	Airplane Zero-lift Angle of Attack Including any Flap Effects	deg
α_{orw}	Wing Root Airfoil Zero-lift Angle of Attack	deg
α_{otw}	Wing Tip Airfoil Zero-lift Angle of Attack	deg
α_{ow}	Airplane Angle of Attack for Wing Zero-lift including any Flap Effects	deg
α_{owf}	Wing-Fuselage zero-lift Angle of Attack including any Flap Effects	deg
$\alpha_{\delta f}$	Change in Airplane Angle of Attack due to Flap Deflection	deg
β	Airplane Sideslip Angle	deg
Δ	Increment	-
ΔC_{D_o}	Increment in Airplane Zero-lift Drag Coefficient	-
$\Delta C_{D_{oA}}$	Change in Airplane Zero-lift Drag Coefficient due to Flaps at Approach Position	-
$\Delta C_{D_{oclean}}$	Increment in Airplane Zero-lift Drag Coefficient due to Compressibility	-
$\Delta C_{D_{oL_down}}$	Increment in Airplane Zero-lift Drag Coefficient due to Landing Flaps and Gear	-
$\Delta C_{D_{oL_up}}$	Increment in Airplane Zero-lift Drag Coefficient due to Landing Flaps, with Gear Retracted	-
$\Delta C_{D_{oOEI}}$	Increment in Airplane Zero-lift Drag Coefficient due to One Engine Inoperative	-
$\Delta C_{D_{oTO_dwn}}$	Increment in Airplane Zero-lift Drag Coefficient due to Takeoff Flaps and Gear	-
$\Delta C_{D_{oTO_up}}$	Increment in Airplane Zero-lift Drag Coefficient due to Takeoff Flaps, with Gear Retracted	-
$\Delta C_{L_{cl-max}}$	Margin of Safety between Airplane Maximum Lift Coefficient and Airplane Lift Coefficient During Climb	-
$\Delta C_{L_c power}$	Change in Canard Lift Coefficient due to Power	-

Symbol	Description	Unit
$\Delta c_{lf0.2}$	Empirical Constant for Split Flap with a Flap Chord to Wing Chord Ratio of 20%	-
$\Delta c_{lf0.2L}$	Empirical Constant at Landing for Split Flap with a Flap Chord to Wing Chord Ratio of 20%	-
$\Delta c_{lf0.2TO}$	Empirical Constant at Take-off for Split Flap with a Flap Chord to Wing Chord Ratio of 20%	-
$\Delta c_{l_{max}} / \Delta c_l$	Ratio of Change in Airfoil Maximum Lift Coefficient to Change in Airfoil Lift Coefficient at Constant Angle of Attack due to Flap Deflection	-
$\Delta C_{Lw\delta da}$	Increment in Wing Lift Coefficient due to Drooped Ailerons	-
$\Delta C_{Lw\delta da L}$	Increment in Wing Lift Coefficient due to Drooped Ailerons at Landing	-
$\Delta C_{Lw\delta da TO}$	Increment in Wing Lift Coefficient due to Drooped Ailerons at Take-off	-
$\Delta C_{Lw_{max} \delta f}$	Increment in Wing Lift Coefficient due to Flaps	-
$\Delta C_{Lw\delta f L}$	Increment in Wing Lift Coefficient due to Flaps at Landing	-
$\Delta C_{Lw\delta f TO}$	Increment in Wing Lift Coefficient due to Flaps at Take-off	-
$\Delta C_{L\delta f}$	Change in Airplane Lift Coefficient due to Flap Deflection	-
$\Delta c_{l\delta f}$	Change in Airfoil Lift Coefficient due to Flap Deflection	-
$\Delta c_{l\delta f L}$	Change in Airfoil Lift Coefficient due to Flap Deflection at Landing	-
$\Delta c_{l\delta f TO}$	Change in Airfoil Lift Coefficient due to Flap Deflection at Take-off	-
ΔW	Component Weight Adjustment	lb
ΔW_E	Iteration Accuracy for Empty Weight	lb
$\Delta W_{F_{used}}$	Weight of Fuel Used in Each Segment	lb
δ_a	Aileron Deflection Angle	deg
δ_{da}	Drooped Aileron Deflection Angle	deg
δ_{daL}	Drooped Aileron Deflection Angle at Landing	deg

Symbol	Description	Unit
δ_{daTO}	Drooped Aileron Deflection Angle at Take-off	deg
δ_e	Elevator Deflection Angle	deg
δ_f	Flap Deflection Angle	deg
δ_{fL}	Flap Deflection Angle at Landing	deg
δ_{fTO}	Flap Deflection Angle at Take-off	deg
δ_{f1}/δ_{f2}	Double Slotted Flap Deflection Angle Ratio	-
$(\delta_{f1}/\delta_{f2})_L$	Double Slotted Flap Deflection Angle Ratio at Landing	-
$(\delta_{f1}/\delta_{f2})_{TO}$	Double Slotted Flap Deflection Angle Ratio at Take-off	-
δ_{f2}	Aft Flap Deflection Angle	deg
δ_{f2L}	Aft Flap Deflection Angle at Landing	deg
δ_{f2TO}	Aft Flap Deflection Angle at Take-off	deg
δ_r	Rudder Deflection Angle	deg
ε_{aw}	Wing Aerodynamic Twist Angle	deg
ε_t	Panel Tip Twist Angle	deg
ϕ_{TEupp}	Flap Trailing Edge Angle	deg
Γ_c	Canard Dihedral Angle	deg
Γ_h	Horizontal Tail Dihedral Angle	deg
Γ_v	Vertical Tail Dihedral Angle	deg
Γ_{vee}	V-Tail Dihedral Angle	deg
Γ_{vf}	Ventral Fin Dihedral Angle	deg
Γ_w	Wing Dihedral Angle	deg
γ	Flight Path Angle	deg
η	Spanwise Chord Station	%
η	Flap Parameter	-
η	Lifting Surface Spanwise Station	%
η_i	Inboard Station in Terms of Span	%
η_{ia}	Aileron Inboard Station in Terms of Wing Half Span	%
η_{ie}	Elevator Inboard Station in Terms of Horizontal Tail Half Span	%
η_{if}	Flap Inboard Station in Terms of Wing Half Span	%
η_{ir}	Rudder Inboard Station in Terms of Vertical Tail Span	%

Symbol	Description	Unit
η_o	Outboard Station in Terms of Span	%
η_{oa}	Aileron Outboard Station in Terms of Wing Half Span	%
η_{oe}	Elevator Outboard Station in Terms of Horizontal Tail Half Span	%
η_{of}	Flap Outboard Station in Terms of Wing Half Span	%
η_{or}	Rudder Outboard Station in Terms of Vertical Tail Span	%
η_{orv}	Ruddervator Outboard Station in Terms of V-Tail Half Span	%
η_p	Propeller Efficiency for the Flight Segment	%
$\Lambda_{c/4c}$	Canard Quarter Chord Sweep Angle	deg
$\Lambda_{c/4h}$	Horizontal Tail Quarter-chord Sweep Angle	deg
$\Lambda_{c/4py}$	Pylon Quarter-Chord Sweep Angle	deg
$\Lambda_{c/4v}$	Vertical Tail Quarter-chord Sweep Angle	deg
$\Lambda_{c/4vee}$	V-Tail Quarter-chord Sweep Angle	deg
$\Lambda_{c/4vf}$	Ventral Fin Quarter-chord Sweep Angle	deg
$\Lambda_{c/4w}$	Wing Quarter-chord Sweep Angle	deg
Λ_{LEc}	Canard Leading Edge Sweep Angle	deg
Λ_{LEh}	Horizontal Tail Leading Edge Sweep Angle	deg
Λ_{LEv}	Vertical Tail Leading Edge Sweep Angle	deg
Λ_{LEvee}	V-Tail Leading Edge Sweep Angle	deg
Λ_{LEvf}	Ventral Fin Leading Edge Sweep Angle	deg
Λ_{LEw}	Wing Leading Edge Sweep Angle	deg
Λ_{TEc}	Canard Trailing Edge Sweep Angle	deg
Λ_{TEh}	Horizontal Tail Trailing Edge Sweep Angle	deg
Λ_{TEv}	Vertical Tail Trailing Edge Sweep Angle	deg
Λ_{TEvee}	V-Tail Trailing Edge Sweep Angle	deg
Λ_{TEvf}	Ventral Fin Trailing Edge Sweep Angle	deg
Λ_{TEw}	Wing Trailing Edge Sweep Angle	deg
λ_c	Canard Taper Ratio	-
λ_h	Horizontal Tail Taper Ratio	-
λ_{py}	Pylon Taper Ratio	-
λ_v	Vertical Tail Taper Ratio	-

Symbol	Description	Unit
λ_{vee}	V-Tail Taper Ratio	-
λ_{vf}	Ventral Fin Taper Ratio	-
λ_w	Wing Taper Ratio	-
μ	Dynamic Viscosity	lb s/ft ²
μ_G	Wheel-ground Rolling Friction Coefficient During Take-off	-
ρ	Air Density at the Specified Altitude	slugs/ft ³
ρ_F	Fuel Density	lb/ft ³
ρ_{12}	Cross-section Control Point Weight Factor (Rho) at Upper Section	-
ρ_{23}	Cross-section Control Point Weight Factor (Rho) at Lower Section	-
σ	Ratio of Air Density at Altitude to that at Sea-level	-

Subscripts

Symbol	Description
air	In the air
A	Approach
Blade	Propeller Blade
clean	Clean Configuration (Flaps Up, Gear Up)
c	Canard
cl	Climb
cr	Cruise
eng	Engine
F	Fuel
f	flap
h	Horizontal Tail
i	i^{th} segment
j	j^{th} segment
L	Landing
ltr	Loiter
l.s.	Lifting Surface
M	Maneuver
M	at a certain Mach Number
Max	Maximum
misc	Miscellaneous
p	Propeller
prof	Profile
prop	Propeller
S	Stall
SL,ISA	Sea level, International Standard Atmosphere
SpExPwr	Specific Excess Power
TO	Take-Off
turn	Turn
refuel	During Refueling Segment
v	Vertical Tail
vf	Ventral Fin
vee	V-Tail
w	Wing

Symbol	Description
wm	Windmilling
x	TO for Take-off, L for Landing

Acronyms

Acronym	Description
AAA	Advanced Aircraft Analysis
AML	Adaptive Modeling Language
AMRaven	Adaptive Modeling Rapid Air Vehicle Engineering
CAD	Computer Aided Design
CFD	Computational Fluid Dynamics
dll	Dynamic link library
FEA	Finite Element Analysis
G.A-CAD	General Aviation Computer Aided Design

1 Introduction

When starting a clean sheet airplane design it is assumed the design requirements are known at the onset of the design process. Often design requirements change during the design process, which leads to redesign work, or even starting over. Changing requirements as well as methods used can lead to a design that eventually does not meet the initial requirements.

The initial conceptual design phase sets the overall size and configuration of the vehicle and thus drives most of the cost of the airplane development project. Many design systems and tools (See Chapter 2) have been developed over the years, but none are fully integrated and each require extensive training to use. A historical overview of available design systems is given in Chapter 2.1. Data exchange between these tools is tedious and error prone. This by itself also drives up the cost of design.

The airplane design system development is described in Chapter 3 and explains the programming languages and development environments used.

The system architecture is managed using an object-oriented modeling language called Adaptive Modeling Language (AML, see Chapter 4), developed and marketed by TechnoSoft, Inc. AML is a mature, commercially-available software development architecture containing many of the objects necessary for developing integrated

design, analysis, and manufacturing tools. AML automatically builds and manages networks of dependencies between objects, so that when an object changes all dependent objects are automatically updated.

TechnoSoft, Inc. started development of a multidisciplinary modeling and analysis environment supporting air vehicle synthesis called AMRaven (AML Rapid Air Vehicle Engineering, see Chapter 4.2), a knowledge-based engineering design and analysis framework using the AML language. AMRaven supports process design automation and integrates design exploration and optimization across multiple disciplines. The framework facilitates rapid vehicle development integrating feature-based 3D geometric modeling, 3D parametric meshing, analysis (aerodynamics, propulsion, trajectory, weight estimation, etc.) and simulation.

Since no conceptual or preliminary airplane design methods were originally part of the AMRaven environment, The University of Kansas, TechnoSoft and DARcorporation teamed to add these tools to AMRaven. These tools used for conceptual and preliminary design and analysis of airplanes are based on the Advanced Aircraft Analysis (AAA, see Section 2.1) tools. The author is the chief software architect of at DARcorporation. The author developed this powerful framework to support the iterative and non-unique process of aircraft conceptual and preliminary design. AAA allows students and preliminary design engineers to rapidly evolve an aircraft configuration from early weight sizing through open loop and

closed loop dynamic stability and sensitivity analysis, while working within regulatory and cost constraints. The program is specifically designed to assist in the design learning process while reserving that individual creative judgment which is essential to the process of airplane design. The design process used is described in Chapter 5.

Starting with the methods developed for the Advanced Aircraft Analysis (AAA) software (described in Chapter 2 and Appendix B for details on the latest version of AAA) a system has been developed to automate the initial design phase. This effort involved the automation of design methods developed for AAA using the Adaptive Modeling Language (AML, see Chapter 4) and integrating these tools into AMRaven (see Chapter 4.2). The theoretical background of all methods used is described in Chapter 6

Chapter 7 shows the implementation and testing of the tools developed on a series of existing airplanes and one new design.

Chapter 8 shows the conclusions of this study and recommendations for further research and development.

2 Airplane Design Systems and Overview of Past Work

Since the methods to be used in the new Knowledge-based system are based on the Advanced Aircraft Analysis (AAA) software, a description is given on the development history of AAA including the first and second generation, leading to development of G.A.-CAD and the current version of AAA (Third Generation), release 3.1. A detailed description of the AAA 3.1 specifications can be found in Appendix B. The current version of AAA is based on the methods of Refs. 1-11 supplemented with methods and procedures from Refs. 12-35.

Many companies and universities have developed conceptual/preliminary airplane design systems. A comprehensive list of paper and article abstracts written on these tools and background are listed in Appendix D. More details can be found in References 36-184. Most references deal with small subsets of design systems, such as geometry representation or concentration on Computational Fluid Dynamics (CFD) and/or finite element analysis (FEA).

Design systems developed by industry and academia are described in Section 2.1. Papers and articles related to aircraft design, written during the last 25 years have been collected and organized. Abstracts of books and papers dealing with general Computer Aided Design (CAD) methods and the mathematics behind CAD systems are described in Appendix C. Papers dealing with configuration design, artificial intelligence in design, knowledge-based design, geometry-based design, general

airplane design and design systems, geometry representations for CFD and FEA are described in Appendix C. All references show the paper abstracts as written by the authors except where noted and are shown in chronological order.

2.1 Design Systems

An overview of currently commercial available airplane design systems and/or university developed systems (not necessarily still operational) are described in the following sections.

2.1.1 CDS: Configuration Development System

Raymer (Ref. 69) describes the design system developed at Rockwell International. CDS contains a configuration development system, which is fully 3D. An aircraft is described as a collection of components, such as wings, engines and fuselages each consisting of three-dimensional cross-sections. An interface to an aerodynamics module has been developed. No additional description beyond 1979 has been found.

2.1.2 Paper Airplane

In the early eighties the Flight Transportation Laboratory of MIT (Ref. 70) started the development of Paper Airplane. The program uses symbolic manipulation (non-numeric computation) to handle objects such as design variables and design functions. The advantage of this is that there is no distinction between input and output parameters. When one parameter is unknown, Paper Airplane will deduce one

parameter from the known parameters. No further documentation beyond 1983 has been found.

2.1.3 ACSYNT: Aircraft Synthesis

This code was developed by the ACSYNT Institute a joint venture between NASA Ames and Virginia Polytechnic Institute (Refs. 73, 77, 87, 91, 92, 96, 107, 111). The code is still in use by quite a few companies and universities. It has developed from a UNIX based system to PC-Windows based and contains a detailed geometry module. It does not contain as much detail in stability and control as does AAA.

2.1.4 ADAS: Aircraft Design and Analysis System

This system has been developed at the Delft University of Technology (Refs. 80, 183) and is written in FORTRAN. It uses the methods from Reference 15. The geometry is defined in MEDUSA, a solid modeling CAD system originally and later used AutoCAD. ADAS is no longer operational. Many methods are still valid today and are similar to methods used in AAA. No detailed stability and control is included. A sizing module for canards and horizontal tails (Ref. 196) has been developed by the author of this dissertation. The author has extensive experience using this design tool. It requires programming experience and detailed CAD experience.

2.1.5 RDS

This program (Refs. 90, 97, 106, 108) developed by Raymer is still MS-DOS based and contains a geometry engine. Optimization methods are included. No detailed stability and control is included. It contains a basic sizing code, similar to Roskam methods. It is still available as a commercial product. It is also available as a student version. The fact that it is still a DOS version limits the usefulness of this program.

2.1.6 Advanced Aircraft Analysis: First Generation

In 1988 at The University of Kansas under guidance of Dr. Jan Roskam, several graduate students (including the author of this dissertation) started automating (Refs. 12, 36, 37, 38) the methods in Refs.1-11. The result of this development was the first version of Advanced Aircraft Analysis (AAA). This software ran on Apollo DN-series workstations (UNIX based), was programmed in Pascal and used Apollo proprietary graphics routines. The language Pascal was chosen since Apollo tools were mostly written in Pascal and the original user-interface tools on the Apollo workstation were written in Pascal (using Apollo GPR graphics primitives) and were originally donated by General Dynamics to The University of Kansas.

A prototype system was installed at the University of Kansas and was used for class instruction purposes only. This first generation of AAA contained the following modules:

1. Weight Sizing
2. Class I Drag
3. Performance Sizing
4. Performance Analysis
5. Class I Weight and Balance
6. Control
7. Dynamics
8. 2D Geometry
9. High Lift

In Class I methods only a minimal amount of input generation is required. With Class II methods more detailed and refined estimates of the airplane can be made but more input information is required.

The first generation of AAA contained a simple user-interface, with input and output sections and a toolbar with a calculate and print button. The symbols used for the input and output parameters were text based, without subscripts, superscripts or Greek symbols. For instance $c_{l\alpha_{rw}}$ was presented as c_l_a_rw. This made it harder to learn the system. Plotting and simple database functions to store and retrieve files were also part of this AAA. A first attempt was made to include all stability and control derivatives, but most of this code was written in FORTRAN and very

unstable. Most figures of Reference 6 were digitized using simple polynomials. All this code was later removed. After the first prototype was constructed, the author of this dissertation added the following modules:

1. Class I Weight Fractions
2. Class I Moments of Inertia
3. Class II Drag
4. Cost Analysis
5. Installed Thrust and Power
6. Rewrite of Stability and Control derivatives (digitizing of figures are based on methods described in Appendix F)

2.1.7 Advanced Aircraft Analysis: Second Generation

In 1991 Design, Analysis and Research Corporation (DARcorporation, the author of this dissertation is the owner and president) of Lawrence, Kansas acquired the rights for AAA and continued development of AAA as a commercial venture. In 1991 DARcorporation released Version 1.0 of AAA running on Apollo Domain and 400-series computers. The author of this dissertation is the chief architect of the second generation and of the current version of the AAA (Third Generation) software and is the owner of DARcorporation.

The program was developed to provide a powerful framework to support the non-unique process of aircraft preliminary design (Refs. 39, 40, 46). The system allows

design engineers to rapidly evolve an aircraft configuration from weight sizing through detailed performance calculations, while working within regulatory constraints. The program is designed to reduce the preliminary design phase cost and to bring advanced design methods to small businesses and universities. The objective was to create a user-friendly computer program that allows designers (not specialists) to rapidly assess the performance, structural weight breakdown, stability and control characteristics of arbitrary new airplane configurations.

AAA requires only a minimum of specialist knowledge (it is also used for teaching purposes, so novice users are expected to be able to quickly get up to speed) and contains a help system which familiarizes the user with the theoretical and methodological background of the various software modules.

During 1991 and 1992 AAA was ported to the X-Window system (see Figure 2.1) for all graphics and user-interface using the programming language C.

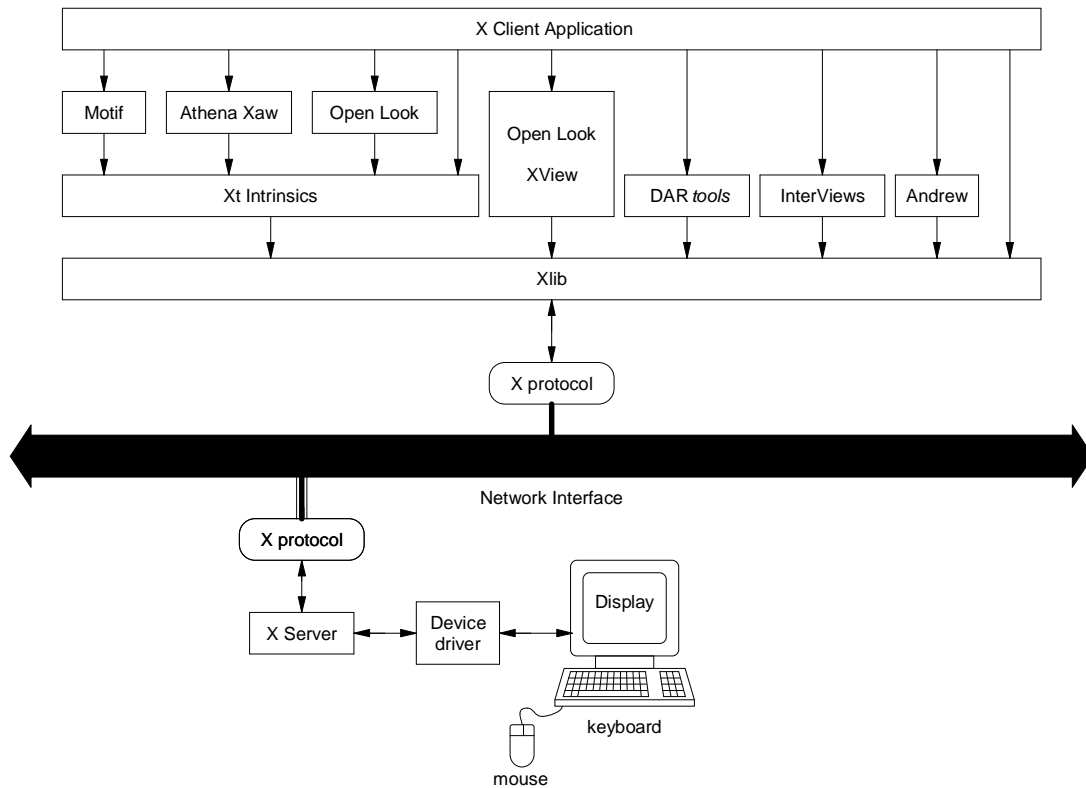


Figure 2.1 AAA(X-Client) in the X-Window System

The *DARtools* program contained the interface between the C-modules dealing with database handling, user-interface and graphics. All AAA methods were programmed in Pascal. The author was responsible for the overall architecture and all Pascal code (airplane design code).

In 1991 through 1992 AAA was ported to the SUN SPARCstation in X-Windows (on SUNOS 4.x and later Solaris 2.x), then followed by Silicon Graphics (IRIX 4.x), IBM RS 6000 (AIX) and Hewlett-Packard 700 series (HP-UX 8.x). The project was code-

named Project-X and resulted in the release of AAA Version 1.3. Through 1993-1995 AAA Version 1.4, 1.5, 1.6 and 1.7 were released with mainly additional modules and bug fixes, (Ref. 36-40). The user-interface was still primitive (See Figure 2.2) and based on the first generation of AAA. The author performed all porting to the different computer platforms.

The second generation AAA software contained thirteen modules, a database and help section and is based on Refs.1-11, supplemented with methods from Refs. 13-35.

In most of the analytical modules the user has the option to use Class I or Class II methods (See Chapter 5). In Class I methods only a minimal amount of input generation is required. With Class II methods more detailed and refined estimates of the airplane can be made but more input information is required.

WEIGHT SIZING	GEOMETRY	DRAG POLAR	WEIGHT & BALANCE	PERF. ANALYSIS	DYNAMICS	COST ANALYSIS	HELP / SETUP
PERFORM. SIZING	HIGH LIFT	STAB. & CONTROL	INSTALLED THRUST	S&C DERIVATIVES	CONTROL	DATA BASE	Q U I T

Flow Regime

SUBSONIC	TRANSONIC	SUPERSONIC	R E T U R N
-----------------	-----------	------------	-------------

Class II Drag Polar Prediction

WING DRAG	VERTICAL TAIL	FUSELAGE DRAG	FLAP DRAG	CANOPY DRAG	TRIM DRAG	MISCELLANEOUS	PLOT DRAG POLAR
HORIZONTAL TAIL	CANARD DRAG	NACELLE/PYLON	GEAR DRAG	STORES DRAG	SPOILER DRAG	TOTAL DRAG	R E T U R N

CALCULATE	THEORY	PRINT PARAMETERS	R E T U R N
-----------	--------	------------------	-------------

Wing Drag Coefficient Prediction

Altitude = ? ft	TR_w = ?	k = ? 10 ⁻³	claw M=0 = ? 1/rad
U_1 = ? kts	$\hat{C}/4_w = ? \text{ deg}$	l_LER_w/c = ? %	f_gap_w = ?
C_L_w = ?	Df_max = ? ft	L_fus = ? ft	epsilon_w = ? deg
S_w = ? ft ²	(t/C)_w_r = ? %	L'_w = ?	
AR_w = ?	(t/C)_w_t = ? %	Xlam/C_w = ? %	

Output Parameters

M_1 = ?	S_wet_w = ? ft ²	C_D_L_w = ?
C_L_a_w = ? 1/rad	C_D_o_w = ?	

Design, Analysis and Research Corporation	Advanced Aircraft Analysis Manual	/users/beta/manual/Business_Jet	February 13, 1996
			12:50 PM

Figure 2.2 AAA Second Generation User Interface

2.1.8 General Aviation Computer Aided Design: G.A.-CAD

In 1993 DARcorporation received a NASA SBIR (Small Business Innovative Research) Phase I contract (Ref. 185) for the development of a prototype design system for General Aviation Airplane Design. The program, called G.A.-CAD for General Aviation Computer Aided Design, is based on Advanced Aircraft Analysis (AAA) as described in Ref. 41. G.A.-CAD runs in a PC Windows environment. Detailed descriptions of G.A.-CAD can be found in Refs. 42-44. As part of G.A.-CAD a computer aided drafting program, Aero-CADD (Ref. 45) has been developed.

The author of this dissertation completely architected the structure of this software and performed most of the software development. Help system and testing were performed by other DARcorporation employees.

The design system identified during SBIR Phase I has been implemented in a personal computer based program during SBIR Phase II, which was awarded by NASA in 1995 (Ref. 186). The end product is a marketable software program which can be used in General Aviation configuration design and analysis. The objectives of Phase II were:

- Research of structural design, flutter analysis and loads
- Research of Computer Aided Design (CAD) methods for entering geometric descriptions in the form of an airplane three-view or wire frame model

- Research in aerodynamic methods, including propulsion and ground effects, currently not available in the Advanced Aircraft Analysis (AAA) software
- Implementation of Phase I and II research into a computer aided design system for General Aviation aircraft
- Development of a help system to augment the user-friendliness of the computer aided design system

During 1994 a limited working prototype of G.A.-CAD was completed. The focus of this prototype program was the preliminary research and development of the design methods required for the G.A.-CAD program. The areas of developmental research have included the user interface and analysis calculation methods. Modeled after the AAA program, the G.A.-CAD user interface follows the same sequence of menus and windows as found in AAA. However, the internal structure and appearance of the G.A.-CAD user-interface differ from the UNIX based AAA program by incorporating the methods required for the Microsoft Windows operating system. The calculation methods implemented in the G.A.-CAD prototype application were transferred directly from the AAA (Second Generation) program.

The G.A.-CAD prototype incorporates a limited working user interface (as shown in Figure 2.3), calculation modules and a Help system. The user interface for the G.A.-CAD application program includes the user manipulation of the menus, Input/Output windows (see Figure 2.4) and command buttons.

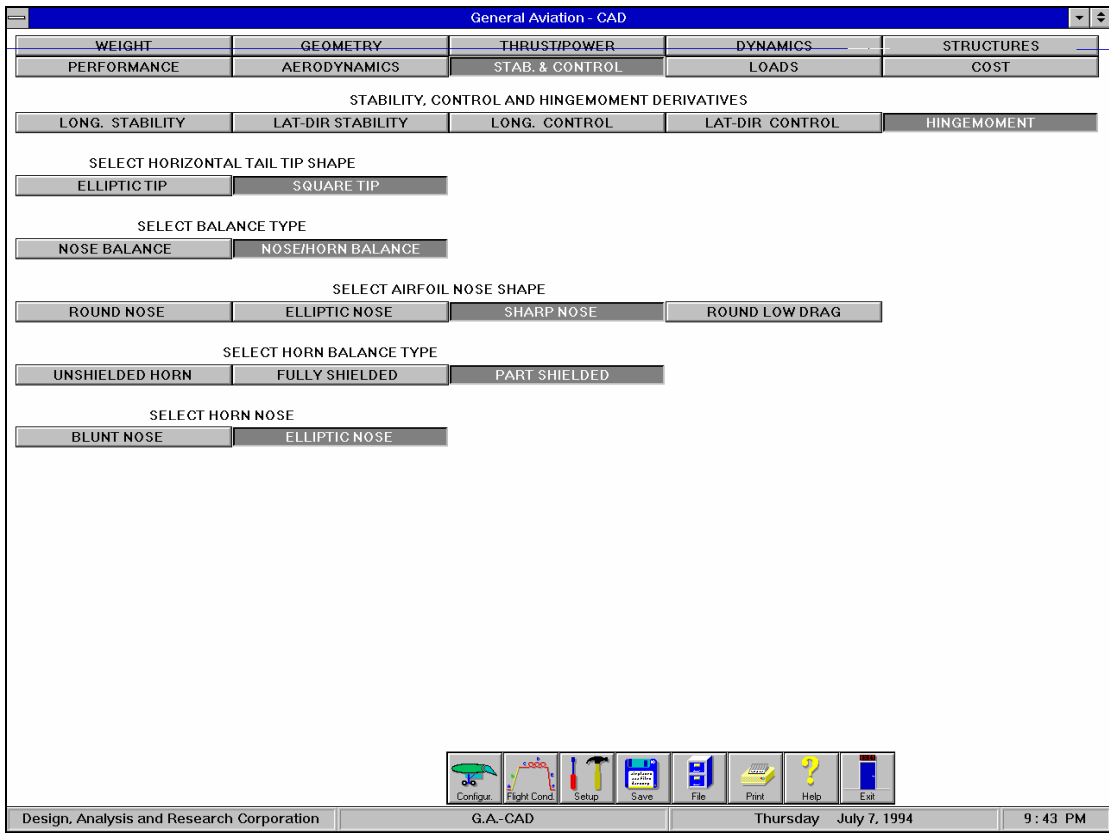


Figure 2.3 G.A.-CAD User Interface

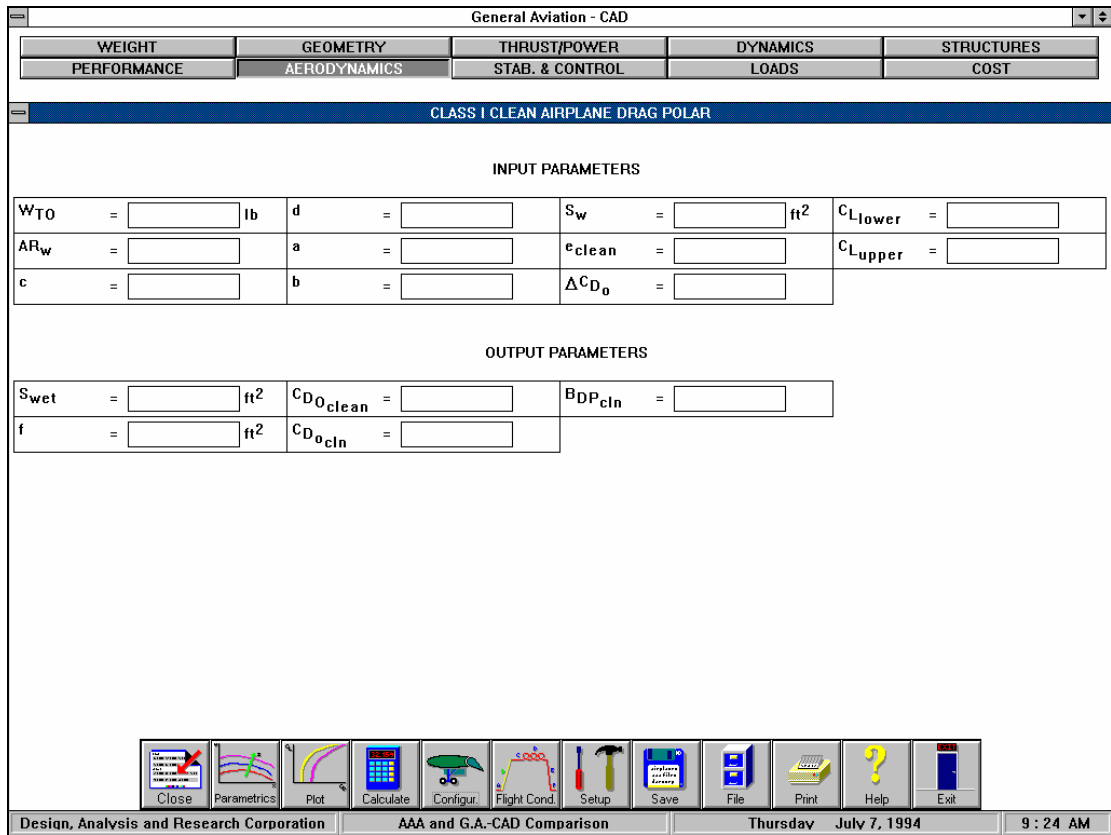


Figure 2.4 Input/Output Window for Class I Clean Airplane Drag Polar

The main difference with AAA 1.0-1.7 was a complete rewrite of the user-interface. Real subscripts, superscripts and Greek characters (see Figure 2.5) were used to make all symbols as used in textbooks and thus making it easier for users to work with the program.

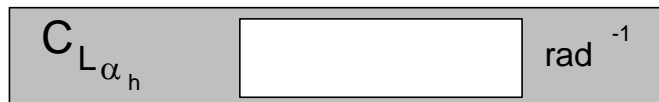


Figure 2.5 Input/Output Parameter Element

As part of the prototype system an elaborate help system was developed. Earlier versions of AAA had limited help in the form of ASCII files with very hard to read equations. The new help system (see Figure 2.6 and Figure 2.7) uses real symbols and equations for ease of understanding.

The screenshot shows a window titled "Class I Drag Help System" with a menu bar (File, Edit, Bookmark, Help) and a toolbar (Contents, Search, Back, History, <<, >>, Copy, Path, Exit). The main content area is titled "Class I Drag Options" and contains the following text:

Theory and methods for constructing airplane drag polars using Class I methods are presented in this help topic. All airplane configurations (clean, take-off gear down, etc.) are covered in this help topic. The theory is based on the methods of Reference 1. Theory is presented in text form which the user can scroll through. If an equation appears in the theory, the user can select it to view further explanation. Some variables and constants have a graphic or table associated with them. These variable or constants can be selected by the user to view the table or graphic.

Class I methods assume a parabolic drag polar of the form:

$$C_D = C_{D0} + \frac{C_L^2}{\pi A e} \quad \text{[eqn.1]}$$

The zero-lift drag coefficient, C_{D0} , can be expressed as:

$$C_{D0} = \frac{f}{S} \quad \text{[eqn.2]}$$

Wetted area and equivalent parasite area can be related by a logarithmic equation arrived at empirically in Reference 1. This equation is:

$$\log_{10} f = a + b \log_{10} S_{wet} \quad \text{[eqn.3]}$$

Similarly, airplane wetted area can be estimated from take-off weight by the following empirically obtained equation (Reference 1):

$$\log_{10} S_{wet} = c + d \log_{10} W_{TO} \quad \text{[eqn.4]}$$

with:

- S_{wet} airplane wetted area
- W_{TO} take-off weight

After calculating equivalent parasite coefficient, C_{D0} , can be calculated. Constants c and d are regression coefficients and e is the efficiency factor, e , are presented in Reference 1:

Configuration	e
Clean	0.80 - 0.85
Take-Off Flaps	0.75 - 0.80

Values for c and d were obtained by correlating wetted area and take-off weight data for various airplane types in Reference 1 and are presented in the following table:

Regression Line Coefficients for Take-off Weight Versus Wetted Area

Airplane Type	c	d
Homebuilts	1.0892	0.4319
Single Engine Propeller Driven	1.0892	0.5147
Twin Engine Propeller Driven	0.8635	0.5632
Agricultural	1.0447	0.5326
Business Jets	0.2263	0.6977
Regional Turboprops	-0.0866	0.8099
Military Trainers (no stores)	0.8565	0.5423
Flying Boats, Amphibious, and Float	0.6295	0.6708

copied from Reference 1.

Figure 2.6 G.A.-CAD Class I Clean Airplane Drag Polar Help System

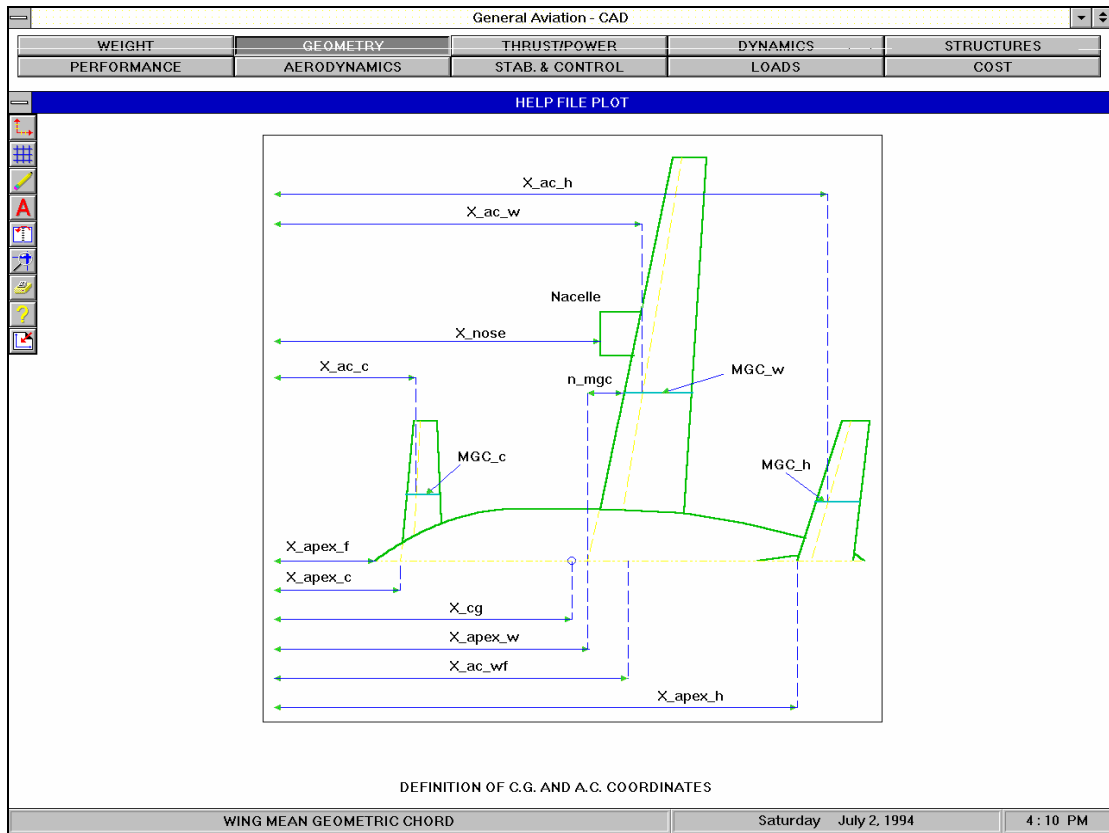


Figure 2.7 G.A.-CAD Graphical Help System

The prototype system was converted to a full design system during 1995-1996 under a NASA SBIR Phase II program. The resulting program called G.A.-CAD for General Aviation Computer Aided Design was released in 1996. It consisted of two parts: an analysis/design program based on AAA and a CAD program called Aero-CAD.

The user interface was changed from the G.A.-CAD prototype system to make it more intuitive (see Figure 2.8 - Figure 2.11).

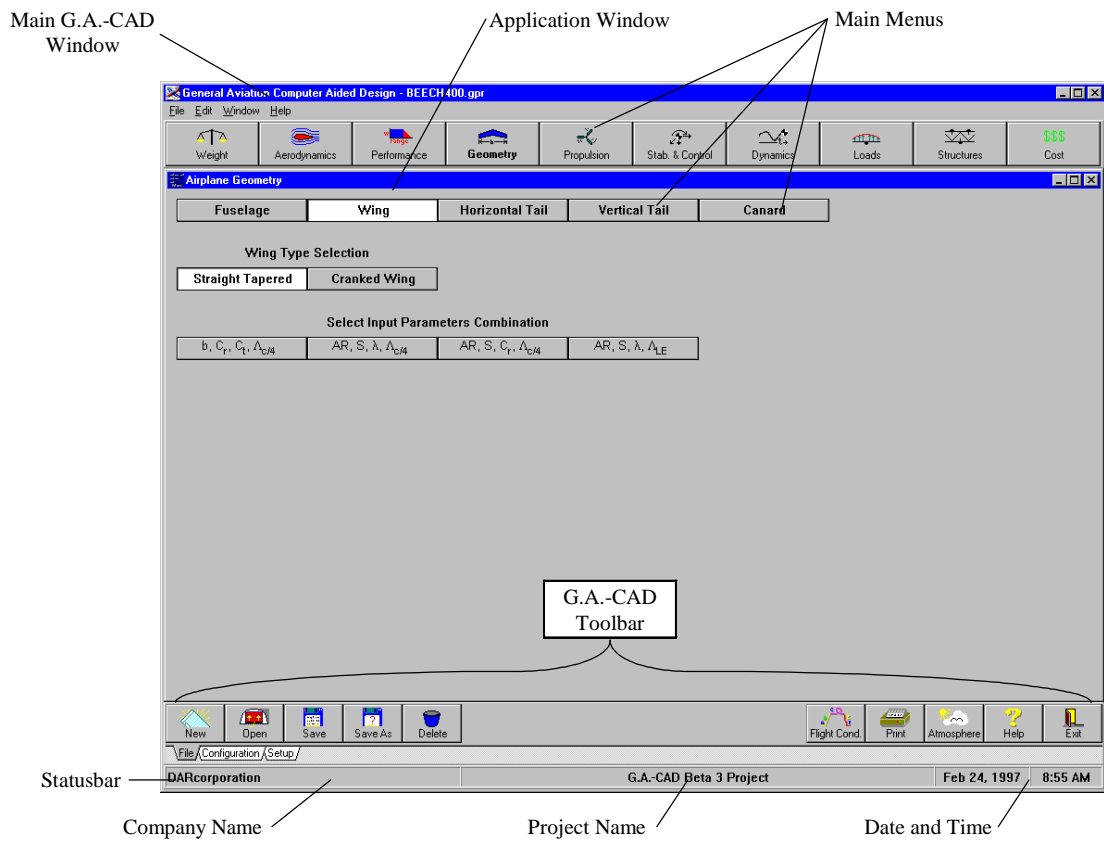


Figure 2.8 G.A.-CAD Window with Main Menu Buttons

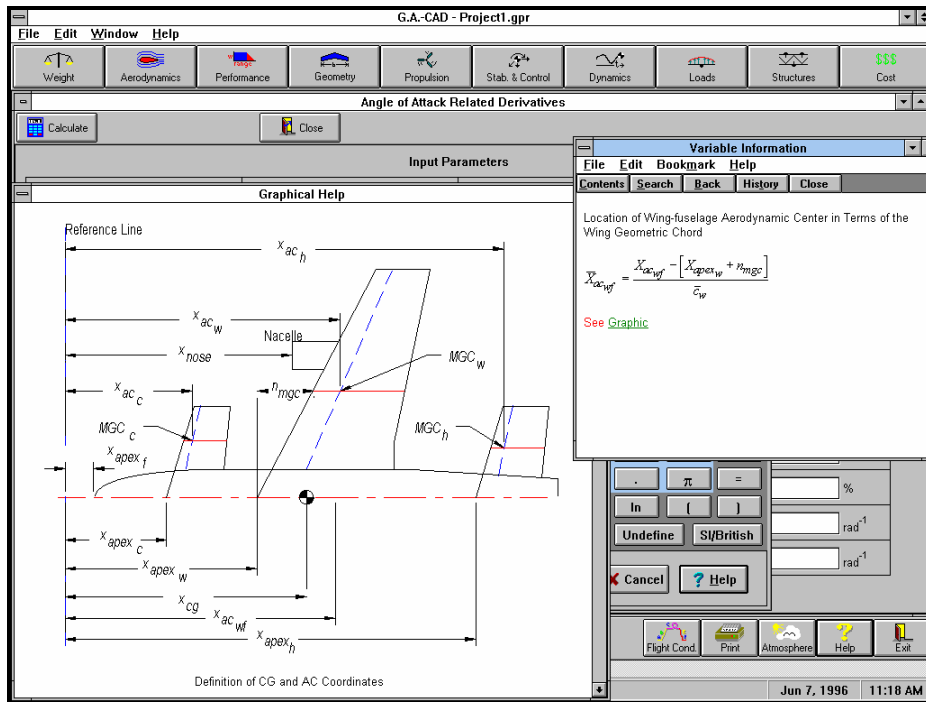


Figure 2.9 G.A.-CAD Graphical Help Window

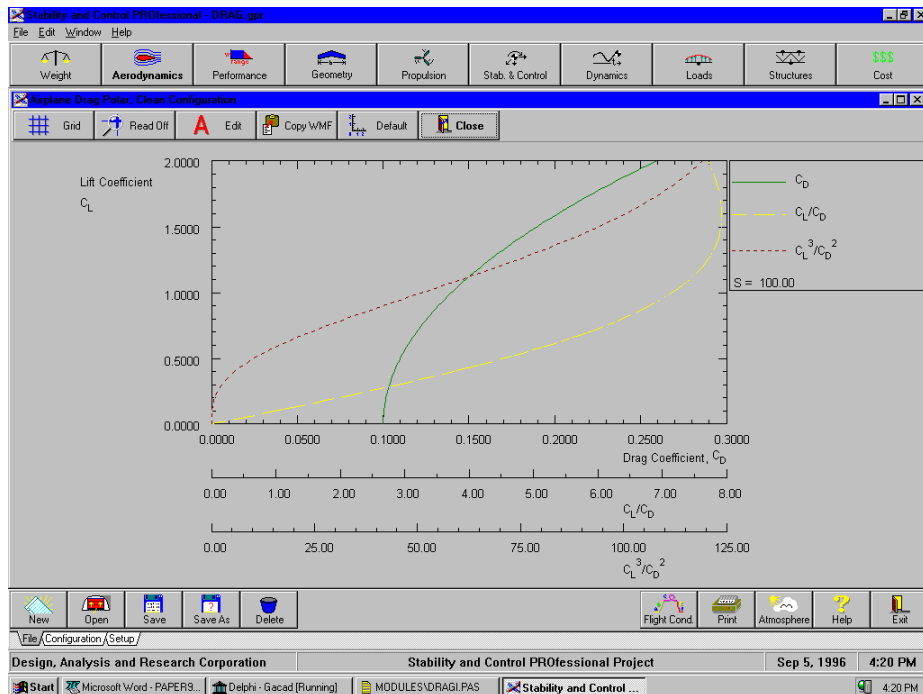


Figure 2.10 Class I Drag Polar Plot

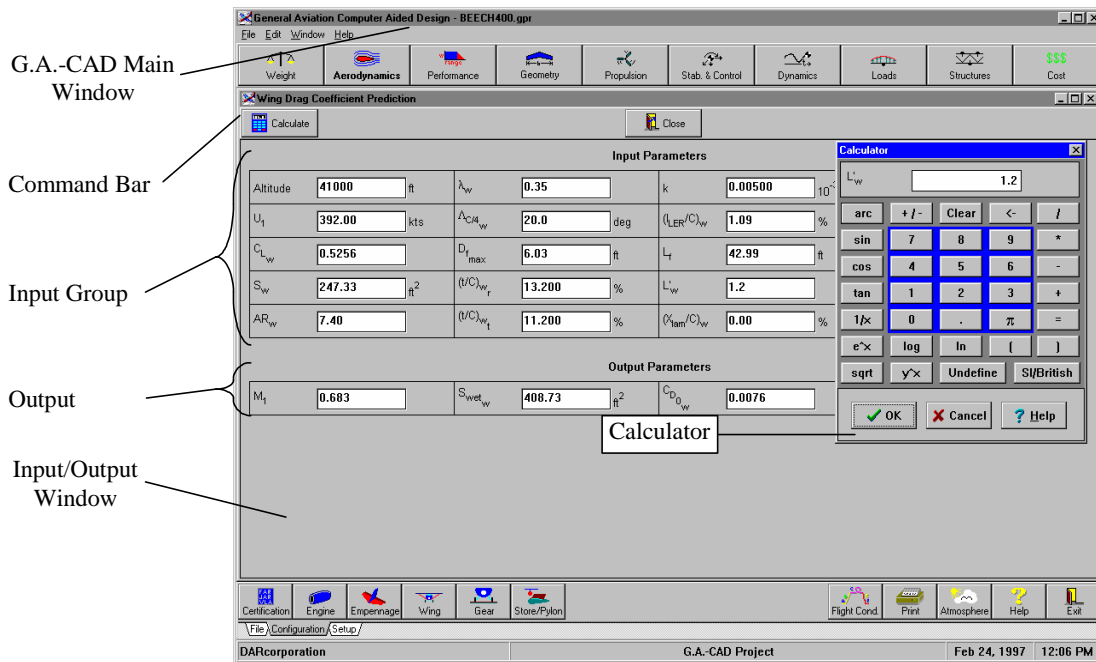


Figure 2.11 Input/Output Window for Class II Wing Drag

This user interface is still in use today in AAA 3.1 (Third Generation) with minor additions. As part of the user-interface development, a new feature was added to AAA, called the flight condition dialog. From version 2.0 on (there were no versions 1.8, 1.9), AAA subdivides all data in flight condition dependent and flight condition independent data. Figure 2.12 shows the first flight condition dialog window as used in G.A.-CAD and AAA 2.0.

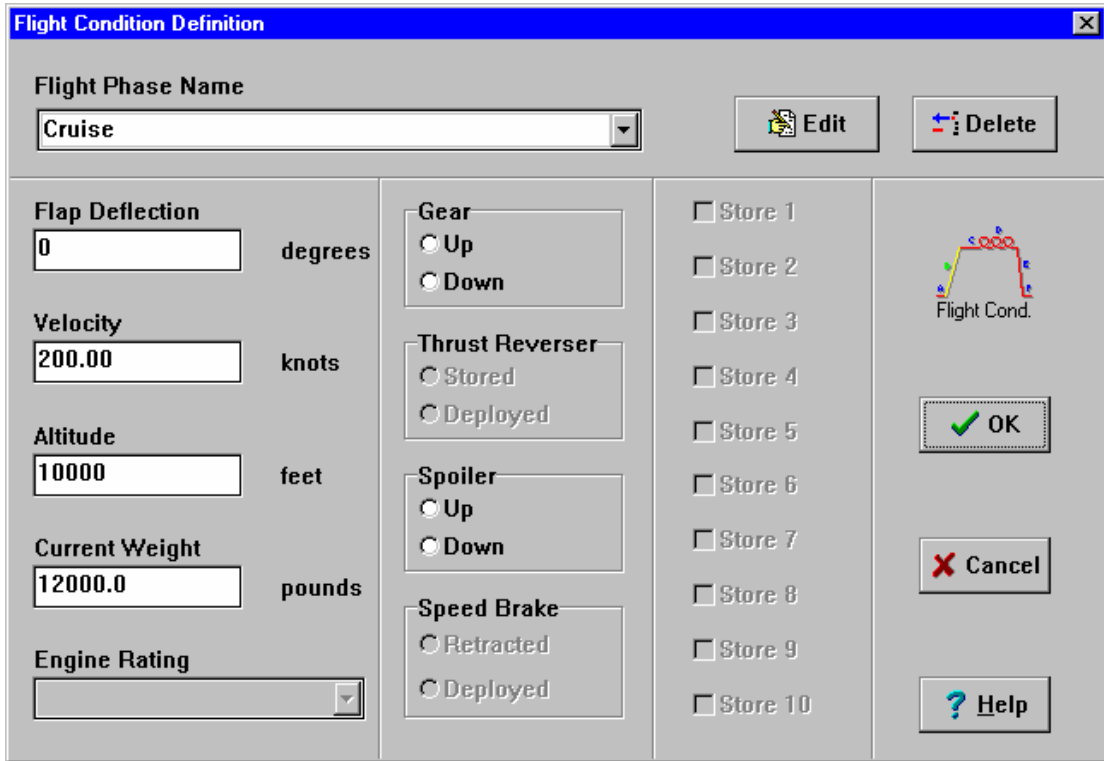


Figure 2.12 Flight Condition Dialog

The UNIX version of AAA was discontinued with the release of G.A.-CAD 1.0 which was later released as two separate programs: AAA and Aero-CADD. The current version of AAA (3.1) contains many of the features developed for G.A.-CAD. Most programming, functionality and architecture for subsequent versions of AAA (since version 2.0) have been performed and developed by the author.

2.2 Knowledge-based Design Systems

In addition to the work described in this dissertation (see also Ref. 61 and Chapter 3), other knowledge based design systems (based on publications from 2002-2006) are currently being developed and researched at universities and research institutes. These systems are described in the following sections.

2.2.1 The University of Texas

Under guidance of Dr. Bernd Chudoba (Ref. 174) a system is developed consisting of a database system, an information-base system and a method library. The author claims to have a first-of-a-kind aerospace conceptual design knowledge-based system, which is an unsubstantiated claim. No tie-in with design requirements is shown. The system appears to be a collection of methods, still under development. It is not clear what development language is used. No tie-in with geometry is described.

2.2.2 Delft University of Technology

Under guidance of Dr. Michel van Tooren (Refs. 147, 170, 175, 178, 180) the ICAD system is used to fully parametrically describe the airplane geometry. ICAD uses IDL (ICAD Design Language) which is Lisp based. It is an Object-Oriented language and uses a similar object tree as AML. Research is primarily focused on CFD and FEA methods and no detail is given on the conceptual design phase. Although one of the papers has conceptual design in the title, it primarily deals with optimization techniques and does not tie it in with specific sizing techniques.

2.2.3 NASA Langley Research Center

A general description of work performed at NASA (Ref. 143) is given. TechnoSoft also works closely together with NASA Langley on software development using Adaptive Modeling Language, AML. Currently work is focused on Vehicle SketchPad (VSP, Ref. 187) which has similar features as AMRaven regarding geometry representation. No papers on VSP have been written yet. Most of design processes used by NASA Langley are based on ACSYNT (Refs. 73, 77, 87, 91, 92, 96, 107, 111) and Model Center (Ref. 165) and are not specifically designed for knowledge capture.

The Intelligent Synthesis Environment (ISE) as it was initially formulated (Ref. 131), was a \$100 Million per year effort that was to span 20+ years in NASA and it was to develop advanced simulation throughout the life cycle of a mission or program. This program began the formulation phase and some momentum was developed over about a 2 year period and then was abruptly eliminated. It was never funded at the level that was initially planned¹. The major supporter for the activity was administrator Daniel Goldin within NASA and when he left NASA the program died.

There were several efforts that started with that program at NASA Langley that have received quite a bit of attention. ISE is the activity that first used Model Center at

¹ Ronnie E. Gillian, NASA Langley, private communication, March 15, 2007

NASA Langley. ISE enhanced the CAPRI interface for different CAD systems and several other small activities but no real product. The planning phase occurred in 1998-2000 and was eliminated in 2001.

3 Development Approach and Architecture

The development of the knowledge-based design system is a two-tier approach consisting of the development of the third generation of AAA and the AAA-AML system. The third generation AAA is used for capturing the methods (knowledge) and design sequence, which is subsequently implemented into AAA-AML. The third generation of AAA is based on object-oriented (Ref. 112) software methods.

3.1 Object-Oriented Programming

An object in a programming language encapsulates data and data-access functions and inherits data and behavior from objects they are derived from (ancestors). The same principle is used in AAA and AAA-AML. Objects are lifting surfaces, bodies, panels, airfoils, etc. A lifting surface can be a wing, canard, vertical or horizontal tail. Lifting surfaces are built-up from panels and airfoils. Fuselages, tailbooms, nacelles are bodies. Objects such as lifting surface panels have properties (data encapsulation), which need to be defined by the user. A lifting surface consists of multiple panels and inherits all data and behavior from these objects. An airplane can be built-up from the different components or objects. A graphical user-interface gives the user feedback on the design. Wings can be designed by entering data related to the panels. Each panel is an object by itself and consists of root chord, tip chord, span, twist angle, root incidence, dihedral and root and tip airfoil. These parameters are the properties of a panel. Supplying airfoils is simplified by using an

airfoil geometric layout tool in AAA containing numerous existing airfoils and also has the capability to enter new airfoil shapes. AMRaven contains similar tools.

Objects encapsulate methods, for instance methods to calculate weights, aerodynamics etc. In AAA these methods are all programmed in separate function and procedure calls. Appendix E gives a subset of these function and procedure calls.

Using object-oriented methods for presenting airplane configuration data makes the design process more structured. Objects created by either AAA or AAA-AML are the same, independent of the program used to create them. Any program that can write or read the object and its properties in a common format can share its data. It is no longer necessary to specify a specific wing, fuselage, etc., but use objects presenting these components instead and giving them a name such as wing and fuselage. Whether a lifting surface is the main wing or a vertical tail does not matter when using object-oriented representation. One of the main advantages of object-oriented programming is re-usability. Here for the first time objects and methods are re-used across two totally different programming languages. Normally re-usability is performed within the same development environment.

The third generation of AAA contains ten main application modules:

- Weight
- Aerodynamics
- Performance

- Geometry
- Propulsion
- Stability and Control
- Dynamics
- Loads
- Structures
- Cost

Except for Structures and the Structural Loads part of Loads, most of the modules have been developed by the author of this dissertation. All architecture of the AAA and AAA-AML has been developed by the author.

The main purpose of also developing AAA-AML is to take advantage of the advanced options of the AML language which are not available in the AAA development environment. AML allows for a further structuring into classes (objects) and tie it in with AMRaven methods (see Section 4.2). AMRaven contains physics based methods for weights based on full 3D geometry and aerodynamics (panel methods, CFD). Reusing these methods will save a major development effort as opposed to developing this using methods used for AAA.

After an initial research period into translating AAA methods in AML using classical programming methods and several programs written by the author to translate AAA Delphi/Pascal code into AML, the decision was made to re-use as much as possible of

AAA-methods in its native Delphi/Pascal language. The AAA methods were converted to dynamic link library (dll) procedures and functions which can be called by AML. In AML a class contains a method, which is linked to a function or procedure call from a AAA dll. Appendix F describes the dll's developed for this project. Switching to dll's instead of a straight AAA translation lead to a major time savings in development.

3.2 Knowledge-Based Design

The knowledge-based conceptual design framework integrates the design domain knowledge of AAA with the multi-disciplinary AML (See Chapter 4) tool. This AAA-AML (this will be part of AMRaven described in Section 4.2, but for clarity, it is called AAA-AML) design tool is designed to capture the domain knowledge and rapidly evolve designs suitable for preliminary design work. The goal is to integrate these designs with advanced analyses like computational structural dynamics and computational fluid dynamics. The program is also designed to reduce the preliminary design phase cost and to bring advanced design methods to businesses which normally do not have the computational and/or modern design/analysis capability.

3.2.1 Common Computational Model

The Common Computational Model (CCM) embodies two aspects of the overall modeling system. First, there is the ability to represent a design geometry,

subsystem, or component in more than one way. This allows the model to contain different aspects of that object (e.g. design, analysis, and manufacturing) or different levels of design fidelity (conceptual, preliminary, and final). Second, there is the standardization of interfaces between the different components of the design model, between analyses, and between the vehicle model and analyses. The creation of these standards allows new design components and analyses to be added to the system and be immediately recognized by those already present.

3.2.2 Model Abstraction, Fidelity and Object Aspects

The differing requirements of various engineering processes may dictate different representations of the same part. The part design features could be different from the part manufacturing or analysis features. To capture this, a single part model can include a number of different object hierarchies representing the requirements of the various disciplines. These hierarchies may be cross-referenced when a property within one hierarchy is dependent on a number of properties from other hierarchies.

The vehicle geometry and configuration evolve through the various stages of the design cycle. At each level, requirements are met through the integration of various tools with the CCM. In addition to closing the loop between the various tools, the CCM enables continuous refinements of the model geometry and attributes while maintaining associations among various model representations with different levels of fidelity. As the design evolves, changes to parameters at any level automatically

trigger the framework's dependency tracking capability to allow model updates by feeding information between the various design levels.

To achieve a reduction in engineering analysis time, the CCM enables the representation and capture of engineering steps as the design cycle evolves from the conceptual into the preliminary design stage. The conceptual model includes the minimal set of design parameters required for first level analyses. For example, these analyses may need only descriptive parameters for the part geometry without any surface geometry details (i.e., fuselage length and area instead of a complete description of the surface). Basic analyses are performed to refine the configuration parameters enabling the definition of the vehicle shape to the level of fidelity needed to generate the preliminary surface geometry as well as panel meshes. The CCM will incorporate any parameterizations and feature relations between the models and analysis tools. The system employs a fully interactive graphical user interface supporting the engineering of a wide range of aircraft designs including agricultural, homebuilt, transport, or business jet. These can be designed to meet any of the requirements ranging from FAR 23 to FAR 25 to Military specifications.

4 Adaptive Modeling Language (AML) and AMRaven

The Adaptive Modeling Language, AML (Refs. 60, 61) is an object-oriented programming language developed by TechnoSoft, Inc. AMRaven, Adaptive Modeling Rapid Air Vehicle Engineering Environment, is also developed in AML by TechnoSoft, Inc.

4.1 AML: Adaptive Modeling Language

As an object-oriented language, AML emphasizes decomposing engineering problems into classified objects. It supports the most powerful feature of object-oriented modeling: the ability to construct a class hierarchy in which complex classes inherit properties from simpler classes. This is the same mechanism that powers human understanding: the ability to make abstractions and then build upon them to create more complex concepts. Part (geometry, features, materials, function, etc.) and process (manufacturing, inspection, analysis) designs are concurrently generated from, and stored in, a single model with automated dependency tracking among various abstractions of common features.

Inheritance (as supported by AML) enables the user to combine a number of existing objects to form a new part definition, modify its behavior, and deduce its processes through using inherited knowledge. It is this functionality that will enable more broad engineering dissemination beyond the realm of aerospace engineering, as many abstractions in related engineering disciplines will begin by inheriting from a similar

object within our proposed framework. As an illustrative example in the selected domain of aerospace vehicle design, Figure 4.1 identifies the object-subobject relationships in a representative vehicle class from the high level abstraction of the vehicle, to low level abstractions of the wing geometry and structural members. Each vehicle component (fuselage, landing gear, etc) is similarly decomposed to lower levels of abstraction. Double headed arrows indicate mutual dependencies between subobjects. At any level of abstraction, varied users may wish to perform functional trade studies and performance calculations. Results of these studies must be available to all users, and the implications of local variations to individual objects must be readily communicated throughout dependent objects. Knowledge-based development environments, such as AML, allow one to capture the object-subobject relationship of Figure 4.1, and re-use it at various levels of abstraction for further trade studies. For example, a Formula 1 race car airfoil may clearly inherit from a wing class, but many assembled beam objects may be able to as well.

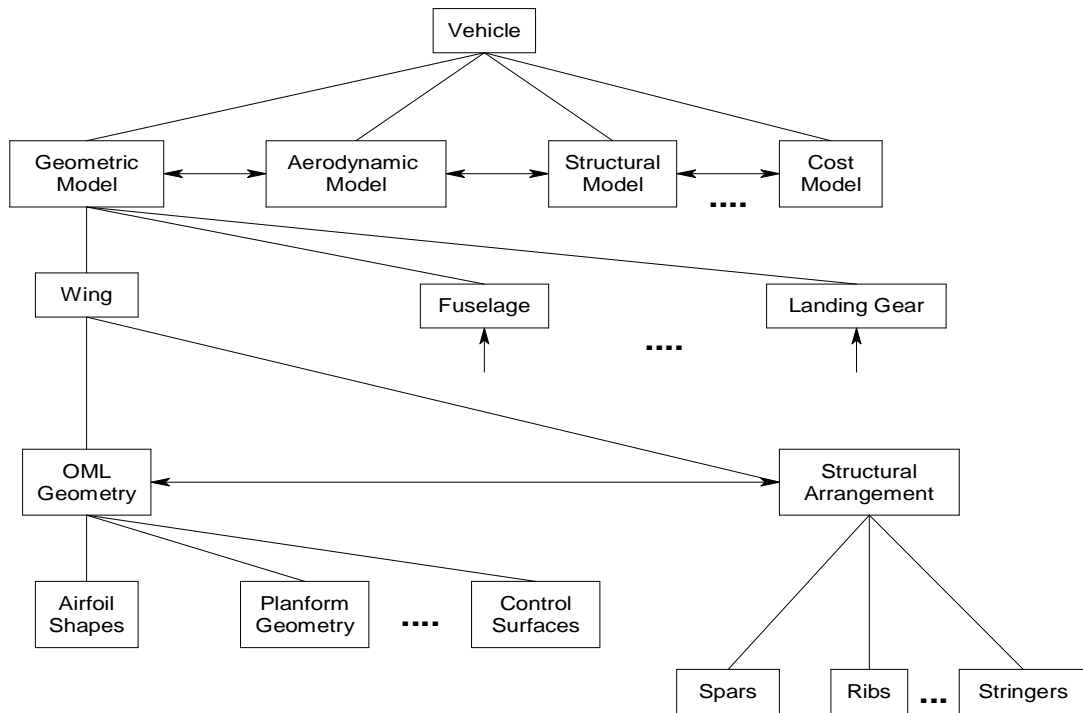


Figure 4.1 Products Decomposed into Decreasing Abstractions while Enforcing Dependencies (Ref. 61)

The AML framework implements a geometry-centric Common Computational Model (CCM) which provides various levels of modeling fidelity and captures the conceptual, preliminary, and detailed design processes. The framework automates and manages dependencies, data transfer, and interactions among users, designs, analyses, and computational tools. The CCM provides a common virtual interface for all related analyses and tools enabling seamless interfacing and exchange of data between the geometric modelers, grid generators, and analyses needed in the synthesis process.

AML is a mature, commercially available architecture that already contains many objects necessary for developing integrated design, analysis and manufacturing tools (e.g. geometric solid modeling, mesh generation, machining analysis, manufacturing process planning, etc.). AML class libraries also support communication over a network, thus inherently supporting collaborative design by distributed design teams. AML and similar languages have illustrated significant success in proprietary industrial research activities. Knowledge-based software systems (Refs. 62-65) have been shown to:

- Reduce time to market by automating repetitive design and engineering tasks
- Facilitate concurrent engineering
- Improve product quality by applying consistent standards and best practices
- Enable continuous improvement by formally capturing existing knowledge, allowing re-use of good practices, and providing a framework for identifying and correcting poor practices.

Previous work using AML by Dr. Richard D. Hale, on an integrated design, analysis and manufacturing system for composite materials and structures was used on the Boeing Joint Strike Fighter Technology Demonstrator program. Use of the tool resulted in documented cost savings of 60% over conventional methods, and first-time quality of all manufactured components (Refs. 62-64).

In other industry sponsored research, Jaguar Cars, a division of Ford Motor Co., has claimed a 94% time savings on its XK8 body panel project, and has reduced cycle time for headlight design from four weeks to one day (Ref. 64). AFRL success stories for aerospace and automotive applications are described in Refs. 64 and 65.

4.2 AMRaven

As indicated before, the AAA-AML will be part of the AMRaven environment. A detailed description of the AMRaven (Adaptive Modeling Rapid Air Vehicle Engineering) environment is given in Refs. 66-67. AMRaven is developed by TechnoSoft Inc. in collaboration with AFRL, NASA and major aerospace companies. AMRaven is an environment enabling integrated design and analysis of air vehicles and is built on the AML object-oriented framework (See Section 4.1). It has a fully automated modeling environment to couple aerodynamic and structural analysis. It contains a feature-based design environment incorporating custom airplane components such as pods, wings, control surfaces, spars, ribs and bulkheads.

AMRaven contains a full 3D modeling environment with a graphical user interface as shown in Figure 4.2. Primitives, surfaces, solids and Boolean operators are supported. Fuselage and wing outer mold lines (OML) (See Figure 4.3) can be created in this environment, as well as internal structure (See Figure 4.4). Note: Figure 4.4 does not show a finalized substructure, but is shown for illustration of the AMRaven capabilities.

AMRaven contains a modular architecture (geometry, structural analysis, meshing module, aerodynamics module) and is object-oriented. All models are composed of a hierarchy of objects representing various aspects of the design.

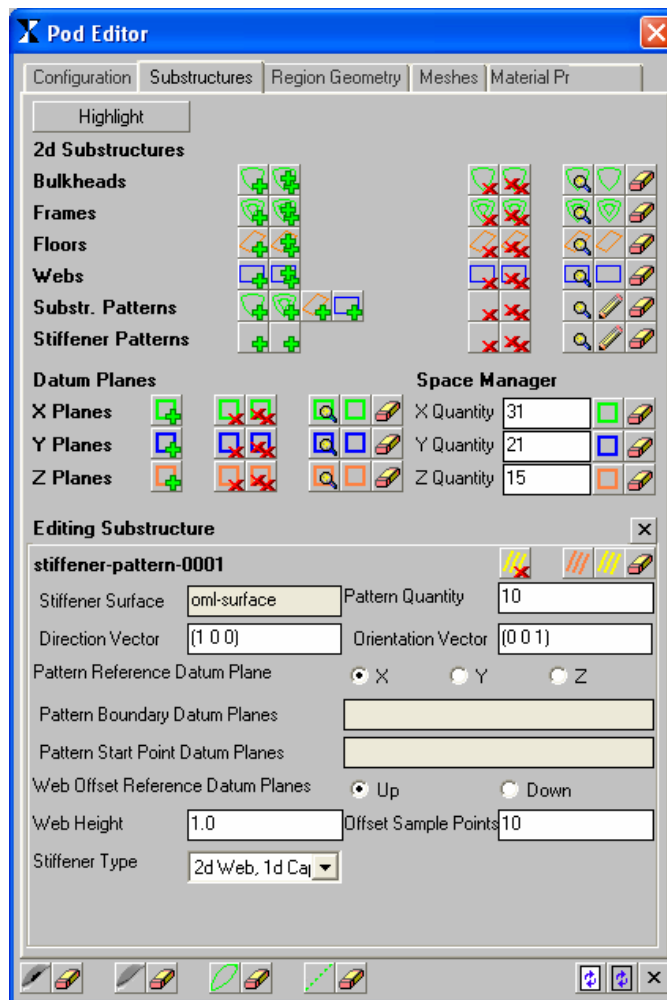


Figure 4.2 AMRaven Pod Editor User Interface (Ref. 67, Courtesy TechnoSoft)

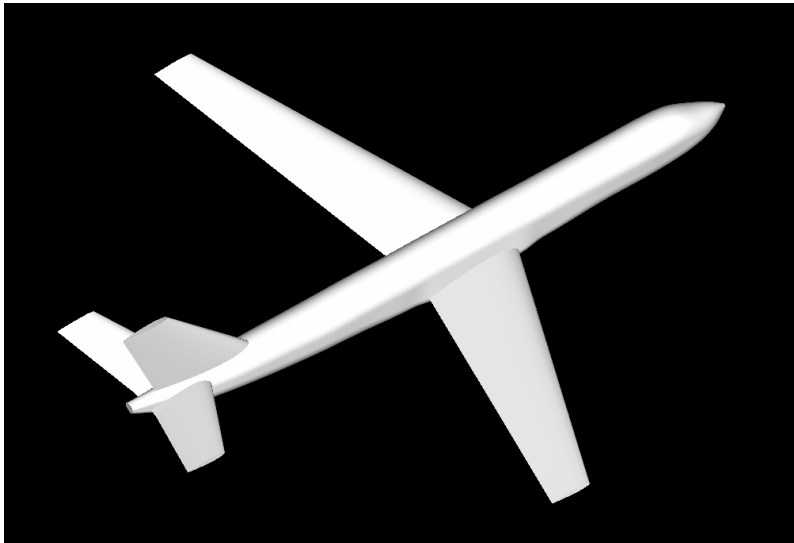


Figure 4.3 AMRaven Airliner Geometry (Ref. 67, Courtesy TechnoSoft)

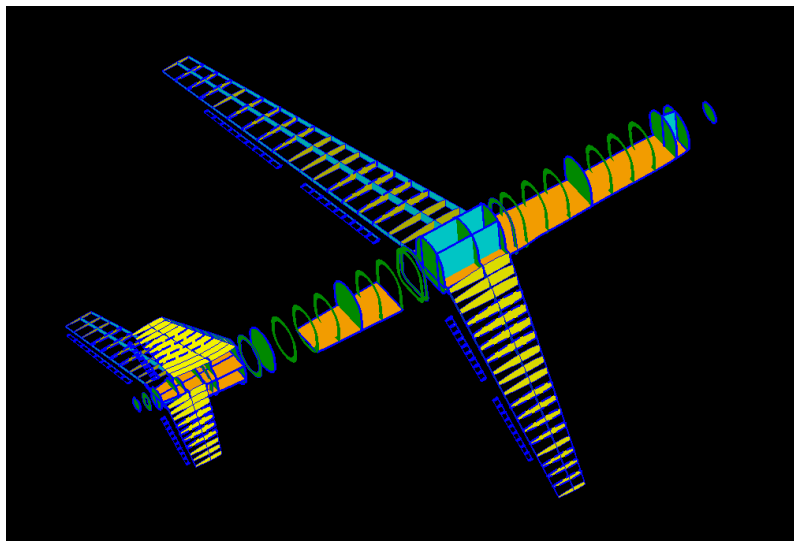


Figure 4.4 AMRaven Airliner Substructure (Ref. 67, Courtesy TechnoSoft)

A major limitation of AMRaven is that the initial configuration must be known and is not coupled to a mission-based design. AAA-AML corrects this shortcoming.

5 Airplane Design Process in AAA and AAA-AML

The preliminary design process consists of a number of interdependent design steps. These steps begin with constraints and requirements in the form of a mission specification, and end with a preliminary design that meets all the specifications of the mission requirement. Figure 5.1 shows these design steps and their relation to each other.

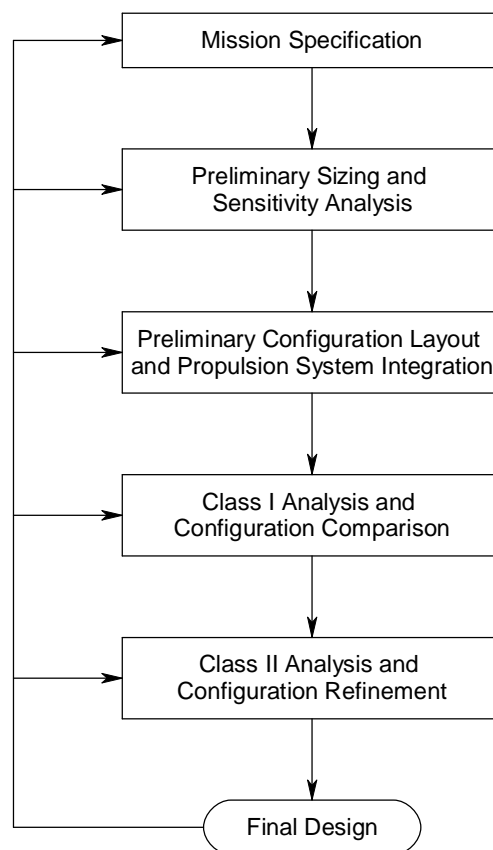


Figure 5.1 Preliminary Design Process

Class I and Class II design and analysis methods consist of several steps. An example of Class I and Class II design steps is presented in Figure 5.2.

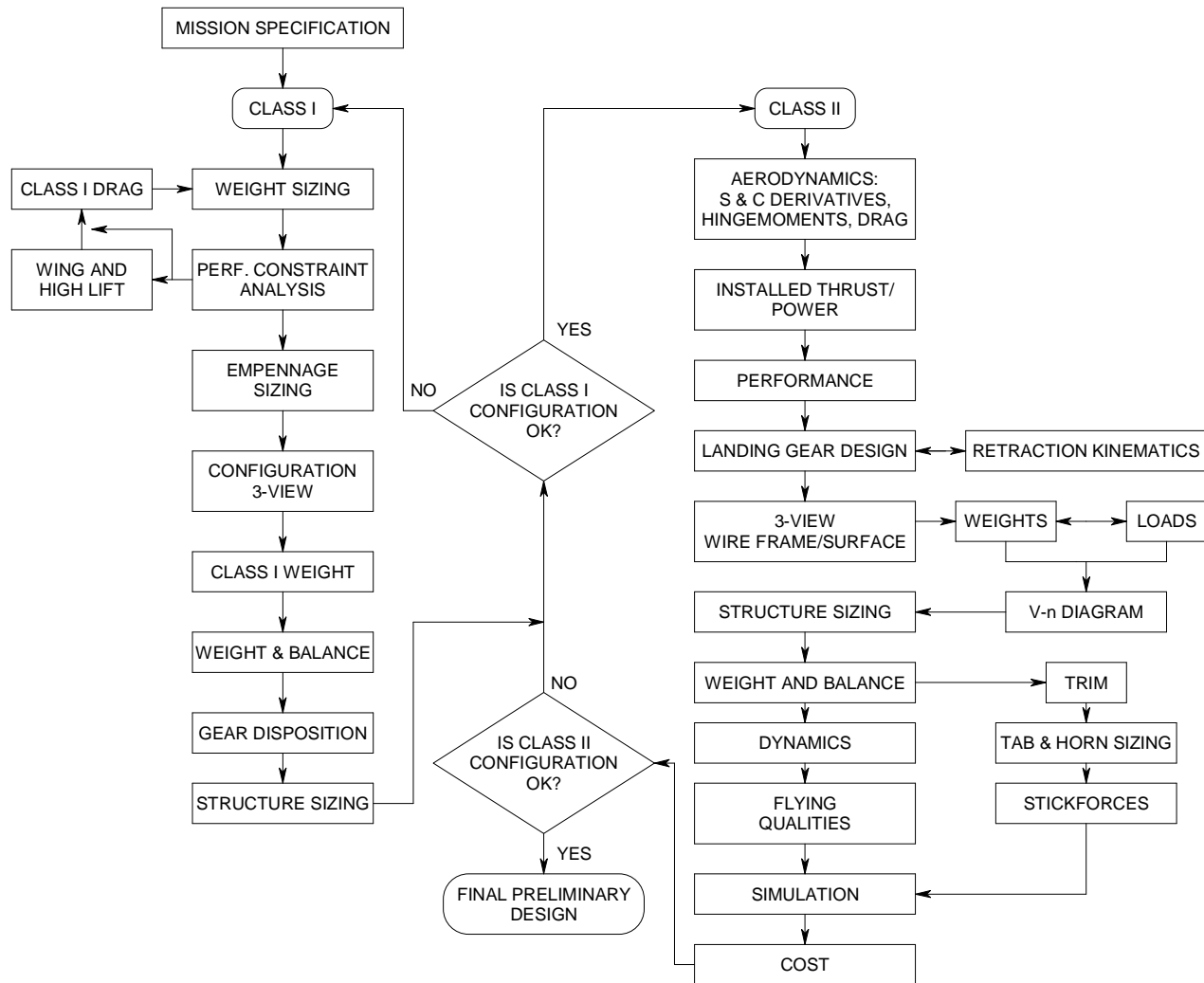


Figure 5.2 Preliminary Design Process Detailed Steps

5.1 Preliminary Design Steps

A preliminary airplane design follows the design steps forward from one step to the next. If a design is found to be unacceptable at any point in the process, it can return to any previous step (iteration). The software can also be used to analyze existing airplanes. In this case, it is possible to enter the design process at any point to perform analysis calculations.

The following subsections describe the preliminary design process steps as presented in Figure 5.1 and Figure 5.2. The methods are based on References 1-11.

These steps are:

- Mission specification
- Preliminary sizing and sensitivity analysis
- Preliminary configuration layout and propulsion system integration
- Class I analysis, configuration design and configuration comparison
- Class II analysis and configuration refinement

5.1.1 Mission Specification

The mission specification usually includes the following parameters:

- payload and type of payload
- range and/or loiter requirements
- cruise speed and altitude
- field length for take-off and for landing
- fuel reserves
- climb requirements
- maneuvering requirements
- certification base (FAR, JAR, VLA, LSA, MIL or AS specs)

Depending on the customer, further performance requirements may be specified.

Preliminary design always starts with a mission specification. Appendix A shows several mission specifications of multiple types of airplanes.

5.1.2 Preliminary Sizing and Sensitivity Studies

At this stage, the following parameters are determined:

- gross take-off weight, W_{TO}
- empty weight, W_E
- mission fuel weight, W_F
- maximum required take-off thrust, T_{TO} , or take-off power, P_{TO}

- wing area, S , wing aspect ratio, A , wing taper ratio and sweep angle
- maximum required clean lift coefficient, $C_{L_{\max}}$
- maximum required take-off lift coefficient, $C_{L_{\max TO}}$
- maximum required landing lift coefficient, $C_{L_{\max L}}$
- airfoil type and thickness
- flap type and flap size

Sensitivity studies can also be performed at this step in the design process. These studies determine how maximum take-off weight varies with several performance and/or weight parameters. The actual detailed methods implemented are described in Chapter 6. Figure 5.3 shows the Class I sizing process implemented in AAA-AML. Currently decisions are still made by the user. So if requirements are not met, the user is still required to change input parameters manually.

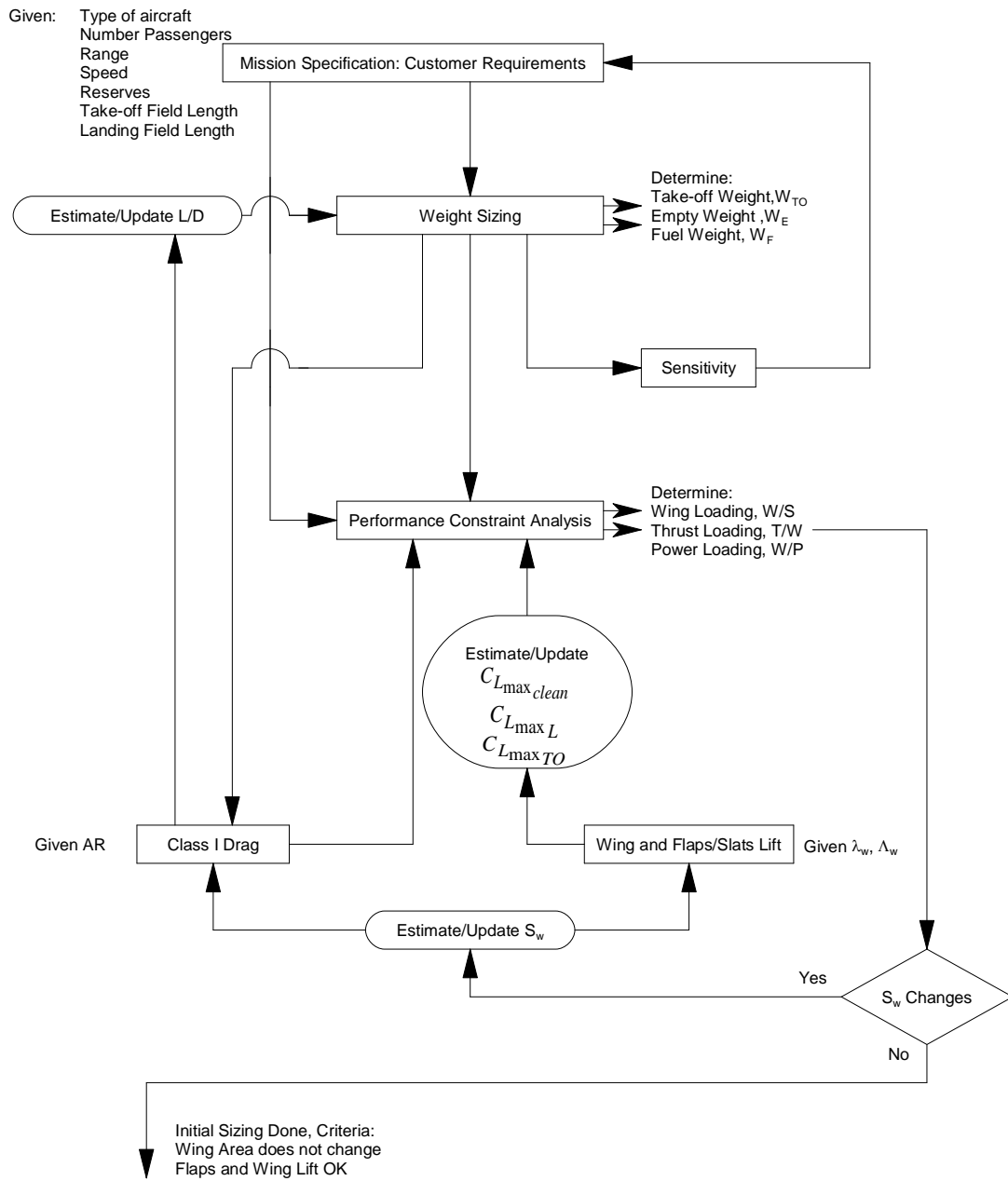


Figure 5.3 Class I Sizing Flow Chart

5.1.3 Preliminary Configuration Layout and Propulsion System Integration

Airplanes with similar mission specifications are studied with a resulting choice of the basic airplane configuration(s) to be studied further. At this point, overall configuration (i.e. conventional, canard, three surface, flying wing, etc.) is chosen along with the propulsion system type (jet, piston engine, etc.), placement and number of engines.

5.1.4 Class I Analysis, Configuration Design and Configuration Comparison

Class I methods (See Ref. 1) require a relatively small amount of engineering person-hours to comprehend and to use. These methods have limited accuracy, but can quickly eliminate bad configuration ideas or arrangements. Using these methods, it is possible for the designer to compare a number of preliminary design ideas and determine which are worthy of more detailed design studies.

Figure 5.4 shows the process flow used in sizing for stability using volume coefficients and the class I weight and balance. At this point more detail on geometry is required, such as taper ratios, sweep angles and aspect ratios.

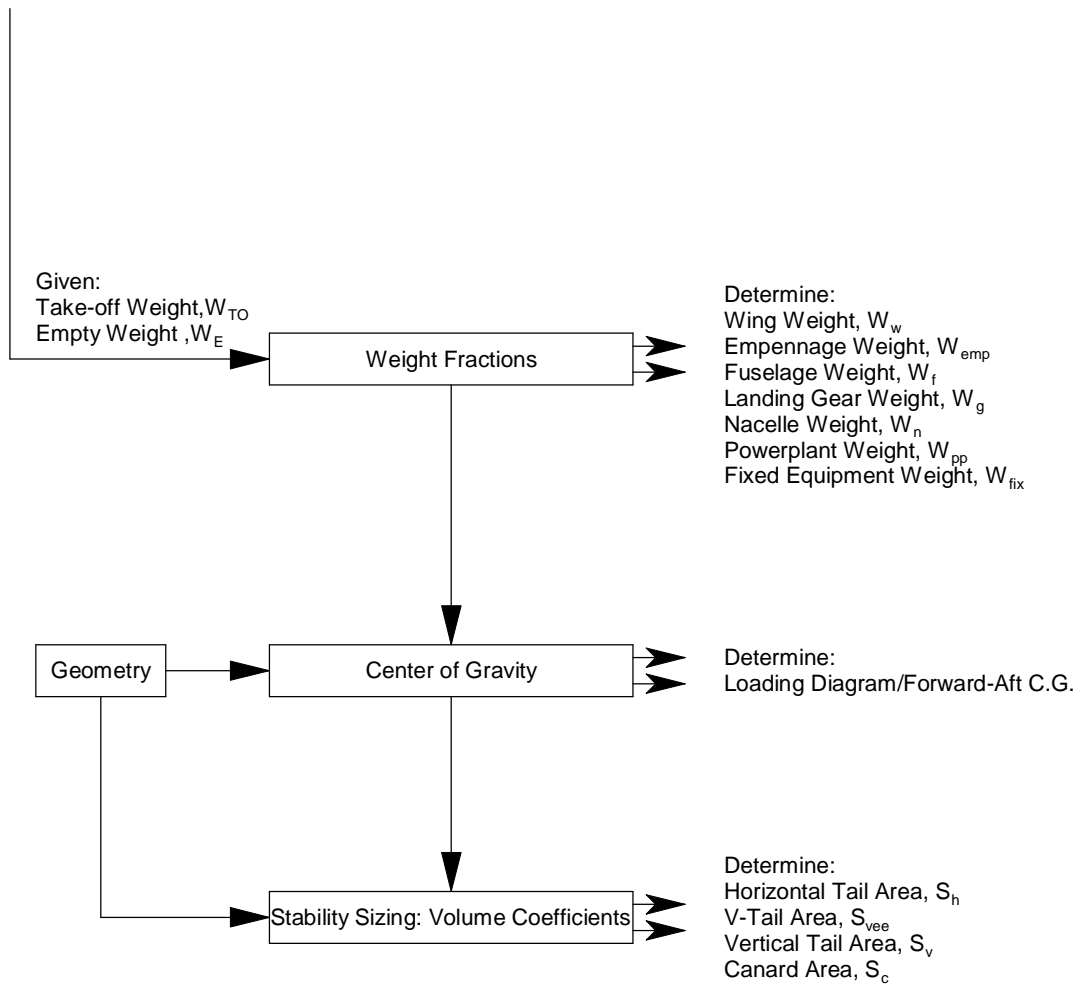


Figure 5.4 Class I Weights and Stability Sizing Flow Chart

5.1.5 Class II Analysis and Configuration Refinement

Class II methods require significantly more engineering person-hours than Class I methods. However, analysis accuracy is significantly improved using Class II methods. These methods are used in that stage of the preliminary design where only

a limited number of design concepts are evaluated. Class II design analysis methods are used in conjunction with more refined design/analysis steps taken in preliminary airplane design.

5.2 Class I and Class II Design and Analysis Methods

The design steps that are part of Class I and Class II design and analysis are highly interdependent and follow a unique path for every airplane design. The design process modeling concentrates on gathering the analysis methods necessary to perform the different design steps.

Most of the design steps in Figure 5.2 are implemented in the Advanced Aircraft Analysis software (See Appendix B for a detailed description of the current version).

A subset of these design methods are implemented in AAA-AML.

The current implementation contains:

1. Mission Profile
2. Weight Sizing including Regression Coefficients
3. Performance Sizing
4. Maximum Lift
5. Flap Lift
6. Class I Drag

7. Lift Distribution
8. Geometry
9. Class I Weights (Weight Fractions)
10. Weight and Balance
11. Class I Moments of Inertia
12. Volume Methods
13. Class II Weights (excluding weight iteration)
14. Class II Drag

The details of the methods implemented including references are described in Chapter 6.

6 Theoretical Background of Implemented Methods

This chapter describes all the mathematical details of the methods implemented in AAA-AML. All methods listed are programmed in AAA 3.1. Several of them are extracted into dynamic link libraries (dll) to be used with AMRaven. A full description of the dll's is listed in Appendix E.

6.1 Class I Sizing Methods

6.1.1 Weight Sizing

The purpose of the Weight Sizing module is to estimate the following weights and/or sensitivity coefficients:

- Take-off weight, W_{TO}
- Empty weight, W_E
- Mission fuel weight, W_F
- Sensitivity of take-off weight to aerodynamic, propulsion and mission parameters

These parameters are estimated on the basis of the following inputs:

- A mission specification
- Statistical relation between empty weight and take-off weight of existing airplanes.

AAA-AML contains four of the AAA Weight Sizing submodules:

1. Mission Profile or Primary Mission in AML: allows the user to calculate the overall mission fuel fraction by entering the flight segments from the start to the end of the mission.
2. Take-off Weight: calculates mission fuel weight, take-off weight and empty weight. A plot showing the iteration process is provided.
3. Regression Coefficients: the user can enter statistical data by providing empty weights and take-off weights in a table and calculate the regression coefficients A and B. A logarithmic plot of the entered data is also provided.
4. Sensitivity Analysis: After entering the Mission Profile and calculating the Take-off Weight, sensitivities of take-off weight for changes in aerodynamic, propulsion and mission parameters can be calculated.

6.1.1.1 Mission Profile

This option allows for the setup of the flight mission profile. In AML a menu is shown consisting of three command buttons:

- Add Segment This command is used to enter a new segment of the mission specification. A selection can be constructed from the twelve mission segments:
 - Warm-up
 - Taxi
 - Take-off

- Climb
- Cruise
- Turn
- Loiter
- Payload Expended
- Refueling
- Descent
- Land/Taxi
- Stall (specifically added to AML)

The newly specified flight segment is added at the end of the previously defined segments. For some flight segments, a calculation can be performed to obtain the fuel-fraction. For other segments, the input will be the fuel-fraction.

- Delete Segment

A segment can be deleted from the flight profile. The user selects a segment that is to be deleted. All data related to this segment will be erased. If the user wishes to exit without deleting a segment, any menu can be selected to exit this command.

- Insert Segment

A flight segment can be inserted between two previously entered segments. When the Insert Segment command is selected, a menu with twelve flight segments as described

in New Segment will appear. Upon selection of a new segment to be inserted, the user must select the position of the new segment within the mission profile. The new segment will be inserted before the segment selected as the new position. Inserting at the end of the table is possible by selecting New Segment instead of Insert Segment.

Input data in a particular flight segment can be changed by selecting the flight segment from the previously created table.

6.1.1.2 Take-off Weight

The airplane take-off weight is calculated from the mission segment fuel fractions and regression coefficients using the methods of Ref. 1. The regression coefficients A and B can either be entered in the input section or calculated in the regression coefficients module. After entering all input data, the empty weight, take-off weight, mission fuel weight, used fuel weight, mission fuel fraction, fuel burned in each flight segment and the fuel available and airplane weight at the beginning of each flight segment will be calculated and displayed.

A linear relationship between the logarithm of the airplane empty weight and the logarithm of the airplane take-off weight is derived for airplanes of same type. The line that represents the relationship is called the Regression line. The take-off weight

regression coefficients, A and B, for different types of airplane are listed in the info of the variables in AAA. Users can also calculate these coefficients in the Regression Coefficients module.

The regression line is as follows:

$$\log_{10} W_E = \frac{\log_{10} W_{TO} - A}{B} \quad (6-1)$$

The take-off Weight, W_{TO} , can be expressed as follows:

$$W_{TO} = W_E + W_{PL} + W_{crew} + W_{PL_{exp}} + W_F - W_{F_{refuel}} + W_{tfo} \quad (6-2)$$

The payload weight excludes expended payload such as bombs and ammunition. Payload dropped during the mission must be specified in the mission profile. Payload, which is not dropped, must be included in payload and crew weights. Refueled fuel weight during the mission must also be specified in the mission profile.

The other parameters are as follows:

$$W_F = (1 + M_{F_{res}}) W_{F_{used}} \quad (6-3)$$

$$W_{F_{used}} = (1 - M_{ff}) W_{TO} \quad (6-4)$$

$$W_{tfo} = M_{tfo} W_{TO} \quad (6-5)$$

Combining equations (6-2), (6-3), (6-4) and (6-5) gives:

$$W_E = \left[1 - (1 - M_{ff})(1 + M_{Fres}) - M_{tfo} \right] W_{TO} - \left(W_{PL} + W_{crew} + W_{PLexp} - W_{Frefuel} \right) \quad (6-6)$$

The above equation can also be written as follows:

$$W_E = CW_{TO} - D \quad (6-7)$$

where:

$$C = 1 - (1 + M_{Fres})(1 - M_{ff}) - M_{tfo} \quad (6-8)$$

$$D = W_{crew} + W_{PL} + W_{PLexp} - W_{Frefuel} \quad (6-9)$$

The calculation leads to one of the following cases:

1. No solutions for take-off weight
2. One solution for take-off weight
3. Two solutions for take-off weight

A plot function is available to show the iteration process used to arrive at these solutions. For case 1, the input data must be changed to obtain a solution. For case 2, no modifications are necessary. If case 3 occurs, the lowest number is automatically chosen.

An iteration method is used to estimate the airplane take-off weight from equations (6-1) and (6-7). The iteration starts with a guessed value of take-off weight (defined by the user).

The mission fuel fraction is estimated from:

$$M_{ff} = \prod_{i=1}^n M_{ffi} + \frac{1}{W_{TO}} \left\{ \sum_{i=1}^{n-1} \left[W_{PLexp_i} \left(1 - \prod_{j=i+1}^n M_{ffj} \right) \right] \right\} - \frac{1}{W_{TO}} \left\{ \sum_{i=1}^{n-1} \left[W_{Frefuel_i} \left(1 - \prod_{j=i+1}^n M_{ffj} \right) \right] \right\} \quad (6-10)$$

or

$$M_{ff} = M_{ffuncor} + \frac{W_{Fcorr}}{W_{TO}} \quad (6-11)$$

The fuel fraction at i^{th} segment is defined as follows:

$$M_{ffi} = \frac{W_i - \Delta W_{Fused_i}}{W_i} \quad (6-12)$$

See Section 6.1.1.3 for the fuel fraction of different flight phases.

The total expended payload weight is calculated from:

$$W_{PLexp} = \sum_{i=1}^n W_{PLexp_i} \quad (6-13)$$

The total refueled fuel weight is given by:

$$W_{F_{refuel}} = \sum_{i=1}^n W_{F_{refuel}_i} \quad (6-14)$$

The airplane empty weights calculated from equations (6-1) and (6-7) are compared. If the two successive calculated empty weights are within 0.05 lbs, the iteration stops. This number is hardwired in the code. The earlier versions of AAA (before version 1.7) contained this number as a user-input, but was later removed to increase ease of use. If the condition is not satisfied, the program will adjust the guessed take-off weight and repeat the calculation until the condition is satisfied.

Once the take-off weight is determined, the weight of the fuel used in the mission is estimated from equation (6-4). The total fuel weight is given by equation (6-3).

The fuel weight at the beginning of each segment is computed from:

$$W_{F_{begin}_i} = W_{F_{begin}_{i-1}} - \Delta W_{F_{used}_i} + W_{F_{refuel}_{i-1}} \quad (6-15)$$

The maximum fuel weight in the fuel tank at any point of the mission is the maximum value of the fuel calculated from equation (6-13):

$$W_{F_{max}} = \max(W_{F_{begin}_i}) \quad (6-16)$$

The airplane weight at the beginning of each segment is computed from:

$$W_{begin_i} = W_{begin_{i-1}} - \Delta W_{Fused_i} + W_{Frefuel_{i-1}} - W_{PLexp_{i-1}} \quad (6-17)$$

The weight iteration method is programmed in WeightSizing.dll (See Appendix E).

6.1.1.3 Mission Profile Fuel Fraction

The fuel fractions for the warm-up, taxi, take-off, descent, and land/taxi segments can be assumed based on typical values for a category of airplanes.

It has been assumed that no fuel is consumed during any of the payload expenditure segments or the refueling segments. Therefore, the fuel fraction for a payload expenditure segment or a refueling segment will be 1.0.

For the Climb, Cruise, Loiter and Turn the fuel fraction can be calculated based on the Breguet range equation.

6.1.1.3.1 Climb Fuel Fraction

For the climb the endurance is calculated from:

$$E = \frac{h}{\text{Climb Rate}} \quad (6-18)$$

For a propeller aircraft the climb fuel fraction is:

$$M_{ff} = e^{\left(\frac{1.151 E_{cl} c_{p_{cl}} V_{cl}}{(375)(60) \eta_{p_{cl}} \left(\frac{L}{D} \right)_{cl}} \right)} \quad (6-19)$$

For a jet aircraft the climb fuel fraction is:

$$M_{ff} = e^{\left(\frac{E_{cl} c_{j_{cl}}}{60 \left(\frac{L}{D} \right)_{cl}} \right)} \quad (6-20)$$

6.1.1.3.2 Cruise Fuel Fraction

For a propeller aircraft the cruise fuel fraction is:

$$M_{ff} = e^{\left(\frac{1.151 R_{cr} c_{p_{cr}}}{375 \eta_{p_{cr}} \left(\frac{L}{D} \right)_{cr}} \right)} \quad (6-21)$$

For a jet aircraft the cruise fuel fraction is:

$$M_{ff} = e^{\left(\frac{R_{cr} c_{j_{cr}}}{V_{cr} \left(\frac{L}{D} \right)_{cr}} \right)} \quad (6-22)$$

6.1.1.3.3 Loiter Fuel Fraction

For a propeller aircraft the loiter fuel fraction is:

$$M_{ff} = e^{\left(\frac{E_{ltr} c_{p_{ltr}} 1.151V_{ltr}}{(375)(60)\eta_{p_{ltr}} \left(\frac{L}{D}\right)_{ltr}} \right)} \quad (6-23)$$

For a jet aircraft the loiter fuel fraction is:

$$M_{ff} = e^{\left(\frac{E_{ltr} c_{j_{ltr}}}{(60)\left(\frac{L}{D}\right)_{ltr}} \right)} \quad (6-24)$$

6.1.1.3.4 Turn Fuel Fraction

For a propeller aircraft the turn fuel fraction is:

$$M_{ff} = e^{\left(\frac{E_{turn} c_{p_{turn}} 1.151V_{turn}}{375 \eta_{p_{turn}} \left(\frac{L}{D}\right)_{turn}} \right)} \quad (6-25)$$

For a jet aircraft the turn fuel fraction is:

$$M_{ff} = e^{\left(\frac{E_{turn} c_{j_{turn}}}{\left(\frac{L}{D}\right)_{turn}} \right)} \quad (6-26)$$

The endurance in the turn is obtained from:

$$E_{turn} = \frac{2\pi(NumberOfTurns)}{3600\left(\frac{\pi}{180}\right)TurnRate} \quad (6-27)$$

where:

$$TurnRate = \frac{180}{\pi} \left(\frac{g}{1.689V_{turn}} \right) \sqrt{(NumberOfTurns^2 - 1)} \quad (6-28)$$

6.1.1.4 Regression Coefficients

This option allows the user to generate a table of empty weights and take-off weights to calculate the regression coefficients, A and B. An empty table will appear with one column each for the airplane name, take-off weight and empty weight. When all input data are entered, this will calculate the intercept A and slope B for a logarithmic relation between take-off and empty weight using a least squares method. AAA uses the methods of Appendix F to calculate the regression coefficients.

6.1.1.5 Sensitivity

This option allows the user to calculate the sensitivity of take-off weight to aerodynamic, propulsion and mission parameters. Once all data from the mission profile and the take-off weight calculation are available, take-off weight sensitivities with respect to payload weight and empty weight can be calculated. The results are shown in a table, which will appear with the flight segments and the corresponding weight sensitivities.

The sensitivity of take-off weight to payload weight, or airplane growth factor due to payload, is determined from:

$$\frac{\partial W_{TO}}{\partial W_{PL}} = \frac{\partial W_{TO}}{\partial W_{crew}} = \frac{-BW_{TO}}{CW_{TO}(1-B) - D + B(1 + M_{F_{res}})\Delta W_F} \quad (6-29)$$

With C defined in equation (6-8) and D in equation (6-9). The fuel weight correction for the expended payload and/or refueled fuel weight is given by:

$$\Delta W_F = \sum_{i=1}^n \left\{ \left(W_{PL_{exp_i}} - W_{F_{refuel_i}} \right) \left(1 - \prod_{j=i+1}^n M_{ff_j} \right) \right\} \quad (6-30)$$

The sensitivity of take-off weight to empty weight, or airplane growth factor due to empty weight is solved from:

$$\frac{\partial W_{TO}}{\partial W_E} = \frac{W_{TO}B}{W_E} \quad (6-31)$$

The sensitivity of take-off weight to expended payload weight at the kth mission profile segment, also known as the airplane growth factor due to expended payload weight, is calculated from:

$$\frac{\partial W_{TO}}{\partial W_{PL_{exp_k}}} = \frac{BW_{TO} \left\{ \left(1 + M_{F_{res}} \right) \left(1 - \prod_{j=k+1}^n M_{ff_j} \right) - 1 \right\}}{CW_{TO}(1-B) - D + B(1 + M_{F_{res}})\Delta W_F} \quad (6-32)$$

The sensitivity of take-off weight to refueled fuel weight at the k^{th} mission profile segment is calculated from:

$$\frac{\partial W_{TO}}{\partial W_{F_{refuel}_k}} = \frac{BW_{TO} \left\{ (1 + M_{F_{res}}) \left(1 - \prod_{j=k+1}^n M_{ff_j} \right) + 1 \right\}}{CW_{TO}(1-B) - D + B(1 + M_{F_{res}}) \Delta W_F} \quad (6-33)$$

The sensitivity of take-off weight to other factors at the k^{th} mission profile segment, such as range, endurance, specific fuel consumption, propeller efficiency, and lift-to-drag ratio, are derived from the following two equation for a particular mission segment depending on whether the segment fuel fraction depends on range (as in cruise) or endurance (climb, loiter and turn):

Range:

$$\frac{\partial W_{TO}}{\partial y_k} = \frac{BW_{TO}^2 (1 + M_{F_{res}}) \left[\prod_{i=1}^n M_{ff_i} - \frac{\sum_{i=1}^{k-1} \left\{ (W_{PL_{exp_i}} - W_{F_{refuel_i}}) \prod_{j=i+1}^n M_{ff_j} \right\}}{W_{TO}} \right] \frac{\partial \bar{R}}{\partial y_k}}{- \left[CW_{TO}(1-B) - D + B(1 + M_{F_{res}}) \Delta W_F \right]} \quad (6-34)$$

Endurance:

$$\frac{\partial W_{TO}}{\partial y_k} = \frac{BW_{TO}^2 (1 + M_{Fres}) \left[\prod_{i=1}^n M_{ff_i} - \frac{\sum_{i=1}^{k-1} \left\{ (W_{PL_{exp_i}} - W_{F_{refuel_i}}) \prod_{j=i+1}^n M_{ff_j} \right\}}{W_{TO}} \right] \frac{\partial \bar{E}}{\partial y_k}}{-[CW_{TO}(1-B) - D + B(1 + M_{Fres})\Delta W_F]} \quad (6-35)$$

The Breguet partial derivative $\frac{\partial \bar{R}}{\partial y_k}$ and $\frac{\partial \bar{E}}{\partial y_k}$ can be determined for the following factors for the kth mission segment:

Range for a propeller driven airplane for a given segment:

$$\frac{\partial \bar{R}}{\partial y} = \frac{c_p}{375\eta_p} \frac{L}{D} \quad (6-36)$$

Range for a jet airplane for a given segment:

$$\frac{\partial \bar{R}}{\partial y} = \frac{c_j}{V} \frac{L}{D} \quad (6-37)$$

Endurance for a propeller driven airplane for a given segment:

$$\frac{\partial \bar{E}}{\partial y} = \frac{V c_p}{375\eta_p} \frac{L}{D} \quad (6-38)$$

Endurance for a jet airplane for a given segment:

$$\frac{\partial \bar{E}}{\partial y} = \frac{c_j}{\left(\frac{L}{D}\right)} \quad (6-39)$$

Specific Fuel Consumption for a propeller driven airplane for a cruise segment:

$$\frac{\partial \bar{R}}{\partial y} = \frac{R}{375 \eta_p \frac{L}{D}} \quad (6-40)$$

Specific Fuel Consumption for a jet airplane for a cruise segment:

$$\frac{\partial \bar{R}}{\partial y} = \frac{R}{V \frac{L}{D}} \quad (6-41)$$

Specific Fuel Consumption for a propeller driven airplane for a climb, loiter or turn segment:

$$\frac{\partial \bar{E}}{\partial y} = \frac{E V}{375 (60) \eta_p \left(\frac{L}{D}\right)} \quad (6-42)$$

Specific Fuel Consumption for a jet airplane for a climb, loiter or turn segment:

$$\frac{\partial \bar{E}}{\partial y} = \frac{E}{60 \left(\frac{L}{D}\right)} \quad (6-43)$$

Propeller Efficiency for a cruise segment:

$$\frac{\partial \bar{R}}{\partial y} = -\frac{R c_p}{375 \eta_p^2 \frac{L}{D}} \quad (6-44)$$

Propeller Efficiency for a climb, loiter or turn segment:

$$\frac{\partial \bar{E}}{\partial y} = -\frac{E V c_p}{375 (60) \eta_p^2 \left(\frac{L}{D}\right)} \quad (6-45)$$

Lift to Drag Ratio for a propeller driven airplane for a cruise segment:

$$\frac{\partial \bar{R}}{\partial y} = -\frac{R c_p}{375 \eta_p \left(\frac{L}{D}\right)^2} \quad (6-46)$$

Lift to Drag Ratio for a jet airplane for a cruise segment:

$$\frac{\partial \bar{R}}{\partial y} = -\frac{R c_j}{V \left(\frac{L}{D}\right)^2} \quad (6-47)$$

Lift to Drag Ratio for a propeller driven airplane for a climb, loiter or turn segment:

$$\frac{\partial \bar{E}}{\partial y} = -\frac{E V c_p}{375 (60) \eta_p \left(\frac{L}{D}\right)^2} \quad (6-48)$$

Lift to Drag Ratio for a jet airplane for a climb, loiter or turn segment:

$$\frac{\partial \bar{E}}{\partial y} = -\frac{E c_j}{60 \left(\frac{L}{D} \right)^2} \quad (6-49)$$

6.1.2 Estimation of Class I Drag Polars

The Class I Drag can be calculated for the following configurations:

- Flaps in take-off configuration with gear down.
- Flaps in take-off configuration with gear up.
- Configuration with no flap deflection and gear up.
- Flaps in landing configuration with gear up.
- Flaps in landing configuration with gear down.
- One engine inoperative configuration.

The methodology used to calculate the drag polar can be found in Chapter 3 of Reference 1. To calculate the drag polar, the user first selects the switch corresponding to the configuration of interest. The other five flight condition options will have similar input and output parameters.

The Class I Drag module relates the total airplane lift coefficient to the total airplane drag coefficient through the drag polar equation:

$$C_D = C_{D_{o_{clean}}} + \Delta C_{D_o} + \frac{1}{\pi AR_w e} C_L^2 \quad (6-50)$$

Where the coefficients are calculated by the program using the methods in Section 3.4.1 of Reference 1.

$$C_{D_{o_{clean}}} = \frac{f}{S_w} \quad (6-51)$$

Where the equivalent parasite area, f , is a function of the regression coefficients, a and b , (Reference 1, Section 3.4.1), and are user-defined.

$$\log_{10} f = a + b \log_{10} S_{wet} \quad (6-52)$$

The wetted area is a function of the regression coefficients, c and d (Reference 1, Section 3.4.1), and are user-defined.

$$\log_{10} S_{wet} = c + d \log_{10} W_{TO} \quad (6-53)$$

6.1.3 Performance Sizing

The purpose of the Performance Sizing submodule is to allow for a rapid estimation of those airplane design parameters having a major impact on airplane performance. Airplanes are usually required to meet performance objectives in different categories depending on the mission profile. Meeting these performance objectives normally results in the determination of a range of values for:

- Wing loading, W/S
- Thrust loading, T/W for a jet or power loading W/P , for a propeller airplane
- Airplane maximum lift coefficients $C_{L_{\max}}$, $C_{L_{\max TO}}$ and $C_{L_{\max L}}$.

The variables listed above are plotted in the form of a performance-matching plot. These plots depend on the type of airplane, the applicable specification and the applicable regulation(s). With the help of such a plot, the combination of the highest possible wing loading and the smallest possible thrust (or highest power) loading, which meets all performance requirements, can be determined. The methodology used for performance sizing can be found in Reference 1.

The sizing options are:

1. Sizing to stall speed requirements.
2. Sizing to take-off distance requirements.
3. Sizing to climb requirements.
4. Sizing to maximum cruise speed requirements.
5. Sizing to maneuvering requirements.
6. Sizing to landing distance requirements.

The user may choose to size an airplane by using any combination (or all) of the above sizing options. Several performance sizing options require input only from the user, while others also provide the user with output. Once all of the inputs for the desired options have been entered, the user may create a matching plot to plot the performance sizing equations. The methods used for use each performance sizing option are presented in the following sections.

6.1.3.1 Sizing to Stall Speed Requirements

To size the aircraft to meet stall speed requirements, the user selects the Stall Speed option. The methodology used in sizing to stall speed requirements is based on Reference 1, Section 3.1. The input and output data for this submodule are for all airplane types and specifications.

Stall speed is defined as the minimum steady flight speed at which the airplane remains controllable. A low stall speed is always preferred for the take-off, landing, approach and climb performance of the airplane. For some airplanes the mission task demands a stall speed not higher than a certain value. In such case, the mission specifications will include a requirement for a maximum stall speed.

FAR 23 certified single engine airplanes may not have a stall speed greater than 61 knots at the airplane take-off weight. In addition, FAR 23 certified multi-engine airplanes with a take-off weight less than 6000 lbs must also have a stall speed of no

more than 61 knots, unless they meet certain climb gradient criteria (FAR 23.49). These stall speed requirements can be met flaps-up or flaps-down at the option of the designer.

There are no requirements for maximum stall speed in the case of FAR 25 certified airplanes.

Given the maximum allowable stall speed for the flight condition at which the stall is to be evaluated, the maximum allowable wing loading at that certain flight condition can be computed from:

$$\left(\frac{W}{S}\right)_S = C_{L_{\max S}} \frac{1}{2} \rho V_S^2 \quad (6-54)$$

The corresponding maximum allowable wing loading at take-off to meet the stall speed requirement can then be calculated from:

$$\left(\frac{W}{S}\right)_{TO} = \frac{W_{TO}}{W_S} \left(\frac{W}{S}\right)_S \quad (6-55)$$

The maximum take-off wing loading to meet stall speed requirement is always a vertical line on the matching plot. To meet the stall speed requirement, the take-off wing loading must be less than the value represented by the stall line.

6.1.3.2 Sizing to Take-off Distance Requirements

This module is used to size the aircraft to take-off distance requirements. The methodology used in sizing to take-off distance requirements can be found in Reference 1, Section 3.2.

The take-off distance of an airplane is determined by the following factors:

1. Take-off weight.
2. Take-off speed (also called lift-off speed).
3. Thrust-to-weight ratio at take-off (or weight-to-power ratio and the corresponding propeller characteristics).
4. Aerodynamic drag coefficient and ground friction coefficient.
5. Pilot technique.

Take-off requirements are normally given in terms of take-off field length requirements. These requirements differ widely and depend on the type of airplane under consideration.

For civil airplanes, the requirements of FAR 23 and FAR 25 must be adhered to. In the case of homebuilt airplanes it is not necessary to design to the FAR's. In that case, the individual designer may set his own take-off requirements.

For military airplanes the requirements are usually set forth in the so-called Request-for-Proposal or RFP. All take-off calculations for military airplanes must be done with the definitions outlined in Military Specification, MIL-C-005011B (USAF).

Depending on the type of mission, the take-off requirements are frequently spelled out in terms of minimum ground run requirements in combination with some minimum climb capability. For Navy airplanes with carrier capability, the limitations of the catapult system on the carrier must be taken into account.

Figure 6.1 shows the take-off distance parameters.

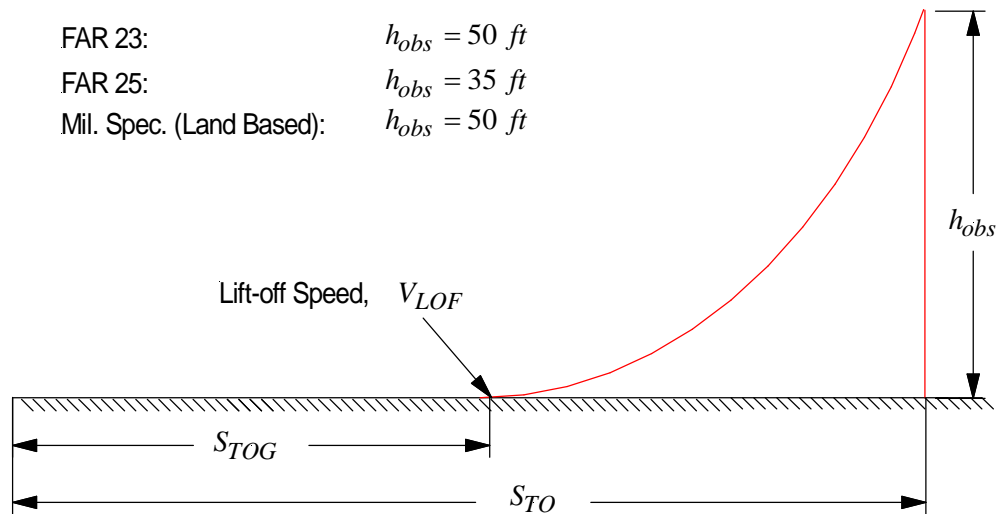


Figure 6.1 Take-off Distance Definition

6.1.3.2.1 Sizing to FAR 23, JAR 23 and VLA Take-off Distance Requirements

For jet driven airplanes, the thrust to weight ratio to meet take-off distance requirements is plotted using the following relationship:

$$\left(\frac{T}{W}\right)_{TO} = \frac{\left(\frac{W}{S}\right)_{TO}}{0.0296 S_{TO} \sigma C_{L_{\max TO}} F_{TO}} \quad (6-56)$$

For propeller powered airplanes, the weight to power ratio to meet take-off distance requirements is plotted using the following relationship:

$$\left(\frac{W}{P}\right)_{TO} = \frac{TOP_{23} \sigma C_{L_{\max TO}} F_{TO}}{\left(\frac{W}{S}\right)_{TO}} \quad (6-57)$$

The FAR 23 take-off parameter is given by:

$$TOP_{23} = -273.0 + \sqrt{7.45 \times 10^3 + 67.11 S_{TOFL}} \quad (6-58)$$

The take-off field length is determined from:

$$\text{If } S_{TO} > 1.66 S_{TOG} \text{ then } S_{TOFL} = 1.66 S_{TOG} \quad (6-59)$$

$$\text{If } S_{TO} < 1.66 S_{TOG} \text{ then } S_{TOFL} = S_{TO} \quad (6-60)$$

$$\text{If } S_{TOG} \text{ is undefined then } S_{TOFL} = S_{TO} \quad (6-61)$$

$$\text{If } S_{TO} \text{ is undefined then } S_{TOFL} = 1.66 S_{TOG} \quad (6-62)$$

Note: Equations used in this topic assume the British unit of the parameter used in the program. For the SI unit system, appropriate conversions must be made.

6.1.3.2.2 Sizing to FAR 25 Take-off Distance Requirements

For jet driven airplanes, the thrust to weight ratio to meet take-off distance requirements is plotted using the following relationship:

$$\left(\frac{T}{W}\right)_{TO} = \frac{\left(\frac{W}{S}\right)_{TO}}{0.0267S_{TO}\sigma C_{L_{maxTO}} F_{TO}} \quad (6-63)$$

For propeller powered airplanes, the weight to power ratio to meet take-off distance requirements is plotted using the following relationship:

$$\left(\frac{W}{P}\right)_{TO} = \frac{0.0773S_{TO}\sigma C_{L_{maxTO}} F_{TO}}{\left(\frac{W}{S}\right)_{TO}} \quad (6-64)$$

Note: Equations used in this topic assume the British unit of the parameter used in the program. For the SI unit system, appropriate conversions must be made.

6.1.3.2.3 Sizing to Military Take-off Distance Requirements

6.1.3.2.3.1 Land Based Airplanes

For jet driven airplanes, the thrust to weight ratio to meet take-off distance requirements is plotted using the following relationship:

$$\left(\frac{T}{W}\right)_{TO} = \frac{\rho@h_{TO,ISA} S_{TOG} \left(0.72C_{D_{o_{TO_down}}} + C_{L_{max_{TO}}} \mu_G\right) + 0.0447 \left(\frac{W}{S}\right)_{TO}}{F_{TO} \rho@h_{TO,ISA} C_{L_{max_{TO}}} S_{TOG} 0.75 \left(\frac{5+BPR}{4+BPR}\right)} \quad (6-65)$$

For propeller powered airplanes, the weight to power ratio to meet take-off distance requirements is plotted using the following relationship:

$$\left(\frac{W}{P}\right)_{TO} = \frac{C_{L_{max_{TO}}} \rho@h_{TO,ISA} S_{TOG} l_p \left(\frac{\sigma}{P_{TO}/ND_p^2}\right)^{1/3} F_{TO}}{\sigma S_{TOG} \left(0.72C_{D_{o_{TO_down}}} + C_{L_{max_{TO}}} \mu_G\right) + 0.0376 \left(\frac{W}{S}\right)_{TO}} \quad (6-66)$$

where:

$$l_p = 4.60 \text{ for fixed pitch propellers;}$$

$$l_p = 5.75 \text{ for variable pitch propellers.}$$

The propeller disk loading is calculated from:

$$P_{TO}/ND_p^2 = \frac{\pi}{4} P_{blade} N_{blades} \quad (6-67)$$

Note: Equations used in the equations above assume the British unit of the parameter used in the program. For the SI unit system, appropriate conversions must be made.

6.1.3.2.3.2 Carrier Based Airplanes

For carrier based airplanes, the limitations of the catapult system need to be taken into account. These limitations are usually stated in terms of relationships between take-off weight and launch speed at the end of the catapult.

At the end of the catapult stroke, the following relationship must be satisfied:

$$\left(\frac{W}{S}\right)_{TO} = \frac{C_{L_{maxTO}}}{1.21} 0.5\rho_{@h_{TO},ISA} (V_{wod} + V_{cat})^2 \quad (6-68)$$

6.1.3.2.4 Climb Sizing

This module is used to size the aircraft to meet climb requirements. Note that the input elements, which pertain to the specification to be satisfied, contain default values. These values can still be modified by the user as needed. The drag polar parameters can be estimated in the Class I Drag submodule. The methodology used in sizing to climb requirements is based on Section 3.4 of Reference 1.

All airplanes must meet certain climb rate or climb gradient requirements. To size an airplane for climb requirements, it is necessary to have an estimate for the airplane drag polar.

For civil airplanes, the climb requirements of either FAR 23 or FAR 25 must be met. For military airplanes either the requirements of the military specifications,

MIL-C-005011B (USAF), or whatever climb requirements are specified in the RFP, must be met.

FAR 23.45, FAR 23.65, and FAR 23.77 requirements must be met for airplane climb sizing in the FAR 23, JAR 23, and VLA categories.

6.1.3.2.4.1 Sizing to FAR 23, JAR 23, and VLA Climb requirements

6.1.3.2.4.1.1 FAR 23.65(a) Rate of Climb (RC)

For jet driven airplanes, the thrust to weight ratio to meet FAR 23.65.a Rate of Climb (RC) requirements is plotted using the following relationship:

$$\left(\frac{T}{W}\right)_{TO} = \frac{1}{F_{MaxCont}} \left[\frac{\left(\frac{RC_{23.65}}{60}\right) \left(\frac{0.5\rho@SL,ISA}{\sqrt{\left(\frac{W}{S}\right)_{TO} \left(\frac{C_{D_oTO_up}}{B_{DP_{TO_up}}}\right)}}\right)^{1/2}}{\sqrt{\left(\frac{W}{S}\right)_{TO} \left(\frac{C_{D_oTO_up}}{B_{DP_{TO_up}}}\right)}} + 2 \left(C_{D_oTO_up} B_{DP_{TO_up}}\right)^{1/2} \right] \quad (6-69)$$

For propeller powered airplanes, the weight to power ratio to meet FAR 23.65.a Rate of Climb (RC) requirements is plotted using the following relationship:

$$\left(\frac{W}{P}\right)_{TO} = F_{MaxCont} \frac{19\eta_p \left(\frac{27}{256 C_{D_o TO_up} B_{DP TO_up}^3} \right)^{1/4}}{\sqrt{\left(\frac{W}{S}\right)_{TO} + \frac{19RC_{23.65}}{33,000} \left(\frac{27}{256 C_{D_o TO_up} B_{DP TO_up}^3} \right)^{1/4}}} \quad (6-70)$$

The parameter B of the airplane drag polar is calculated from:

$$B_{DP TO_up} = \frac{1}{\pi AR_w e_{TO}} \quad (6-71)$$

Note: Equations used in this topic assume the British unit of the parameter used in the program. For the SI unit system, appropriate conversions must be made.

6.1.3.2.4.1.2 FAR 23.65(a) Climb Gradient (CGR)

For jet driven airplanes, the thrust to weight ratio to meet FAR 23.65.a Climb Gradient (CGR) requirements is plotted using the following relationship:

$$\left(\frac{T}{W}\right)_{TO} = \frac{CGR_{23.65} + (L/D)^{-1}}{F_{MaxCont}} \quad (6-72)$$

The lift to drag ratio at take-off with gear retracted is calculated from:

$$L/D = \frac{0.5}{\sqrt{C_{D_o TO_up} B_{DP TO_up}}} \quad (6-73)$$

The parameter B of the airplane drag polar is calculated from:

$$B_{DP_{TO_up}} = \frac{1}{\pi A R_w e_{TO}} \quad (6-74)$$

For propeller powered airplanes, the weight to power ratio to meet FAR 23.65.a Climb Gradient (CGR) requirements is plotted using the following relationship:

$$\left(\frac{W}{P}\right)_{TO} = \frac{18.97 F_{MaxCont} \eta_p \sqrt{\left(C_{L_{maxTO}} - \Delta C_{L_{Cl-Max}}\right)}}{\sqrt{\left(\frac{W}{S}\right)_{TO} \left[CGR_{23.65} + \frac{C_{D_{oTO_up}} + B_{DP_{TO_up}} \left(C_{L_{maxTO}} - \Delta C_{L_{Cl-Max}}\right)^2}{C_{L_{maxTO}} - \Delta C_{L_{Cl-Max}}} \right]}} \quad (6-75)$$

The parameter B of the airplane drag polar is calculated from:

$$B_{DP_{TO_up}} = \frac{1}{\pi A R_w e_{TO}} \quad (6-76)$$

Note: Equations used in this topic assume the British unit of the parameter used in the program. For the SI unit system, appropriate conversions must be made.

6.1.3.2.4.1.3 FAR 23.67(c)(2)(i) Rate of Climb (RC) One Engine Inoperative

For jet driven airplanes, thrust to weight ratio to meet FAR 23.67(c)(2)(i) Rate of Climb (RC) requirements is plotted using the following relationship:

$$\left(\frac{T}{W}\right)_{TO} = \frac{2N_{eng} \left[\frac{\frac{RC}{V_S^2} \left(\frac{W}{S}\right)_{TO}^{1/2} \left(\frac{C_{D_o OEI}}{B_{DP OEI}}\right)^{1/4}}{(1.689)^2 60 C_{L_{max clean}} (2\rho_{@ 5000, ISA})^{1/2} + \left(C_{D_o OEI} B_{DP OEI}\right)^{1/2}} \right]}{F_{5000} (N_{eng} - 1)} \quad (6-77)$$

For propeller powered airplanes, the weight to power ratio to meet FAR 23.67(c)(2)(i)

Rate of Climb (RC) requirements is plotted using the following relationship:

$$\left(\frac{W}{P}\right)_{TO} = \frac{(27)^{1/4} 18.97 \eta_p F_{5000} \left(\frac{N_{eng} - 1}{N_{eng}}\right) \sqrt{\sigma_{@ 5000, ISA}}}{\left[256 C_{D_o OEI} B_{DP OEI}^3 \left(\frac{W}{S}\right)_{TO}^2 \right]^{1/4} + \frac{2(27)^{1/4} (18.97) \sqrt{\sigma_{@ 5000, ISA}} \frac{RC}{V_S^2} \left(\frac{W}{S}\right)_{TO}}{(1.689)^2 33000 \rho_{@ 5000, ISA} C_{L_{max clean}}} \quad (6-78)$$

The parameter B of the airplane drag polar at One Engine Inoperative Condition is calculated from:

$$B_{DP OEI} = \frac{1}{\pi A R_w e_{OEI}} \quad (6-79)$$

Note: Equations used in this topic assume the British unit of the parameter used in the program. For the SI unit system, appropriate conversions must be made.

6.1.3.2.4.1.4 FAR 23.67(c)(2)(i) Climb Gradient (CGR) One Engine Inoperative

For jet driven airplanes, the thrust to weight ratio to meet FAR 23.67(c)(2)(i) Climb Gradient (CGR) requirements is plotted using the following relationship:

$$\left(\frac{T}{W}\right)_{TO} = \frac{\left(CGR_{23.65} + \left(\frac{L}{D}\right)^{-1}\right)N_{eng}}{F_{5000}(N_{eng} - 1)} \quad (6-80)$$

The lift to drag ratio with one engine inoperative is determined from:

$$\frac{L}{D} = \frac{0.5}{\sqrt{C_{D_{oOEI}} B_{DP_{OEI}}}} \quad (6-81)$$

The parameter B of the airplane drag polar is calculated from:

$$B_{DP_{OEI}} = \frac{1}{\pi AR_w e_{OEI}} \quad (6-82)$$

For propeller powered airplanes, the weight to power ratio to meet 23.67(c)(2)(i) Climb Gradient (CGR) requirements is plotted using the following relationship:

$$\left(\frac{W}{P}\right)_{TO} = \frac{F_{5000} 18.97 \eta_p \sqrt{\sigma_{@5000,ISA}} C_{L_{max_{clean}}} \left(\frac{N_{eng} - 1}{N_{eng}}\right)}{\sqrt{\left(\frac{W}{S}\right)_{TO} \left[CGR_{23.67} + \frac{\left(C_{D_{oOEI}} + B_{DP_{OEI}} \left(C_{L_{max_{clean}}}\right)^2\right)}{C_{L_{max_{clean}}}\right]}} \quad (6-83)$$

The parameter B of the airplane drag polar is calculated from:

$$B_{DP_{OEI}} = \frac{1}{\pi AR_w e_{OEI}} \quad (6-84)$$

Note: Equations used in this topic assume the British unit of the parameter used in the program. For the SI unit system, appropriate conversions must be made.

6.1.3.2.4.1.5 FAR 23.67(c)(2)(ii) Rate of Climb (RC) One Engine Inoperative

For jet driven airplanes, the thrust to weight ratio to meet FAR 23.67(c)(2)(ii) Rate of Climb (RC) requirements is plotted using the following relationship:

$$\left(\frac{T}{W}\right)_{TO} = \frac{2N_{eng} \left[\frac{\frac{RC}{V_S^2} \left(\frac{W}{S}\right)_{TO}^{1/2} \left(\frac{C_{D_o_{OEI}}}{B_{DP_{OEI}}}\right)^{1/4}}{(1.689)^2 60 C_{L_{max_{clean}}} (2\rho@5000,ISA)^{1/2}} + \left(C_{D_o_{OEI}} B_{DP_{OEI}}\right)^{1/2} \right]}{F_{5000} (N_{eng} - 1)} \quad (6-85)$$

For propeller powered airplanes, the weight to power ratio to meet FAR 23.67(c)(2)(ii) Rate of Climb (RC) requirements is plotted using the following relationship:

$$\left(\frac{W}{P}\right)_{TO} = \frac{(27)^{1/4} 18.97 \eta_p F_{5000} \left(\frac{N_{eng} - 1}{N_{eng}}\right) \sqrt{\sigma_{@ 5000, ISA}}}{\left[256 C_{D_o OEI} B_{DP OEI}^3 \left(\frac{W}{S}\right)_{TO}^2 \right]^{1/4} + \frac{2(27)^{1/4} (18.97) \sqrt{\sigma_{@ 5000, ISA}} \frac{RC}{V_S^2} \left(\frac{W}{S}\right)_{TO}}{(1.689)^2 33000 \rho_{@ 5000, ISA} C_{L_{max clean}}}} \quad (6-86)$$

The parameter B of the airplane drag polar is calculated from:

$$B_{DP OEI} = \frac{1}{\pi A R_w e_{OEI}} \quad (6-87)$$

Note: Equations used in this topic assume the British unit of the parameter used in the program. For the SI unit system, appropriate conversions must be made.

6.1.3.2.4.1.6 FAR 23.67(c)(2)(ii) Climb Gradient (CGR) One Engine Inoperative

For jet driven airplanes, the thrust to weight ratio to meet FAR 23.67(c)(2)(ii) Climb Gradient (CGR) requirements is plotted using the following relationship:

$$\left(\frac{T}{W}\right)_{TO} = \frac{\left(CGR_{23.67 OSA} + \left(\frac{L}{D}\right)^{-1}\right) N_{eng}}{(N_{eng} - 1) F_{OSA5000}} \quad (6-88)$$

The lift to drag ratio with one engine inoperative is calculated from:

$$L/D = \frac{0.5}{\sqrt{C_{D_{oOEI}} B_{DP_{OEI}}}} \quad (6-89)$$

The 'B' of the airplane drag polar with one engine inoperative is calculated from:

$$B_{DP_{OEI}} = \frac{1}{\pi AR_w e_{OEI}} \quad (6-90)$$

For propeller powered airplanes, the weight to power ratio to meet 23.67(c)(2)(ii) Climb Gradient (CGR) requirements is plotted using the following relationship:

$$\left(\frac{W}{P}\right)_{TO} = \frac{F_{OSA5000} \left(18.97 \eta_p \sqrt{\sigma_{@5000,+40^\circ F}} C_{L_{max_{clean}}}\right) \left(\frac{N_{eng} - 1}{N_{eng}}\right)}{\left[CGR_{23.67_{OSA}} + \frac{\left(C_{D_{oOEI}} + B_{DP_{OEI}} \left(C_{L_{max_{clean}}}\right)^2\right)}{C_{L_{max_{clean}}}} \right] \sqrt{\left(\frac{W}{S}\right)_{TO}}} \quad (6-91)$$

The parameter B of the airplane drag polar is calculated from:

$$B_{DP_{OEI}} = \frac{1}{\pi AR_w e_{OEI}} \quad (6-92)$$

Note: Equations used in this topic assume the British unit of the parameter used in the program. For the SI unit system, appropriate conversions must be made.

6.1.3.2.4.1.7 FAR 23.77(a) Climb Gradient (CGR)

For jet driven airplanes, the thrust to weight ratio to meet FAR 23.77(a) Climb Gradient (CGR) requirements is plotted using the following relationship:

$$\left(\frac{T}{W}\right)_{TO} = \frac{W_L}{W_{TO}} \left(CGR_{23.77} + (L/D)^{-1} \right) \quad (6-93)$$

The lift to drag ratio at landing with gear down is calculated from:

$$L/D = \frac{0.5}{\sqrt{C_{D_{oL_down}} B_{DPL_down}}} \quad (6-94)$$

The parameter B of the airplane drag polar is calculated from:

$$B_{DPL_down} = \frac{1}{\pi A R_w e_L} \quad (6-95)$$

For propeller powered airplanes, the weight to power ratio to meet FAR 23.77(a) Climb Gradient (CGR) requirements is plotted using the following relationship:

$$\left(\frac{W}{P}\right)_{TO} = \frac{18.97 \eta_p \left(C_{L_{\max L}} - \Delta C_{L_{Cl-Max}} \right)^{1/2} \left(\frac{W_L}{W_{TO}} \right)^{-2/3}}{\sqrt{\left(\frac{W}{S}\right)_{TO} \left(CGR_{23.77} + \frac{C_{D_{oL_down}} + B_{DPL_down} \left(C_{L_{\max L}} - \Delta C_{L_{Cl-Max}} \right)^2}{C_{L_{\max L}} - \Delta C_{L_{Cl-Max}}} \right)}} \quad (6-96)$$

The parameter B of the airplane drag polar is calculated from:

$$B_{DPL_down} = \frac{1}{\pi A R_w e_L} \quad (6-97)$$

Note: Equations used in this topic assume the British unit of the parameter used in the program. For the SI unit system, appropriate conversions must be made.

6.1.3.2.4.1.8 FAR 23.77(b) Rate of Climb (RC)

For jet driven airplanes, the thrust to weight ratio to meet FAR 23.77(b) Rate of Climb (RC) requirements is plotted using the following relationship:

$$\left(\frac{T}{W}\right)_{TO} = \frac{W_L}{W_{TO}} \left(\frac{\frac{RC_{5000OSA}}{60}}{\left(\frac{W_{TO}}{W_L} \left(\frac{W}{S}\right)_{TO}\right)^{1/2}} \sqrt{\frac{(0.5\rho_{@5000,+40^\circ F})}{\left(\frac{C_{D_oL_down}}{B_{DPL_down}}\right)^{1/2}}} + 2 \left(\frac{C_{D_oL_down}}{B_{DPL_down}}\right)^{1/2} \right) \quad (6-98)$$

For propeller powered airplanes, the weight to power ratio to meet FAR 23.77(b) Rate of Climb (RC) requirements is plotted using the following relationship:

$$\left(\frac{W}{P}\right)_{TO} = \frac{W_{TO}}{W_L} \left(\frac{19\eta_p \frac{(27)^{1/4} (\sigma_{@ 5000,+40^\circ F})^{1/2}}{\left(256C_{D_{oL_down}} B_{DPL_down}^3\right)^{1/4}}}{\left(\frac{W_L}{W_{TO}} \left(\frac{W}{S}\right)_{TO}\right)^{1/2} + \frac{19(27)^{1/4} RC_{5000OSA} (\sigma_{@ 5000,+40^\circ F})^{1/2}}{33000 \left(256C_{D_{oL_down}} B_{DPL_down}^3\right)^{1/4}}} \right) \quad (6-99)$$

The parameter B of the airplane drag polar is calculated from:

$$B_{DPL_down} = \frac{1}{\pi AR_w e_L} \quad (6-100)$$

Note: Equations used in this topic assume the British unit of the parameter used in the program. For the SI unit system, appropriate conversions must be made.

6.1.3.2.4.2 Sizing to FAR 25 Climb requirements

6.1.3.2.4.2.1 FAR 25.111 Climb, One Engine Inoperative

For jet driven airplanes, thrust to weight ratio to meet FAR 25.111 One Engine Inoperative Climb requirements is plotted using the following relationship:

$$\left(\frac{T}{W}\right)_{TO} = \left(CGR_{25.111} + \frac{C_D + C_{D_{wm}}}{C_L} \right) \frac{N_{eng}}{N_{eng} - 1} \quad (6-101)$$

For propeller powered airplanes, the weight to power ratio to meet FAR 25.111 One Engine Inoperative Climb requirements is plotted using the following relationship:

$$\left(\frac{W}{P}\right)_{TO} = \frac{\left(18.97\eta_p \left(C_L\sigma_{@h_{TO},ISA}\right)^{1/2}\right) \frac{N_{eng} - 1}{N_{eng}}}{\left(CGR_{25.111} + \frac{C_D + C_{D_{prop}}}{C_L}\right) \sqrt{\left(\frac{W}{S}\right)_{TO}}} \quad (6-102)$$

The lift coefficient is determined from:

$$C_L = \frac{C_{L_{maxTO}}}{1.44} \quad (6-103)$$

The drag coefficient is calculated from:

$$C_D = C_{D_{oTO_up}} + B_{DP_{TO_up}} C_L^2 \quad (6-104)$$

The parameter B of the airplane drag polar is calculated from:

$$B_{DP_{TO_up}} = \frac{1}{\pi A R_w e_{TO}} \quad (6-105)$$

Note: Equations used in this topic assume the British unit of the parameter used in the program. For the SI unit system, appropriate conversions must be made.

6.1.3.2.4.2.2 FAR 25.121 Climb, One Engine Inoperative, Transition

For jet driven airplanes, the thrust to weight ratio to meet FAR 25.121 One Engine Inoperative, Transition Climb requirements is plotted using the following relationship:

$$\left(\frac{T}{W}\right)_{TO} = \left(CGR_{25.121T} + \frac{C_D + C_{D_{wm}}}{C_L} \right) \frac{N_{eng}}{N_{eng} - 1} \quad (6-106)$$

For propeller powered airplanes, the weight to power ratio to meet FAR 25.121 One Engine Inoperative, Transition Climb requirements is plotted using the following relationship:

$$\left(\frac{W}{P}\right)_{TO} = \frac{\left(18.97\eta_p \left(C_L \sigma_{@h_{TO,ISA}} \right)^{1/2} \right) \frac{N_{eng} - 1}{N_{eng}}}{\left(CGR_{25.121T} + \frac{C_D + C_{D_{prop}}}{C_L} \right) \sqrt{\left(\frac{W}{S}\right)_{TO}}} \quad (6-107)$$

The lift coefficient is determined from:

$$C_L = \frac{C_{L_{maxTO}}}{1.21} \quad (6-108)$$

The drag coefficient is calculated from:

$$C_D = C_{D_{oTO_down}} + B_{DP_{TO_down}} C_L^2 \quad (6-109)$$

The parameter B of the airplane drag polar is calculated from:

$$B_{DP_{TO_down}} = \frac{1}{\pi A R_w e_{TO}} \quad (6-110)$$

Note: Equations used in this topic assume the British unit of the parameter used in the program. For the SI unit system, appropriate conversions must be made.

6.1.3.2.4.2.3 FAR 25.121 Climb, One Engine Inoperative, Second Segment

For jet driven airplanes, the thrust to weight ratio to meet FAR 25.121 One Engine Inoperative, Second Segment Climb requirements is plotted using the following relationship:

$$\left(\frac{T}{W}\right)_{TO} = \left(CGR_{25.121S} + \frac{C_D + C_{D_{wm}}}{C_L} \right) \frac{N_{eng}}{N_{eng} - 1} \quad (6-111)$$

For propeller powered airplanes, the weight to power ratio to meet FAR 25.121 One Engine Inoperative, Second Segment Climb requirements is plotted using the following relationship:

$$\left(\frac{W}{P}\right)_{TO} = \frac{\left(18.97 \eta_p \left(C_L \sigma_{@h_{TO}, ISA} \right)^{1/2} \right) \frac{N_{eng} - 1}{N_{eng}}}{\left(CGR_{25.121S} + \frac{C_D + C_{D_{prop}}}{C_L} \right) \sqrt{\left(\frac{W}{S}\right)_{TO}}} \quad (6-112)$$

The lift coefficient is determined from:

$$C_L = \frac{C_{L_{\max TO}}}{1.44} \quad (6-113)$$

The drag coefficient is calculated from:

$$C_D = C_{D_{oTO_up}} + B_{DP_{TO_up}} C_L^2 \quad (6-114)$$

The parameter B of the airplane drag polar is calculated from:

$$B_{DP_{TO_up}} = \frac{1}{\pi A R_w e_{TO}} \quad (6-115)$$

Note: Equations used in this topic assume the British unit of the parameter used in the program. For the SI unit system, appropriate conversions must be made.

6.1.3.2.4.2.4 FAR 25.121 Climb, One Engine Inoperative, Enroute

For jet driven airplanes, the thrust to weight ratio to meet FAR 25.121 One Engine Inoperative, Enroute Climb requirements is plotted using the following relationship:

$$\left(\frac{T}{W}\right)_{TO} = \left(CGR_{25.121ER} + \frac{C_D + C_{D_{wm}}}{C_L} \right) \left(\frac{N_{eng}}{N_{eng} - 1} \right) \frac{1}{F_{MaxCont}} \quad (6-116)$$

For propeller powered airplanes, the weight to power ratio to meet FAR 25.121 One Engine Inoperative, Enroute Climb requirements is plotted using the following relationship:

$$\left(\frac{W}{P}\right)_{TO} = \frac{18.97\eta_p F_{MaxCont} \sqrt{C_L \sigma_{@h_{TO}, ISA}} \left(\frac{N_{eng} - 1}{N_{eng}}\right)}{\left(CGR_{25.121ER} + \frac{C_D + C_{Dprop}}{C_L}\right) \sqrt{\left(\frac{W}{S}\right)_{TO}}} \quad (6-117)$$

The lift coefficient is determined from:

$$C_L = \frac{C_{Lmaxclean}}{(1.25)^2} \quad (6-118)$$

The drag coefficient is calculated from:

$$C_D = C_{D0clean} + B_{DPclean} C_L^2 \quad (6-119)$$

The parameter B of the airplane drag polar is calculated from:

$$B_{DPclean} = \frac{1}{\pi AR_w e_{clean}} \quad (6-120)$$

Note: Equations used in this topic assume the British unit of the parameter used in the program. For the SI unit system, appropriate conversions must be made.

6.1.3.2.4.2.5 FAR 25.121 Climb, One Engine Inoperative, Approach

For jet driven airplanes, the thrust to weight ratio to meet FAR 25.121 One Engine Inoperative, Approach Climb requirements is plotted using the following relationship:

$$\left(\frac{T}{W}\right)_{TO} = \frac{W_L}{W_{TO}} \left(CGR_{25.121L} + \frac{C_D + C_{D_{wm}}}{C_L} \right) \frac{N_{eng}}{N_{eng} - 1} \quad (6-121)$$

For propeller powered airplanes, the weight to power ratio to meet FAR 25.121 One Engine Inoperative, Approach Climb requirements is plotted using the following relationship:

$$\left(\frac{W}{P}\right)_{TO} = \frac{18.97\eta_p \sqrt{C_L \sigma_{@hL,ISA}} \left(\frac{N_{eng} - 1}{N_{eng}} \right)}{\left(CGR_{25.121L} + \frac{C_D + C_{D_{prop}}}{C_L} \right) \left(\frac{W_L}{W_{TO}} \right)^{3/2} \sqrt{\left(\frac{W}{S} \right)_{TO}}} \quad (6-122)$$

The lift coefficient is determined from:

$$C_L = \frac{C_{L_{maxA}}}{2.25} \quad (6-123)$$

The drag coefficient is calculated from:

$$C_D = C_{D_{oA}} + B_{DPL_down} C_L^2 \quad (6-124)$$

The zero lift drag coefficient during approach is dependent on the value of the change in zero-lift drag due to approach:

$$\text{if } \Delta C_{D_{oA}} = 0 \text{ then } C_{D_{oA}} = \frac{C_{D_{oL_down}} + C_{D_{oTO_down}}}{2} \quad (6-125)$$

$$\text{if } \Delta C_{D_{oA}} > 0 \text{ then } C_{D_{oA}} = C_{D_{oL_down}} - \Delta C_{D_{oA}} \quad (6-126)$$

The parameter B of the airplane drag polar is calculated from:

$$B_{DPL_down} = \frac{1}{\pi AR_w e_L} \quad (6-127)$$

Note: Equations used in this topic assume the British unit of the parameter used in the program. For the SI unit system, appropriate conversions must be made.

6.1.3.2.4.2.6 FAR 25.121 Climb, All Engines Operative, Landing

For jet driven airplanes, the thrust to weight ratio to meet FAR 25.121 All Engines Operative Landing Climb requirements is plotted using the following relationship:

$$\left(\frac{T}{W}\right)_{TO} = \frac{W_L \left(CGR_{25.119} + \frac{C_D}{C_L} \right)}{W_{TO} F_{8sec}} \quad (6-128)$$

For propeller powered airplanes, the weight to power ratio to meet FAR 25.121 All Engines Operative Landing Climb requirements is plotted using the following relationship:

$$\left(\frac{W}{P}\right)_{TO} = F_{8,sec} \frac{18.97\eta_P \sqrt{C_L \sigma_{@h_L,ISA}}}{\left(CGR_{25.119} + \frac{C_D}{C_L}\right) \left(\frac{W_L}{W_{TO}}\right)^{3/2} \sqrt{\left(\frac{W}{S}\right)_{TO}}} \quad (6-129)$$

The lift coefficient is determined from:

$$C_L = \frac{C_{L_{maxL}}}{1.69} \quad (6-130)$$

The drag coefficient is calculated from:

$$C_D = C_{D_{O_{L_down}}} + B_{D_{P_{L_down}}} C_L^2 \quad (6-131)$$

The parameter B of the airplane drag polar is calculated from:

$$B_{D_{P_{L_down}}} = \frac{1}{\pi A R_w e_L} \quad (6-132)$$

Note: Equations used in this topic assume the British unit of the parameter used in the program. For the SI unit system, appropriate conversions must be made.

6.1.3.2.4.3 Sizing to Military Climb requirements

6.1.3.2.4.3.1 Military Climb: Take-off, Gear down

For jet driven airplanes, the take-off thrust to weight ratio to meet Military Take-off Climb requirements with landing gear extended is plotted using the following relationship:

$$\left(\frac{T}{W}\right)_{TO} = \left(CGR_{TO} + \frac{C_D}{C_L}\right) F_{engine} \quad (6-133)$$

For propeller powered airplanes, the take-off weight to power ratio to meet Military Take-off Climb requirements with landing gear extended is plotted using the following relationship:

$$\left(\frac{W}{P}\right)_{TO} = \frac{18.97 \eta_p \sqrt{C_L \sigma @ h_{TO, ISA}}}{F_{engine} \left(CGR_{TO} + \frac{C_D}{C_L}\right) \sqrt{\left(\frac{W}{S}\right)_{TO}}} \quad (6-134)$$

The airplane lift coefficient at the given flight condition is determined from:

$$C_L = \frac{C_{L_{maxTO}}}{1.21} \quad (6-135)$$

The airplane drag coefficient at the given flight condition is calculated from:

$$C_D = C_{D_{oTO_down}} + B_{DP_{TO_down}} C_L^2 \quad (6-136)$$

The parameter B of the airplane drag polar with take-off flaps and landing gear deployed is calculated from:

$$B_{DP_{TO_down}} = \frac{1}{\pi A R_w e_{TO}} \quad (6-137)$$

The engine factor accounts for the number of engines on the airplane with one engine inoperative, and is calculated from:

$$\text{if } N_{eng} = 1 \text{ then } F_{engine} = 1 \quad (6-138)$$

$$\text{if } N_{eng} > 1 \text{ then } F_{engine} = \frac{N_{eng}}{N_{eng} - 1} \quad (6-139)$$

Note: Equations used in this topic assume the British unit of the parameter used in the program. For the SI unit system, appropriate conversions must be made.

6.1.3.2.4.3.2 Military Climb: Take-off, Gear up

For jet driven airplanes, the take-off thrust to weight ratio to meet Military Take-off Climb requirements with landing gear retracted is plotted using the following relationship:

$$\left(\frac{T}{W}\right)_{TO} = \left(CGR_{TO50} + \frac{C_D}{C_L}\right) F_{engine} \quad (6-140)$$

For propeller powered airplanes, the take-off weight to power ratio to meet Military Take-off Climb requirements with landing gear retracted is plotted using the following relationship:

$$\left(\frac{W}{P}\right)_{TO} = \frac{18.97\eta_p\sqrt{C_L\sigma_{@h_{TO,ISA}}}}{F_{engine}\left(CGR_{TO50} + \frac{C_D}{C_L}\right)\sqrt{\left(\frac{W}{S}\right)_{TO}}} \quad (6-141)$$

The airplane lift coefficient at the given flight condition is determined from:

$$C_L = \frac{C_{L_{maxTO}}}{(1.15)^2} \quad (6-142)$$

The airplane drag coefficient at the given flight condition is calculated from:

$$C_D = C_{D_{oTO_up}} + B_{DP_{TO_up}}C_L^2 \quad (6-143)$$

The parameter B of the airplane drag polar with takeoff flaps and landing gear retracted is calculated from:

$$B_{DP_{TO_up}} = \frac{1}{\pi AR_w e_{TO}} \quad (6-144)$$

The engine factor accounts for the number of engines on the airplane with one engine inoperative, and is calculated from:

$$\text{if } N_{eng} = 1 \text{ then } F_{engine} = 1 \quad (6-145)$$

$$\text{if } N_{eng} > 1 \text{ then } F_{engine} = \frac{N_{eng}}{N_{eng} - 1} \quad (6-146)$$

Note: Equations used in this topic assume the British unit of the parameter used in the program. For the SI unit system, appropriate conversions must be made.

6.1.3.2.4.3.3 Military Climb: Landing

For jet driven airplanes, the take-off thrust to weight ratio to meet Military Balked Landing Climb requirements is plotted using the following relationship:

$$\left(\frac{T}{W}\right)_{TO} = \frac{W_L}{W_{TO}} \left(CGR_L + \frac{C_D}{C_L} \right) F_{engine} \quad (6-147)$$

For propeller powered airplanes, the take-off weight to power ratio to meet Military Balked Landing Climb requirements is plotted using the following relationship:

$$\left(\frac{W}{P}\right)_{TO} = \frac{18.97 \eta_p \sqrt{C_L \sigma @ h_L, ISA}}{F_{engine} \left(CGR_L + \frac{C_D}{C_L} \right) \left(\frac{W_L}{W_{TO}} \right)^{3/2} \sqrt{\left(\frac{W}{S} \right)_{TO}} \quad (6-148)$$

The airplane lift coefficient at the given flight condition is determined from:

$$C_L = \frac{C_{LmaxA}}{1.44} \quad (6-149)$$

The airplane drag coefficient at the given flight condition is calculated from:

$$C_D = C_{D_{oA}} + B_{DPL_up} C_L^2 \quad (6-150)$$

The zero-lift drag coefficient during approach landing is dependent on the value of the change in zero-lift drag due to flaps at approach position:

$$\text{if } \Delta C_{D_{oA}} = 0 \quad \text{then } C_{D_{oA}} = \frac{C_{D_{oL_up}} + C_{D_{oTO_up}}}{2} \quad (6-151)$$

$$\text{if } \Delta C_{D_{oA}} > 0 \quad \text{then } C_{D_{oA}} = C_{D_{oL_up}} - \Delta C_{D_{oA}} \quad (6-152)$$

The parameter B of the airplane drag polar with landing flaps and gear up is calculated from:

$$B_{DPL_up} = \frac{1}{\pi A R_w e_L} \quad (6-153)$$

The engine factor accounts for the number of engines on the airplane with one engine inoperative, and is calculated from:

$$\text{if } N_{eng} = 1 \quad \text{then } F_{engine} = 1 \quad (6-154)$$

$$\text{if } N_{eng} > 1 \quad \text{then } F_{engine} = \frac{N_{eng}}{N_{eng} - 1} \quad (6-155)$$

Note: Equations used in this topic assume the British unit of the parameter used in the program. For the SI unit system, appropriate conversions must be made.

6.1.3.2.4.3.4 Military Time to Climb

For jet driven airplanes, the take-off thrust to weight ratio to meet Military Time to Climb requirements is plotted using the following relationship:

$$\left(\frac{T}{W}\right)_{TO} = \frac{F_1}{\sqrt{\left(\frac{W}{S}\right)_{TO}}} + A_1 \quad (6-156)$$

The calculation parameters A_1 and F_1 are dependent on the flight path angle:

$$\text{if } \gamma < 15.0^\circ \text{ then } A_1 = (L/D)^{-1} \quad (6-157)$$

$$F_1 = RC \sqrt{0.5\rho_{@SL,ISA} C_L} \quad (6-158)$$

$$\text{if } \gamma > 15.0^\circ \text{ then } A_1 = 0 \quad (6-159)$$

$$F_1 = \frac{RC \sqrt{0.5\rho_{@SL,ISA} C_L}}{A - \sqrt{A^2 - A + \frac{1}{1 + (L/D)^2}}} \quad (6-160)$$

The lift to drag ratio is calculated from:

$$L/D = \frac{C_L}{C_{D_{oclean,M}} + B_{DP_{clean}} C_L^2} \quad (6-161)$$

The airplane lift coefficient at the flight condition is determined from:

$$C_L = \sqrt{\frac{C_{D_{oclean,M}}}{B_{DP_{clean}}}} \quad (6-162)$$

The parameter B of the drag polar is calculated from:

$$B_{DP_{clean}} = \frac{1}{\pi A R_w e_{clean}} \quad (6-163)$$

The rate of climb is calculated from:

$$RC = \frac{h_{abs}}{60 t_{Cl}} \ln \left(\frac{1}{1 - \frac{h_{Cl_{end}}}{h_{abs}}} \right) \quad (6-164)$$

The calculation parameter, A, is determined from:

$$A = \frac{\left(\frac{L}{D}\right)^2}{1 + \left(\frac{L}{D}\right)^2} \quad (6-165)$$

For propeller powered airplanes, the take-off weight to power ratio to meet Military Time to Climb requirements is plotted using the following relationship:

$$\left(\frac{W}{P}\right)_{TO} = \frac{19 \eta_p \sqrt{\frac{L^3}{D^2}}}{\sqrt{\left(\frac{W}{S}\right)_{TO} + \frac{19}{33000} RC \sqrt{\frac{L^3}{D^2}}} \quad (6-166)$$

The ratio of the cube of lift to the square of the drag is determined from:

$$\frac{L^3}{D^2} = \frac{C_L^3}{\left(C_{D_{oclean,M}} + B_{DP_{clean}} C_L^2 \right)^2} \quad (6-167)$$

The airplane lift coefficient at the given flight condition is determined from:

$$C_L = \sqrt{\frac{3C_{D_{oclean,M}}}{B_{DP_{clean}}}} \quad (6-168)$$

The parameter B of the drag polar is calculated from:

$$B_{DP_{clean}} = \frac{1}{\pi A R_w e_{clean}} \quad (6-169)$$

Note: Equations used in this topic assume the British unit of the parameter used in the program. For the SI unit system, appropriate conversions must be made.

6.1.3.2.4.3.5 Military Ceiling

For jet driven airplanes, the take-off thrust to weight ratio to meet Military Ceiling requirements is plotted using the following relationship:

$$\left(\frac{T}{W} \right)_{TO} = \frac{F_1}{\sqrt{\left(\frac{W}{S} \right)_{TO}}} + A_1 \quad (6-170)$$

The calculation parameters A_1 and F_1 are dependent on the flight path angle:

$$\text{if } \gamma < 15.0^\circ \text{ then } A_1 = \left(\frac{L}{D}\right)^{-1} \quad (6-171)$$

$$F_1 = RC \sqrt{0.5 \rho_{@SL,ISA} C_L} \quad (6-172)$$

$$\text{if } \gamma > 15.0^\circ \text{ then } A_1 = 0 \quad (6-173)$$

$$F_1 = \frac{RC \sqrt{0.5 \rho_{@SL,ISA} C_L}}{A - \sqrt{A^2 - A + \frac{1}{1 + \left(\frac{L}{D}\right)^2}}} \quad (6-174)$$

The lift to drag ratio is calculated from:

$$\frac{L}{D} = \frac{C_L}{C_{D_{o_{clean,M}}} + B_{DP_{clean}} C_L^2} \quad (6-175)$$

The airplane lift coefficient at the flight condition is determined from:

$$C_L = \sqrt{\frac{C_{D_{o_{clean,M}}}}{B_{DP_{clean}}}} \quad (6-176)$$

The parameter B of the drag polar is calculated from:

$$B_{DP_{clean}} = \frac{1}{\pi A R_w e_{clean}} \quad (6-177)$$

The calculation parameter, A, is determined from:

$$A = \frac{\left(\frac{L}{D}\right)^2}{1 + \left(\frac{L}{D}\right)^2} \quad (6-178)$$

For propeller powered airplanes, the take-off weight to power ratio to meet Military Ceiling requirements is plotted using the following relationship:

$$\left(\frac{W}{P}\right)_{TO} = \frac{19\eta_p \sqrt{\frac{L^3}{D^2}}}{\sqrt{\left(\frac{W}{S}\right)_{TO} + \frac{19}{33000} RC \sqrt{\frac{L^3}{D^2}}}} \quad (6-179)$$

The ratio of the cube of lift to the square of the drag is determined from:

$$\frac{L^3}{D^2} = \frac{C_L^3}{\left(C_{D_{o_{clean},M}} + B_{DP_{clean}} C_L^2\right)^2} \quad (6-180)$$

The airplane lift coefficient at the given flight condition is determined from:

$$C_L = \sqrt{\frac{3C_{D_{o_{clean},M}}}{B_{DP_{clean}}}} \quad (6-181)$$

The parameter B of the drag polar is calculated from:

$$B_{DP_{clean}} = \frac{1}{\pi AR_w e_{clean}} \quad (6-182)$$

Note: Equations used in this topic assume the British unit of the parameter used in the program. For the SI unit system, appropriate conversions must be made.

6.1.3.2.4.3.6 Military Specific Excess Power

For jet driven airplanes, the take-off thrust to weight ratio to meet Military Specific Excess Power requirements is plotted using the following relationship:

$$\left(\frac{T}{W}\right)_{TO} = \frac{P_{SpExPwr} W_{Cl}}{60 V_{SpExPwr} W_{TO} F_{SpExPwr}} + \frac{C_{D_{o\ clean, M}} \bar{q}}{F_{SpExPwr}} + \frac{\left(\frac{W_{Cl}}{W_{TO}}\right)^2 B_{DP_{clean}}}{F_{SpExPwr} \bar{q}} \left[\left(\frac{W}{S}\right)_{TO}\right]^2$$

(6-183)

The speed for the excess power calculation is calculated from:

$$V_{SpExPwr} = \sqrt{\frac{2\bar{q}}{\rho_{@ h_{SpExPwr, ISA}}}}$$

(6-184)

The dynamic pressure at the altitude of the specific excess power calculation is calculated from:

$$\bar{q} = 1482 \left(\frac{V_{Cl}}{a_{@ h_{SpExPwr, ISA}}} \right)^2 \delta_{@ h_{SpExPwr, ISA}}$$

(6-185)

The parameter B of the drag polar is calculated from:

$$B_{DP_{clean}} = \frac{1}{\pi A R_w e_{clean}}$$

(6-186)

Note: Equations used in this topic assume the British unit of the parameter used in the program. For the SI unit system, appropriate conversions must be made.

6.1.3.2.5 Sizing to Maximum Cruise Speed Requirements

This module is used to size the aircraft to maximum cruise speed requirements. The methodology used in sizing to maximum cruise speed requirements is based on Section 3.6 of Reference 1.

For jet driven airplanes, the thrust to weight ratio to meet maximum cruise speed requirements is plotted using the following relationship:

$$\left(\frac{T}{W}\right)_{TO} = \bar{q} \frac{C_{D_o\ clean, M}}{F_{Cr} \left(\frac{W}{S}\right)_{TO}} + \left(\frac{W_{Cr}}{W_{TO}}\right)^2 \frac{B_{DP\ clean}}{\bar{q} F_{Cr}} \left(\frac{W}{S}\right)_{TO} \quad (6-187)$$

The dynamic pressure is determined from:

$$\bar{q} = 0.5 \rho_{@Altitude, ISA} V_{Cr_{max}}^2 \quad (6-188)$$

The parameter B of the drag polar is calculated from:

$$B_{DP\ clean} = \frac{1}{\pi A R_w e_{clean}} \quad (6-189)$$

The cruise Mach number shown in the output is solved from the flight altitude and maximum cruise speed.

For propeller powered airplanes, the weight to power ratio to meet maximum cruise speed requirements is plotted using the following relationship:

$$\left(\frac{W}{P}\right)_{TO} = \left(\frac{W}{S}\right)_{TO} \frac{F_{Cr}}{\sigma_{@Altitude,ISA} I_{power}^3} \quad (6-190)$$

Note: Equations used in this topic assume the British unit of the parameter used in the program. For the SI unit system, appropriate conversions must be made.

6.1.3.2.6 Sizing to Maneuvering Requirements

This module is used to size the aircraft to meet maneuvering requirements. This submodule sizes the airplane for both pull-up (or push-over) load factor and a specific turn rate in the level turn maneuver. The methodology used in sizing to maneuvering requirements is based on Reference 1, Section 3.5.

For jet driven airplanes, the thrust to weight ratio to meet maneuvering requirements is plotted using the following relationship:

$$\left(\frac{T}{W}\right)_{TO} = \frac{\bar{q} C_{D_{o\ clean,M}}}{F_M \left(\frac{W}{S}\right)_{TO}} + \left(\frac{W}{S}\right)_{TO} \left(\frac{nW_M}{W_{TO}}\right)^2 \frac{B_{DP\ clean}}{\bar{q} F_M} \quad (6-191)$$

The dynamic pressure during maneuvering is determined from:

$$\bar{q} = 0.5\rho_{@h_M,ISA} V_M^2 \quad (6-192)$$

The parameter B of the drag polar is calculated from:

$$B_{DP_{clean}} = \frac{1}{\pi AR_w e_{clean}} \quad (6-193)$$

For propeller powered airplanes, the weight to power ratio to meet maneuvering requirements is plotted using the following relationship:

$$\left(\frac{W}{P}\right)_{TO} = \frac{\left(\frac{W}{S}\right)_{TO}}{\bar{q} C_{D_o_{clean,M}} T + \left(\frac{nW_M}{W_{TO}}\right)^2 B_{DP_{clean}} \frac{T}{\bar{q}} \left(\frac{W}{S}\right)_{TO}^2} \quad (6-194)$$

The parameter, T, is determined from:

$$T = \frac{1.689V_M}{550\eta_p F_M} \quad (6-195)$$

Note: Equations used in this topic assume the British unit of the parameter used in the program. For the SI unit system, appropriate conversions must be made.

6.1.3.2.7 Sizing to Landing Distance Requirements

This module is used to size the aircraft to meet landing distance requirements. The methodology used in sizing to landing requirements is based on Reference 1, Section 3.3. Landing distances of airplanes are determined by the following factors:

1. Landing weight;
2. Approach speed;
3. Deceleration method used;
4. Flying qualities of the airplane;
5. Pilot technique.

Kinetic energy considerations suggest that the approach speed should have a "square" effect on the total landing distance. After an airplane has touched down the following deceleration methods can be used:

- a. Brakes
- b. Thrust reversers
- c. Parachutes
- d. Arresting systems (field-based or carrier-based)
- e. Crash barriers

For civil airplanes, the requirements of FAR 23 and FAR 25 are in force. In the case of homebuilt airplanes, it is not necessary to design to FAR landing distance requirements. For military airplanes, the requirements are usually laid down in the Request for Proposal. Ground runs are sometimes specified without their accompanying air distances. In the case of Navy airplanes, the capabilities of the on-deck arresting system need to be taken into consideration.

6.1.3.2.7.1 Land based Airplanes

The landing distance parameters are shown in Figure 6.2.

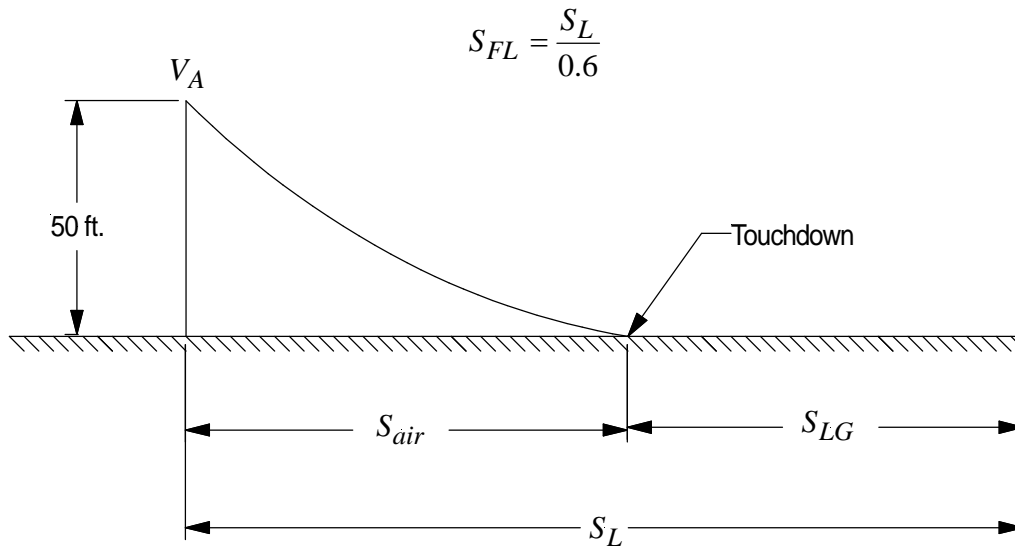


Figure 6.2 Landing Distance Definition

The wing loading to meet landing distance requirements is plotted using the following relationship:

$$\left(\frac{W}{S}\right)_L = 0.5 \rho_{@h_L, ISA} C_{L_{\max L}} S_L F_1 \frac{W_{TO}}{W_L} \quad (6-196)$$

with:

$F_1 = 5.547$ for FAR 23, JAR 23 and VLA certification, also used for LSA;

$F_1 = 9.365$ for FAR 25 certification;

$F_1 = 10.990$ for Military and AS certification.

For FAR 25, Military and AS certification:

$$S_{FL} = \frac{S_L}{0.6} \quad (6-197)$$

6.1.3.2.7.2 Carrier based Airplanes

The wing loading to meet landing distance requirements is plotted using the following relationship:

$$\left(\frac{W}{S}\right)_L = \frac{1}{2} \rho_{@h_L, ISA} C_{L_{\max L}} \left(\frac{1.689V_A}{1.1}\right)^2 \left(\frac{W_{TO}}{W_L}\right) \quad (6-198)$$

Note: Equations used in this topic assume the British unit of the parameter used in the program. For the SI unit system, appropriate conversions must be made.

6.2 Airplane and Wing Maximum Lift

6.2.1 Airfoil Maximum Lift Coefficient

The tip and root sectional lift coefficients are obtained from Figure 7.1 in Airplane Design Part II (Ref. 2):

$$c_{l_{\max}} = f\left(\text{Re}, \frac{t}{c}, \text{airfoil}\right) \quad (6-199)$$

The root chord Reynolds number is calculated from:

$$\text{Re}_r = \frac{\rho V_s c_r}{\mu} \quad (6-200)$$

The tip chord Reynolds number is similarly calculated from:

$$\text{Re}_t = \frac{\rho V_s c_t}{\mu} \quad (6-201)$$

If airfoil data is known from wind tunnel data, the $c_{l_{\max}}$ can be entered as an input instead.

6.2.2 Wing Maximum Lift Coefficient

The following method applies to the calculation of the maximum lift coefficient of any lifting surface. The lifting surface maximum lift coefficient without any flap effects is calculated from:

$$C_{L_{w \max \text{ clean}}} = k_{\lambda_w} \frac{\cos \Lambda_{c/4w} (c_{l_{\max r_w}} + c_{l_{\max t_w}})}{2} \quad (6-202)$$

The lifting surface taper ratio factor is determined from:

$$k_{\lambda_w} = -0.117\lambda_w + 0.997 \quad (6-203)$$

The lifting surface taper ratio is calculated from:

$$\lambda_w = \frac{c_{t_w}}{c_{r_w}} \quad (6-204)$$

The wing maximum lift coefficient without any flap effects is sufficient to meet the clean airplane maximum lift coefficient requirement if the following condition is met:

$$\frac{\left| \frac{C_{L_{\max w \text{ clean}}}}{f_{\text{couple}}} - C_{L_{\max \text{ clean}}} \right|}{C_{L_{\max \text{ clean}}}} < 0.05 \quad (6-205)$$

Note: If the wing under consideration cannot meet the required value of the maximum lift coefficient within 5%, it will be necessary to redesign the wing planform and/or select different airfoils until it does.

The coupling factor, f_{couple} , accounts for the "tail down-load to trim" or for a canard "canard up-load to trim" on the wing. The coupling factor is:

$$f_{couple} = 1.05 \quad \text{for short coupled airplanes, } \frac{l_h}{\bar{c}_w} \text{ or } \frac{l_c}{\bar{c}_w} < 3.0$$

$$f_{couple} = 1.10 \quad \text{for long coupled airplanes, } \frac{l_h}{\bar{c}_w} \text{ or } \frac{l_c}{\bar{c}_w} > 5.0$$

6.3 Flap Sizing

The purpose of this module is to size the trailing edge flap for the wing using the Class I method, given the required maximum airplane lift coefficients at clean, take-off and landing configurations. The result is the flapped wing area (see Figure 6.3) to the wing area ratio that is required to produce the additional lift at take-off or landing condition. This area ratio in turn gives the required flap outboard station.

The calculations are performed for the following types of flaps:

- Plain Flap
- Split Flap
- Single-Slotted Flap
- Fowler Flap
- Type I Double-Slotted Flap
- Type II Double-Slotted Flap
- Triple Slotted Flap

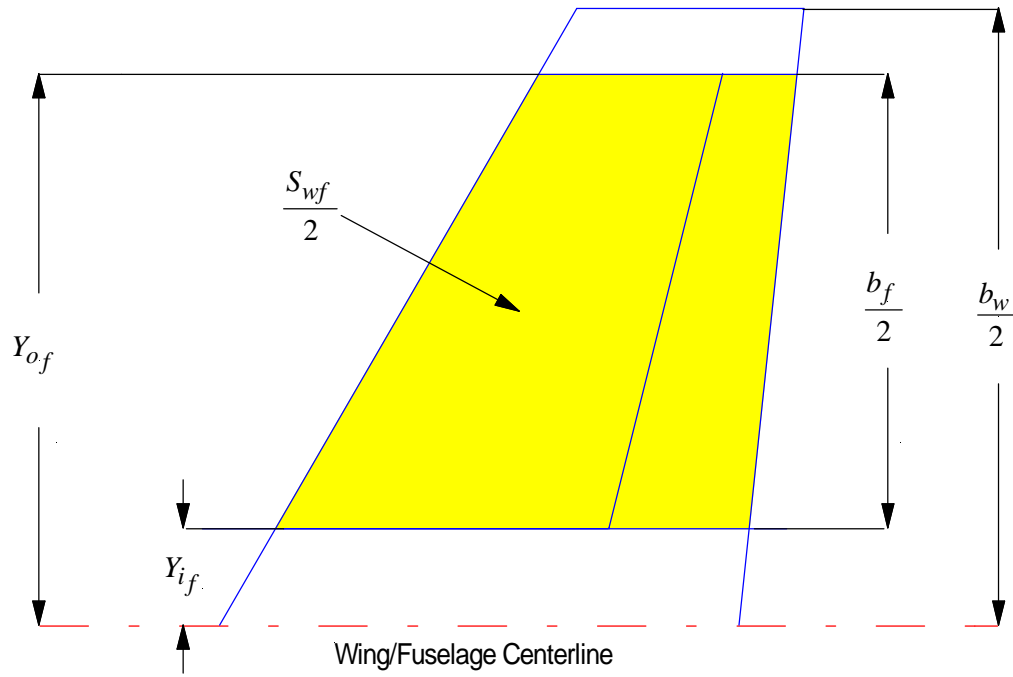


Figure 6.3 Flapped Area Definition

The outboard station of the flap is solved using the following relation for the flapped wing area ratio:

$$\frac{S_{wf}}{S_w} = \frac{(\eta_{of} - \eta_{if})}{1 + \lambda_w} \left[2 - (1 - \lambda_w)(\eta_{of} + \eta_{if}) \right] \quad (6-206)$$

The flapped wing area ratio for take-off is solved from:

$$\frac{S_{wf}}{S_w} = \frac{\Delta C_{L_{w\delta_{FTO}}}}{\frac{\Delta c_{l_{max}}}{\Delta c_l} \Delta c_{l\delta_{FTO}} \left(\cos^{3/4} \Lambda_{c/4_w} \right) \left(1.0 - 0.08 \cos^2 \Lambda_{c/4_w} \right)} \quad (6-207)$$

The flapped wing area ratio for landing is solved from:

$$\frac{S_{wf}}{S_w} = \frac{\Delta C_{Lw\delta fL}}{\frac{\Delta c_{l_{\max}}}{\Delta c_l} \Delta c_{l\delta fL} \left(\cos^{3/4} \Lambda_{c/4w} \right) \left(1.0 - 0.08 \cos^2 \Lambda_{c/4w} \right)} \quad (6-208)$$

The flapped wing area ratio is sized for the condition, either take-off or landing, which requires the highest flap area to meet the required lift coefficient.

The increment in wing maximum lift coefficient due to flap deflection at take-off is calculated using:

$$\Delta C_{Lw\delta fTO} = K_{trim} \left(C_{L_{\max TO}} - C_{L_{\max \text{clean}}} \right) - \Delta C_{Lw\delta daTO} \quad (6-209)$$

The increment in wing maximum lift coefficient due to flap deflection at landing is calculated using:

$$\Delta C_{Lw\delta fL} = K_{trim} \left(C_{L_{\max L}} - C_{L_{\max \text{clean}}} \right) - \Delta C_{Lw\delta daL} \quad (6-210)$$

The ratio of the increment in the maximum sectional lift coefficient due to flaps to the increment in the sectional lift coefficient due to flaps can be determined from Figure 7.4 in Airplane Design Part II (Ref. 2) as a function of flap chord ratio and the flap

type:

$$\frac{\Delta c_{l_{\max}}}{\Delta c_l} = f\left(\frac{c_f}{c_w}, \text{flap type}\right) \quad (6-211)$$

The change in airfoil lift coefficient due to flap deflection depends on the type of flaps.

6.3.1 Plain Flap

For a plain flap (See Figure 6.4), the increment in the sectional lift coefficient due to flaps is calculated from:

$$\Delta c_{l_{\delta f_x}} = c_{l_{\delta f}} K'_x \delta_{f_x} \frac{\pi}{180} \quad (6-212)$$

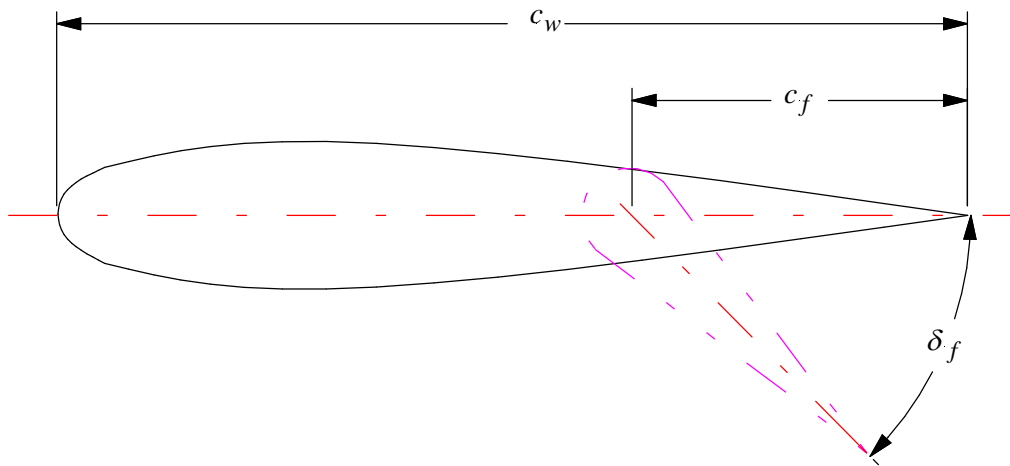


Figure 6.4 Plain Flap

The subscript, x, denotes the take-off, landing or actual flight condition.

The derivative of sectional lift coefficient with flap deflection is determined from Figure 7.5 of Airplane Design Part II (Ref. 2) as a function of the flap chord ratio and the wing thickness ratio at the spanwise station of wing mean geometric chord. The figure is digitized as follows:

$$c_{l\delta_f} = f\left(\frac{c_f}{c_w}, \left(\frac{t}{c}\right)_w\right) = \sum_{i=0}^6 \sum_{j=0}^3 c_{i,j} \left(\frac{c_f}{c_w}\right)^i \left(\frac{t}{c}\right)_w^j \quad (6-213)$$

The wing thickness ratio at the spanwise station of wing mean geometric chord is determined from:

$$\left(\frac{t}{c}\right)_w = \frac{\left(\frac{t}{c}\right)_{r_w} - \frac{1+2\lambda_w}{3(1+\lambda_w)} \left[\left(\frac{t}{c}\right)_{r_w} - \left(\frac{t}{c}\right)_{t_w} \lambda_w \right]}{1 - \frac{1+2\lambda_w}{3(1+\lambda_w)} (1-\lambda_w)} \quad (6-214)$$

The correction factor which accounts for non-linearity at high flap deflections is determined from Figure 7.6 of Airplane Design Part II (Ref. 2) as a function of the flap deflection angle and the flap chord ratio. The figure is digitized as follows:

$$K'_x = f\left(\delta_{f_x}, \frac{c_f}{c_w}\right) = \sum_{i=0}^4 \sum_{j=0}^4 c_{i,j} \delta_{f_x}^i \left(\frac{c_f}{c_w}\right)^j \quad (6-215)$$

6.3.2 Split Flap

For a split flap (See Figure 6.5), the increment in the sectional lift coefficient due to flaps is calculated from:

$$\Delta c_{l\delta f_x} = k_{SplitFlap} \Delta c_{l_f 0.2_x} \quad (6-216)$$

The subscript, x, denotes the take-off, landing or actual flight condition.

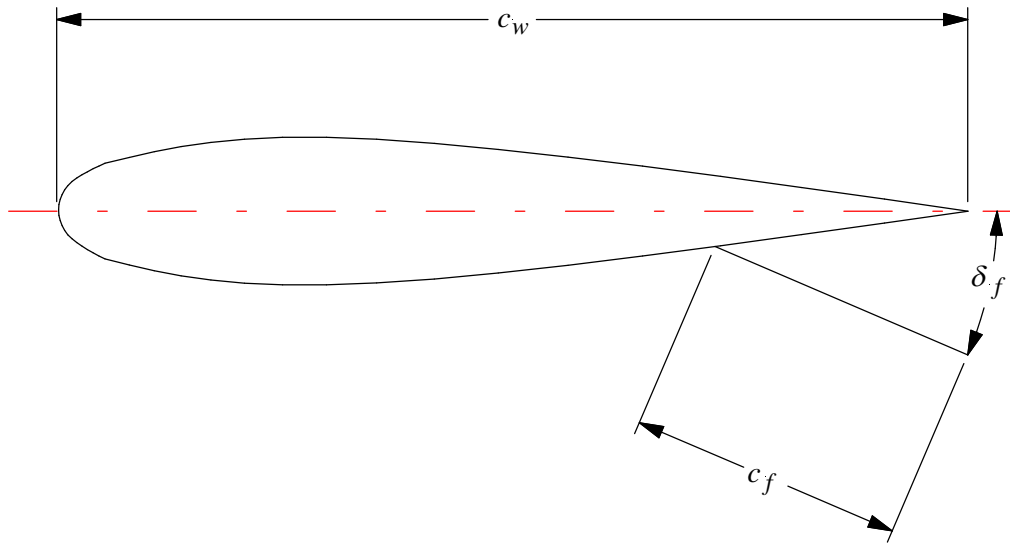


Figure 6.5 Split Flap

The split flap factor is determined from Figure 7.7 of Airplane Design Part II (Ref. 2) as function of the flap chord ratio. The figure is digitized as follows:

$$k_{SplitFlap} = f\left(\frac{c_f}{c_w}\right) = \sum_{i=0}^6 c_i \left(\frac{c_f}{c_w}\right)^i \quad (6-217)$$

The increment in section-lift-coefficient-due-to-flap-deflection derivative with a flap chord ratio of 0.2 is determined from Figure 7.7 of Airplane Design Part II (Ref. 2) as a function of the wing thickness ratio at the spanwise station of wing mean geometric chord and the flap deflection angle. The figure is digitized as follows:

$$\Delta c_{l_{f0.2x}} = f\left(\delta_{f_x}, \left(\frac{\bar{t}}{c}\right)_w\right) = \sum_{i=0}^6 \sum_{j=0}^3 c_{i,j} \delta_{f_x}^i \left(\frac{\bar{t}}{c}\right)_w^j \quad (6-218)$$

The wing thickness ratio at the spanwise station of wing mean geometric chord is determined from equation (9-213).

6.3.3 Single Slotted Flap

For a single-slotted flap (See Figure 6.6), the increment in the sectional lift coefficient due to flaps is calculated from:

$$\Delta c_{l_{\delta_{f_x}}} = c_{l_{\alpha_w}} @ M=0 \alpha_{\delta_{f_x}} \delta_{f_x} \frac{\pi}{180} \quad (6-219)$$

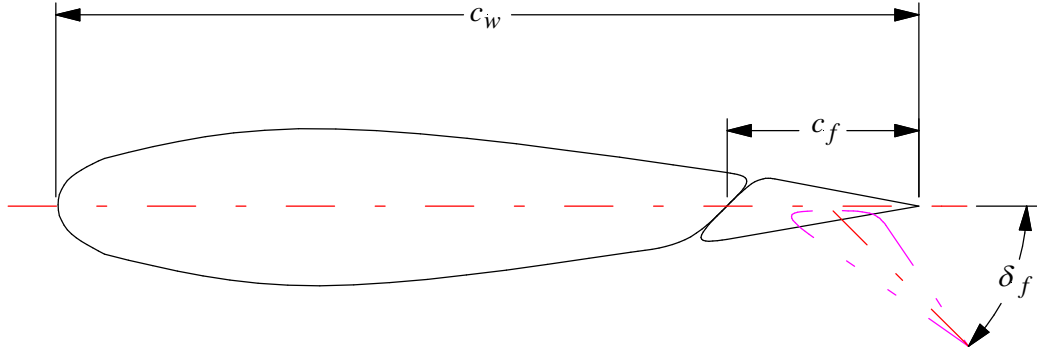


Figure 6.6 Single Slotted Flap

The subscript, x, denotes the take-off, landing or actual flight condition.

The wing airfoil lift effectiveness parameter is determined from Figure 7.8 of Airplane Design Part II (Ref. 2) as a function of flap deflection angle and wing thickness ratio at the spanwise station of the wing mean geometric chord. The figure is digitized as follows:

$$\alpha_{\delta_{f_x}} = f\left(\delta_{f_x}, \frac{c_f}{c_w}\right) = \sum_{i=0}^7 \sum_{j=0}^4 c_{i,j} \delta_{f_x}^i \left(\frac{c_f}{c_w}\right)^j \quad (6-220)$$

6.3.4 Type I Double Slotted Flap

For a type I double slotted flap (See Figure 6.7), the increment in the sectional lift coefficient due to flap deflection is given by the equation:

$$\Delta c_{l_{\delta_{f_x}}} = \eta_{1_x} c_{l_{\delta_{f_1}}} \left(\delta_{f_x} - \delta_{f_{2_x}}\right) \left(1 + \frac{c_1}{c_w}\right) + \eta_{2_x} c_{l_{\delta_{f_2}}} \delta_{f_x} \frac{c'_w}{c_w} \quad (6-221)$$

The subscript, x, denotes the take-off, landing or actual flight condition.

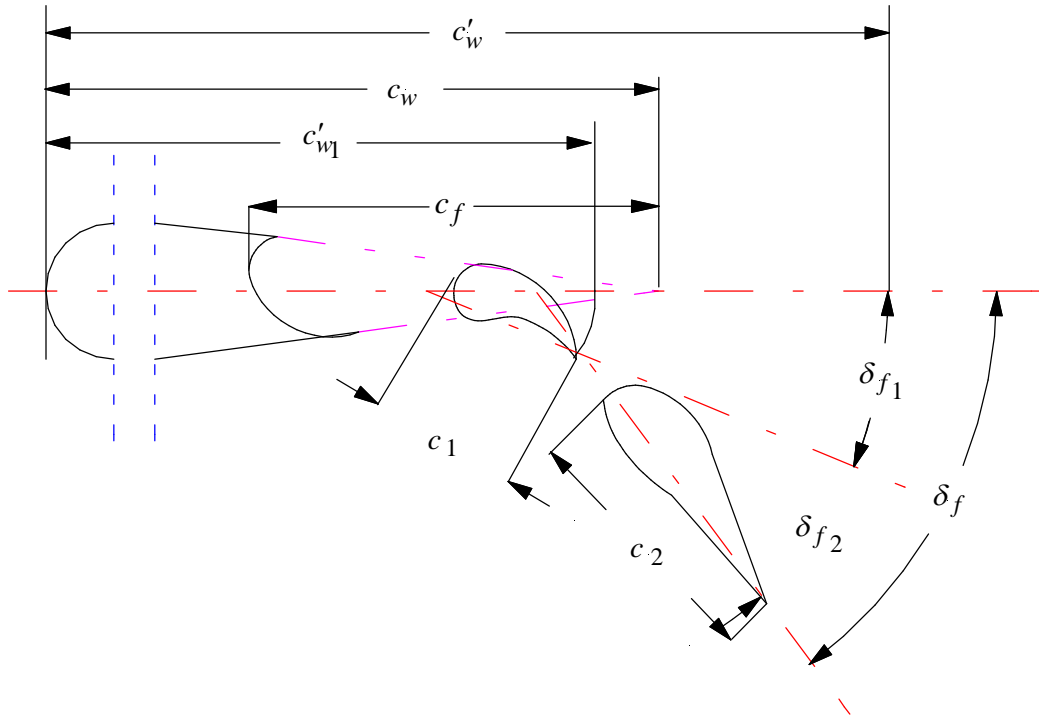


Figure 6.7 Type I Double Slotted Flap

The empirical lift efficiency factor is determined from Figure 8.20 of Airplane Design Part VI (Ref. 6) as a function of effective turning angle of the flap segment and the segment chord ratio:

$$\eta_{k_x} = f\left(\Phi_{k_x}, \frac{c_k}{c_w}\right) = \sum_{i=0}^6 \sum_{j=0}^2 c_{i,j} \Phi_{k_x}^i \left(\frac{c_k}{c_w}\right)^j \quad (6-222)$$

The subscript k is either 1 or 2. The effective turning angle of the first flap segment is determined from:

$$\Phi_{1x} = \delta_{f_x} - \delta_{f_{2x}} + \Phi_{TE_{upp}} \quad (6-223)$$

The effective turning angle of the second flap segment is determined from:

$$\Phi_{2x} = \delta_{f_x} + \Phi_{TE_{upp}} \quad (6-224)$$

The lifting effectiveness is determined from Figure 8.21 of Airplane Design Part VI (Ref. 6) as a function of flap segment chord to wing chord ratio:

$$c_{l\delta_{f_k}} = f\left(\frac{c_k}{c_w}\right) = \sum_{i=0}^6 c_i \left(\frac{c_k}{c_w}\right)^i \quad (6-225)$$

The extended wing chord to wing chord ratio is given by:

$$\frac{c'_w}{c_w} = 1 + \left(\frac{\Delta c_w}{c_f}\right)_x \frac{c_f}{c_w} \quad (6-226)$$

The increment in wing chord due to flap deflection to flap chord ratio can be determined from Figure G-7 of Synthesis of Subsonic Airplane Design (Ref. 15) as a function of the flap deflection angle and flap type:

$$\left(\frac{\Delta c_w}{c_f}\right)_x = f(\delta_{f_x}) = \sum_{i=0}^6 c_i \delta_{f_x}^i \quad (6-227)$$

6.3.5 Type II Double Slotted Flap

For a type II double slotted flap (Figure 6.8), the increment in the sectional lift coefficient due to flap deflection is given by:

$$\Delta c_{l_{\delta f_x}} = \eta_{1_x} c_{l_{\delta f_1}} (\delta_{f_x} - \delta_{f_{2x}}) \left(\frac{c'_{w_1}}{c_w}\right) + \eta_{2_x} \eta_{t_x} c_{l_{\delta f_2}} \delta_{f_{2x}} \left(1 + \frac{c'_w}{c_w} - \frac{c'_{w_1}}{c_w}\right) \quad (6-228)$$

The subscript, x, denotes the take-off, landing or actual flight condition.

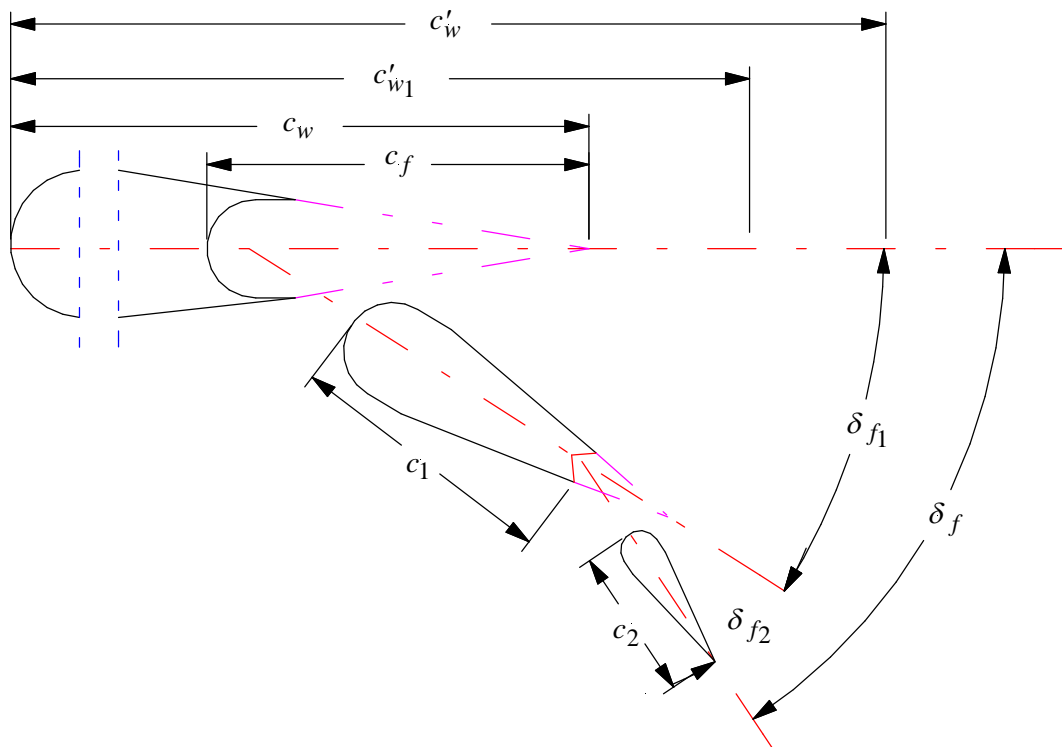


Figure 6.8 Type II Double Slotted Flap

The empirical lift efficiency factor, η_{ik} , is determined from Figure 8.20 of Airplane Design Part VI (Ref. 6) as function of effective turning angle of the flap segment and the segment chord ratio.

The lifting effectiveness, $c_{l_{\delta_{fk}}}$, is determined from Figure 8.21 of Airplane Design Part VI (Ref. 6) as function of flap segment chord to wing chord ratio.

The extended wing chord to wing chord ratio is given by:

$$\frac{c'_w}{c_w} = 1 + \left(\frac{\Delta c_w}{c_f} \right)_x \left(\frac{c_1}{c_w} + \frac{c_2}{c_w} \right) \quad (6-229)$$

The increment in wing chord due to flap deflection to flap chord ratio can be determined from Figure G-7 (Type III) of Synthesis of Subsonic Airplane Design (Ref. 15) as function of flap deflection angle and flap type:

$$\left(\frac{\Delta c_w}{c_f} \right)_x = f_{\text{Type III}}(\delta_{f_x}) = 0.3065 \frac{\delta_{f_x}}{15} \text{ for } \delta_{f_x} \leq 15 \text{ deg} \quad (6-230)$$

$$\left(\frac{\Delta c_w}{c_f} \right)_x = f_{\text{Type III}}(\delta_{f_x}) = 0.3065 + 0.4225 \frac{(\delta_{f_x} - 15)}{45} \text{ for } \delta_{f_x} > 15 \text{ deg} \quad (6-231)$$

Similarly, the extended wing chord (measured to the trailing edge of the first flap segment only) to wing chord ratio is given by:

$$\frac{c'_{w_1}}{c_w} = 1 + \left(\frac{\Delta c_{w_1}}{c_f} \right)_x \frac{c_f}{c_w} \quad (6-232)$$

The increment in wing chord due to forward flap-segment deflection to flap chord ratio can be determined from Figure G-7 (Type IVb) of Synthesis of Subsonic Airplane Design (Ref. 15) as function of the flap deflection angle and flap type:

$$\left(\frac{\Delta c_{w_1}}{c_f} \right)_x = f(\delta_{f_x}) = \sum_{i=0}^5 c_i \delta_{f_x}^i \quad (6-233)$$

The factor accounting for reduced effectiveness of the aft flap, η_{t_x} , is determined from Figure 8.22 of Airplane Design Part VI (Ref. 6) as function of total flap deflection angle and the deflection angle of the second flap segment:

$$\eta_{t_x} = f(\delta_{f_{1x}}, \delta_{f_{2x}}) = 1 + \left(\sum_{i=0}^5 c_i \delta_{f_{2x}}^i - 1 \right) \frac{\delta_{f_{1x}}}{20} \quad (6-234)$$

The deflection angle ratio is calculated from:

$$\left(\frac{\delta_{f_1}}{\delta_{f_2}} \right)_x = \frac{\delta_{f_x}}{\delta_{f_{2x}}} - 1 \quad (6-235)$$

6.3.6 Fowler Flap

For a Fowler flap (See Figure 6.9), the increment in the sectional lift coefficient due to flaps is given by:

$$\Delta c_{l_{\delta_{fx}}} = c_{l_{\alpha_w @ M=0}} \alpha_{\delta_{fx}} \left(1 + \frac{c_f}{c_w} \right) \delta_{fx} \frac{\pi}{180} \quad (6-236)$$

The subscript, x, denotes the take-off, landing or actual flight condition.

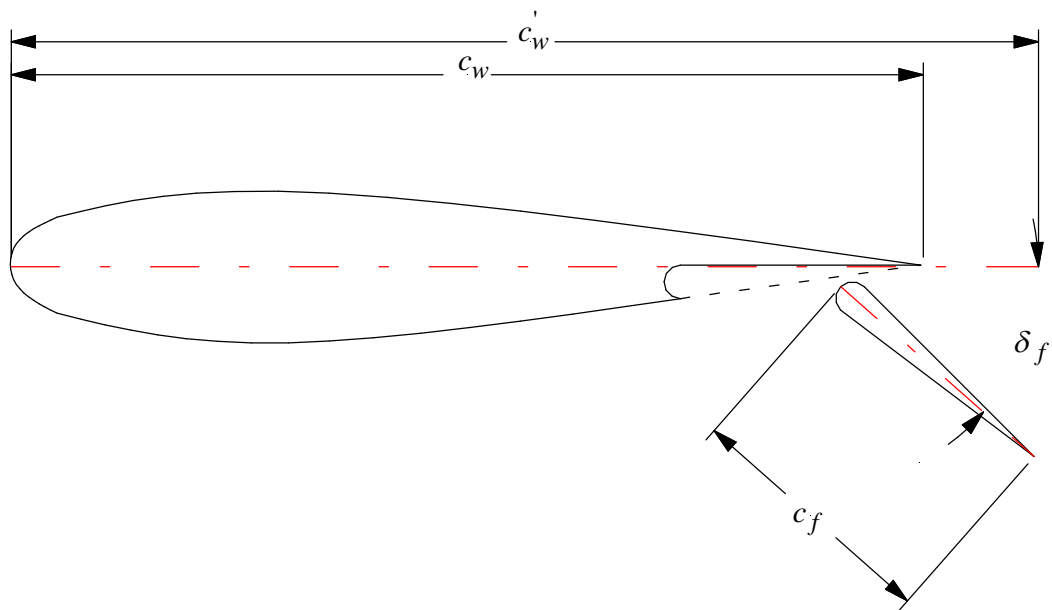


Figure 6.9 Fowler Flap

The wing airfoil lift effectiveness parameter, $\alpha_{\delta_{f_x}}$, is determined from Figure 7.8 of Airplane Design Part II (Ref. 2) as function of flap deflection angle and flap chord ratio:

$$\alpha_{\delta_{f_x}} = f\left(\delta_{f_x}, \frac{c_f}{c_w}\right) = \sum_{i=0}^7 \sum_{j=0}^4 c_{i,j} \delta_{f_x}^i \left(\frac{c_f}{c_w}\right)^j \quad (6-237)$$

6.3.7 Triple Slotted Flap

For a triple slotted flap (See Figure 6.10), the increment in the sectional lift coefficient due to flaps is calculated from:

$$\Delta c_{l_{\delta_{f_x}}} = \eta_{\delta} c_{l_{\alpha_w}} \alpha_{\delta_{f_x}} \delta_{f_x} \frac{\pi}{180} \quad (6-238)$$

The subscript, x, denotes the take-off, landing or actual flight condition.

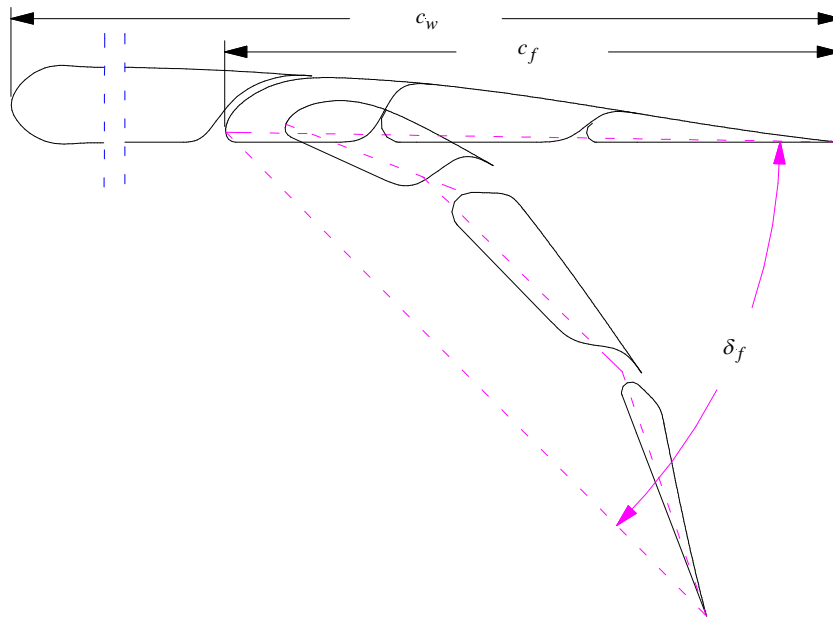


Figure 6.10 Triple Slotted Flap

Flap lift effectiveness, η_δ , is determined from Figure G-6 of Synthesis of Subsonic Airplane Design (Ref. 15).

The theoretical flap lift factor is calculated from:

$$\alpha_{\delta_{fx}} = 1 - \frac{\theta_f - \sin \theta_f}{\pi} \quad (6-239)$$

The angle characterizing relative flap chord is determined from:

$$\theta_f = \cos^{-1} \left(2 \frac{c'_f}{c'} - 1 \right) \quad (6-240)$$

The flap chord extension to wing chord extension ratio is given by:

$$\frac{c'_f}{c'} = \frac{c_f + \Delta c}{c + \Delta c} = \frac{1 + \frac{\Delta c}{c_f}}{\frac{c}{c_f} + \frac{\Delta c}{c_f}} \quad (6-241)$$

6.3.8 Lift Distribution

The method assumes that the quarter chord line of the wing is approximately straight. The method also accounts for compressibility at speeds below the critical Mach number.

The sectional lift coefficient can be plotted along the half span of the wing. The sectional lift coefficient at spanwise station, η , is divided into basic lift and additional lift:

$$c_l(\eta) = c_{l_b}(\eta) + c_{l_a}(\eta) \quad (6-242)$$

Basic lift is the sectional lift coefficient due to wing twist at zero wing lift. Additional lift is the sectional lift coefficient due to a change of the wing angle of attack.

The additional sectional lift coefficient at spanwise station, η , is given by:

$$c_{l_a}(\eta) = \frac{C_{L_w} S_w}{\sqrt{S_w A R_w}} \frac{L_a(\eta)}{c(\eta)} \quad (6-243)$$

The non-dimensional additional sectional lift at spanwise station, η , is computed from:

$$L_a(\eta) = C_1(\eta) c(\eta) \frac{\sqrt{S_w A R_w}}{S_w} + C_2(\eta) \frac{4}{\pi} \sqrt{1 - \eta^2} + C_3(\eta) f(\eta) \quad (6-244)$$

The intermediate coefficients at spanwise station, η , are obtained from Figure E-5 in Synthesis of Subsonic Airplane Design (Ref. 15) as function of the lifting surface aspect ratio, the lifting surface airfoil lift curve slope at spanwise station, η , and the lifting surface quarter chord sweep angle:

$$C_1(\eta) = f\left(\frac{2\pi AR_w}{c_{l_\alpha}(\eta)\cos\Lambda_{c/4w}}\right) = \sum_{i=0}^3 c_i \left(\frac{2\pi AR_w}{c_{l_\alpha}(\eta)\cos\Lambda_{c/4w}}\right)^i \quad (6-245)$$

$$C_2(\eta) = f\left(\frac{2\pi AR_w}{c_{l_\alpha}(\eta)\cos\Lambda_{c/4w}}\right) = \sum_{i=0}^4 c_i \left(\frac{2\pi AR_w}{c_{l_\alpha}(\eta)\cos\Lambda_{c/4w}}\right)^i \quad (6-246)$$

$$C_3(\eta) = 1 - C_1(\eta) - C_2(\eta) \quad (6-247)$$

The lifting surface sectional lift curve slope at spanwise station, η , is calculated from:

$$c_{l_\alpha}(\eta) = c_{l_{\alpha r_w}} - \eta \left(c_{l_{\alpha r_w}} - c_{l_{\alpha t_w}} \right) \quad (6-248)$$

The lift distribution factor at spanwise station, η , is computed from:

$$f(\eta) = f(\Lambda_\beta, \eta) = \sum_{i=0}^9 \sum_{j=0}^5 c_{i,j} \eta^i \Lambda_\beta^j \quad (6-249)$$

The lifting surface semi-chord sweep angle corrected for Mach effects is given by:

$$\Lambda_\beta = \tan^{-1}\left(\frac{\tan\Lambda_{c/2w}}{\beta}\right) \quad (6-250)$$

The Prandtl-Glauert transformation factor is obtained from:

$$\beta = \sqrt{1 - M_1^2} \quad (6-251)$$

The sectional basic lift coefficient at spanwise station, η , is computed from:

$$c_{lb}(\eta) = \frac{S_w}{\sqrt{S_w AR_w}} \beta \varepsilon_{a_w} \cos \Lambda_\beta \frac{c_{l\alpha}(\eta)}{c(\eta)} L_a(\eta) C_4(\eta) \left(\frac{\varepsilon(\eta)}{\varepsilon_{a_w}} + \alpha_{o1} \right) \quad (6-252)$$

The lifting surface aerodynamic twist angle is determined from:

$$\varepsilon_{a_w} = \varepsilon_{g_w} + \alpha_{orwM} - \alpha_{otrM} \quad (6-253)$$

The root or tip airfoil zero-lift angle of attack corrected for Mach number is calculated from:

$$\alpha_{o(x)wM} = \left(\frac{\alpha_{o_w M}}{\alpha_{o_w M=0.3}} \right)_{(x)_w} \alpha_{o(x)w} \quad (6-254)$$

where "x" represents the root or tip airfoil.

The ratio of the lifting surface airfoil zero-lift angle of attack at Mach to the vertical tail airfoil zero-lift angle of attack at $M = 0.3$ is obtained from Figure 8.42 in Airplane Design Part VI (Ref. 6).

$$\left(\frac{\alpha_{o_w M}}{\alpha_{o_w M=0.3}} \right)_{(x)_w} = f \left(M_1, \Lambda_{c/4_w}, \left(\frac{t}{c} \right)_{(x)_w} \right) \quad (6-255)$$

The intermediate coefficient, $C_4(\eta)$, at spanwise station, η , is obtained from Figure E-3 in Synthesis of Subsonic Airplane Design (Ref. 15) as a function of the lifting surface aspect ratio, the lifting surface sectional lift curve slope at spanwise station, η , and the lifting surface quarter chord sweep angle:

$$C_4(\eta) = \frac{1}{\sqrt{1 + \frac{36}{\left(\frac{2\pi AR_w}{c_{l_\alpha}(\eta)\cos\Lambda_{c/4w}}\right)^2} + \frac{6}{\frac{2\pi AR_w}{c_{l_\alpha}(\eta)\cos\Lambda_{c/4w}}}}} \quad (6-256)$$

The local aerodynamic twist at the spanwise station for which the sectional basic lift is zero is calculated from:

$$\alpha_{o1} = -\int_0^1 \frac{\varepsilon(\eta)}{\varepsilon_{a_w}} L_a(\eta) d\eta \quad (6-257)$$

In the program, the computation has been simplified by assuming a linear twist distribution:

$$\varepsilon(\eta) = \eta\varepsilon_{a_w} \quad (6-258)$$

The wing maximum lift coefficient can be determined by varying the wing lift coefficient until the spanwise lift distribution curve first touches the maximum airfoil lift line.

6.4 Class I Weights

The Class I weight estimation method allows a rapid estimation of airplane component weights. The method relies on the assumption that within each airplane category it is possible to express the weight of major airplane components (or groups) as a simple fraction of the airplane flight design gross weight. The Class I weight estimation method is also referred to as the Weight Fraction method from Ref. 5.

The following fractions are used:

$$F_{W_{gross}} = \frac{W_{gross}}{W_{TO}} \quad (6-259)$$

$$F_{W_{fix}} = \frac{W_{fix}}{W_{gross}} \quad (6-260)$$

$$F_{W_{emp}} = \frac{W_{emp}}{W_{gross}} \quad (6-261)$$

$$F_{W_f} = \frac{W_f}{W_{gross}} \quad (6-262)$$

$$F_{W_{gear}} = \frac{W_{gear}}{W_{gross}} \quad (6-263)$$

$$F_{W_n} = \frac{W_n}{W_{gross}} \quad (6-264)$$

$$F_{W_{pp}} = \frac{W_{pp}}{W_{gross}} \quad (6-265)$$

$$F_{W_{structure}} = \frac{W_{structure}}{W_{gross}} \quad (6-266)$$

$$F_{W_w} = \frac{W_w}{W_{gross}} \quad (6-267)$$

$$F_{W_E} = \frac{W_E}{W_{gross}} \quad (6-268)$$

Where:

$$F_{W_{structure}} = F_{W_{emp}} + F_{W_f} + F_{W_w} + F_{W_{gear}} + F_{W_n} \quad (6-269)$$

$$F_{W_E} = F_{W_{structure}} + F_{W_{pp}} + F_{W_{fix}} \quad (6-270)$$

The airplane flight design gross weight is that weight at which the airplane can sustain its design ultimate load factor. For civil airplanes, the airplane flight design gross weight and the airplane take-off weight are often the same, although there are exceptions. For military airplanes, the airplane flight design gross weight and the airplane take-off weight are frequently quite different.

Step 1: Select similar airplanes from the list of predefined airplanes.

From the list of airplanes of the same category, decide on which ones to use. Frequently it will be sufficient to use average fraction values obtained from a number of airplanes with similar configuration and with missions not too much different from

the mission of the airplane being designed. It is of great importance to observe whether:

- a. an airplane has a strutted (braced) wing
- b. an airplane is pressurized
- c. the landing gear is mounted on the fuselage or on the wing
- d. the engines are mounted on the wing or fuselage

Most of the airplanes included are aluminum airplanes. If the airplane being designed will have to contain a significant amount of primary structure made from composites, from lithium-aluminum or from other materials, it will be necessary to modify the weight fractions.

Step 2: Compute the average weight fractions.

The weight fractions for the various components of the airplane are defined by taking an average of the selected airplanes.

$$F_{W_{component}} = \frac{\sum F_{W_{component}}}{\# \text{ of Airplanes}} \quad (6-271)$$

Step 3: Estimate the component Class I weights from these averaged weight fractions in the Weights module.

First, the airplane flight design gross weight is obtained from:

$$W_{gross} = F_{W_{gross}} W_{TO} \quad (6-272)$$

Then, a first estimate of the Class I weight of each component is computed from:

$$W'_{estimate_{component}} = F_{W_{component}} W_{gross} \quad (6-273)$$

When the first estimated component Class I weights are summed, they yield a weight which could be different from the airplane empty weight calculated in weight sizing. Since the empty weight from weight sizing is considered the correct one at this stage, all weights will be adjusted. This difference between calculated and actual empty weight:

$$\Delta W_E = W_E - W'_E \quad (6-274)$$

is to be distributed over all items in proportion to their component weight value listed in the First Estimates column by computing an adjustment:

$$\Delta W_{component} = \Delta W_E \cdot \frac{W'_{component}}{W'_E} \quad (6-275)$$

The actual Class I weight of the components is therefore computed from:

$$W_{component} = W'_{estimate_{component}} + \Delta W_{component} \quad (6-276)$$

The following table shows all components.

Table 6-1 Component Weights

Component	Weight Fraction	First Estimate [lb]	Adjustment [lb]	Class I Weight [lb]
Wing	F_{W_w}	W'_w	ΔW_w	W_w
Empennage	$F_{W_{emp}}$	W'_{emp}	ΔW_{emp}	W_{emp}
Fuselage	$F_{W_{fus}}$	W'_f	ΔW_f	W_f
Nacelles	$F_{W_{nac}}$	W'_n	ΔW_n	W_n
Landing Gear	$F_{W_{gear}}$	W'_{gear}	ΔW_{gear}	W_{gear}
Structures	$F_{W_{structure}}$	$W'_{structure}$	$\Delta W_{structure}$	$W_{structure}$
Powerplant	$F_{W_{pp}}$	W'_{pp}	ΔW_{pp}	W_{pp}
Fixed Equipment	$F_{W_{fix}}$	W'_{fix}	ΔW_{fix}	W_{fix}
Empty Weight	F_{W_E}	W'_E	ΔW_E	W_E

For the Empty Weight module, the total weight is calculated by summing the individual weights of the components.

6.5 Class I Center of Gravity

The center of gravity of each of the components is determined from the following equations:

$$X_{cg} = \frac{\sum (W_{component} X_{cg,component})}{W_E} \quad (6-277)$$

$$Y_{cg} = \frac{\sum (W_{component} Y_{cg,component})}{W_E} \quad (6-278)$$

$$Z_{cg} = \frac{\sum (W_{component} Z_{cg,component})}{W_E} \quad (6-279)$$

6.6 Class I Moments of Inertia

The Class I methods for determining the moments of inertia are based on comparison to similar aircraft. It is assumed that within a category of airplane a radius of gyration can be identified. Therefore, by averaging the radius of gyration of similar airplanes, the moments of inertia can be determined from the following equations:

About the X-body axis:

$$I_{xxB} = \frac{b_w^2 W_{gross} \bar{R}_x^2}{4g} \quad (6-280)$$

About the Y-body axis:

$$I_{yyB} = \frac{L^2 W_{gross} \bar{R}_y^2}{4g} \quad (6-281)$$

About the Z-body axis:

$$I_{zzB} = \frac{e^2 W_{gross} \bar{R}_z^2}{4g} \quad (6-282)$$

where the parameter e is defined as:

$$e = \frac{b_w + L}{2} \quad (6-283)$$

The non-dimensional radii of gyration is determined by calculating the average non-dimensional radius of gyration for the selected airplanes.

$$\bar{R}_x = \frac{\begin{matrix} \text{\# of Similar} \\ \text{Airplanes} \end{matrix} \sum_{i=1} (\bar{R}_x)_i}{\text{\# of Similar Airplanes}} \quad (6-284)$$

$$\bar{R}_y = \frac{\begin{matrix} \text{\# of Similar} \\ \text{Airplanes} \end{matrix} \sum_{i=1} (\bar{R}_y)_i}{\text{\# of Similar Airplanes}} \quad (6-285)$$

$$\bar{R}_z = \frac{\begin{matrix} \text{\# of Similar} \\ \text{Airplanes} \end{matrix} \sum_{i=1} (\bar{R}_z)_i}{\text{\# of Similar Airplanes}} \quad (6-286)$$

For each similar airplane, the non-dimensional radii of gyration is obtained from:

$$(\bar{R}_x)_i = \frac{2(R_x)_i}{(b_w)_i} \quad (6-287)$$

$$(\bar{R}_y)_i = \frac{2(R_y)_i}{(L)_i} \quad (6-288)$$

$$(\bar{R}_z)_i = \frac{2(R_z)_i}{(e)_i} \quad (6-289)$$

The radii of gyration for each airplane is calculated from:

$$(R_x)_i = \sqrt{\frac{(I_{xxB})_i g}{(W_{gross})_i}} \quad (6-290)$$

$$(R_y)_i = \sqrt{\frac{(I_{yyB})_i g}{(W_{gross})_i}} \quad (6-291)$$

$$(R_z)_i = \sqrt{\frac{(I_{zzB})_i g}{(W_{gross})_i}} \quad (6-292)$$

6.7 Class I Stability: Volume Methods

The area of the lifting surface can be solved by using volume coefficients. Two separate methods can be used, one based on distance between quarter chords of the lifting surfaces (geometric volume coefficient) and one based on distance between aerodynamic center and center of gravity (volume coefficient). Definitions of different lengths and coordinates are given in Figure 6.11.

The horizontal tail area is given by:

$$S_h = \frac{\bar{V}_{hg} S_w \bar{c}_w}{l_h} \quad (6-293)$$

with:

$$l_h = X_{apexh} + x_{mgc_h} + \frac{\bar{c}_h}{4} - X_{apexw} - x_{mgc_w} - \frac{\bar{c}_w}{4} \quad (6-294)$$

or

$$S_h = \frac{\bar{V}_h S_w \bar{c}_w}{X_{ac_h} - X_{cg}} \quad (6-295)$$

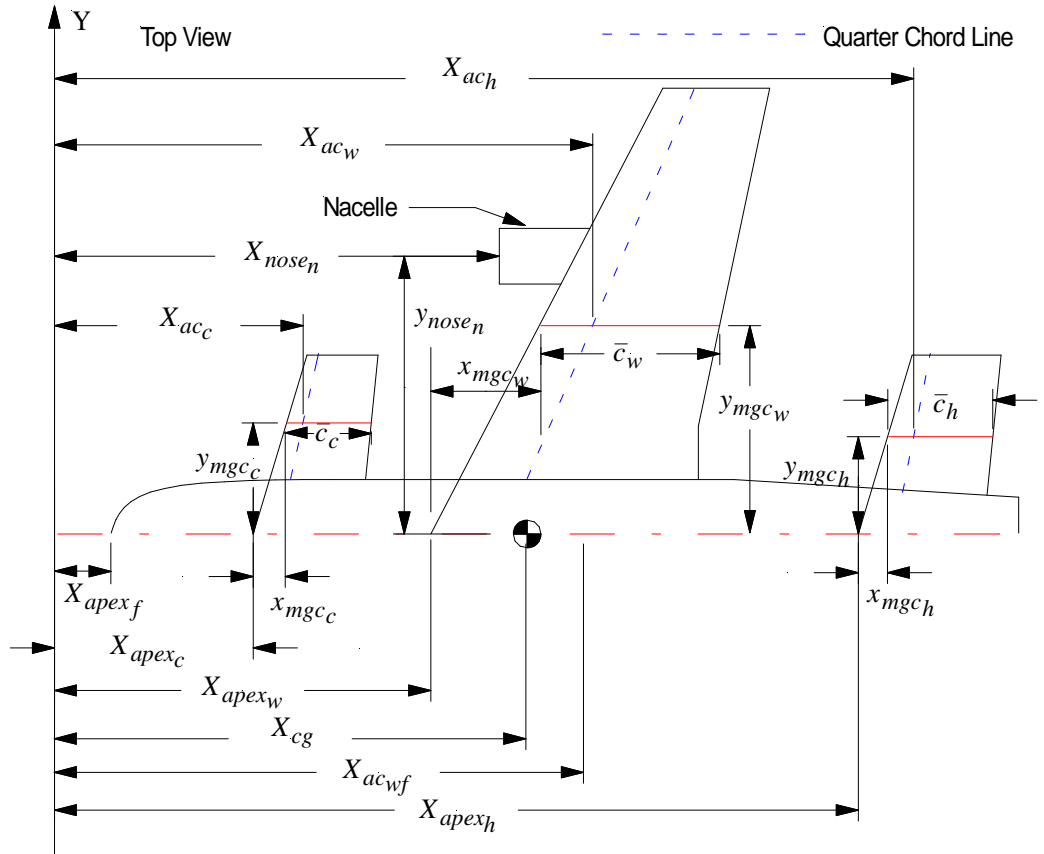


Figure 6.11 Definition of Coordinates

The canard area is given by:

$$S_c = \frac{\bar{V}_{c_g} S_w \bar{c}_w}{l_c} \quad (6-296)$$

with:

$$l_c = X_{apex_w} + x_{mgc_w} + \frac{\bar{c}_w}{4} - X_{apex_c} - x_{mgc_c} - \frac{\bar{c}_c}{4} \quad (6-297)$$

or

$$S_c = \frac{\bar{V}_c S_w \bar{c}_w}{X_{cg} - X_{ac_c}} \quad (6-298)$$

The vertical tail area is given by:

$$S_v = \frac{\bar{V}_{v_g} S_w b_w}{l_v} \quad (6-299)$$

with:

$$l_v = X_{apex_v} + x_{mgc_v} + \frac{\bar{c}_v}{4} - X_{apex_w} - x_{mgc_w} - \frac{\bar{c}_w}{4} \quad (6-300)$$

or

$$S_v = \frac{\bar{V}_v S_w b_w}{X_{ac_v} - X_{cg}} \quad (6-301)$$

The v-tail area is given by:

$$S_{vee} = \frac{\bar{V}_{vee_g} S_w \bar{c}_w}{l_{vee}} \quad (6-302)$$

with:

$$l_{vee} = X_{apex_{vee}} + x_{mgc_{vee}} + \frac{\bar{c}_{vee}}{4} - X_{apex_w} - x_{mgc_w} - \frac{\bar{c}_w}{4} \quad (6-303)$$

or

$$S_{vee} = \frac{\bar{V}_{vee} S_w \bar{c}_w}{X_{ac_{vee}} - X_{cg}} \quad (6-304)$$

Note: For twin vertical tail, the same equation is used. The resulting value is the area of ONE panel only. For a v-tail, the resulting area value is the area of BOTH panels.

6.8 Geometry

The geometry used is either based on lifting surfaces (wing, horizontal tail, vertical tail, canard, pylon) or on a body (fuselage, nacelle, tailboom, store).

6.8.1 Lifting Surfaces

6.8.1.1 Straight Tapered

All pertinent geometry parameters are shown in Figure 6.12.

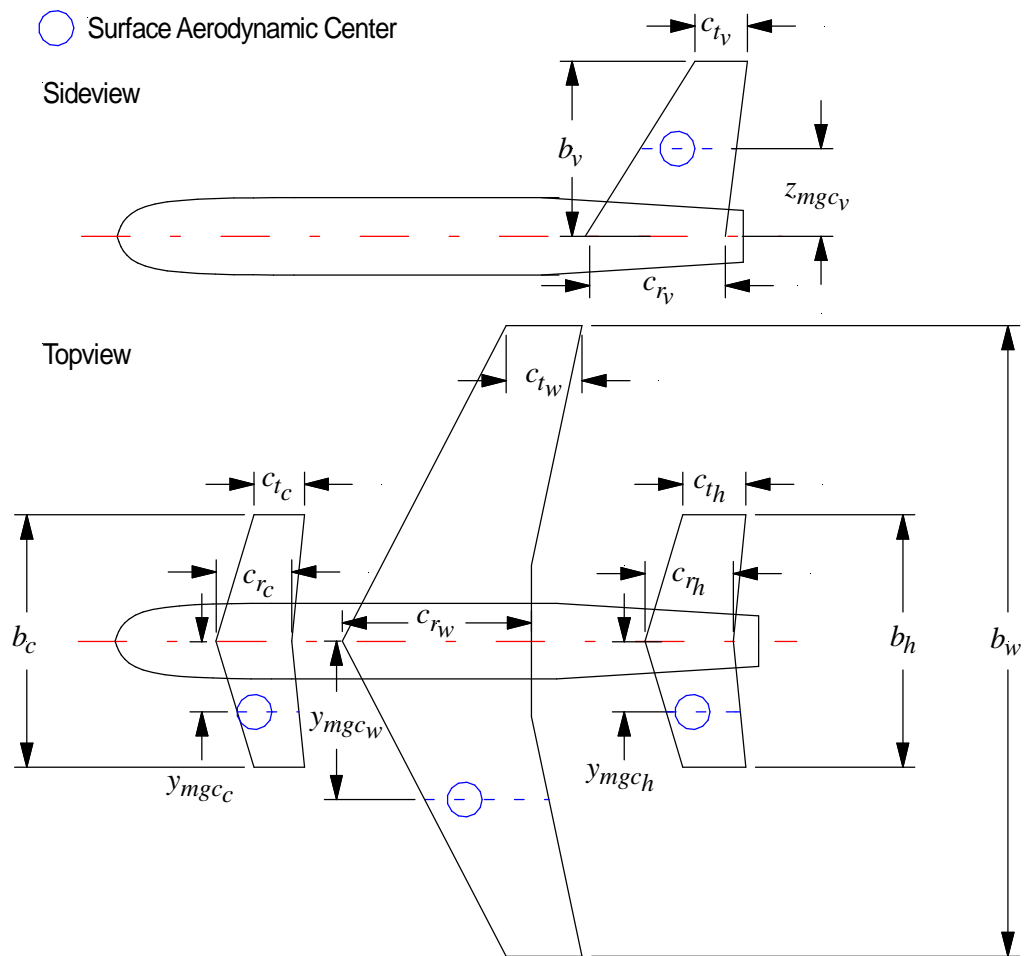


Figure 6.12 Lifting Surface Parameters

All equations use the subscript l.s. to indicate a lifting surface: wing, horizontal tail, canard, V-tail or vertical tail.

The area of the lifting surface is determined from:

$$S_{l.s.} = \frac{b_{l.s.} (c_{\eta_{l.s.}} + c_{\eta_{l.s.}})}{2} \quad (6-305)$$

The aspect ratio for the lifting surface is solved from:

$$AR_{l.s.} = \frac{b_{l.s.}^2}{S_{l.s.}} \quad (6-306)$$

The lifting surface taper ratio is defined as:

$$\lambda_{l.s.} = \frac{c_{\eta_{l.s.}}}{c_{\eta_{l.s.}}} \quad (6-307)$$

The mean geometric chord of the corresponding lifting surface is obtained from:

$$\bar{c}_{l.s.} = \frac{2 c_{\eta_{l.s.}} (1 + \lambda_{l.s.} + \lambda_{l.s.}^2)}{3 (1 + \lambda_{l.s.})} \quad (6-308)$$

The Y-distance between the lifting surface apex and lifting surface mean geometric chord is located from:

$$y_{mgc_{l.s.}} = \frac{b_{l.s.} (1 + 2\lambda_{l.s.})}{6 (1 + \lambda_{l.s.})} \quad (6-309)$$

The Y-distance between the ventral fin apex and lifting surface mean geometric chord is determined with:

$$y_{mgc_{vf}} = \frac{b_{vf} (1 + 2\lambda_{vf})}{3 (1 + \lambda_{vf})} \quad (6-310)$$

The z-distance between the vertical tail apex and the vertical tail mean geometric chord is determined from:

$$z_{mgc_v} = b_v \frac{(1 + 2\lambda_v)}{3 (1 + \lambda_v)} \quad (6-311)$$

The z-distance between the ventral fin apex and the ventral fin mean geometric chord is determined from:

$$z_{mgc_{vf}} = b_{vf} \frac{(1 + 2\lambda_{vf})}{3 (1 + \lambda_{vf})} \sin \Gamma_{vf} \quad (6-312)$$

The sweep angles of the lifting surface (except vertical tail) are calculated from (See Figure 6.13).

$$\Lambda_{TE_{l.s.}} = \tan^{-1} \left\{ \tan \Lambda_{LE_{l.s.}} - \frac{4(1-\lambda_{l.s.})}{AR_{l.s.}(1+\lambda_{l.s.})} \right\} \quad (6-313)$$

$$\Lambda_{LE_{l.s.}} = \tan^{-1} \left\{ \tan \Lambda_{c/4_{l.s.}} + \frac{(1-\lambda_{l.s.})}{AR_{l.s.}(1+\lambda_{l.s.})} \right\} \quad (6-314)$$

$$\Lambda_{c/4_{l.s.}} = \tan^{-1} \left\{ \tan \Lambda_{LE_{l.s.}} - \frac{(1-\lambda_{l.s.})}{AR_{l.s.}(1+\lambda_{l.s.})} \right\} \quad (6-315)$$

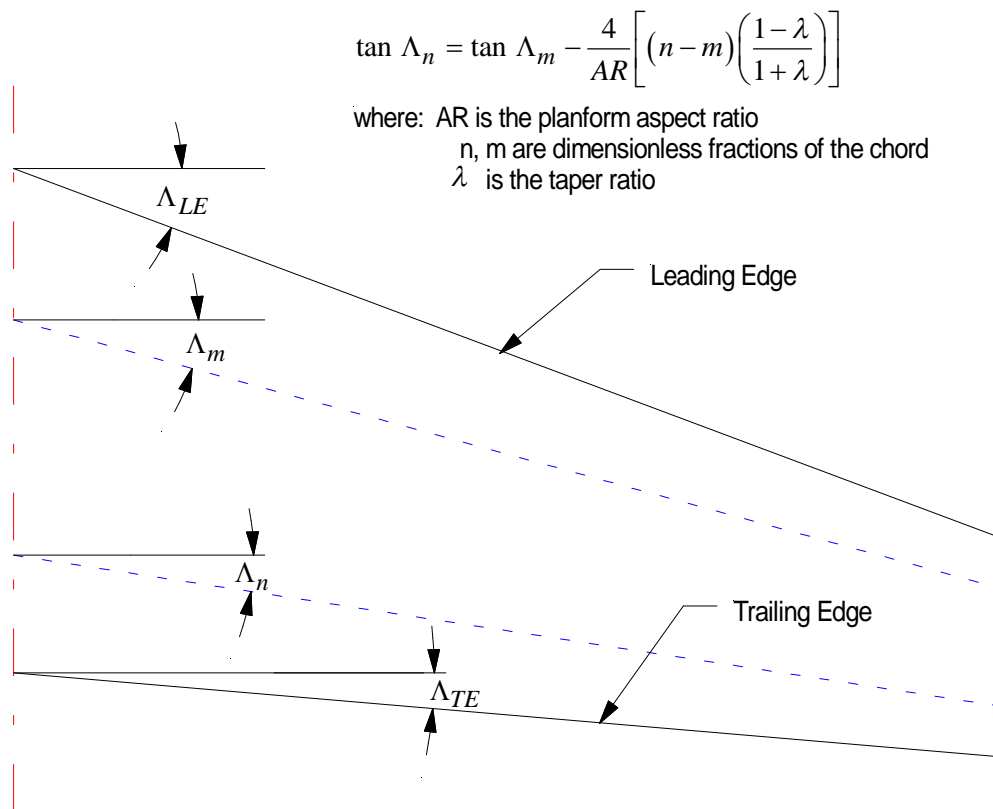


Figure 6.13 Sweep Angle Definition

The vertical tail sweep angles are determined from:

$$\Lambda_{LE_v} = \tan^{-1} \left\{ \tan \Lambda_{c/4_v} + \frac{(1-\lambda_v)}{2AR_v(1+\lambda_v)} \right\} \quad (6-316)$$

$$\Lambda_{TE_v} = \tan^{-1} \left\{ \tan \Lambda_{LE_v} - \frac{4(1-\lambda_v)}{2AR_v(1+\lambda_v)} \right\} \quad (6-317)$$

$$\Lambda_{c/4_v} = \tan^{-1} \left\{ \tan \Lambda_{LE_v} - \frac{(1-\lambda_v)}{2AR_v(1+\lambda_v)} \right\} \quad (6-318)$$

The ventral fin sweep angles are determined from:

$$\Lambda_{LE_{vf}} = \tan^{-1} \left\{ \tan \Lambda_{c/4_{vf}} + \frac{(1-\lambda_{vf})}{2AR_{vf}(1+\lambda_{vf})} \right\} \quad (6-319)$$

$$\Lambda_{TE_{vf}} = \tan^{-1} \left\{ \tan \Lambda_{LE_{vf}} - \frac{4(1-\lambda_{vf})}{2AR_{vf}(1+\lambda_{vf})} \right\} \quad (6-320)$$

The X-location of the lifting surface mean geometric chord leading edge relative to the lifting surface apex is calculated from:

$$x_{mgcl.s.} = y_{mgcl.s.} \tan \Lambda_{LEl.s.} \quad (6-321)$$

For the vertical tail:

$$x_{mgc_v} = z_{mgc_v} \tan \Lambda_{LE_v} \quad (6-322)$$

For ventral fin:

$$x_{mgc_{vf}} = b_{vf} \frac{(1+2\lambda_{vf})}{3(1+\lambda_{vf})} \tan \Lambda_{LE_{vf}} \quad (6-323)$$

6.8.1.2 Cranked Surfaces

An equivalent wing (canard, horizontal tail, vertical tail) is a wing with the same net wing area and the same wing tip as the cranked wing. The user may specify a wing panel (see Figure 6.14) or part of a wing panel inside the fuselage to calculate the equivalent wing area. The first wing panel may start at the fuselage centerline or at the wing-fuselage intersection. Defining the first wing panel from the wing-fuselage intersection prevents overestimation of the area for wings with strakes and wings with large leading edge or trailing edge sweep.

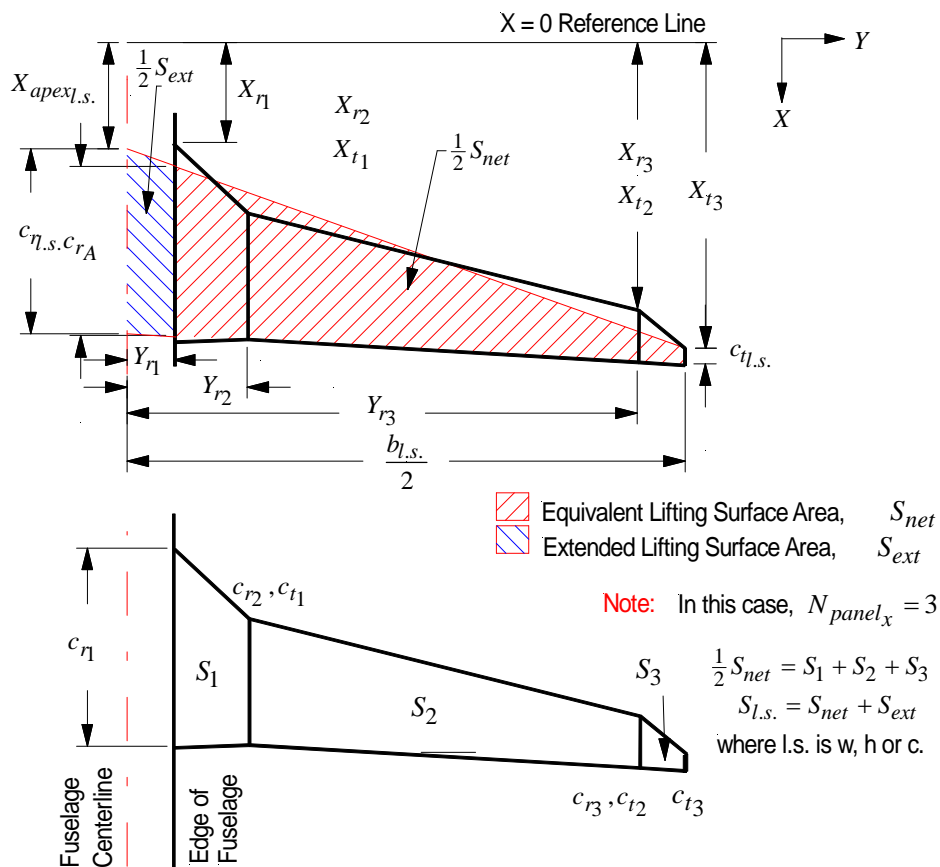


Figure 6.14 Cranked Surfaces Definition

For a wing consisting of N panels, the method used to construct an equivalent wing is as follows with the parameters used for each wing panel:

- $N_{panel_{l.s.}}$ number of panels that make up half of the lifting surface (wing, horizontal tail or canard) or the whole vertical tail. For simplicity, it will be replaced by 'N' in the theory presented below.
- c_r root chord length of the i^{th} panel.
- c_t tip chord length of the i^{th} panel.
- Y_r Y-distance of the i^{th} panel root chord from the fuselage centerline.
- Z_r Z-coordinate of the i^{th} panel root chord leading edge.
- X_r X-coordinate of the i^{th} panel root chord leading edge.
- X_t X-coordinate of the i^{th} panel tip chord leading edge.
- ε_t twist angle at the tip of the i^{th} panel.

The tip chord of the equivalent lifting surface is defined as the tip chord of the N^{th} panel of the wing planform is:

$$c_{l.s.} = c_{tN} \quad (6-324)$$

The root chord of the equivalent lifting surface is solved from:

$$c_{r_{l.s.}} = \left(\frac{c_{r_A} - c_{l.s.}}{b_{l.s.} - Y_{r_1}} \right) Y_{r_1} + c_{r_A} \quad (6-325)$$

For a vertical tail:

$$c_{r_v} = \left(\frac{c_{r_A} - c_{t_v}}{b_v - (Z_{r_1} - Z_{apex_v})} \right) (Z_{r_1} - Z_{apex_v}) + c_{r_A} \quad (6-326)$$

The chord length of the equivalent lifting surface at the root of the first panel is solved from:

$$c_{r_A} = \frac{S_{net}}{\frac{b_{l.s.}}{2} - Y_{r_1}} - c_{l.s.} \quad (6-327)$$

The area of the equivalent lifting surface is determined from:

$$S_{net} = \sum_{i=1}^N [(Y_{r_{i+1}} - Y_{r_i})(c_{r_i} + c_{t_i})] \quad (6-328)$$

with:

$$Y_{r_{i+1}} = \frac{b_{l.s.}}{2} \quad (6-329)$$

For a vertical tail:

$$c_{r_A} = \frac{2S_{net}}{b_v - (Z_{r_1} - Z_{apex_v})} - c_{t_v} \quad (6-330)$$

$$S_{net} = \frac{1}{2} \sum_{i=1}^N [(Z_{r_{i+1}} - Z_{r_i})(c_{r_i} + c_{t_i})] \quad (6-331)$$

with:

$$Z_{r_{N+1}} = Z_{apex_v} + b_v \quad (6-332)$$

The lifting surface (also applicable to the vertical tail) area is:

$$S_{l.s.} = (c_{r_{l.s.}} + c_{t_{l.s.}}) \frac{b_{l.s.}}{2} \quad (6-333)$$

The leading edge sweep angle of the equivalent lifting surface is determined with:

$$\Lambda_{LE_{l.s.}} = \tan^{-1} \left\{ \frac{2(X_{t_N} - X_{r_1}) \left(\frac{b_{l.s.}}{2} - Y_{r_1} \right) - \sum_{i=1}^N (X_{r_i} + X_{t_i} - 2X_{r_i}) (Y_{r_{i+1}} - Y_{r_i})}{\left(\frac{b_{l.s.}}{2} - Y_{r_1} \right)^2} \right\} \quad (6-334)$$

For the vertical tail, the leading edge sweep angle is determined from:

$$\Lambda_{LE_v} = \tan^{-1} \left\{ \frac{2(X_{t_N} - X_{r_1}) (b_v + Z_{apex_v} - Z_{r_1}) - \sum_{i=1}^N (X_{r_i} + X_{t_i} - 2X_{r_i}) (Z_{r_{i+1}} - Z_{r_i})}{(b_v + Z_{apex_v} - Z_{r_1})^2} \right\} \quad (6-335)$$

The X-coordinate of the lifting surface apex is determined from:

$$X_{apex_{l.s.}} = X_{t_N} - \frac{b_{l.s.}}{2} \tan \Lambda_{LE_{l.s.}} \quad (6-336)$$

For a vertical tail:

$$X_{apex_v} = X_{t_N} - b_v \tan \Lambda_{LE_v} \quad (6-337)$$

The aspect ratio, taper ratio, mean geometric chord, spanwise locations of mean geometric chord, sweep angles are as defined in the previous section.

6.8.2 Volume Coefficient

The horizontal tail volume coefficient is given by:

$$\bar{V}_h = \frac{S_h (X_{ach} - X_{cg})}{S_w \bar{c}_w} \quad (6-338)$$

The canard volume coefficient is given by:

$$\bar{V}_c = \frac{S_c (X_{cg} - X_{ac_c})}{S_w \bar{c}_w} \quad (6-339)$$

The vertical tail volume coefficient is given by:

$$\bar{V}_v = \frac{S_v (X_{ac_v} - X_{cg})}{S_w b_w} \quad (6-340)$$

The V-Tail volume coefficient is given by:

$$\bar{V}_{vee} = \frac{S_{vee} (X_{ac_{vee}} - X_{cg})}{S_w \bar{c}_w} \quad (6-341)$$

The volume coefficients listed above are based on center of gravity and aerodynamic center of the lifting surface. The geometric volume coefficients are as follows:

The horizontal tail geometric volume coefficient is given by:

$$\bar{V}_{hg} = \frac{S_h l_h}{S_w \bar{c}_w} \quad (6-342)$$

where the x-distance between the horizontal tail and wing mean geometric chord quarter chord points is determined from:

$$l_h = X_{apex_h} + x_{mgc_h} + \frac{\bar{c}_h}{4} - X_{apex_w} - x_{mgc_w} - \frac{\bar{c}_w}{4} \quad (6-343)$$

The canard geometric volume coefficient is given by:

$$\bar{V}_{cg} = \frac{S_c l_c}{S_w \bar{c}_w} \quad (6-344)$$

where:

$$l_c = X_{apex_w} + x_{mgc_w} + \frac{\bar{c}_w}{4} - X_{apex_c} - x_{mgc_c} - \frac{\bar{c}_c}{4} \quad (6-345)$$

The vertical tail geometric volume coefficient is given by:

$$\bar{V}_{vg} = \frac{S_v l_v}{S_w b_w} \quad (6-346)$$

where:

$$l_v = X_{apex_v} + x_{mgc_v} + \frac{\bar{c}_v}{4} - X_{apex_w} - x_{mgc_w} - \frac{\bar{c}_w}{4} \quad (6-347)$$

The V-Tail geometric volume coefficient is given by:

$$\bar{V}_{veeg} = \frac{S_{vee}l_{vee}}{S_w\bar{c}_w} \quad (6-348)$$

where:

$$l_{vee} = X_{apex_{vee}} + x_{mgc_{vee}} + \frac{\bar{c}_{vee}}{4} - X_{apex_w} - x_{mgc_w} - \frac{\bar{c}_w}{4} \quad (6-349)$$

6.8.3 Fuel Volume

The methods are based on Ref. 15. The following assumptions are made:

- a. The wing fuel is carried in a wet wing. A wet wing is a wing that has no separate fuel tanks. The wing torque box, which is the part of the wing structure between the front and the rear spar, is sealed and forms the fuel tank.
- b. No fuel can be carried beyond the 85 percent span point. This is to prevent lightning strikes, which are most likely to hit the airplane extremities, from starting an in-flight fire. Fuel may be carried in wingtips or in tiptanks, provided the skin is locally beefed up to assure that lightning strikes have enough metal to disperse. It is up to the user to determine the extra fuel volume in such case.

The wing maximum fuel tank volume is computed from:

$$V_{F_w} = F_F \frac{0.54}{(1 + \lambda_w)^2} \left(\frac{S_w^2}{b_w} \right) \left[\left(\frac{t}{c} \right)_{r_w} + \lambda_w \sqrt{\left(\frac{t}{c} \right)_{r_w} \left(\frac{t}{c} \right)_{t_w}} + \lambda_w^2 \left(\frac{t}{c} \right)_{t_w} \right] \quad (6-350)$$

where:

$$F_F = 1 - F_{F \text{ expansion}} \quad (6-351)$$

The maximum fuel weight limited by the fuel tank volume is obtained from:

$$W_{F_{max_w}} = \left(\frac{1 \text{ gallon}}{0.13368 \text{ ft}^3} \right) \rho_F V_{F_w} \quad (6-352)$$

The program always checks that $W_{F_{max_w}} > W_{F_{max}}$.

If the above condition is not fulfilled, it is up to the user to enlarge the wing or to place the excess fuel somewhere else.

6.8.4 Bodies

All bodies are described by cross-sections along the body axis (stations). Each cross-section consists of four conic sections. Each conic is defined by three sets of coordinates and a rho-value.

Figure 6.15 shows the definition of the conics and coordinates.

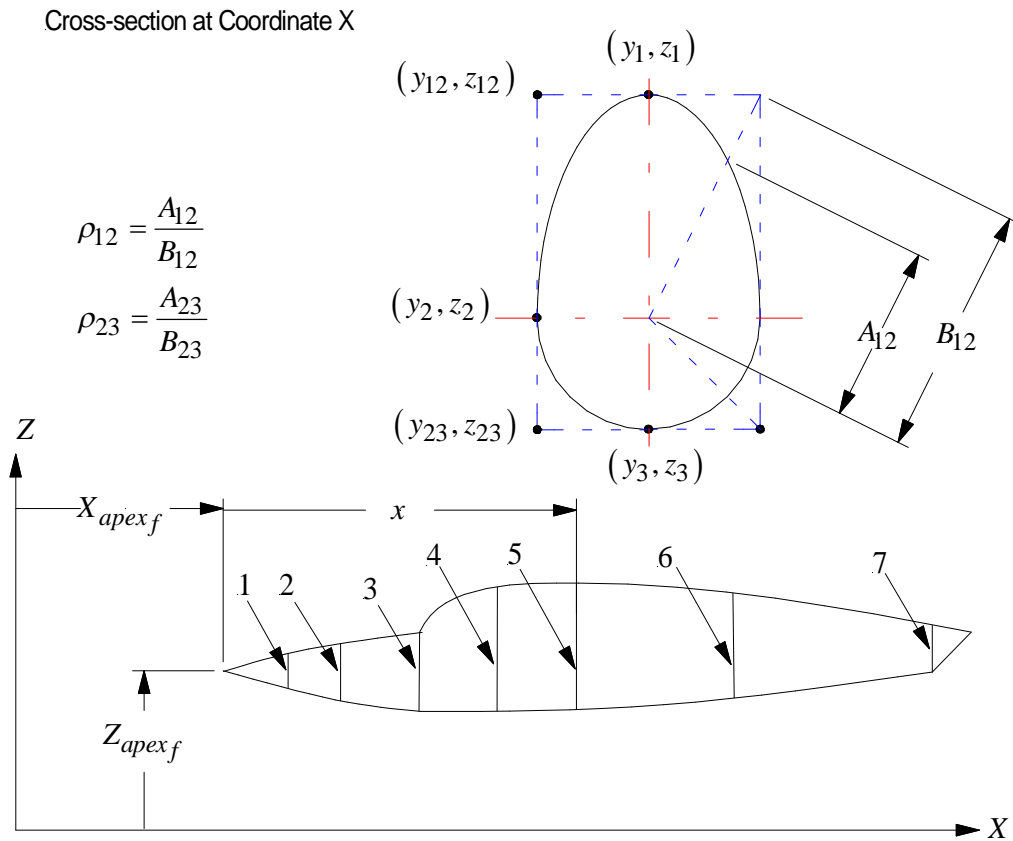


Figure 6.15 Cross-section Definition

x is the X-location of the cross-section with respect to the component apex (nose) or absolute X-location, depending on the Coordinate System Definition chosen by the user.

y_1, z_1 are the Y- and Z-location of the cross-section upper section point 1 with respect to the component apex (nose) or absolute X-location, depending on the Coordinate System Definition chosen by the user.

y_2, z_2 are the Y- and Z-location of the cross-section point 2 with respect to the component apex (nose) or absolute X-location, depending on the Coordinate System Definition chosen by the user.

y_3, z_3 are the Y- and Z-location of the cross-section lower section point 3 with respect to the component apex (nose) or absolute X-location, depending on the Coordinate System Definition chosen by the user.

y_{12}, z_{12} are the Y- and Z-location of the cross-section upper section control point with respect to the component apex (nose) or absolute X-location, depending on the Coordinate System Definition chosen by the user.

ρ_{12} is the cross section upper section control point weight factor.

y_{23}, z_{23} are the Y- and Z-location of the cross-section lower section control point with respect to the component apex (nose) or absolute X-location, depending on the Coordinate System Definition chosen by the user.

ρ_{23} is the cross section lower section control point weight factor.

In parametric format the top part conic is described by (Ref. 50, 183):

$$y = \frac{y_1 t^2 + 2y_{12} t(1-t)\rho_{12} + y_2 (1-t)^2}{t^2 + 2t(1-t)\rho_{12} + (1-t)^2} \quad (6-353)$$

$$z = \frac{z_1 t^2 + 2z_{12} t(1-t)\rho_{12} + z_2 (1-t)^2}{t^2 + 2t(1-t)\rho_{12} + (1-t)^2} \quad (6-354)$$

and the bottom part conic is described by:

$$y = \frac{y_2 t^2 + 2y_{23} t(1-t)\rho_{23} + y_3(1-t)^2}{t^2 + 2t(1-t)\rho_{23} + (1-t)^2} \quad (6-355)$$

$$z = \frac{z_2 t^2 + 2z_{23} t(1-t)\rho_{23} + z_3(1-t)^2}{t^2 + 2t(1-t)\rho_{23} + (1-t)^2} \quad (6-356)$$

Where t varies from 0 to 1 along the curve.

The Coordinate System Definition is defined as where the (0,0,0) reference point is located. For the Airplane Coordinate System, the reference point is located at the absolute (0,0,0) of the user coordinate system. For the Fuselage, Nacelles, Stores, Tailbooms Coordinate System, the reference point is located at the apex points of the component.

6.9 Class II Analysis Methods

6.9.1 Class II Drag

The Class II Drag (Ref. 6) is composed of the zero-lift drag and drag due to lift of each component. The following drag components are accounted for:

- Wing Drag
- Horizontal Tail Drag
- V-Tail Drag
- Canard Drag
- Vertical Tail Drag
- Fuselage Drag
- Flap Drag
- Canopy Drag
- Float Drag
- Gear Drag
- Inlet Drag
- Nozzle Drag
- Pylon Drag
- Speed Brake Drag
- Store Drag
- Windmilling Drag
- Windshield Drag
- Tailboom Drag
- Trim Drag
- Miscellaneous Drag

Most methods are a direct adaptation of the methods on Airplane Design Part VI (Ref. 6). Components that are not described or where different methods are used, are described in the following sections. The methods are divided into a subsonic regime ($M < 0.6$), transonic regime ($0.6 < M < 1.2$) and supersonic regime ($M > 1.2$). All procedures and functions used to determine drag are programmed in two dll's (see Appendix E): DragCoefficient.dll and FuselageDrag.dll.

6.9.1.1 Tailboom Drag

The tailboom drag is based on the fuselage drag as described in Ref. 6.

6.9.1.2 Trim Drag

The total trim drag coefficient is determined from:

$$C_{D_{trim}} = \Delta C_{D_{trim_{prof}}} \quad (6-357)$$

The trim drag coefficient due to the profile drag is determined by treating each control surface as a plain flap:

$$\begin{aligned}
\Delta C_{D_{trim_{prof}}} &= \left(\Delta C_{D_p} \right)_{\Lambda_c/4_h=0} \cos \Lambda_c/4_h \frac{S_{ef}}{S_h} \frac{S_h}{S_w} + \left(\Delta C_{D_p} \right)_{\Lambda_c/4_c=0} \cos \Lambda_c/4_c \frac{S_{cf}}{S_c} \frac{S_c}{S_w} \\
&+ \left(\Delta C_{D_p} \right)_{\Lambda_c/4_{vee}=0} \cos \Lambda_c/4_{vee} \frac{S_{veef}}{S_{vee}} \frac{S_{vee}}{S_w} \\
&+ \left(\Delta C_{D_p} \right)_{\Lambda_c/4_v=0} \cos \Lambda_c/4_v \frac{S_{vf}}{S_v} \frac{S_v}{S_w} \\
&+ \left(\Delta C_{D_p} \right)_{\Lambda_c/4_w=0} \cos \Lambda_c/4_w \frac{S_{wf}}{S_w}
\end{aligned} \tag{6-358}$$

The profile drag coefficient due to the lifting surface control surface, is determined from Figure 4.44 in Airplane Design Part VI (Ref. 6):

$$\left(\Delta C_{D_p} \right)_{\Lambda_c/4_{l.s.}=0} = f \left(\delta_{control}, \frac{c_{control}}{c_{surface}} \right) \tag{6-359}$$

The horizontal tail flapped area due to elevator is defined in Figure 4.72 in Ref. 6:

$$S_{ef} = f \left(\eta_{ie}, \eta_{oe}, \lambda_h \right) \tag{6-360}$$

The canard flapped area due to canardvator is defined in Figure 4.72 in Ref. 6:

$$S_{cf} = f \left(\eta_{ic}, \eta_{oc}, \lambda_c \right) \tag{6-361}$$

The V-Tail flapped area due to ruddervator is defined in Figure 4.72 in Ref. 6:

$$S_{rvf} = f \left(\eta_{ivr}, \eta_{orv}, \lambda_{vee} \right) \tag{6-362}$$

The vertical tail flapped area due to rudder is defined in Figure 4.72 in Ref. 6:

$$S_{rf} = f(\eta_{ir}, \eta_{or}, \lambda_v) \quad (6-363)$$

The wing flapped area due to elevon is defined in Figure 4.72 in Ref. 6:

$$S_{elf} = f(\eta_{iel}, \eta_{oel}, \lambda_w) \quad (6-364)$$

6.9.1.3 Miscellaneous Drag

Other causes of drag such as struts, antennas, or other items may be added to the Class II drag calculation. Miscellaneous drag may be calculated as a function of airplane lift coefficient, angle of attack, or both.

The total miscellaneous drag is calculated from:

$$C_{D_{misc}} = C_{D_{misc}C_{L1}} + C_{D_{misc}\alpha} \quad (6-365)$$

Miscellaneous drag as a function of the airplane lift coefficient is determined from:

$$C_{D_{misc}C_{L1}} = C_{D_{o_{misc}}} + B_{CD_{1misc}} C_{L1} + B_{CD_{2misc}} C_{L1}^2 + B_{CD_{3misc}} C_{L1}^3 + B_{CD_{4misc}} C_{L1}^4 + B_{CD_{5misc}} C_{L1}^5 \quad (6-366)$$

Miscellaneous drag as a function of the airplane angle of attack is calculated from:

$$C_{D_{misc\alpha}} = C_{D_{0misc}} + B_{CD_{1misc}} \alpha + B_{CD_{2misc}} \alpha^2 + B_{CD_{3misc}} \alpha^3 + B_{CD_{4misc}} \alpha^4 + B_{CD_{5misc}} \alpha^5 \quad (6-367)$$

This method is the same for all speed regimes.

6.9.1.4 Total Drag

The total airplane drag coefficient is broken down into the following components:

$$C_{D_t} = C_{D_{0w}} + C_{D_{Lw}} + C_{D_{0h}} + C_{D_{Lh}} + C_{D_{0v}} + C_{D_{Lv}} + C_{D_{0c}} + C_{D_{Lc}} + C_{D_{0f}} + C_{D_{Lf}} + C_{D_p} + C_{D_n} + C_{D_{flap}} + C_{D_{slot}} + C_{D_{sl}} + C_{D_{fixed}} + C_{D_{retract}} + C_{D_{canopy}} + C_{D_{wx}} + C_{D_{store}} + C_{D_{trim}} + C_{D_{sp}} + C_{D_{wm}} + C_{D_{prop}} + C_{D_{misc}} \quad (6-368)$$

The method is the same for all speed regimes.

6.9.2 Class II Weights

The following methods based on Ref. 5, are used in the calculation of the Class II weights:

- Cessna Method: This method is used for small, relatively low performance type airplanes with max. speeds below 200 kts.
- USAF Method: This method is used for light and utility type airplanes with performance up to 300 kts.
- Torenbeek Method: This method is used for light transport airplanes with take-off weights below 12,500 lb.
- GD Method: This method is used for airplanes with the following parameter ranges:
 - Maximum wing thickness ratio: 0.08 to 0.15
 - Maximum aspect ratio: 4 to 12
 - Maximum mach number at sea level: 0.4 to 0.8

The weight estimation equations for the weight components are available for the following types of airplanes:

- General Aviation Airplanes
- Commercial Transport Airplanes
- Military Patrol, Bomb and Transport Airplanes
- Fighter and Attack Airplanes

The Class II weight estimating method focuses on estimating the components of the airplane empty weight, defined as:

$$W_E = W_{structure} + W_{pp} + W_{fix} \quad (6-369)$$

The Class II take-off weight is then calculated from:

$$W_{TO} = \frac{W_E + W_{PL} + W_{PLexp} - W_{Frefuel}}{M_{ff} (1 + M_{Fres}) - M_{Fres} - M_{tfo}} \quad (6-370)$$

Class II Structure Weight, Class II Powerplant Weight and Class II Fixed Equipment Weight are based on the methods described in Ref. 5.

With an initial estimated take-off weight, the component weights are calculated. The sum of the component weights defines a new empty weight, which in turn gives a Class II take-off weight:

$$W_{TOII} = \frac{W_{fix} + W_{structure} + W_{pp} + W_{crew} + W_{PL} + W_{PLexp} - W_{Frefuel}}{M_{ff} (1 + M_{Fres}) - M_{Fres} - M_{tfo}} \quad (6-371)$$

Since the fixed equipment weight, the structure weight and the powerplant weight vary with take-off weight, these weights need to be recalculated. That again, yields a new Class II take-off weight. The program iterates until the difference between the take-off weight resulted from the new component weights and the take-off weight used to compute those component weights is within 5% of the previous step. This

iteration is not yet implemented in AAA-AML. Several figures used in the calculations of class II weights are programmed in the dll: WeightII.dll (see Appendix E).

6.10 Atmospheric Properties

The theory used to calculate atmospheric properties is based on References 16 and 11. The methods are programmed in the dll: Atmosphere.dll (See Appendix E). The earth's atmosphere consists of four regions, troposphere, stratosphere, ionosphere and exosphere. The International Civil Aviation Organization (ICAO) has established standard properties of the atmosphere. The U.S. Standard Atmosphere is identical to the ICAO atmosphere for altitudes below 65,617 ft. According to the standard atmosphere the sea-level properties are as follows (Ref. 11):

$$g_o = 32.17 \text{ ft/s}^2 = 9.806 \text{ m/s}^2$$

$$P_o = 29.92 \text{ in Hg} = 2,116.2 \text{ lb/ft}^2 = 101,325 \text{ N/m}^2$$

$$T_o = 59 \text{ }^\circ\text{F} = 518.69 \text{ }^\circ\text{R} = 288.15 \text{ K}$$

$$\rho_o = 0.002377 \text{ slug/ft}^3 = 1.225 \text{ Kg/m}^3$$

Properties at the Tropopause (36,089 ft) are:

$$P_1 = 472.7 \text{ lb/ft}^2 = 22,632 \text{ N/m}^2$$

$$T_1 = 390 \text{ }^\circ\text{R} = 216.65 \text{ K}$$

Figure 6.16 shows how the atmospheric properties vary with altitude.

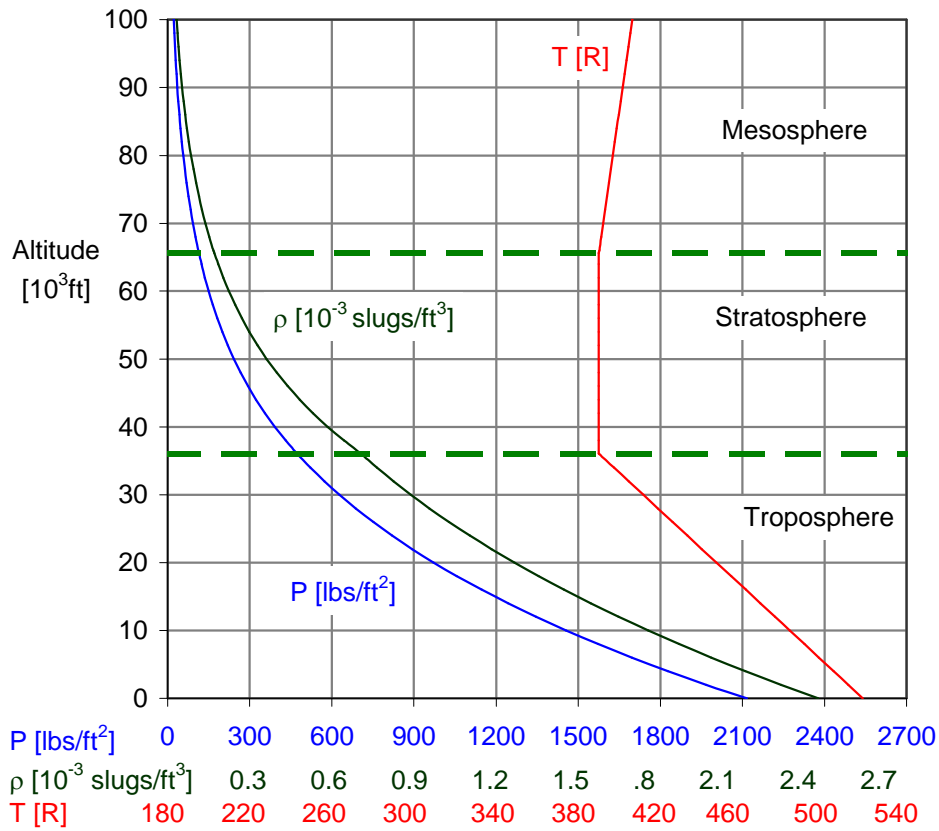


Figure 6.16 Atmospheric Properties in British Units

6.10.1 Temperature in Standard Atmosphere

The temperature is calculated as function of the geometric altitude, h , and the temperature offset, ΔT .

All theory is based on the geopotential altitude, H , which is calculated from the geometric altitude with:

$$H = \frac{20855532h}{20855532 + h} \quad (6-372)$$

For altitudes < 36,089 ft (11,000 m):

The atmospheric temperature is determined from:

$$T = T_B + LH_P \quad (6-373)$$

The pressure altitude is iteratively calculated from:

$$H_P = H - \frac{\Delta T}{L} \ln \left(\frac{T_o + LH_P}{T_B - \Delta T} \right) \quad (6-374)$$

For altitudes > 36,089 ft (11,000 m) and < 65,617 ft (20,000 m):

The atmospheric temperature is determined from:

$$T = T_B + \Delta T \quad (6-375)$$

The pressure altitude is calculated from:

$$H_P = H_{P_{TP}} + (H - H_{TP}) \frac{T_{TP} - \Delta T}{T_{TP}} \quad (6-376)$$

with: $H_{P_{TP}} = 36,089 \text{ ft}$

The tropopause temperature can be calculated with:

$$T_{TP} = T_B + \Delta T \quad (6-377)$$

The geopotential altitude H_{TP} , for the pressure altitude $H_{P_{TP}}$, is solved from:

$$H_{TP} = H_{P_{TP}} + \frac{\Delta T}{L} \ln \left(\frac{T_o + LH_{P_{TP}}}{T_o} \right) \quad (6-378)$$

where:

British Units	H < 36,089 ft	36,089 ft < H < 65,617 ft
H_B	0.0 ft	36,089 ft
L	-0.0036 °R/ft	0.0 °R/ft
P_B	2,116.2 lb/ft ²	472.7 lb/ft ²
T_B	518.69 °R	390.0 °R

SI Units	H < 11,000 m	11,000 m < H < 20,000 m
H_B	0.0 m	11,000 m
L	-0.0065 K/m	0.0 K/m
P_B	101,325 N/m ²	22,632 N/m ²
T_B	288.15 K	216.65 K

The temperature ratio is calculated with:

$$\theta = \frac{T}{T_o} \quad (6-379)$$

6.10.2 Pressure in Standard Atmosphere

The pressure is calculated as function of the altitude, H , and the temperature offset, ΔT .

For altitudes < 36,089 ft (11,000 m), the pressure at altitude is determined from:

$$P = P_o \left(\frac{T - \Delta T}{T_o} \right)^{\frac{-g}{RL}} \quad (6-380)$$

with: $R = 1716.49 \text{ ft}^2/\text{°R/s}$

For altitudes $> 36,089 \text{ ft}$ (11,000 m) and $< 65,617 \text{ ft}$ (20,000 m), the pressure at altitude is determined from:

$$P = P_1 e^{-g \left(\frac{HP - 36,089}{RT_1} \right)} \quad (6-381)$$

where P_1 and T_1 are the pressure and temperature at the pressure altitude of the Tropopause (36,089 ft).

The pressure ratio is determined from:

$$\delta = \frac{P}{P_o} \quad (6-382)$$

6.10.3 Density in Standard Atmosphere

The density at altitude is determined from:

$$\rho = \frac{P}{RT} \quad (6-383)$$

The density ratio is calculated from:

$$\sigma = \frac{\rho}{\rho_0} \quad (6-384)$$

6.10.4 Speed of Sound in Standard Atmosphere

The local speed of sound is calculated from:

$$a = \sqrt{\gamma RT} \quad (6-385)$$

with: $\gamma = 1.4$

6.10.5 Kinematic Viscosity in Standard Atmosphere

The kinematic viscosity is calculated from:

$$v = \frac{\mu}{\rho} \quad (6-386)$$

The coefficient of viscosity is given by:

$$\mu = 0.3170 \times 10^{-10} T^{3/2} \frac{734.7}{T + 216} \left(\frac{\text{lb} \cdot \text{sec}}{\text{ft}^2}, T \text{ in } ^\circ\text{R} \right) \quad (6-387)$$

or

$$\mu = 1.458 \times 10^{-6} T^{3/2} \frac{1}{T + 110.4} \left(\frac{\text{N} \cdot \text{sec}}{\text{m}^2}, T \text{ in } ^\circ\text{K} \right) \quad (6-388)$$

7 Implementation and Testing of AAA and AAA-AML

The project consisted of development of AAA and AAA-AML. The third generation of AAA has been under development since 1994 (See Section 2.1.8) and has been released as a commercial product by DARcorporation. The current version is 3.1. Many methods from AAA have then been re-used in AAA-AML either through direct implementation by translation from Delphi (Ref. 188) to AML or in the form of function and procedure calls in dynamic link libraries (dll). The following sections show the AAA and AAA-AML implementation and testing.

7.1 Advanced Aircraft Analysis

The Advanced Aircraft Analysis (AAA) software has been under development for many years (Sections 2.1.6, 2.1.7, 2.1.8). The author is the main architect and software developer. AAA is currently written in Borland Delphi (Ref. 188). Delphi is an object-oriented development environment for the Windows platform. AAA makes extensive use of the object-oriented technology. AAA is heavily focused on methods.

The main architecture is driven by the design process as outlined in Section 5. The focus is on methods such as weights, aerodynamics, geometry, cost, stability and control, dynamics, propulsion, structures and loads. These are the main modules of the software. It is up to the user (designer) to decide which modules to use and in what order. The program does not force the user into a certain design path. The

object-oriented structure is then primarily method driven. Each module has a path that leads to a calculation (i.e the method).

7.1.1 Structure of the Software

The software uses windows, toolbars and dialog boxes to communicate with the user.

This section describes the structural elements of the software, their purpose and their functionality. The following elements of the software are described in this section:

- Windows and command bars
- Toolbars
- Menu bar

7.1.1.1 Windows and Command Bars

The software is started by selecting the program icon in the Airplane Design and Analysis program group in Windows. When the program is started, the main window (Figure 7.1) is displayed. This window is open as long as the program is running.

The main window contains a Windows menu bar at the top, the main menu of application modules, the software toolbars and the status bar. The status bar is located at the bottom of the main window and contains the company name and project name as specified by the user, and the current date and time. When an element of the status bar is double clicked with the mouse button, a dialog box appears to change the content or format of that element.

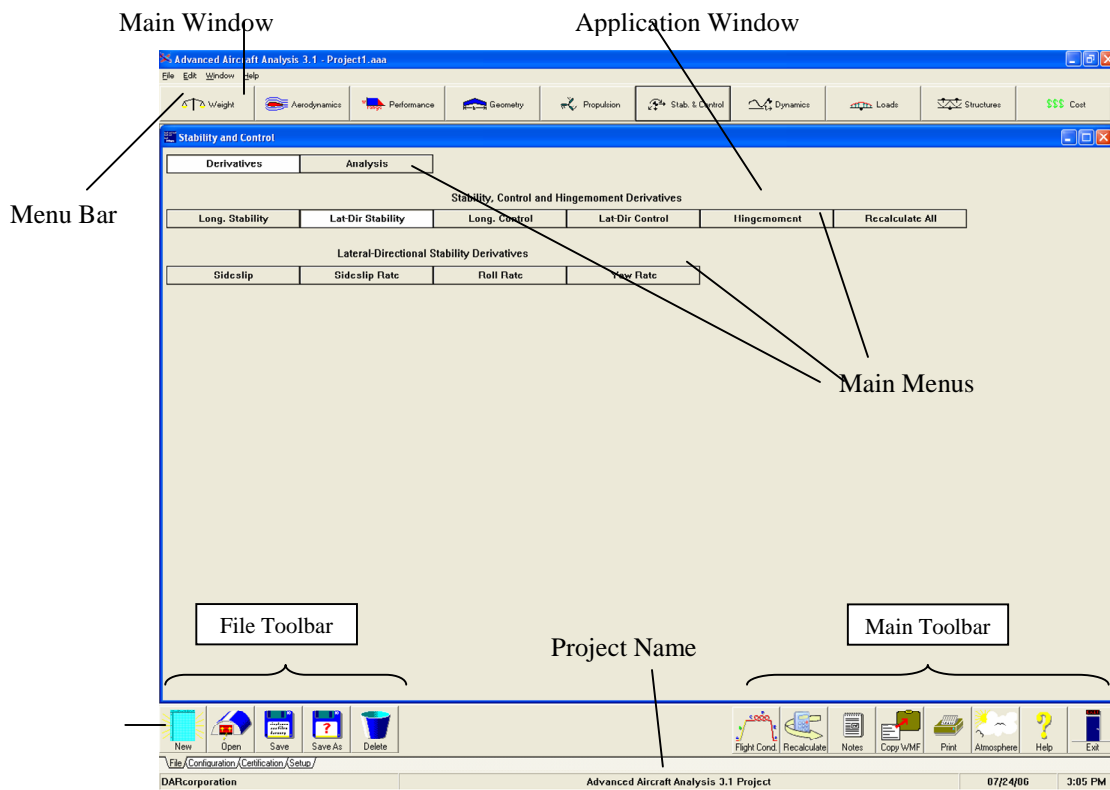


Figure 7.1 The AAA Main Window

Three types of windows can be contained within the main window. There are application windows, input/output windows and plot windows. Application windows, input/output windows and plot windows are child windows and are always displayed within the main window. Descriptions of each of these window types and their components are presented in the following subsections:

- 7.1.1.1.1 Application windows
- 7.1.1.1.2 Input/Output windows
- 7.1.1.1.3 Input/Output window command bar
- 7.1.1.1.4 Plot windows
- 7.1.1.1.5 Plot window command bar

7.1.1.1.1 Application Windows

When one of the application buttons at the top of the main window is selected, the corresponding application window is displayed (see Figure 7.1). The application window contains menu button selections that allow the user to select a calculation to be performed. The software uses a flow chart method for the user interface as shown in Figure 7.1. This allows the user to see the path selected in reaching a certain location.

The software consists of various calculation modules that can be accessed through the application windows. Table 7-1 and Table 7-2 present the application buttons in the main window and the calculation modules accessed by that application module.

Table 7-1 Application Modules of the Program

Application Button	Calculation Modules
Weight	<ul style="list-style-type: none"> • Class I take-off weight and fuel calculation • Class I and Class II weight & balance analysis and center of gravity calculation for current loading
Aerodynamics	<ul style="list-style-type: none"> • Class I wing and high lift devices design • Class I lifting surface and airplane lift calculation • Class I and Class II drag polar calculation • Lift, drag and moment distributions over a lifting surface • Airplane aerodynamic center calculation • Power effects on airplane lift and pitching moment • Ground effects of airplane lift and pitching moment • Dynamic Pressure Ratio
Performance	<ul style="list-style-type: none"> • Class I performance sizing • Class II performance analysis
Geometry	<ul style="list-style-type: none"> • Class I wing, fuselage and empennage layout • Aero-Pack Interface • Lateral tip-over analysis • Scale
Propulsion	<ul style="list-style-type: none"> • Class I installed thrust/power calculation • Inlet/Nozzle sizing

Table 7-2 Application Modules of the Program Continued

Application Button	Calculation Modules
Stab. & Control	<ul style="list-style-type: none"> • Longitudinal and lateral-directional stability and control derivatives, including thrust/power • Control surface and trim tab hinge moment derivatives • Class I stability & control empennage sizing • Class II longitudinal and lateral-directional trim, including stick force and pedal force calculations
Dynamics	<ul style="list-style-type: none"> • Open loop dynamics analysis • Automatic control system analysis
Loads	<ul style="list-style-type: none"> • Velocity-Load Factor (V-n) diagram generation • Structural component internal load estimation
Structures	<ul style="list-style-type: none"> • Material property tables • Class I component structural sizing
Cost	<ul style="list-style-type: none"> • Airplane program cost estimation

Clicking on the appropriate buttons in the application window activates each module.

When the menu buttons leading to a calculation module have been selected, the input/output window for that calculation module is opened.

7.1.1.1.2 Input/Output Windows

The input/output window opens after selecting the type of calculation to be performed. The input/output window contains numeric data necessary to perform a calculation. For some calculations, information about the airplane configuration and airplane certification type are required so that the correct calculation method can be used. Before the input/output window is displayed, the program will display a dialog box allowing the user to specify configuration choices. For example, the program will ask the user to define empennage surfaces before the input/output window for longitudinal stability calculations is displayed.

Input/output windows contain a command bar at the top of the window, an input group and an output group (See Figure 7.2). The command bar contains a menu of buttons, one for each command available to the input/output window. The input/output window command bar is described in Subsection 7.1.1.1.3.

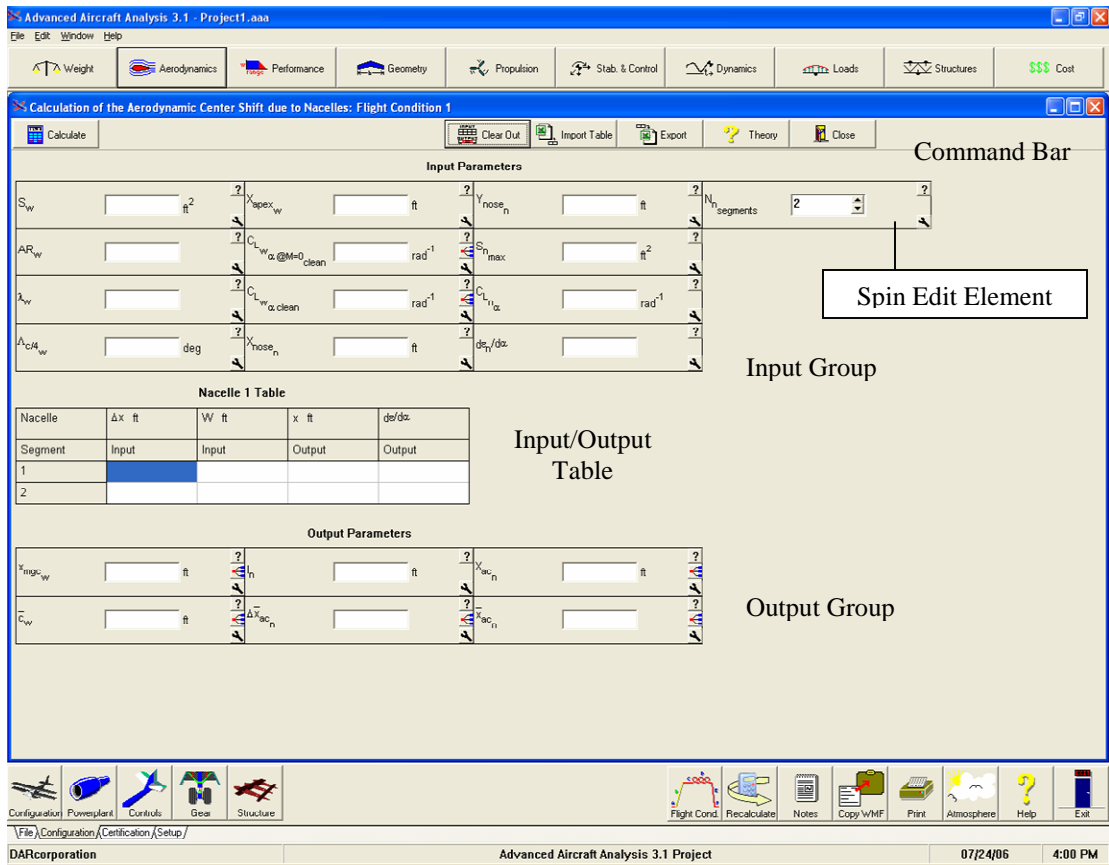
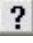




Figure 7.2 Input/Output Window

Input/output windows contain one or more input/output elements. Figure 7.3 shows an input/output element. The input/output element contains the following:

- Variable Symbol
- Edit Box for keyboard input
- Unit (SI or British)
- Info  button
- Go To  button
- Work Pad  button

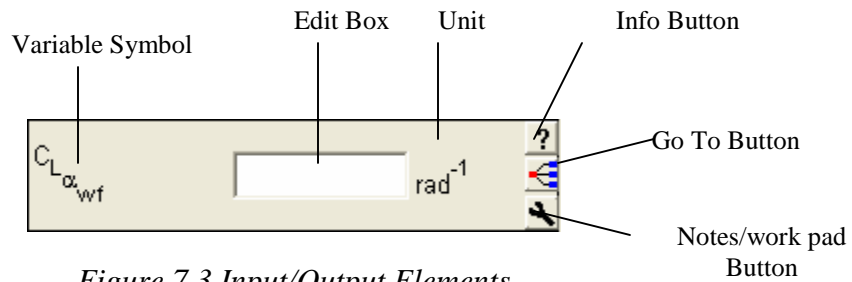


Figure 7.3 Input/Output Elements

When the cursor is positioned over an input/output element, a brief description of the parameter is displayed. When the cursor is located over the edit box of the input/output element, it appears as a vertical bar. When the edit box is selected with the left mouse button, a vertical insertion bar appears in the edit box, and the keyboard can be used to type numeric input. When the cursor is positioned outside the edit box, it appears as a small calculator. When the left mouse button is clicked while the cursor appears as a calculator, the program calculator is opened.

When the **Info** button is clicked, an information window is displayed for that variable. The information window contains a definition of the variable with graphics and suggested values when available.

Figure 7.4 shows the Notes/Work Pad window. When the **Work Pad** button is clicked, this window is displayed and allows the user to type notes about that variable. These notes are specific to that variable and will be saved with the project.

Notes may also be designated one of six colors to identify certain stages of the design process. This is done by simply clicking on the desired color in the “Set Current Note Color” box of the Work Pad Window. If a color is not selected from this portion of the Work Pad Window, the default color will be used with that particular note. If notes have been entered for a variable, the **Work Pad** button will change colors to the default notes color. The default notes color can be set or changed in the Program Options window under Setup. The Work Pad Window also has options to allow the user to lock the value of the variable so that it does not get recalculated, export the value to an ASCII text file, or select whether or not the variable is flight condition dependent. The “Default Unit” box in the Work Pad Window allows the user to change the units for the variable associated with the window without changing the default units for the entire project.

The **Go To** button appears next to parameters which have been calculated by AAA in another module. Selecting the **Go To** button will display the module in which the corresponding parameter was calculated. This allows the user to see what variables were used in producing the parameter, and confirm its validity. Clicking on the **Go To** button a second time will return the user to the previous module.

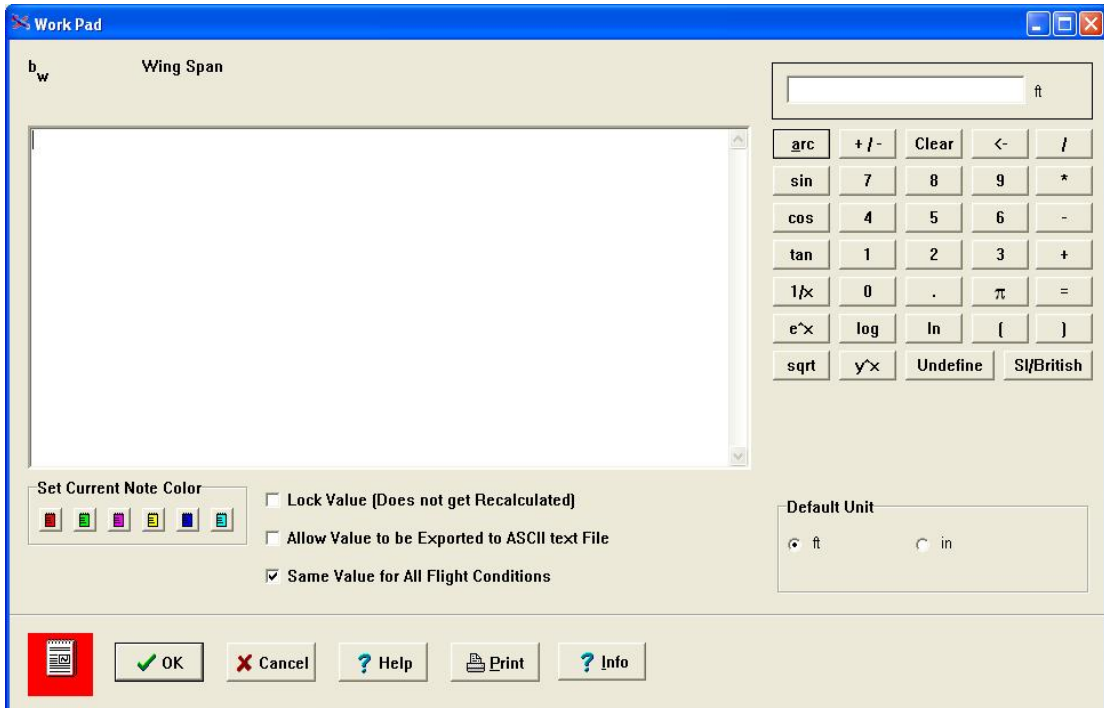


Figure 7.4 Work Pad Window

An input/output window can also contain a table for numeric input and output data (see Figure 7.2). Rows can be added to or subtracted from certain tables to account for multiple inputs of the same form. For example, the fuselage can be divided into two or more sections for moment calculations. Figure 7.2 shows an input/output window with a table for fuselage section input. The table can be resized (rows added or subtracted) using the spin edit element, which appears as the last element in the input menu (see Figure 7.2). The spin edit element is similar in appearance to an input/output element. The number of rows of a table can be changed by clicking on the arrows in the spin edit element.

The work pad window can be used to maintain notes of a particular project. This window can also be used to change the units of a specific parameter and maintain notes about the parameter (see Figure 7.4). The input menu of the input/output window may also contain a combo box element (see Figure 7.5). The combo box element is similar in appearance to an input/output element, but does not contain an edit box. The combo box element contains a list of choices that affect the calculation results. The list of choices is displayed by clicking on the arrow at the right side of the element and holding down the left mouse button. A choice can then be made by moving the cursor to the appropriate choice and releasing the mouse button.

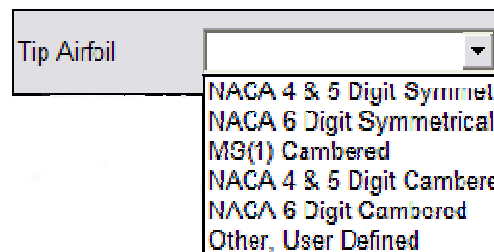


Figure 7.5 Combo Box Element

Most input/output windows contain an output group of elements showing the results of the calculation performed in the window. The output group can contain output elements or a table of values. The output results of some input/output windows can be displayed as a graph or plot. The plot of the output is presented in a plot window when the Plot button on the input/output window command bar is selected.












7.1.1.1.3 Input/Output Window Command Bar

The input/output window command bar is displayed at the top of the input/output window. The input/output window command bar is shown in Figure 7.6. Each button in the command bar represents an action that can be performed in the input/output window. A command bar button is not displayed if its action is not available for the particular input/output window. The Close button in the command bar closes the input/output window and is always displayed. The remaining buttons that can be displayed in the input/output command bar are shown and described in Table 7-3.



Figure 7.6 Input/Output Window Command Bar Buttons

Table 7-3 Input/Output Window Command Bar Functions

 Calculate	<p>Calculate: Using the specified input, the calculations for the input/output window are performed. The results of the calculations are displayed in the output parameters.</p>
 Plot	<p>Plot: Opens the corresponding Plot window when applicable.</p>
 Next Nacelle  Next Tailboom  Next Store  Next Float	<p>Next Item: If there are multiple tables of input (for example, tables for different nacelles, tailbooms and stores) needed for the calculation, the next table of parameters will be displayed. If the last table is currently displayed, the first table will be displayed after selecting this button.</p>
 Clear Out	<p>Clear Out: Allows the user to erase all output parameters in the output section of the calculation window.</p>
 Import Table	<p>Import: Imports an Excel file in the same format as the table in the active window</p>
 Export	<p>Export: Export input and output data to a text file (ASCII), or to an Excel Spreadsheet.</p>
 Theory	<p>Theory: Opens a Help window containing the calculation methods corresponding to the input/output window.</p>
 Close	<p>Close Window: Closes the input/output window. The window minimize button can be used to iconize the window if desired.</p>

7.1.1.1.4 Plot Windows

The plot window contains a graphical representation of a calculation in an input/output window. Figure 7.7 shows a plot window of a Class I drag polar of a jet-powered airplane. The plot window contains a command bar at the top.

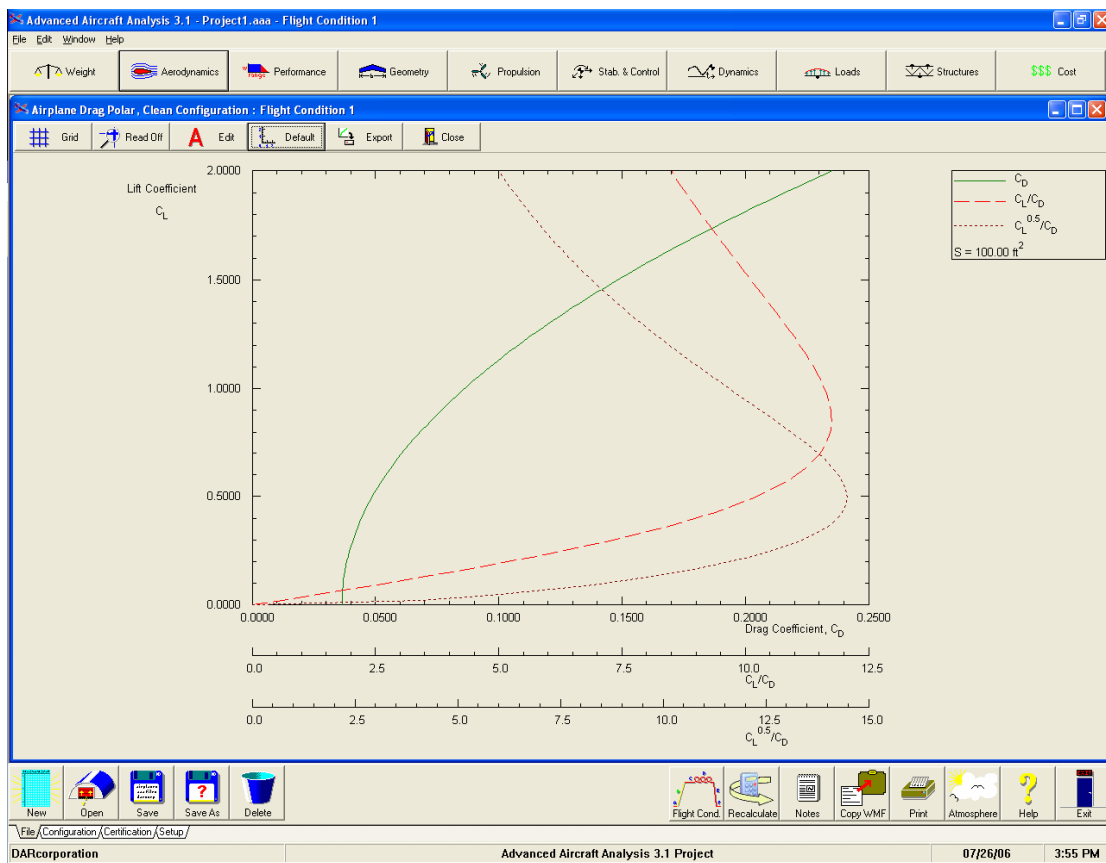


Figure 7.7 Plot Window

Most plot windows contain a legend at the top right corner of the window. Plot windows also contain one or more vertical and one or more horizontal axes. When the cursor is moved over an axis, it appears as horizontal and vertical axes. When the

cursor changes, the left mouse button can be double clicked, and a dialog will be displayed allowing the user to change the axes (see Figure 7.8). The minimum and maximum values, the major and minor divisions and the number of displayed decimal places can be changed. If the axes are expanded beyond the original range of the calculation, the plotted parameters will not be recalculated for the expanded range. To recalculate the parameters, the user should close the plot window, and increase the range of calculation in the input/output window. The first time the program creates a specific plot, the software calculates the plot area to encompass the entire graph. The values defining the first plot area will be saved and used the next time the plot is generated. If the axes are changed to redefine the plot area, those parameters will be saved and used the next time the graph is generated. The parameters are saved for every plot that can be generated in the software. The parameters are saved in the user database. The user can always have the program recalculate the plot area to show the entire graph by selecting the **Default** button in the plot window command bar.

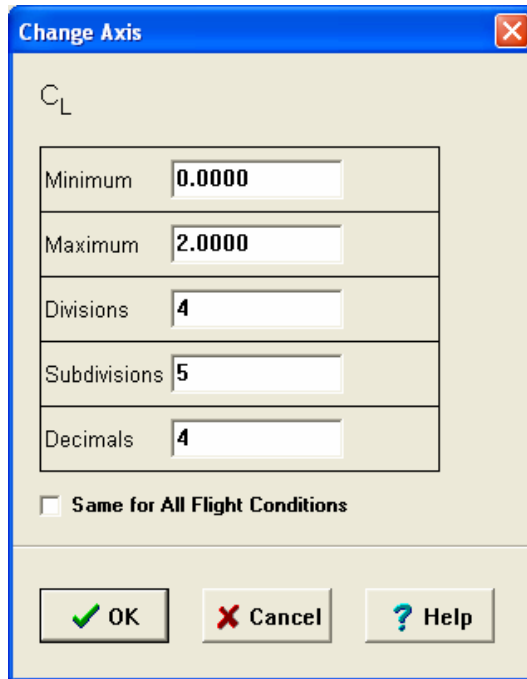


Figure 7.8 Change Axis Dialog

The functionality of the plot window command bar buttons is described in the next subsection.

7.1.1.1.5 Plot Window Command Bar

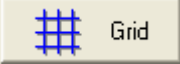
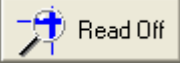


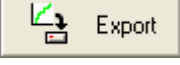

The plot window command bar is displayed at the top of the plot window. The plot window command bar is shown in Figure 7.9. Each button in the command bar represents an action that can be performed in the plot window. A command bar button is not displayed if its action is not available for the particular plot window. The Close button in the command bar closes the plot window and is always

displayed. The remaining buttons that can be displayed in the plot command bar are shown and described in Table 7-4.



Figure 7.9 Plot Window Command Bar Buttons

Table 7-4 Plot Window Command Bar Buttons

	<p>Grid: Allows the user to turn the axis grid on or off on the plot.</p>
	<p>Read Off Graph: Allows the user to read a value from the plot. When selected, the corresponding X and Y coordinates are displayed when the user positions the cross hairs on the plot by holding down the left mouse button. The cross hairs will be set at the instant that the mouse button is released.</p>
	<p>Edit: Allows the user to modify the font of all text displayed on the plot window.</p>
	<p>Default: Recalculates the axes so that the whole graph will show up on the plot window.</p>
	<p>Export: Export input and output data to a text file (ASCII), or to an Excel Spreadsheet.</p>
	<p>Close: Closes the plot window. The window minimize button can be used to iconize the window if desired.</p>

7.1.1.2 Toolbars

The program main window contains five toolbars located above the status bar (see Figure 7.1). The main toolbar is located on the right and is always visible. The four remaining toolbars can be displayed by clicking on the corresponding tab underneath the currently displayed toolbar on the left side of the main window. The five toolbars are described in the following subsections:

- 7.1.1.2.1 Main toolbar (see Figure 7.1)
- 7.1.1.2.2 File toolbar, displayed by clicking on the File tab (see Figure 7.1)
- 7.1.1.2.3 Configuration toolbar, displayed by clicking on the Configuration tab
- 7.1.1.2.4 Certification toolbar, displayed by clicking on the Certification tab
- 7.1.1.2.5 Setup toolbar, displayed by clicking on the Setup tab


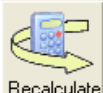






7.1.1.2.1 Main Toolbar

The main toolbar (Figure 7.10) consists of seven fixed bitmap buttons at the bottom right of the main window. The main toolbar supplies general functions needed throughout the program. The functionality of the buttons in the main toolbar is described in Table 7-5.



Figure 7.10 Main Toolbar

Table 7-5 Toolbar Buttons

 <p>Flight Cond.</p>	<p>Flight Condition: Set and define each flight condition to be included in the analysis. An airplane project can have up to 95 flight conditions defined.</p>
 <p>Recalculate</p>	<p>Recalculate: Calculates the output parameters of different modules for selected flight conditions.</p>
 <p>Notes</p>	<p>Notes: Record general notes about the current project. Notes are saved with the project.</p>
 <p>Copy WMF</p>	<p>Copy WMF: Copy a representation of the active window into the clipboard in Windows Metafile Format. The contents of the clipboard can then be pasted into a word processing or drawing program that supports Windows Metafiles. The contents can also be saved to files if the <i>Copy WMF to File</i> option in the Program Options dialog box in the Setup toolbar is checked.</p>
 <p>Print</p>	<p>Print: Make a hard copy of the data currently displayed on the screen on the selected printer.</p>
 <p>Atmosphere</p>	<p>Atmosphere: Display an input/output window for calculation of properties of the standard atmosphere at a given altitude and temperature offset. The module also calculates Mach number and Reynolds number per unit length.</p>
 <p>Help</p>	<p>Help: Display the help system associated with the software.</p>
 <p>Exit</p>	<p>Exit: Exit the program.</p>

The **Flight Condition** button displays the Flight Condition Definition dialog box, which is shown in Figure 7.11.

Flight Condition Definition

Flight Phase Name
 Flight Condition 1

New Edit Delete Move Copy

Flap Deflection deg

Velocity kts

Altitude ft

Temperature Offset deg F

Current Weight lb

C.G. X-Location ft

C.G. Z-Location ft

Engine Rating

Include Power Effects
 Include Ground Effects
 Include in Recalculate
 Include in Export

Stores				Engines Operating					
On	Off	On	Off	On	Off	On	Off		
1	<input type="checkbox"/>	<input type="checkbox"/>	6	<input type="checkbox"/>	<input type="checkbox"/>	1	<input type="checkbox"/>	6	<input type="checkbox"/>
2	<input type="checkbox"/>	<input type="checkbox"/>	7	<input type="checkbox"/>	<input type="checkbox"/>	2	<input type="checkbox"/>	7	<input type="checkbox"/>
3	<input type="checkbox"/>	<input type="checkbox"/>	8	<input type="checkbox"/>	<input type="checkbox"/>	3	<input type="checkbox"/>	8	<input type="checkbox"/>
4	<input type="checkbox"/>	<input type="checkbox"/>	9	<input type="checkbox"/>	<input type="checkbox"/>	4	<input type="checkbox"/>	9	<input type="checkbox"/>
5	<input type="checkbox"/>	<input type="checkbox"/>	10	<input type="checkbox"/>	<input type="checkbox"/>	5	<input type="checkbox"/>	10	<input type="checkbox"/>

Gear Up Down
 Speed Brake Retracted Deployed
 Spoiler Retracted Deployed
 C.G. Location Forward Aft Other

Notes

Flight Condition / Flying Qualities Category

Flight Condition Definition

Flight Phase Name
 Flight Condition 1

New Edit Delete Move Copy

Flight Phase Category
 A B C

Flight Condition / Flying Qualities Category

Figure 7.11 Flight Condition Dialog Box (Both Pages)

The options available to the user in the Flight Condition Definition dialog box are as follows:

- **Flight Phase Name:** The user can select the name of the flight phase for which the present analysis is to be performed (i.e. take-off, climb, cruise, etc.). The defined phases appear in the drop-down list to be selected by the user. Only one flight phase can be analyzed at one time. The program can handle up to 95 different flight conditions.
- **New:** The user can define a new flight phase.
- **Edit:** The user can change the name of the current flight phase.
- **Delete:** The user can delete a flight phase from the current project. All information associated with the selected flight phase will be deleted.
- **Move:** The user can move a flight phase within the current project.
- **Copy:** The user can copy a flight phase within the current project.
- **Flap Deflection:** After defining trailing edge flap in the Wing dialog box, the user enters the flap deflection angle corresponding to the flight condition.
- **Velocity:** The user enters the velocity for the defined flight condition. British or S.I. units are automatically supplied depending on the setting in the Units dialog box.
- **Altitude:** The user enters the altitude corresponding to the defined flight phase.
- **Current Weight:** The user enters the current weight of the aircraft corresponding to the defined flight phase.
- **C.G. X-Location:** The user enters the current Center of Gravity location along the X-axis for the defined flight condition.
- **C.G. Z-Location:** The user enters the current Center of Gravity location along the Z-axis for the defined flight condition.
- **Engine Rating:** The user may select the following options using this drop down list

1. Take-off
2. Max. Continuous
3. Max Cruise
4. % Max Cruise
5. Thrust from Drag

- The user may select any of the given options “Include in Recalculate”, “Include Power Effects”, etc..
- Stores: After defining stores in the Configuration dialog box, the user can specify which stores are on the airplane in the specified flight condition.
- Engines Operating: The user can indicate which engines are operating in that flight condition.
- Gear: After defining the number and location of the gear in the Gear dialog box, the user can select landing gear position, retracted (up) or extended (down) for the corresponding flight phase.
- Speed Brake: After selecting speed brake in the Configuration dialog box, the user can specify if the speed brake is retracted or deployed for the corresponding flight phase.
- Spoilers: After selecting spoiler in the Configuration dialog box, the user can specify if the spoiler is retracted or deployed for the corresponding flight phase.
- C.G. Location: The user can specify whether the flight condition corresponds to forward or aft C.G. or any other C.G. location.
- Flight Phase and Category: The flight phase and category (used in flying quality evaluation) can be specified for the flight condition.
- The user may enter notes that will be saved with the flight condition.

The **Recalculate** button (see Figure 7.12) on the main toolbar allows the user to recalculate:

- a. Class II Weight
- b. Component C.G.
- c. Empty Weight C.G.
- d. Fuel Weight C.G.
- e. C.G.
- f. Forward/Aft C.G.
- g. Lift
- h. Maximum Lift
- i. Stability and Control Derivatives
- j. Critical Mach Number
- k. Class II Drag
- l. Class II Drag Trend Line
- m. Trimmed Lift
- n. Trimmed Horizontal Tail Lift
- o. Transfer Functions
- p. Flying Qualities
- q. Static Margin
- r. Lateral Tip Over
- s. Trim Diagram

This can be done for each flight condition separately where the user can select which features need to be recalculated, or the user can choose to automatically run through a series of flight conditions marked in the Flight Condition window. Trim diagrams can automatically be exported to WMF files and saved to the harddisk for each flight condition. Marked variables can also be exported automatically to Excel spreadsheets.

This powerful tool allows the user to quickly and accurately create a picture of the aircraft aerodynamics and stability and control issues through a wide range of flight conditions at the click of a button.

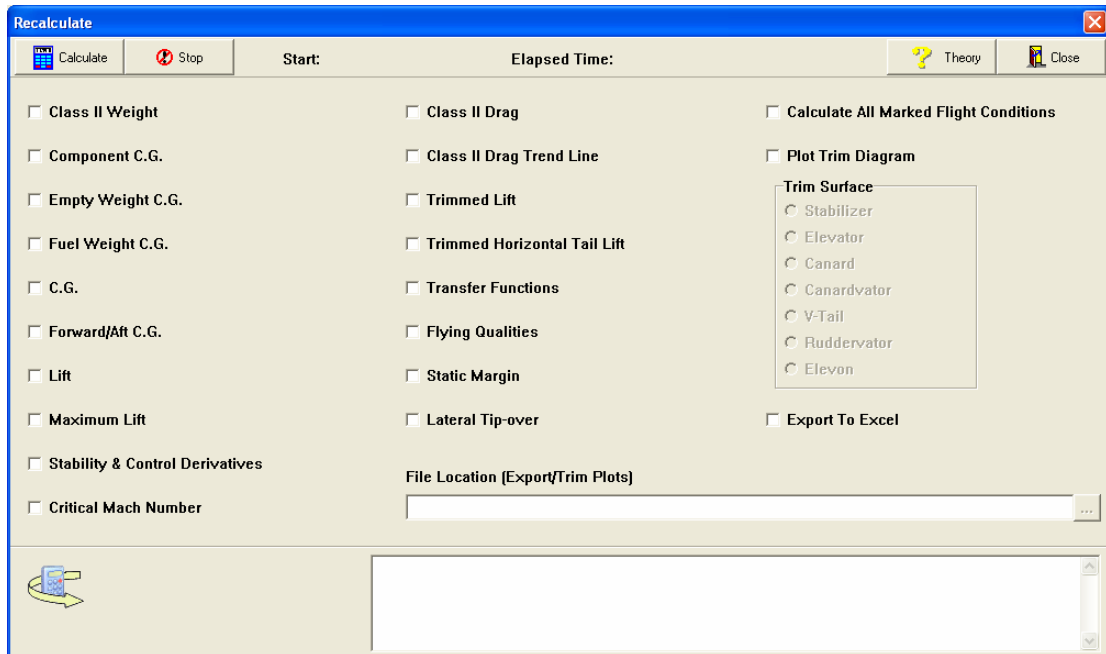


Figure 7.12 Recalculate Dialog

When the **Print** button on the main toolbar is selected, the current print settings defined in Print and Print Setup under the File menu are used to print the output directly with no user interaction. Using Print and Print Setup under the File menu, the user can manipulate the print style, (see Figure 7.13) before the print command is sent to the printer.

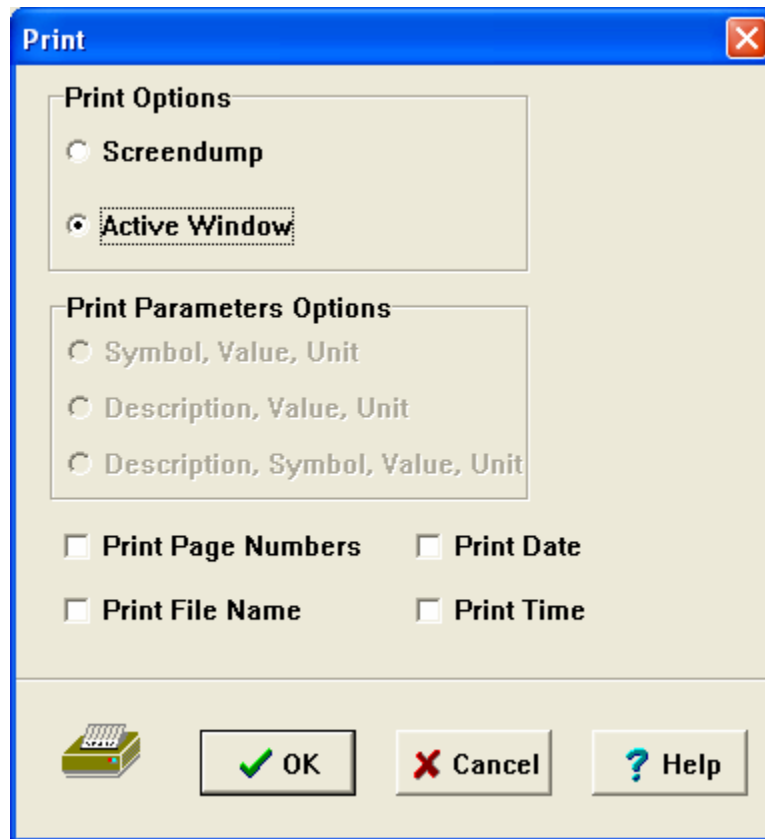


Figure 7.13 The Print Dialog

The Print dialog box options are:

- **Screendump:** Prints a bitmap representation of the main window and any other open and visible windows.
- **Active Window:** Prints a graphic representation of the active application, input/output, or plot window.
- **Print Parameters:** Prints a list of the input and output parameters in an input/output window. The Print Parameters option has three options:
 - **Symbol, Value, Unit:** Prints the parameter symbol, the value, and the unit.
 - **Description, Value, Unit:** Prints the description of the parameter, the value, and the unit.

- Description, Symbol, Value, Unit: Prints the parameter description, symbol, value, and unit
- The user can also choose whether to show the date, time, page number and file name on the print out.

7.1.1.2.2 The File Toolbar

The File toolbar (Figure 7.14) consists of five bitmap buttons at the bottom of the main window. The File toolbar buttons can be used to manage projects and files of the software. The functionality of the buttons is described in Table 7-6.

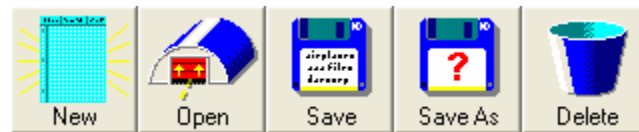



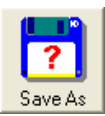



Figure 7.14 File Toolbar

Table 7-6 File Management Toolbar Buttons

 <p>New</p>	<p>New: Create a new project.</p>
 <p>Open</p>	<p>Open: Open an existing project (*.analys files from AAA Versions 1.0 through 1.7 and *.gpr files from AAA 2.0 through AAA 2.2 can also be opened).</p>
 <p>Save</p>	<p>Save: Quickly save the current project under its current name and directory. Files have an *.aaa extension.</p>
 <p>Save As</p>	<p>Save As: Save the current project under a different name and/or folder. The project is saved in a directory (folder) with the same name as the project.</p>
 <p>Delete</p>	<p>Delete: Remove any Project.</p>

Each of the buttons in the File Management toolbar opens a dialog window corresponding to that function.




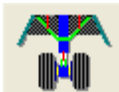

7.1.1.2.3 Configuration Setup Toolbar

The Configuration Setup toolbar (Figure 7.15) consists of six bitmap buttons at the bottom of the main window. The Configuration Setup toolbar buttons can be used to define the airplane configuration for the current project. The functionality of the buttons on the Configuration Setup toolbar is described in Table 7-7.



Figure 7.15 Configuration Setup Toolbar

Table 7-7 Configuration Setup Toolbar Buttons

 <p>Configuration</p>	<p>Configuration: Define the basic configuration of the airplane, which includes empennage, amphibious hull, nacelle(s), store(s), pylon(s), tailboom(s), speed brake, spoiler and pressurization. In the case of stores, speed brake and spoiler, the flight condition dialog box is used to define whether the devices are deployed in the current flight phase.</p>
 <p>Powerplant</p>	<p>Engine: Define various aspects of the propulsion system of the airplane.</p>
 <p>Controls</p>	<p>Controls: Define longitudinal and directional control surfaces for the airplane.</p>
 <p>Gear</p>	<p>Gear: Define the type of landing gear position, retraction and attachment point. In the case of retractable gears, the Flight Condition dialog is used to define whether the gear is extended or retracted in the flight phase.</p>
 <p>Structure</p>	<p>Structure: Define the cross-section structure type of wing and empennage.</p>

Each of the buttons in the Configuration Setup toolbar opens a dialog window when selected. Ref. 193 shows more details for each window.

7.1.1.2.4 Certification Toolbar



The Certification toolbar (Figure 7.16) consists of two bitmap buttons at the bottom of the main window. The Certification toolbar buttons can be used to specify airplane

certification type and class. The functionality of the buttons on the Certification toolbar is described in Table 7-8.



Figure 7.16 Certification Toolbar

Table 7-8 Certification Toolbar Buttons

 Certification	Certification: Define the airplane type, category and certification under civil and military regulations.
 Classification	Classification: Define the class of the airplane for US military flying qualities regulations to evaluate flying qualities for both civilian and military airplanes.

Ref. 193 shows more details for each window.

7.1.1.2.5 System Setup Toolbar

The System Setup toolbar (Figure 7.17) consists of seven bitmap buttons at the bottom of the main window. The System Setup toolbar buttons can be used to manage the program environment. The functionality of the buttons on the System Setup toolbar is described in Table 7-9.

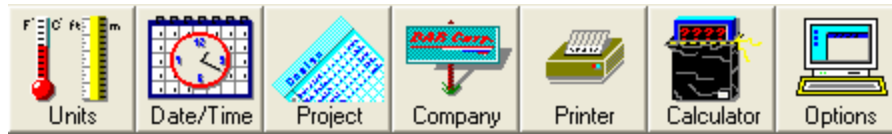


Figure 7.17 System Setup Toolbar

Table 7-9 System Setup Toolbar Buttons

<p>Units</p>	<p>Units: Select British or S.I. units for the input and output parameters.</p>
<p>Date/Time</p>	<p>Date/Time: Select the date and time format in the status bar.</p>
<p>Project</p>	<p>Project: Specify the name of the project to be displayed in the status bar.</p>
<p>Company</p>	<p>Company: Specify the company name to be displayed in the status bar.</p>
<p>Printer</p>	<p>Printer: Access the system print manager to define various printer attributes.</p>
<p>Calculator</p>	<p>Calculator: Select the calculator type: Standard or RPN.</p>
<p>Options</p>	<p>Options: Select the size of the toolbar buttons. Choose whether parameter info and notes buttons are displayed on input/output elements. Choose whether to save WMF to file and specify the length of the recovery project auto-saving interval.</p>

Ref. 193 shows more details for each window.

7.1.2 Objects in AAA

The object-oriented methods in AAA primarily center around the calculations and their organization. All application modules have their calculations organized in an input/output window. This is an object with the following structure:

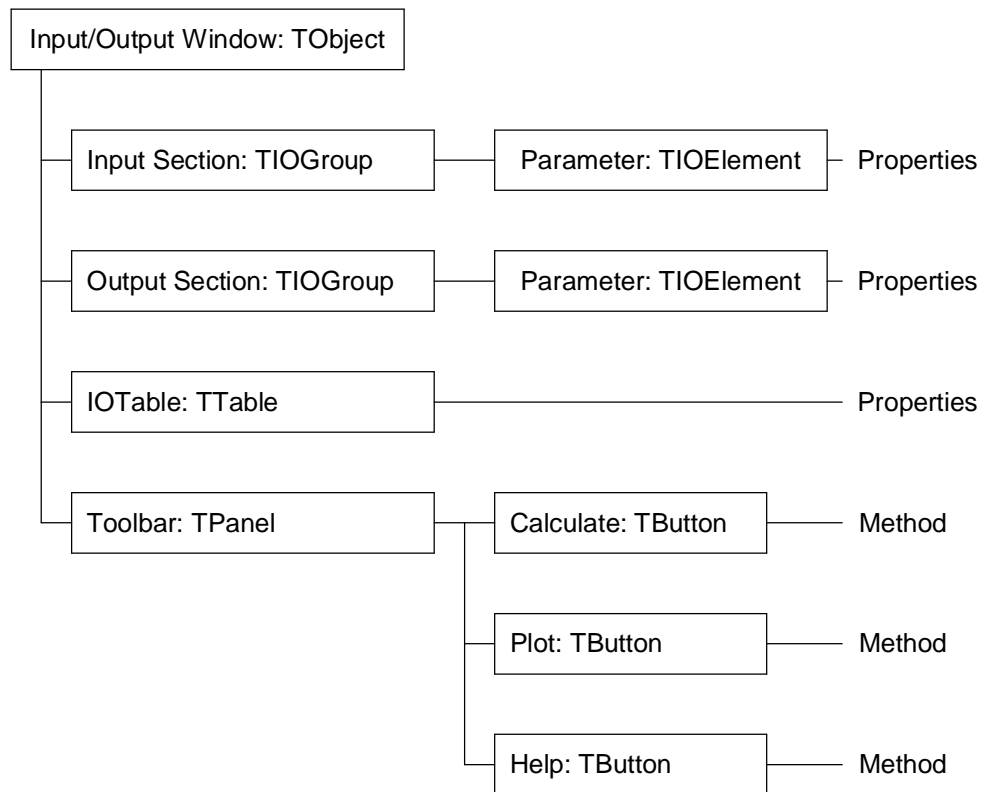


Figure 7.18 Input/Output Window Object Structure

All parameters are organized in an input or output section or in a table. The toolbar has buttons and has methods to calculate or plot the data. The methods are the procedures or functions to calculate the output parameters.

Each parameter (currently over 4,100 parameters are used in AAA) has the following properties:

1. Label
2. Value
3. British unit
4. SI unit
5. SI unit conversion factor
6. Alternate unit
7. Alternate unit conversion factor
8. Number of Decimals (British)
9. Number of Decimals (SI)
10. Hint (text string describing the parameter)
11. Flight Condition dependent (true/false)
12. Go to location, used to jump to the window where the parameter is calculated
13. Notes

The airplane configuration is also organized in an object structure, although it is a different structure in AAA as compared to the object structure used in AAA-AML. The airplane is broken down in different objects as indicated in Figure 7.19. It is important to note, that this object structure does not contain methods. As will be shown later in Section 7.2, this is one of the major differences in object structure used between AAA and AAA-AML.

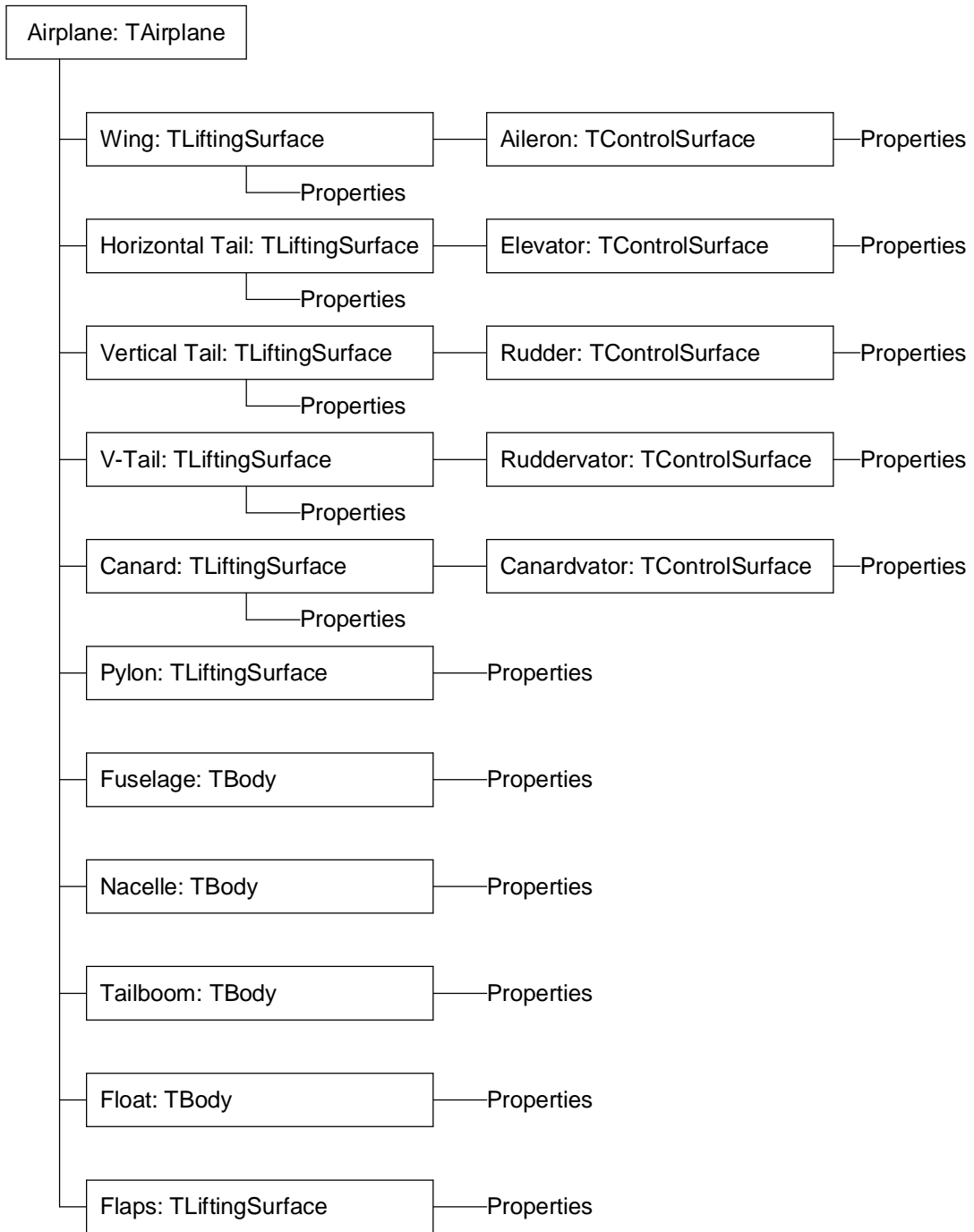


Figure 7.19 Airplane Configuration Object Structure

7.1.3 AAA and Airplane Design

Since the initial development of AAA, all methods used have been carefully tested and checked for accuracy. All methods implemented have been tested by at least two different people, who did not perform the original development or implementation. Hand calculations and spreadsheet calculations have been performed to check correctness. All methods have been tested for a range of airplane types: military, civil, fighters, bombers, general aviation, jets and piston-propeller powered airplanes. As a commercial product, AAA is under constant development, which includes new methods and bug fixes. AAA has been used in over 200 different engineering consulting projects at DARcorporation. The third generation of Advanced Aircraft Analysis (AAA) software, currently in release 3.1, is now used by 279 manufacturers and universities in 45 countries with over 1000 licenses installed. The number of installations is an indication of its acceptance as a standard for conceptual and preliminary airplane design. Constant customer feedback is used to improve the tool.

The efficiency of AAA has been proven by using it on several consulting projects at DARcorporation. One such project dealt with generating all stability and control derivatives, aerodynamic coefficients (lift, drag and pitching moment) and hingemoment coefficients for the Raytheon King Air 350. This project took approximately 500 person-hours over a twelve week period. AAA version 2.1 was used for that project. Several years later for the same company the same data was generated for the Mitsubishi Mu-2. Eight different versions of the MU-2 were

analyzed. Using AAA with the new Recalculate All feature (see 7.1.1.2.1) it was possible to cut analysis time with more than 80%. Not only time was cut, but also errors due to more automation of tedious calculations. With the “Recalculate All” feature it was no longer necessary to go into each module and press calculate manually.

Automation of several aerodynamics methods related to propeller slipstream effects, significantly reduced analysis time for several projects performed for Air Tractor. Early analysis was performed with the second generation of AAA without the option to handle multiple flight conditions within one project and without the propeller effects. The latter was done by using spreadsheet methods. Aerodynamic analysis that used to take approximately 200 person-hours using the second generation of AAA, now takes less than 40 person-hours using the third generation AAA.

As a last example of improved efficiency, AAA 3.1 was used to generate the data to determine the forward and aft center of gravity limits of a General Aviation airplane. Figure 7.20 shows the results generated by AAA and plotted in a spreadsheet chart. Before AAA 3.1 this chart could only be generated using spreadsheet methods. Setting up the spreadsheet, verifying data and copying data from other sources took about 20 person-hours. With AAA 3.1 and a spreadsheet plot, this was cut down to two person-hours, from which most was spent on generating the graph in the spreadsheet.

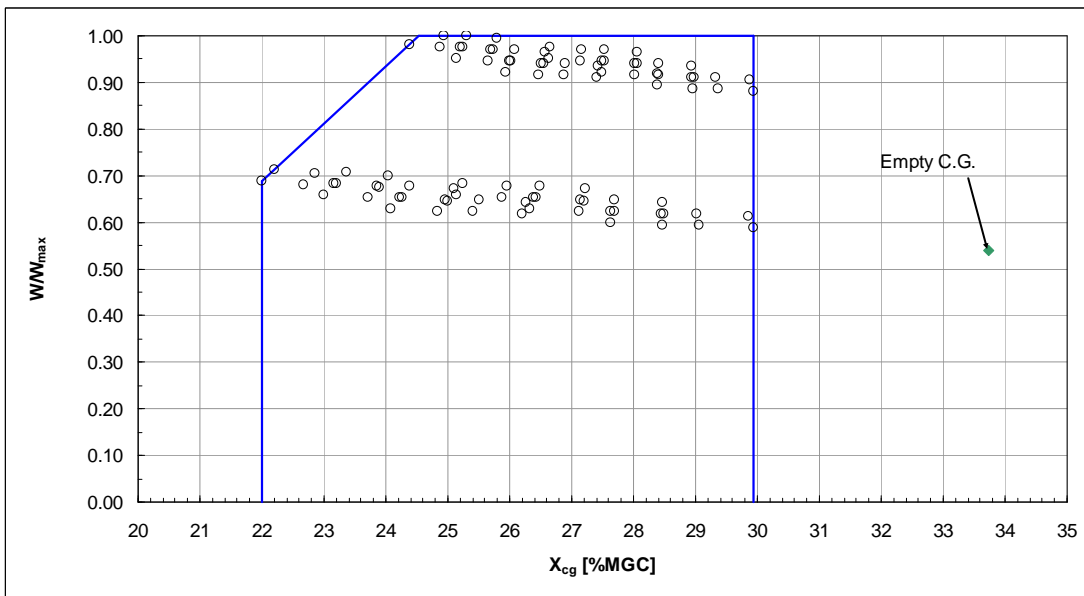


Figure 7.20 Forward and Aft Center of Gravity Limits

In the over 200 engineering projects AAA has been used at DARcorporation, other significant time savings have been demonstrated over conventional hand calculations, spreadsheet methods or first and second generation AAA.

7.2 Advanced Aircraft Analysis Methods Implemented in AML

As indicated in Chapter 3 a new approach has been implemented to capture design knowledge to be used in the conceptual and preliminary design phase. The AAA methods described in Chapter 6 have been implemented in AML either by direct translation or by creating AML classes and methods that call procedures and functions from dynamic link libraries (dll, see Appendix E). These dll's contain the exact same code as used in AAA 3.1.

7.2.1 Implementation

The implemented modules include the following:

1. Mission Profile
2. Weight Sizing including Regression Coefficients
3. Class I Drag
4. Performance Sizing
5. Maximum Lift
6. Flap Lift
7. Lift Distribution
8. Geometry
9. Class I Weights (Weight Fractions)
10. Weight and Balance
11. Class I Moments of Inertia
12. Volume Methods

13. Class II Weights (excluding weight iteration)

14. Class II Drag

The theory used in these modules is described in detail in Chapter 6.

These modules are integrated to support the model evolution through the various stages of the design. A design is initiated by assigning various input parameters including mission profile description (flight segments), engine type (jet/propeller) and class of aircraft (general aviation, commercial, etc.). Additional parameters are recommended for selection such as aircraft thrust-to-weight-ratio and wing-loading. Various criteria for selection based on historical data are provided to assist in the decision making progress.

Aircraft configuration parameters are provided to aid the user in customizing the design. These parameters describe horizontal tails, canards, tailbooms, floats, pylons, control surfaces, etc. Furthermore, selection of control surface type (flap, slat, etc.) is made available. Flap lift coefficients can be determined and flap sizing is implemented for both take-off and landing conditions.

The main structure of the program in AML is different from the object structure used in AAA. Figure 7.21 shows the object model tree.

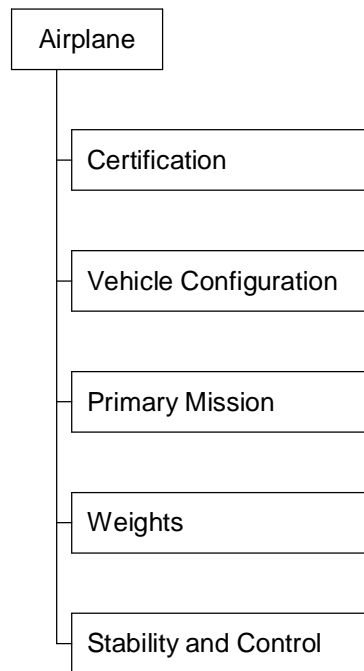


Figure 7.21 Model Tree in AML

The structure is configuration and mission based, as opposed to AAA, which is methods based. Each branch in the model tree represents a class in AML and is divided in subclasses. Classes are linked through inheritance which create dependencies. Dependencies are automatically resolved by AML. This means that if the user enters a value for a parameter and another parameter depends on it, by demanding the value (either by clicking on the exclamation mark next to the parameter, or regenerating a plot) all other parameters are updated. The program will traverse through the tree and resolve all dependencies automatically. This means that there is no specific user action required to go through each branch of the tree. One requirement for this to work properly is that all parameters must have a default value.

The primary mission can be expanded and several flight segments can be added (see Figure 7.22)

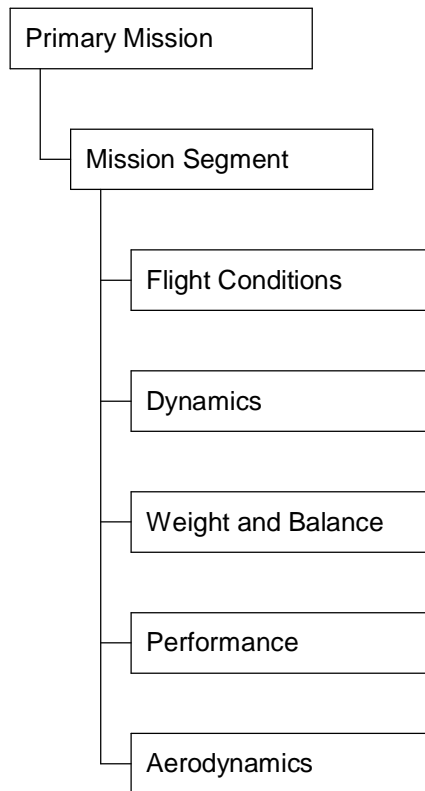


Figure 7.22 Primary Mission in AML

Under this mission segment several branches are shown similar to the methods used in AAA.

The Vehicle Configuration branch contains all geometry information, including all 3D Outer Mold Line geometry. This is one of the most useful features in AAA-AML, because it gives the user an instant visual feedback whether all components of the vehicle are properly defined and attached to the correct locations. AAA does not

have this feature, which makes early design error prone. Unless geometry is exported to a CAD program no visual feedback exists in AAA. This geometry in AAA-AML can be used in AMRaven to create substructures, perform aerodynamic analysis using panel codes or CFD analysis. AAA does not have any of these features. By clicking the regenerate button, the 3D geometry is immediately redisplayed when any changes to geometry parameters are made.

7.2.2 Testing

The implemented methods have been tested against the Advanced Aircraft Analysis (AAA) software to check accuracy and completeness. Separate test programs have been made to check results from the dll's to verify if data is correctly passed between the AML environment and the dll, the same test have been run using AAA and the Delphi development environment (Ref. 188). All results from the dll's were an exact match.

To cover the wide range of types of airplanes, the following examples have been implemented in AAA and in AAA-AML:

- AAI Shadow 600 (UAV)
- Adam A500 (Twin engine piston propeller, General Aviation)
- Bede BD-10 (Single engine fighter)
- BeechJet 400A (Twin engine business jet)
- Boeing 737-900 (Twin engine commercial airliner)

- Boeing 747-400 (Four engine commercial airliner)
- Boeing 777-200 (Twin engine commercial airliner)
- Bombardier Learjet 24F (Twin engine business jet)
- Cessna 172R Skyhawk (Single piston engine propeller, General Aviation)
- Cessna 208 (Single turboprop engine propeller, General Aviation)
- Cessna 210 Centurion (Single piston engine propeller, General Aviation)
- Cessna 310 (Twin piston engine propeller, General Aviation)
- Cessna CJ2 (Twin engine business jet)
- Cirrus SR20 (Single piston engine propeller, General Aviation)
- Diamond DA40(Single piston engine propeller, General Aviation)
- Eclipse 500 (Twin engine business jet)
- Embraer EMB-312 Tucano (Single engine turboprop trainer)
- Embraer EMB-120 Brasilia (Twin engine turboprop commuter)
- FA-22 Raptor (Twin jet fighter/bomber)
- Fairchild T-46 (Single engine jet trainer)
- Falcon 20 (Twin engine business jet)
- Global Hawk (Single jet engine UAV)
- Learfan 2100 (Single turboprop business airplane)
- Lockheed Martin F-16 Fighting Falcon (Single engine jet fighter)
- Piper PA-30 Twin Comanche (Twin piston engine propeller, General Aviation)
- Raytheon Premier 1 (Twin engine business jet)

- KU CReSIS Meridian (Single engine turboprop UAV)

Data is retrieved from Ref. 189 and pilot operating handbooks and flight manuals available for each airplane type. First a model is created in the Advanced Aircraft Analysis software. Then the same input data is used in AAA-AML.

A separate bug tracking tool for this project has been setup. The bug tracking software Mantis (Ref. 190) can be accessed from TechnoSoft, Inc, The University of Kansas and DARcorporation. All problems found using AAA-AML are logged in the system. As of writing of this dissertation 108 problems are still listed to be fixed. Most of them deal with specific implementations not working properly for certain types of airplanes because of missing input parameters. None of the problems were serious enough to halt a full test of the capabilities of the system.

Besides testing on existing airplanes, also one new design has been implemented using AAA-AML. To check for accuracy also AAA was used in conjunction with AAA-AML. The following sections show the details on AAA-AML modules using a Light Sport Aircraft (LSA) as an example.

7.2.2.1 Light Sport Aircraft Requirements

In 2004 the FAA finalized the Sport Pilot/Light Sport Aircraft (LSA) category. This category of affordable aircraft is intended to make owning an aircraft more accessible. There are two airworthiness certification categories:

1. A special light-sport aircraft (S-LSA), sold ready-to-fly that maybe used for flight training, rental, or personal flight, including personal flight instruction.
2. An experimental light-sport aircraft (E-LS), sold in a kit form that may be used for personal recreational flight or personal flight training.

This chapter describes a design applicable to the first category: S-LSA. The aircraft is primarily used for recreational purposes and a sport pilot only operates this airplane during daylight hours. The occupants are seated in tandem formation. A three-surface design is chosen for its aerodynamic efficiency (see Figure 7.23).

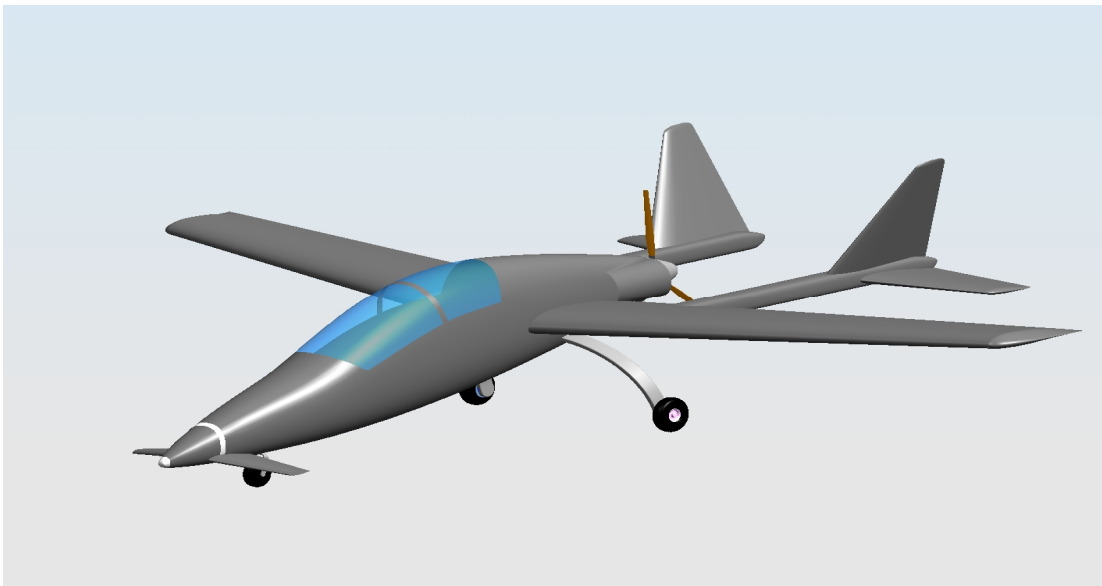


Figure 7.23 Tandem Seater LSA

This chapter describes the design requirements, weight sizing, performance sizing, weight and balance, aerodynamics, stability and geometry as implemented in AAA-AML.

The performance specifications of the aircraft are listed below. The mission profile, which consists of 7 flight segments, is shown in Figure 7.24.

- Range:** 1,000 nm at full payload at 5,000 ft altitude and 10% reserves
- Weight:** 1 crew members, 1 passenger (190 lb each and 10 lb of baggage each)
- Altitude:** 5,000 ft maximum
- Speed:** 120 kts at 5,000 ft altitude
- Climb:** 500 ft/min at maximum weight
- Powerplant:** UL 260i, 95 HP

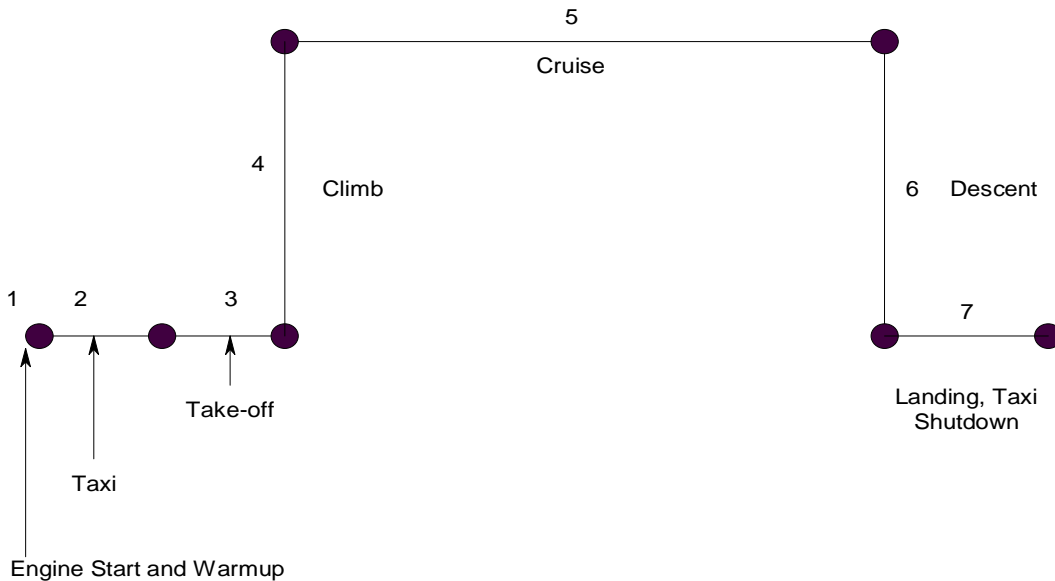


Figure 7.24 Mission Profile of the Tandem Seater LSA

7.2.2.2 Starting AAA-AML

Starting the program is either done through a short-cut “Airplane Design Vehicle Synthesis” or starting AML XEMACS from Start > All Programs. Then select the “Run AML” button to start the Airplane Design and Analysis window.

Select Model > New (opening an existing model, select retrieve). A dialog window with an edit box shows up to define the class name (Figure 7.25).

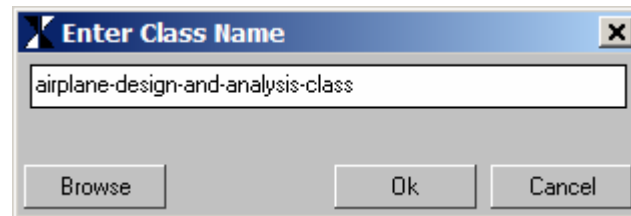


Figure 7.25 Airplane Design and Analysis Class Name

For the class enter airplane-design-and-analysis-class, or use Browse. Enter the airplane name (no spaces, everything after the spaces is left out in the name)

This will bring up the Airplane Design and Analysis user interface (Figure 7.26).

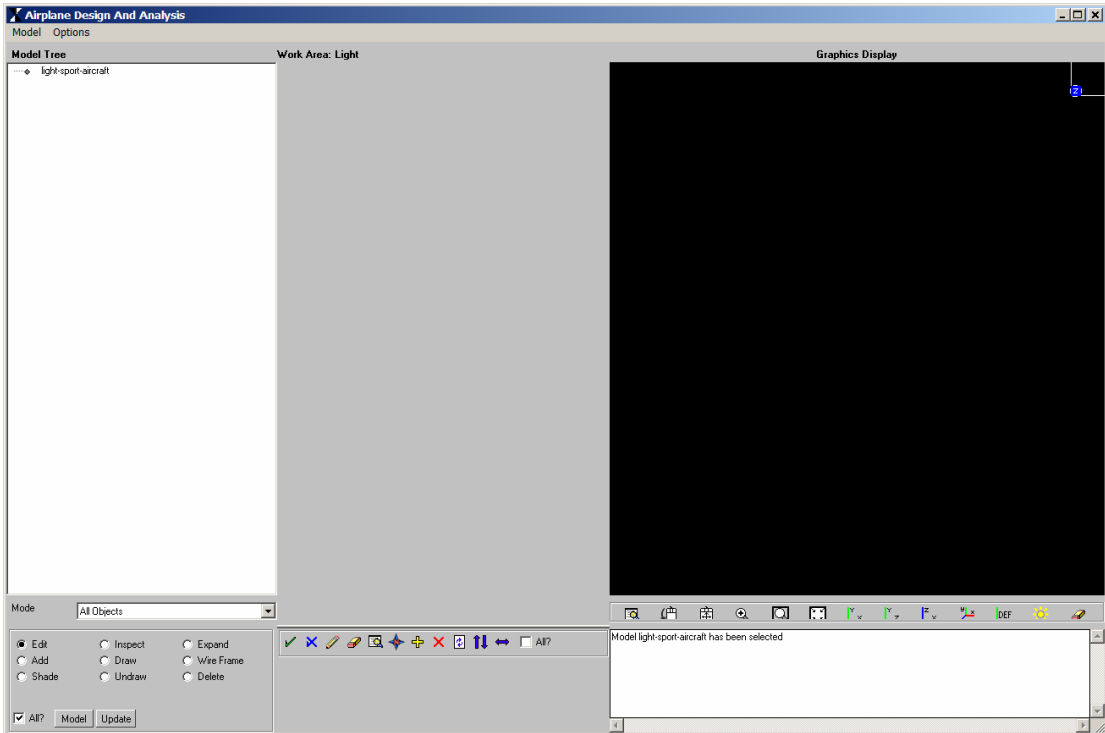


Figure 7.26 Airplane Design and Analysis Design Environment

The Model Tree is where all the modules and calculations are organized. The main modules in the model tree are (see Figure 7.27):

1. Vehicle Certification: a window where the type of airplane is selected, the FAR or Military requirements to which the aircraft will be designed.
2. Vehicle Configuration: the main geometry module for the airplane. All the lifting surfaces, fuselage, nacelles, stores, etc. are defined here.
3. Primary Mission: the main sizing module for the airplane. The mission profile is defined here, and all the Aerodynamics and Performance options are submodules of each mission segment.

4. Weights: the weight calculator for AAA-AML. It uses the inputs from the primary mission and regression data from similar airplanes to calculate a take-off and empty weight for the airplane.
5. Stability and Control: this module is uses most of the AAA stability and control modules with a similar layout and options.

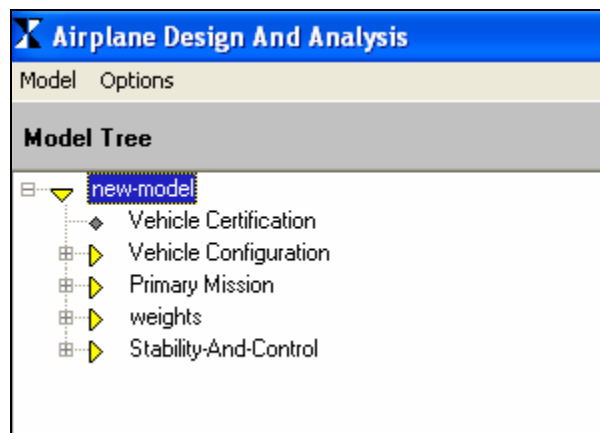


Figure 7.27 Airplane Design and Analysis Design Model Tree

7.2.2.2.1 Vehicle Certification

In the Vehicle Certification window (see Figure 7.28) the Military/Civil designation will be defined, the certification base (here FAR23, since LSA has not yet been implemented in AAA-AML, it is available in AAA 3.1).

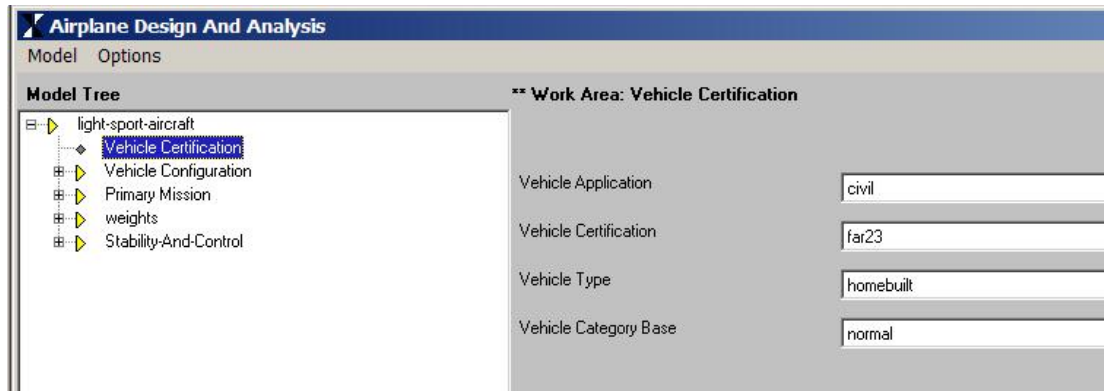


Figure 7.28 Airplane Design and Analysis Design Model Tree

- Military/Civil: The user can select from military or civil airplane types
- Vehicle Type: Depending on the Military/Civil choice, the user can choose the airplane type
- Vehicle Certification: The user can select the following certification standards:
 - FAR 23: Federal Aviation Regulations, Part 23
 - JAR 23: Joint Airworthiness Requirements, Part 23
 - FAR 25: Federal Aviation Regulations, Part 25
 - VLA: Very Light Aircraft
 - Mil Specs.: Military Specifications (MIL-F-8785C and MIL-STD 1797A)
 - AS Specs.: Naval Air Systems Command Specifications
 - Light Sport: Light Sport Requirements (not implemented yet)
- Vehicle Category Base: Under FAR 23 or JAR 23, one of the following airplane categories can be defined:

- Normal
- Utility
- Acrobatic
- Commuter
- Base: Under Mil Specs or AS Specs, the airplane base can be selected as land, carrier or both.

7.2.2.2.2 Vehicle Configuration

When the Vehicle Configuration is expanded and selected, the Vehicle Configuration box is displayed (see Figure 7.29). The user can define the basic configuration of the airplane. For vertical tail, nacelles, stores, tailbooms, floats, pylons and ventral fins the number of each device can also be defined using this dialog window.

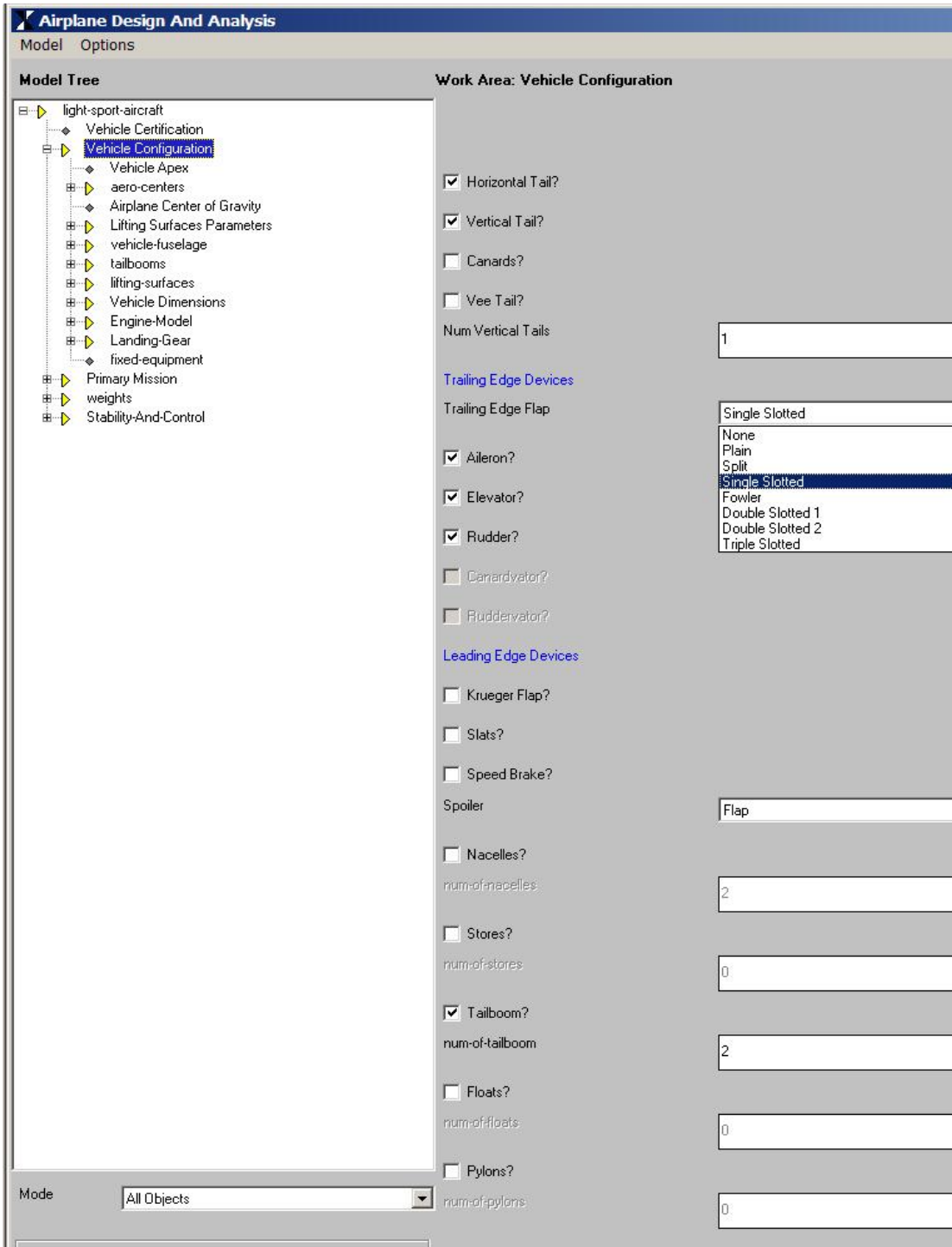


Figure 7.29 Vehicle Configuration Model Tree

7.2.2.2.3 Engine Model

Select the type and number of engines (see Figure 7.30). There are other options in this module, but they do not matter at this time. The engine type (either propeller or jet) will determine which methods will be used for the rest of the calculations.

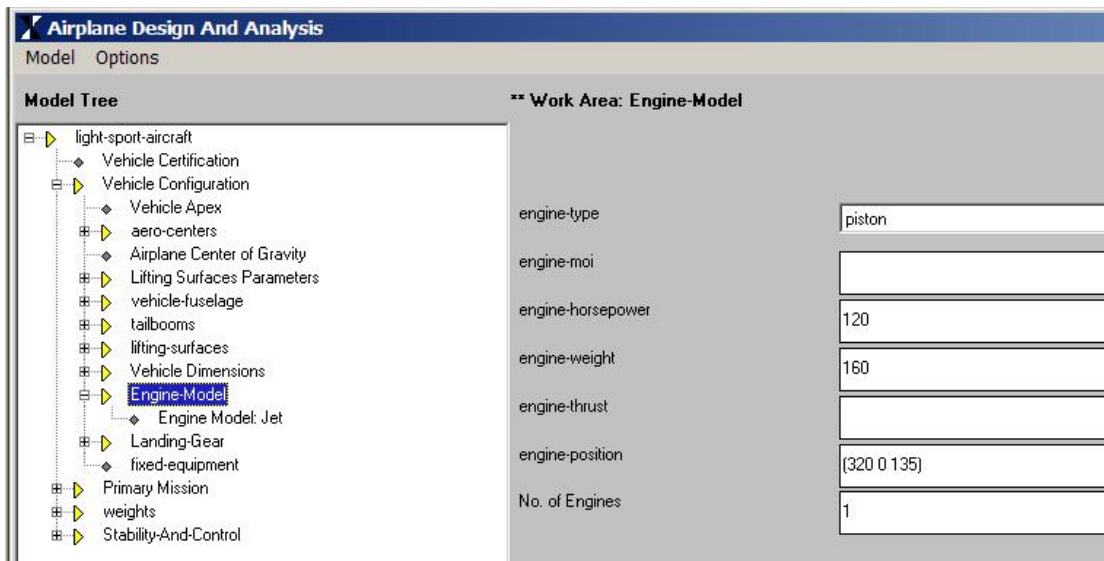


Figure 7.30 Engine Model

7.2.2.3 Weight Sizing

The purpose of weight sizing is to define the gross take-off weight, empty weight and mission fuel weight, while satisfying a given mission profile. For the given mission outlined in section 7.2.2.1, the weights are estimated. For each flight segment, the fuel-fraction is either calculated or selected from the statistical data listed in Reference 1. The fuel-fraction for each phase is defined as the ratio of end weight to begin weight. The segment fuel fractions help in determining the fuel weight, take-off weight, and the empty weight of the airplane. An iterative method is used to calculate the take-off and the empty weight of an airplane (see Section 6.1.1).

7.2.2.3.1 Primary Mission

After collapsing the Vehicle Configuration, the Primary Mission can be expanded. Options are shown for editing and defining mission segments (see Figure 7.32).

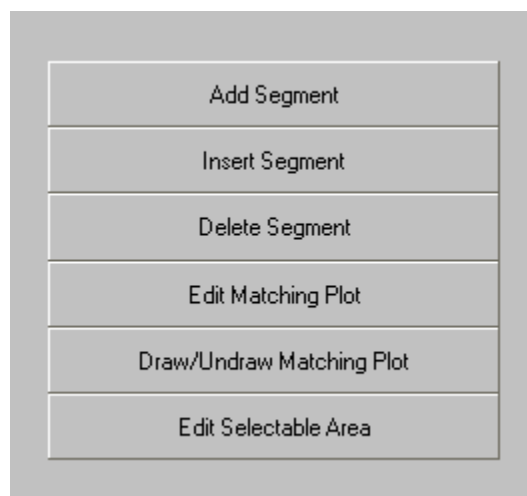


Figure 7.31 Segment Menu

Mission segments are added as shown in Figure 7.32

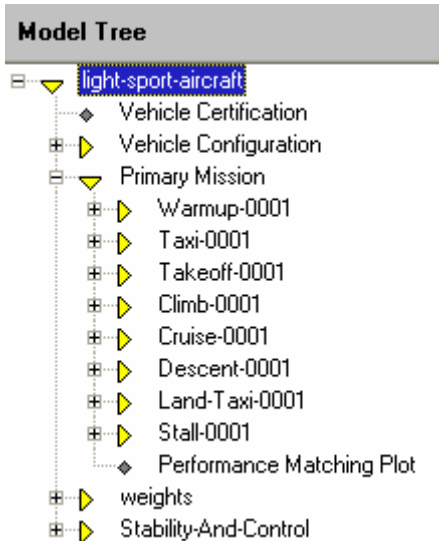


Figure 7.32 Mission Segment Definition

The following flight segments match the mission profile and list the fuel fractions or other input data required:

Warm-up: Fuel-fraction = 0.998

Taxi: Fuel-fraction = 0.998

Take-off: Fuel-fraction = 0.998

Climb: Altitude = 5,000 ft

Initial climb rate = 500 ft/min

Lift-to-drag ratio = 10.7

Specific fuel consumption = 0.375 lb/hr/lb at 90 kts

Propeller Efficiency = 0.60

Calculated fuel-fraction = 0.997

Cruise: Range = 750 nm

Cruise speed = 110 kts

Lift-to-drag ratio = 7.7

Specific fuel consumption = 0.340 lb/hr/lb

Propeller Efficiency = 0.85

Calculated fuel-fraction = 0.8974

Descent: Fuel-fraction = 0.995

Land/Taxi: Fuel fraction = 0.995

Each Flight Segment can be expanded to show other properties or methods associated with each segment (Figure 7.33).

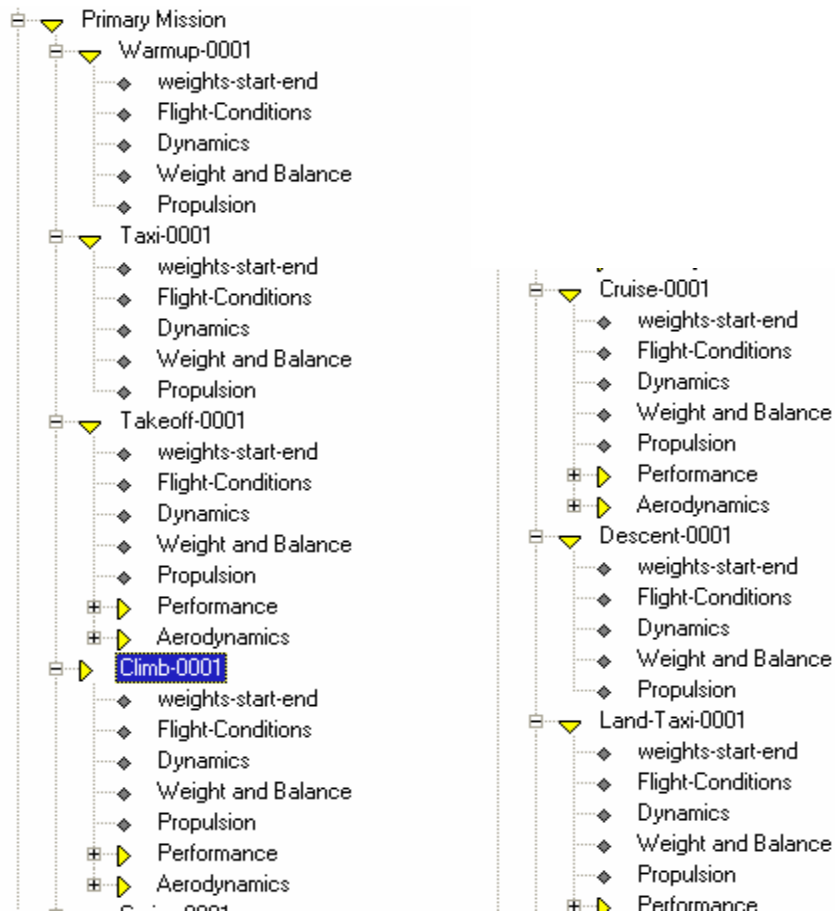


Figure 7.33 Mission Segments Expanded

The mission fuel fraction for each segment is either input (Figure 7.34) by the user or calculated (Figure 7.35) based on certain parameters .

Work Area: Climb-0001

Inputs

Active Engines List	
Rate of Climb	500.0
L/D	10.67
Prop-Efficiency	0.6
Speed	90
C_p	0.375

Figure 7.34 Climb Segment Input Data

Outputs

Change in Altitude	5000	!
Segment Endurance	10.0	!
M_{ff}	0.9973	!

Figure 7.35 Climb Segment Output Data

7.2.2.3.2 Regression

After all flight segments are filled out, the regression module is selected.

The regression coefficients A and B are calculated based on published actual airplane data (References 189-191). These weights are listed in Table 7-10. Results are shown in Figure 7.36.

Table 7-10 Weight Data for Sport Planes and Experimental Airplanes

#	Airplane Name	Take-off Weight [lb]	Empty Weight [lb]
1	P-Swift	520	250
2	Silent Club	530	300
3	Silent Club AE-1	661	441
4	Silent Club IN	639	375
5	Exel	683	432
6	Lafayette Classic Storch	937	452
7	Lafayette Wallaby	937	458
8	Velocity Elite RG	2,250	1,250
9	Velocity SE-FG	2,300	1,300
10	Velocity SUV	2,250	1,235
11	Velocity XL FG	2,700	1,700
12	Velocity XL RG	2,800	1,700
13	Jabiru J250	1,232	700
14	Jabiru J400	1,540	700
15	Jabiru SF	1,540	870

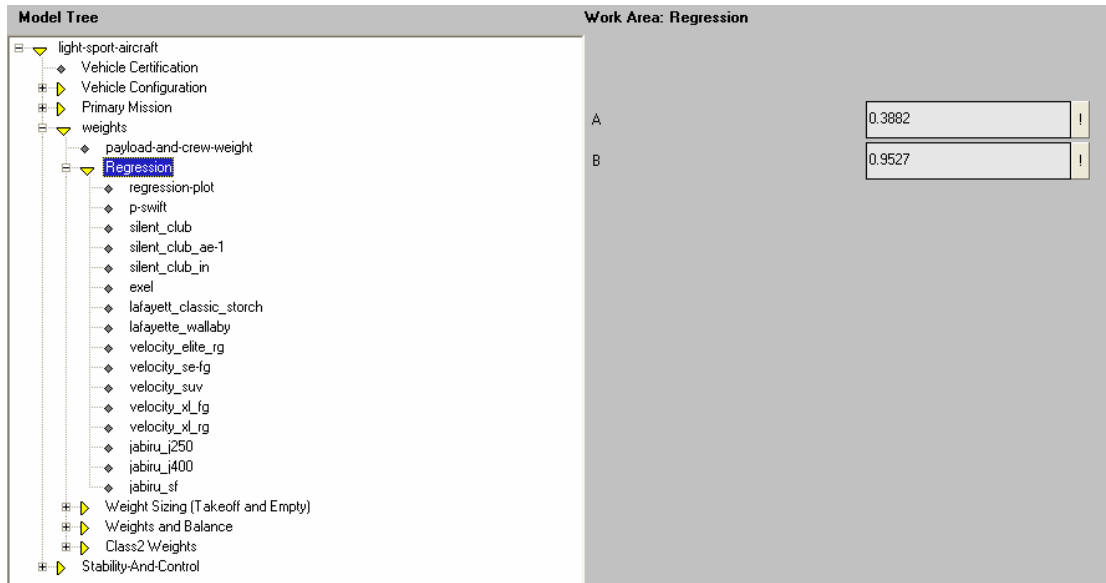


Figure 7.36 Weight Regression Coefficients

7.2.2.3.3 Weight Sizing

Entering the Weight Sizing (Take-off and Empty) module will show other inputs such as: trapped fuel and oil weight fraction, reserve fuel fraction and the airplane regression coefficients (see Figure 7.37). Payload and crew weight are entered in the payload-and-crew-weight section.

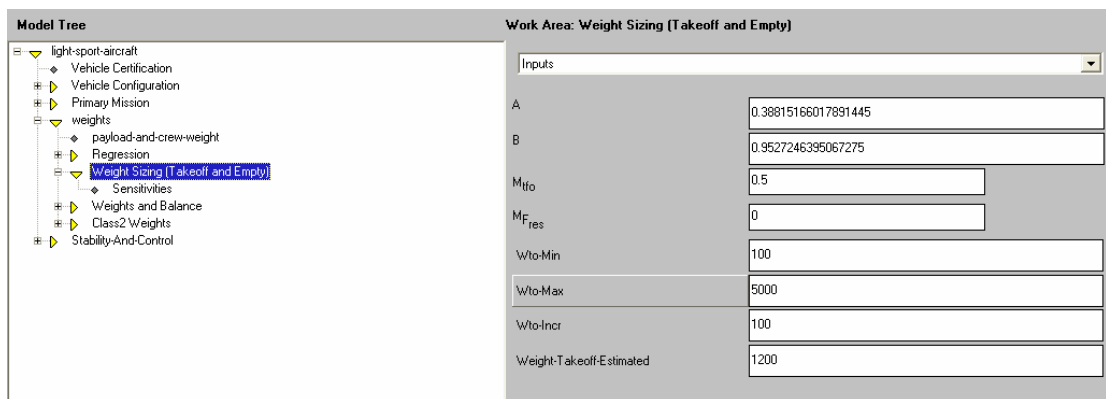


Figure 7.37 Weight Sizing: Input

The overall mission fuel fraction is calculated using the fuel fractions of the individual segments.

The take-off weight, empty weight, fuel weight, trapped fuel weight and reserve fuel weights are calculated (see Figure 7.38).

The airplane weight at the beginning and end of each segment is calculated and tabulated (Figure 7.39). A plot of the take-off and empty weight with the calculated design point at the intersection of the two curves is generated (see Figure 7.40).

Sensitivities of design parameters on take-off weight can be calculated as shown in Figure 7.41.

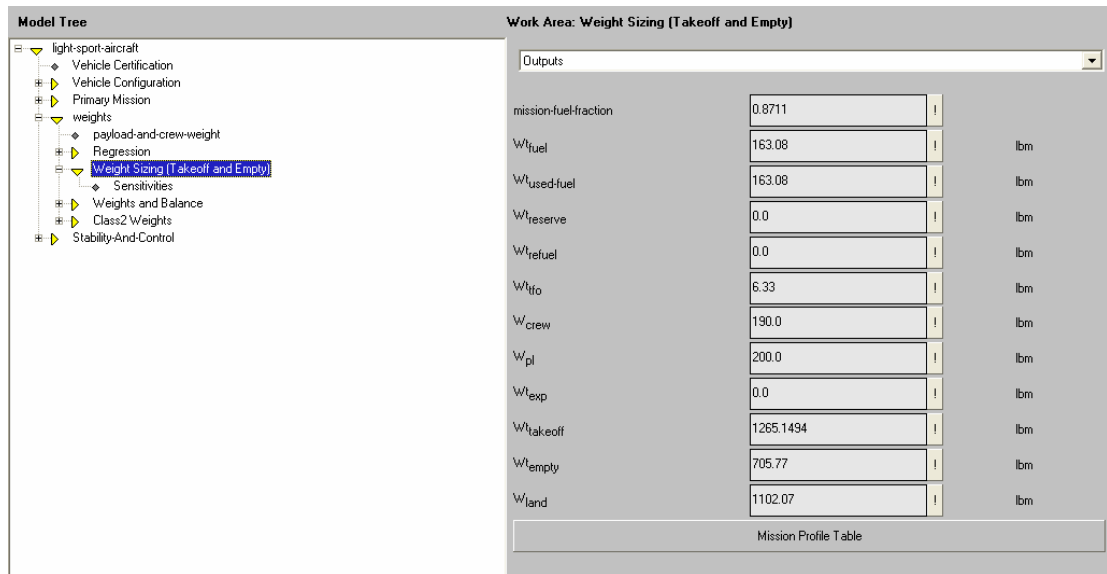


Figure 7.38 Weight Sizing: Output

	W-Begin (lbs)	DeltaWF-Used (lbs)	WF-Begin (lbs)
Warmup-0001	1265.15	2.53	163.08
Taxi-0001	1262.62	2.53	160.55
Takeoff-0001	1260.09	2.52	158.02
Climb-0001	1257.57	3.38	155.5
Cruise-0001	1254.19	141.02	152.12
Descent-0001	1113.17	5.57	11.1
Land-Taxi-0001	1107.61	5.54	5.54
Stall-0001	1102.07	0.0	0.0

Figure 7.39 Weight Sizing: Mission Profile Table

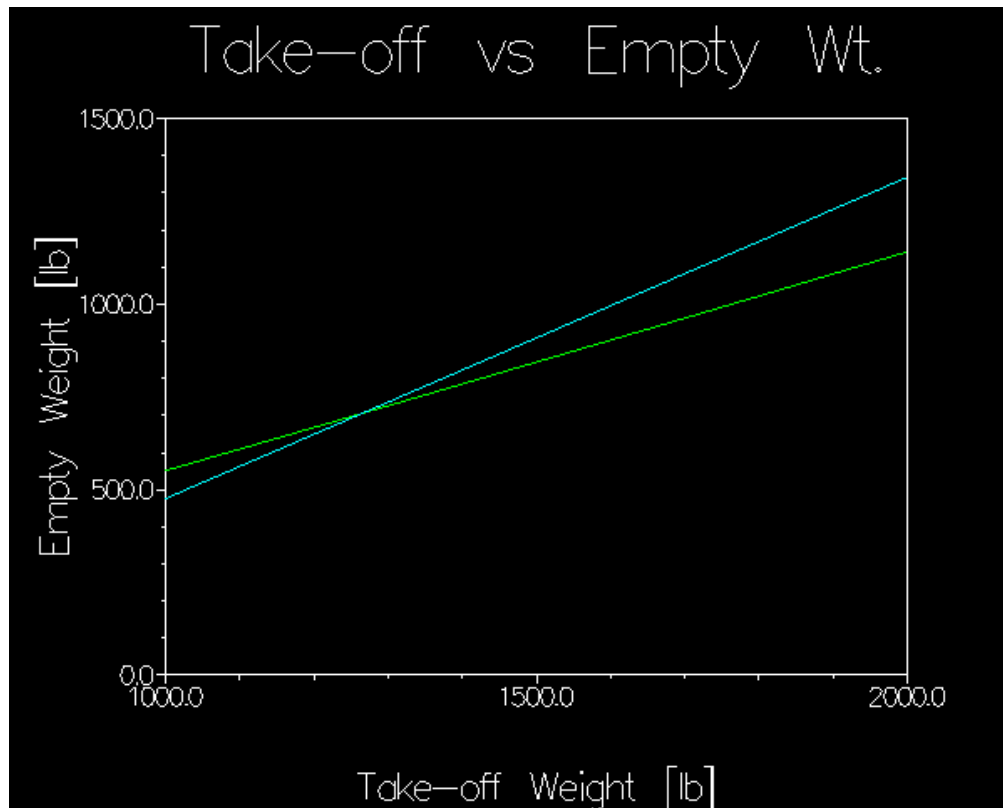


Figure 7.40 Weight Iteration

	Expended Payload	Wt. Refuelling	Specific Fuel Consumption lb-hr	Range lb/nm	Lift to Drag Ratio lb	Endurance lb/hr	Propeller Efficiency
Warmup-0001							
Taxi-0001							
Takeoff-0001							
Climb-0001			15.94		-0.56	35.87	-9.96
Cruise-0001			777.62	0.35	-34.25		-311.05
Descent-0001							
Land-Taxi-0001							
Stall-0001							

Figure 7.41 Take-off Weight Sensitivity

7.2.2.4 Class I Drag

To calculate the Class I drag input data is needed defined in the primary mission. Regression coefficients and Oswald's efficiency factors are defined as shown in Figure 7.42.

Parameter	Value
e_{Clean}	0.8
e_{TD}	0.77
e_L	0.72
e_{OEI}	0.75
a	-2.0458
b	1.0
c	1.2362
d	0.4319
$C_{L_{maxclean}}$	1.4

Figure 7.42 Input for Class I Drag Polar

The reason these parameters are shown here is that they are used in several of the flight segments. As an example the cruise clean Class I drag is calculated. Input parameters are shown in Figure 7.43.

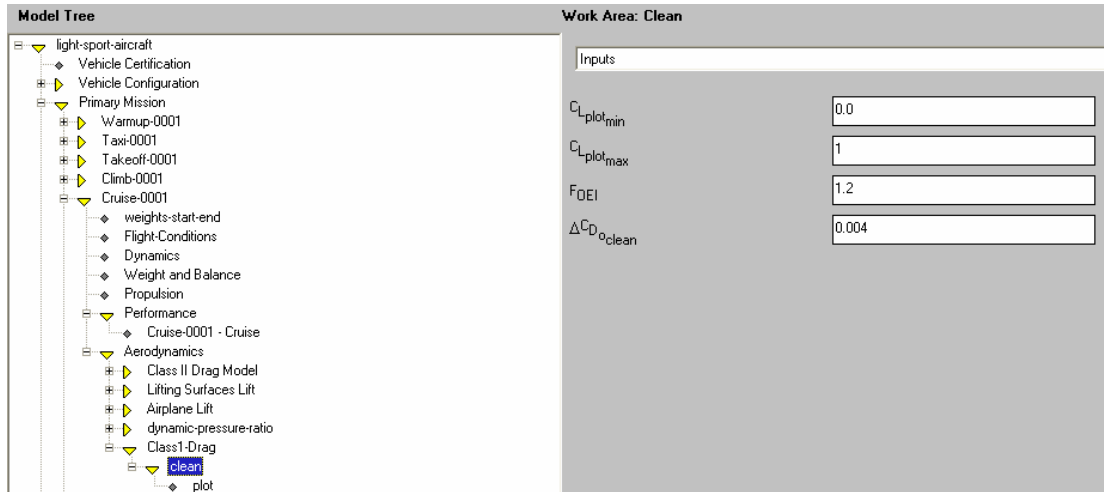


Figure 7.43 Input for Clean Class I Drag Polar

The drag coefficients can be calculated for different flight conditions: take-off gear down, take-off gear up, landing gear down, landing gear up, etc.

The output for the clean drag polar is shown in Figure 7.44.

Work Area: Clean		
Outputs		
W_{TO}	1265.1494	!
S_w	131.7864	!
AR_w	8	!
a	-2.0458	!
b	1.0	!
c	1.2362	!
d	0.4319	!
S_{wet}	376.7168	!
f	3.3901	!
$C_{D_{oclean}}$	0.0257	!
e_L	0.77	!
$C_{D_{oclean}}$	0.0297	!
$B_{DP_{clean}}$	0.0517	!

Figure 7.44 Output for Clean Class I Drag Polar

The lift coefficient can be plotted against the drag coefficient. Figure 7.45 shows the clean configuration drag polar plot.

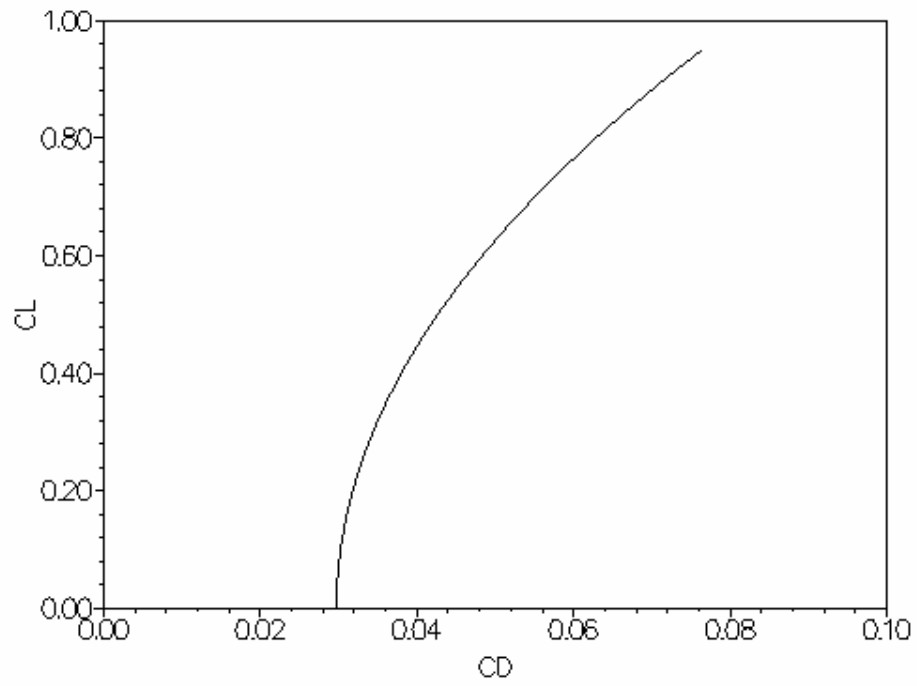


Figure 7.45 Drag Polar

7.2.2.5 Performance Sizing

This module is used to determine the wing loading as well as the power/thrust loading to meet the various performance requirements.

The sizing is based on requirements for climb, stall speed, maximum cruise speed, take-off distance, landing etc. Since the LSA requirements are not yet programmed, FAR23 requirements are used instead. Where needed, LSA requirements for stall speed and maximum speed are used.

For the following flight segments, performance requirements can be constructed:

- Take-off Field Requirements (Figure 7.46)
- Climb (Figure 7.47)
- Maximum Cruise Speed (Figure 7.48)
- Landing Field Requirements (Figure 7.49)
- Stall Speed (Figure 7.50)

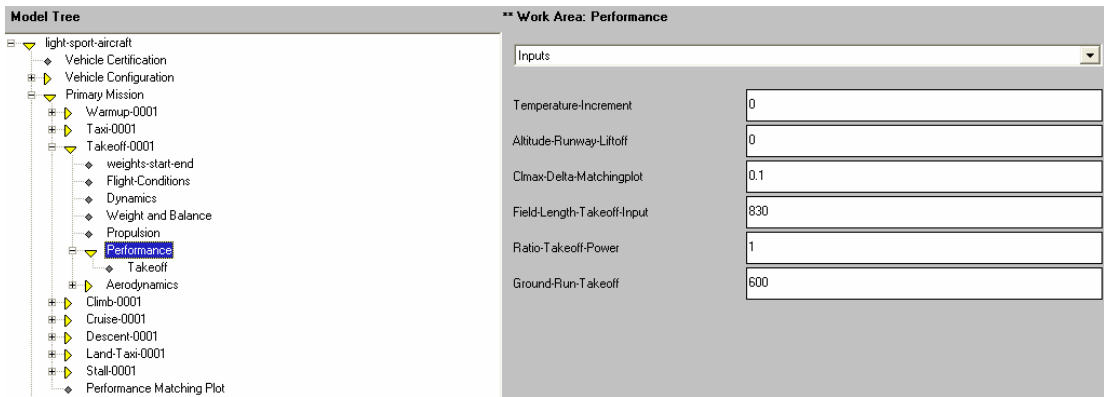


Figure 7.46 Take-off Performance Input

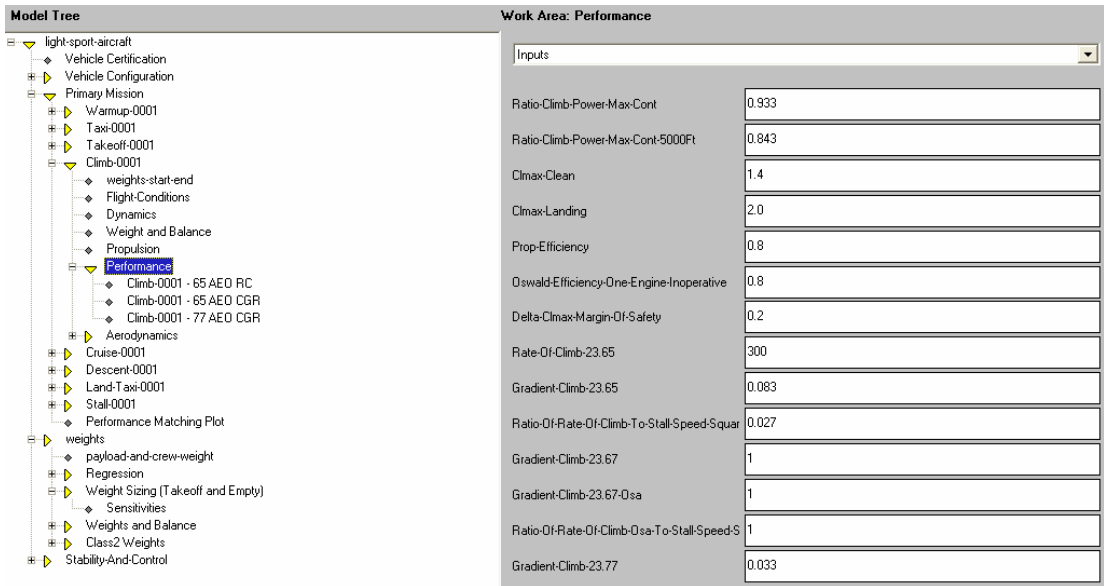


Figure 7.47 Climb Performance Input

Note: FAR23.67 is not applicable to Piston-driven airplanes.

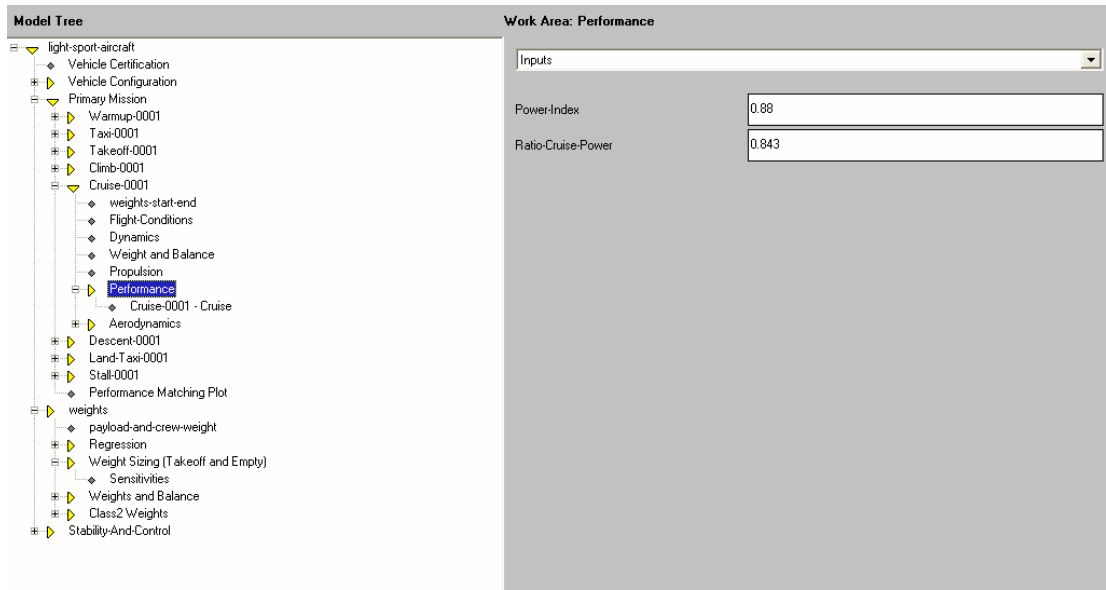


Figure 7.48 Cruise Performance Input

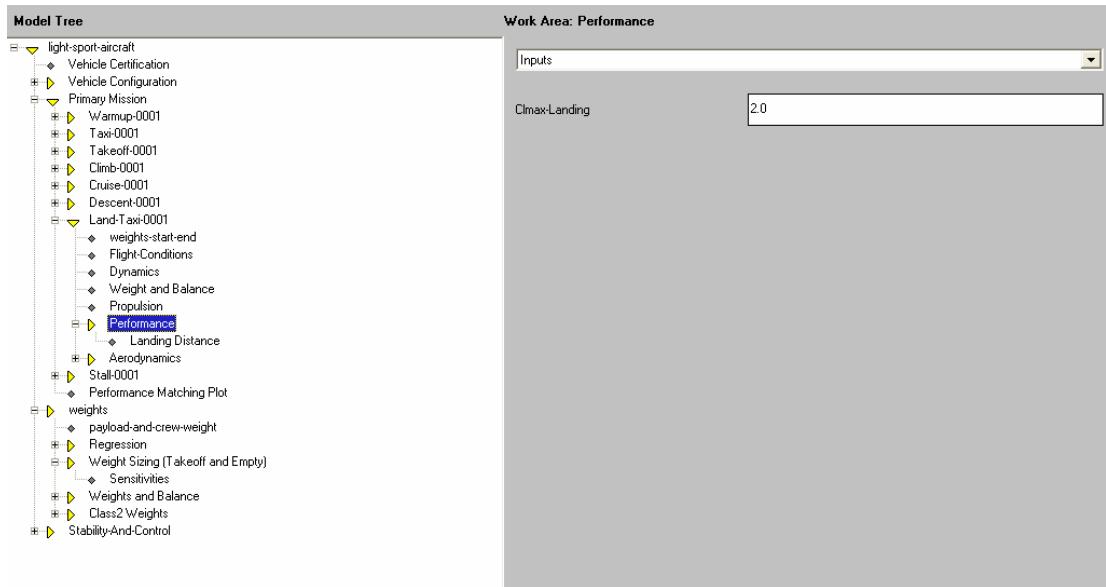


Figure 7.49 Landing Performance Input

Note: the landing distance is not shown, but is defined as a property and is set to 700 ft.

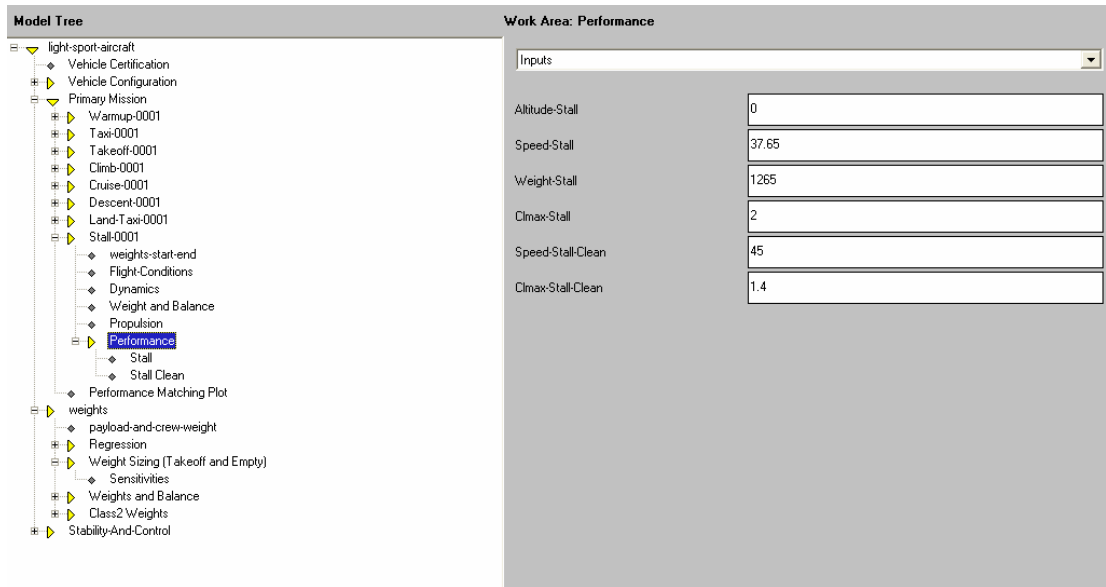


Figure 7.50 Stall Performance Input

A plot of thrust loading (T/W) or power loading (W/P) and wing loading (W/S) is generated for each requirement (Figure 7.51).

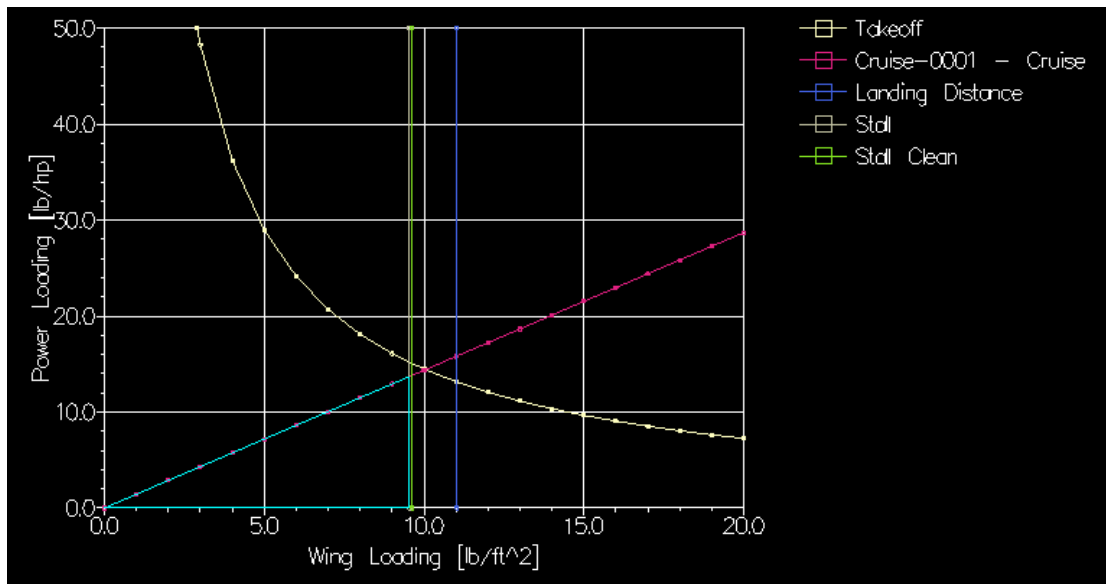


Figure 7.51 Performance Sizing Plot

The matching plot guidelines are built into the system to determine the area under a given curve where the requirement is met. This is done automatically for jet as well as propeller powered airplanes. The user chooses the set of requirements to be satisfied and the system graphically depicts the common area under the curve where the selection of the wing-loading and the thrust-loading is valid (See Figure 7.51). At this point, the user must manually select a point from the selectable area. An option using input weighting factors where the system automatically calculates the design point is under development.

7.2.2.6 Aerodynamics

This module is used to calculate the maximum lift with and without flaps and to determine the lift distribution over the lifting surface span.

7.2.2.6.1 Wing Maximum Lift

Depending on the flight segment the maximum lift can be calculated for airfoils and for the lifting surface. In this case the wing maximum lift coefficient is calculated. Since this airplane uses an airfoil not listed in the list, the airfoil maximum lift coefficient must be defined by the user. This data can come from another software program or from wind tunnel data. Figure 7.52 shows an example using an LS(1)-417 MOD airfoil with lift coefficients determined from wind tunnel data (Ref. 192).

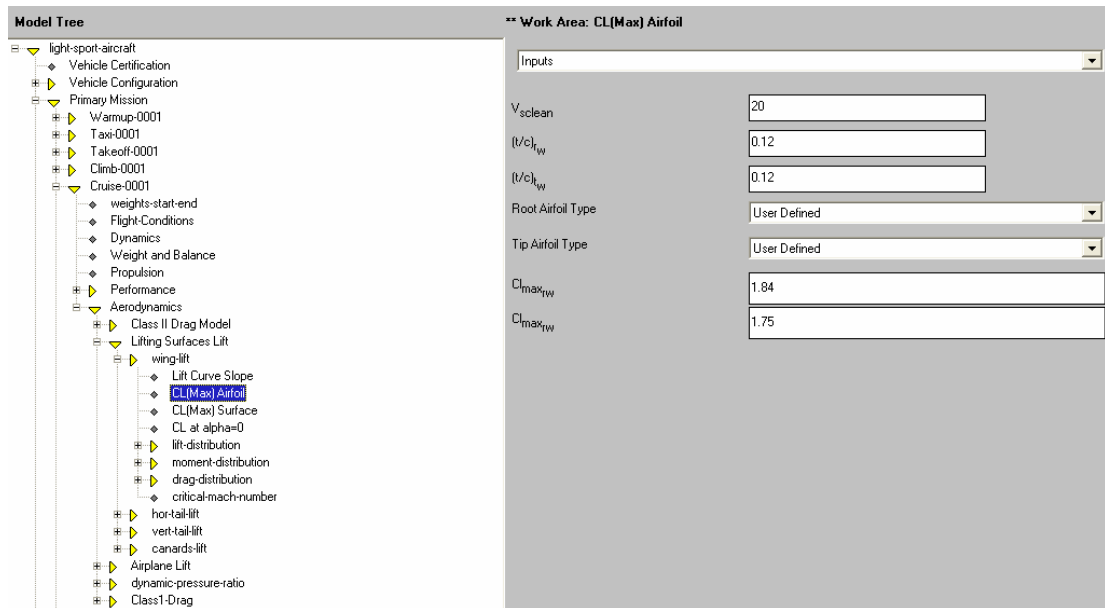


Figure 7.52 Airfoil Maximum Lift Coefficient

With the root and tip airfoil maximum lift coefficient known, the total wing maximum lift coefficient can be calculated.

7.2.2.6.2 Flap Sizing

From the performance sizing module, the maximum lift coefficients at take-off and landing are known. Also the clean wing maximum lift coefficient is known.

In the take-off and landing segment in the primary Mission, several input parameters must be specified under Aerodynamics > Class I Flap and Lift Sizing (Figure 7.53).

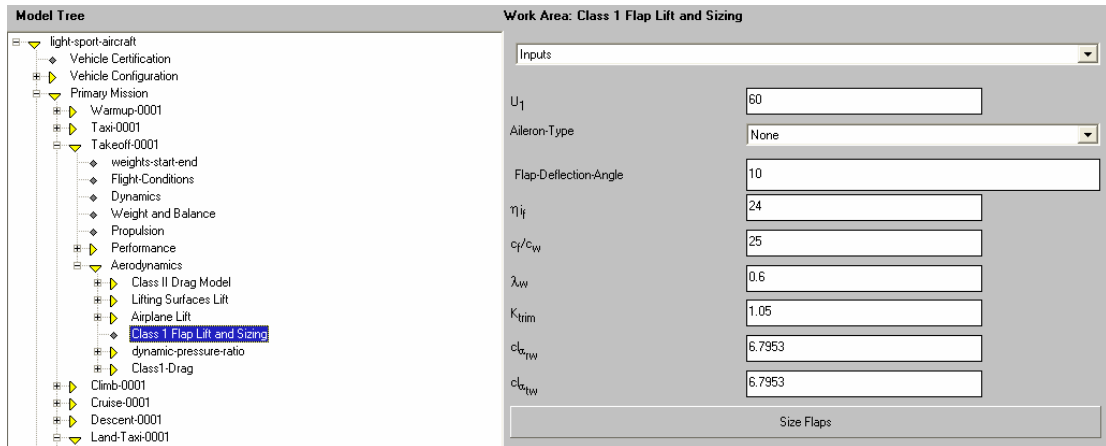


Figure 7.53 Flap Maximum Lift Input

Selecting Size Flaps will create the output parameters and determines the outboard flap station (Figure 7.54).

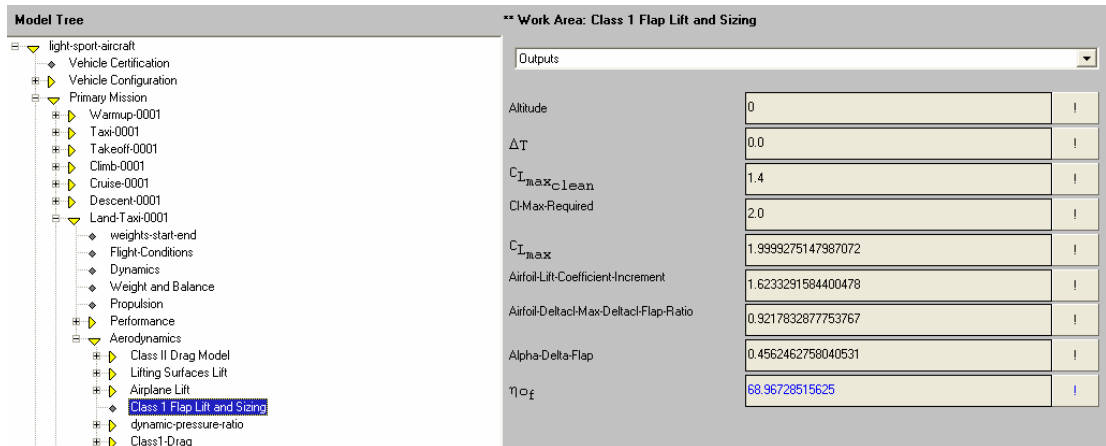


Figure 7.54 Flap Maximum Lift Output

7.2.2.6.3 Wing Lift Distribution

A plot of the wing lift distribution across the span of the wing can be generated with a breakdown of the basic and the additional lift coefficients. Input data needed is shown in Figure 7.55.

Inputs	
lift-coefficient-without-flaps	0.25
area	131.7864
aspect-ratio	8
quarter-chord-sweep-angle	10
spanwise-location	1
root-chord-length	5.0734
tip-chord-length	3.044
altitude	5000
twist-angle	-2
root-thickness-ratio	17.0
tip-thickness-ratio	17.0
root-airfoil-zero-lift-alpha	-3.5
tip-airfoil-zero-lift-alpha	-3.5
root-airfoil-lift-curve-slope	6.7953
tip-airfoil-lift-curve-slope	6.7953

Figure 7.55 Wing Lift Distribution Input Data

Figure 7.56 shows a plot of the lift distribution on the wing.

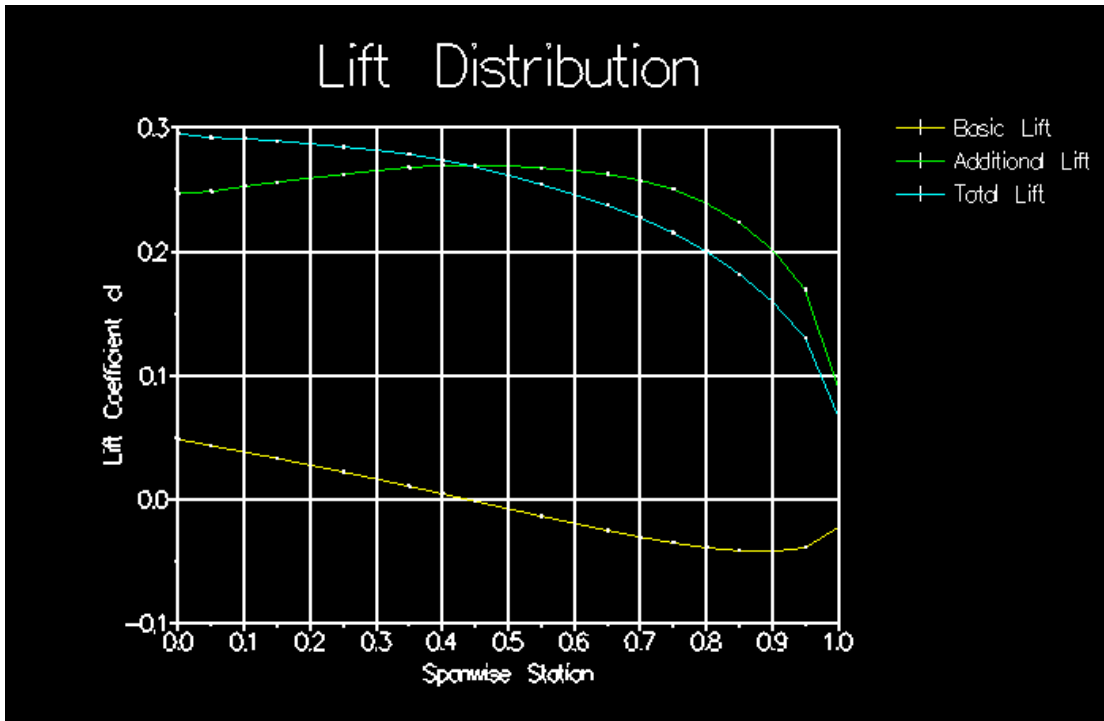


Figure 7.56 Wing Lift Distribution

7.2.2.7 Volume Methods

The horizontal tail, vertical tail and canard locations are calculated using volume methods for given areas. The methods are described in Section 6.7.

Figure 7.57 Shows typical output for the horizontal tail.

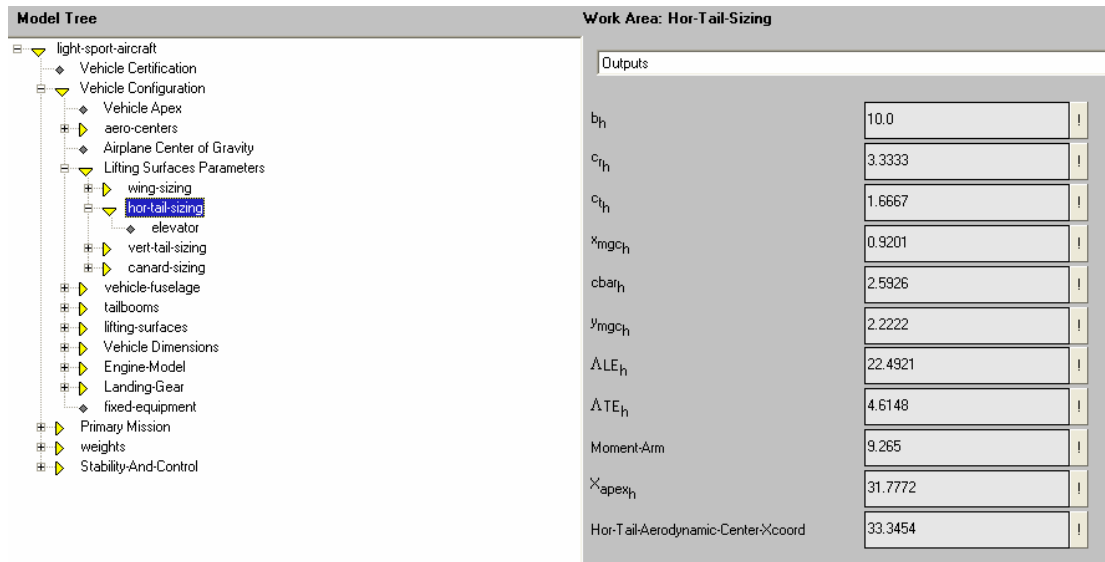


Figure 7.57 Horizontal Tail Volume Method Output

7.2.2.8 Class I Weight and Balance

7.2.2.8.1 Weight Fractions

Under Weight and Balance the weight-fractions module is selected. After supplying the file name with predefined weight fractions, the “+”-sign is used to add airplane to a list. AAA-AML will use these airplanes to average the fractions of the different weight components. For this example, four different airplanes are chosen as shown in Figure 7.58.

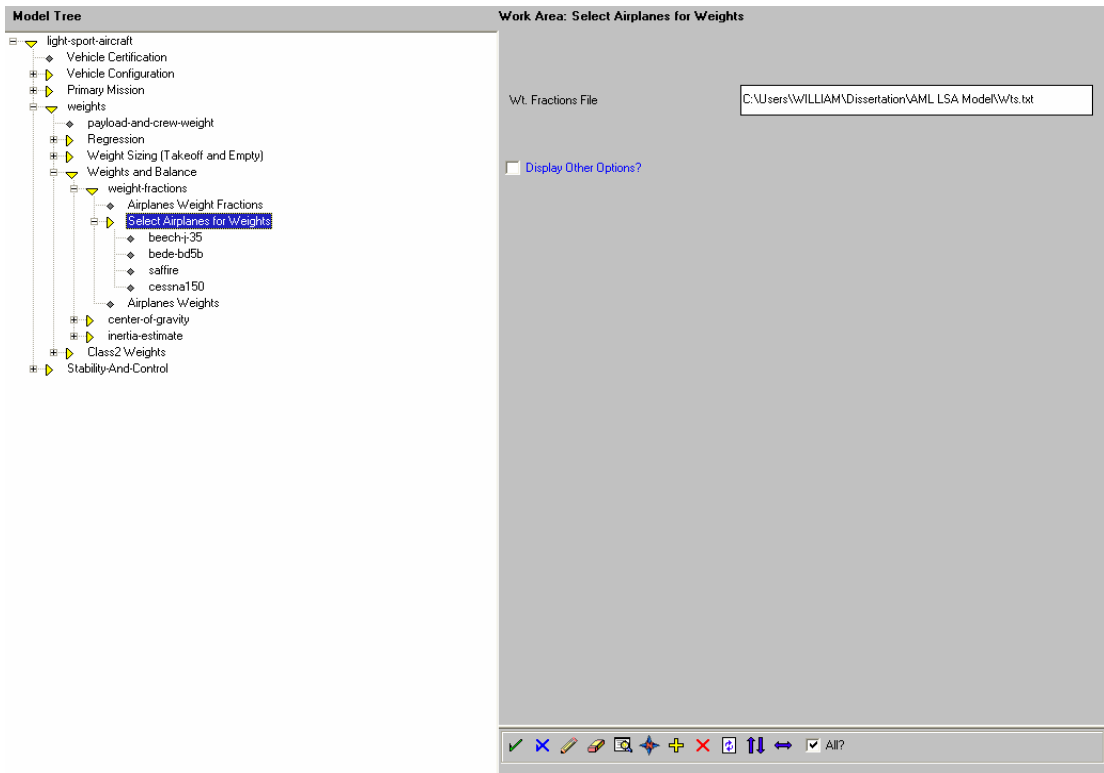


Figure 7.58 Weight Fractions

Selection Airplane Weight Fractions and demanding the output will result in the average weight fractions (Figure 7.59).

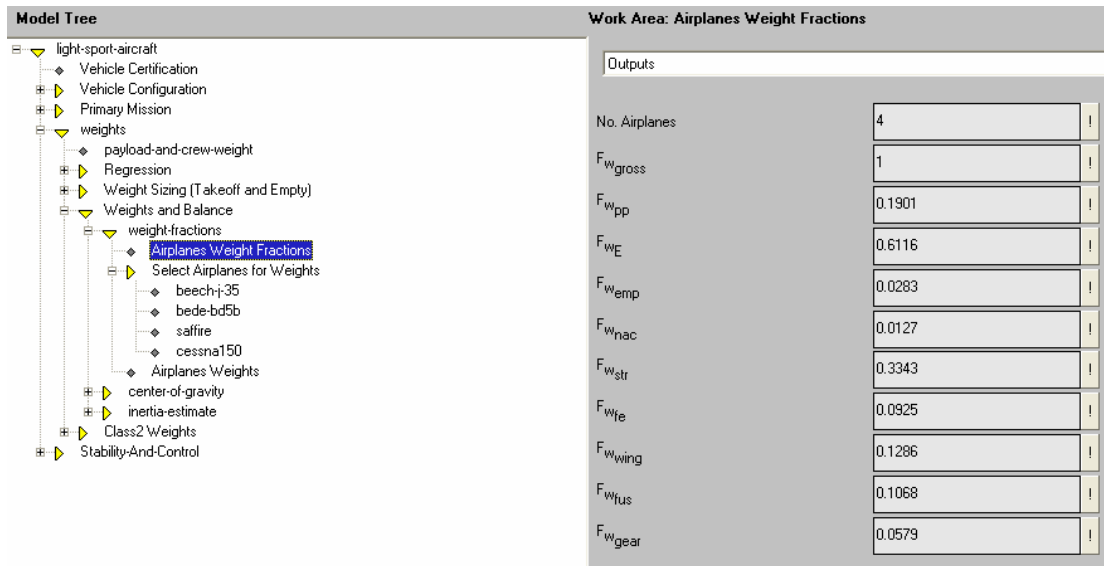


Figure 7.59 Average Weight Fractions

Selecting Airplane Weights and demanding the output results on the component weights as shown in Figure 7.60.

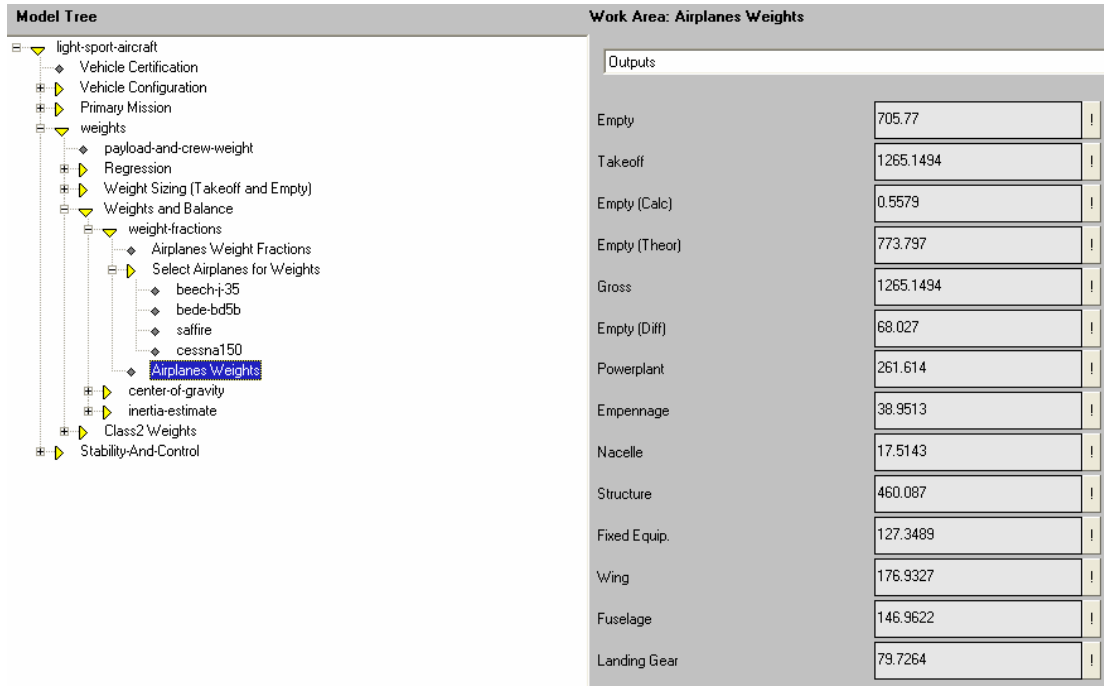


Figure 7.60 Average Weights

7.2.2.8.2 Weight and Balance

To determine the empty weight center of gravity in x-,y- and z-direction, the center-of-gravity module is selected (Figure 7.61). Entering the (x,y,z) coordinates in AML list format and then demanding the output, will show the empty weight center of gravity location (Figure 7.62).

The screenshot displays a software interface with two main panels. The left panel, titled 'Model Tree', shows a hierarchical structure of modules for a 'light-sport-aircraft'. The 'center-of-gravity' module is expanded, and 'Empty Weight (From Fractions)' is selected. The right panel, titled 'Work Area: Empty Weight (From Fractions)', shows a table of inputs for various aircraft components.

Component	Input Value
Fuselage-Group-Cg	(list 9.75 0 9.92)
Wing-Group-Cg	(list 22.54 0 9.42)
Empennage-Group-Cg	(list 22.6 0 9.31)
Landing-Gear-Group-Cg	(list 20.08 0 7.94)
Nacelle-Group-Cg	(list 0 0 0)
Powerplant-Group-Cg	(list 26.67 0 9.83)
Fixed-Equipment-Group-Cg	(list 21.67 0 9.58)

Figure 7.61 Empty Weight Component C.G.

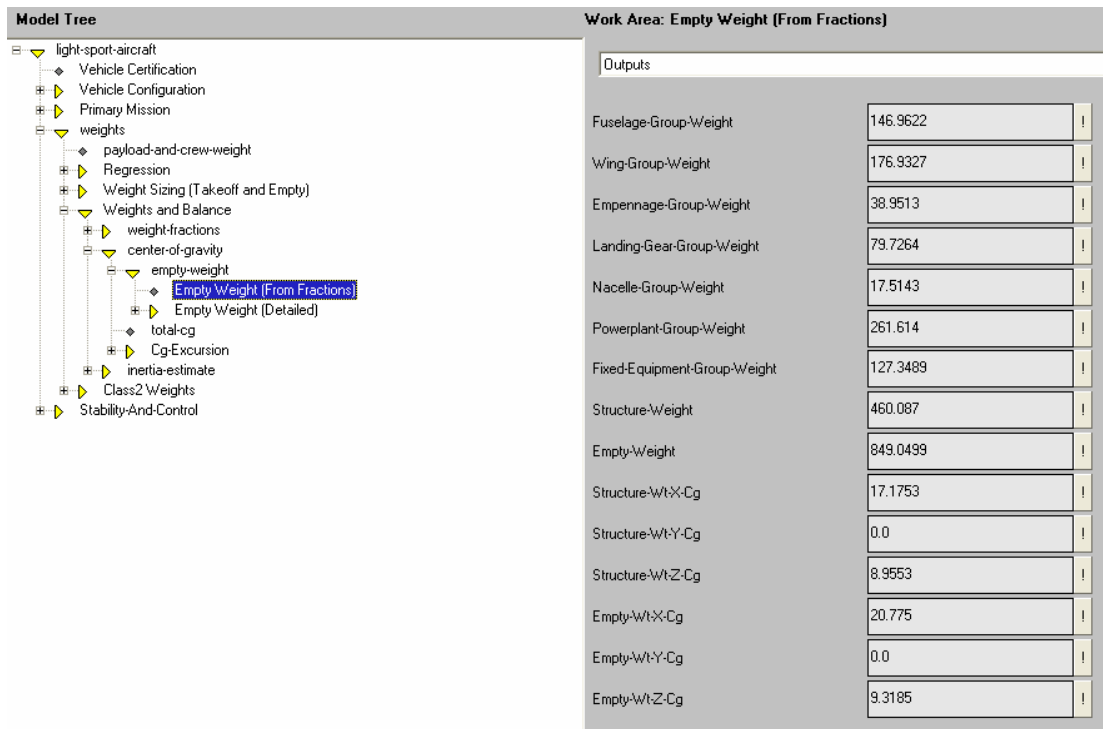


Figure 7.62 Empty Weight C.G.

7.2.2.8.3 Class I Moments of Inertia

Similar to weight fractions, a file must be selected to obtain statistical data on radii of gyration to calculate moments of inertia. Methods are described in Chapter 6.

Similar airplanes are selected from the file and added to the list (Figure 7.63).

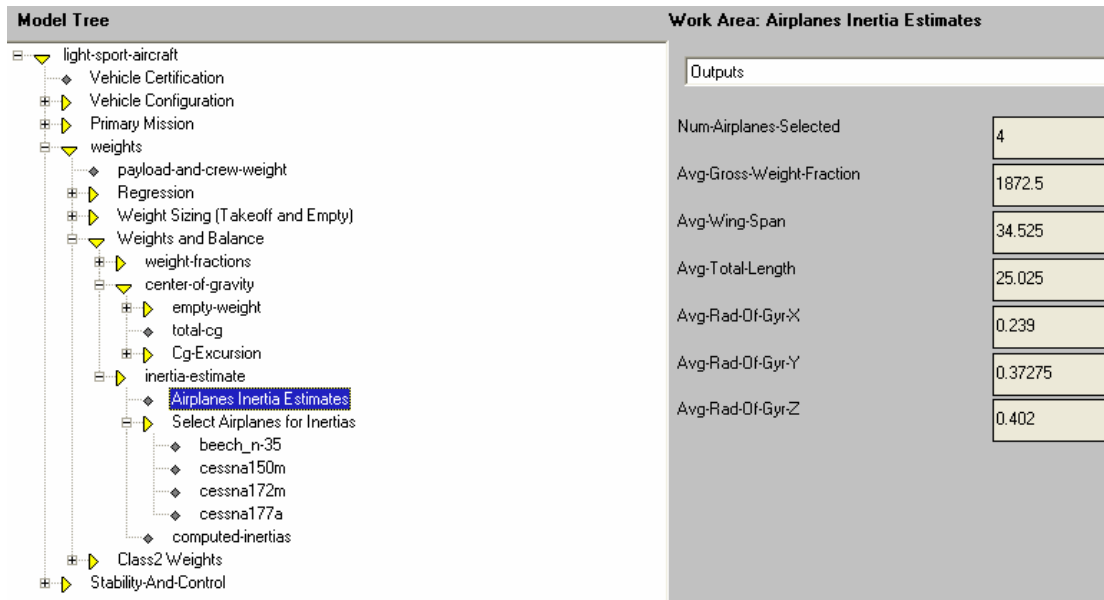


Figure 7.63 Radius of Gyration

With the average radii of gyration, the overall length and wing span, the moments of inertia are calculated as shown in Figure 7.64.

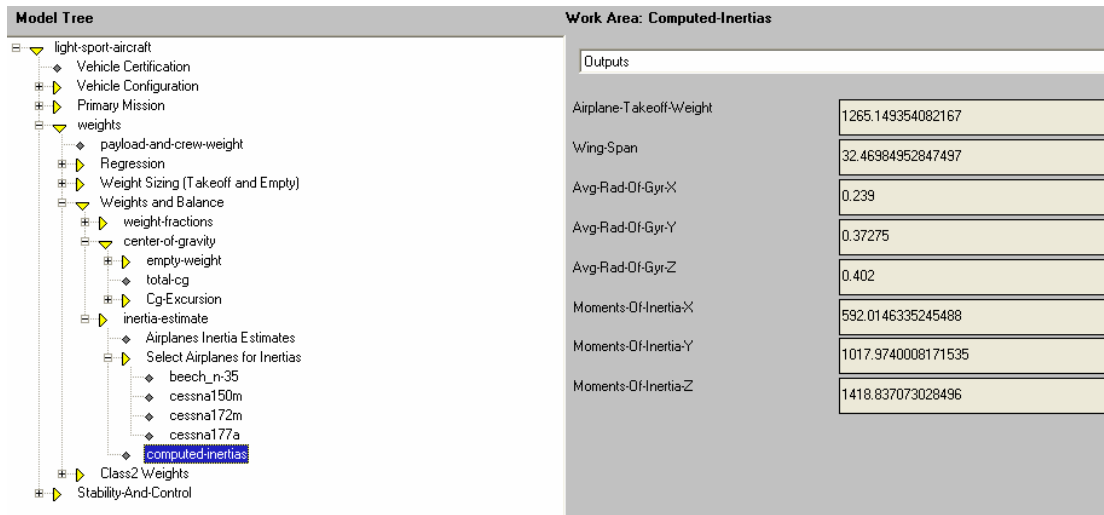


Figure 7.64 Moments of Inertia

7.2.2.9 Class II Weights

This module calculates all the major weights in a similar fashion as AAA. Currently only input/output windows with classes and methods are created. All modules calculate weights for each component. Integration into an iterative process to recalculate the new overall take-off weight is not implemented.

7.2.2.10 Class II Drag

Under the different flight segments, Class II drag can be found under aerodynamics. Currently only methods and classes are implemented. No plotting functions have been integrated. Calculations are performed in a similar matter as AAA.

7.2.2.11 Geometry and Configuration Layout

This module supports the 3D and parametric geometry design, configuration and layout of wing, fuselage, tailbooms, horizontal and vertical tail and canard.

The geometry configuration parameters such as wing span, wing aspect ratio, etc. can be defined in the configuration section and the system generates the geometry based on these parameters (see Figure 7.65). With calculated planform parameters the outer mold lines and surfaces can be drawn in the graphics display of the AML development environment (see Figure 7.66).

Inputs	
Wing Loading	9.6
λ_w	0.6
AR_w	8
$\Delta c/4_w$	10
Z_{apex_w}	10.58
$Z_{ct/4_w}$	10.58
Γ_{g_w}	2.6
i_w	0
ϵ_{g_w}	-3
x_{apex_w}	21.5
t/c_{t_w} (%)	17
t/c_{t_w} (%)	17

Figure 7.65 AAA-AML Wing Geometry Input

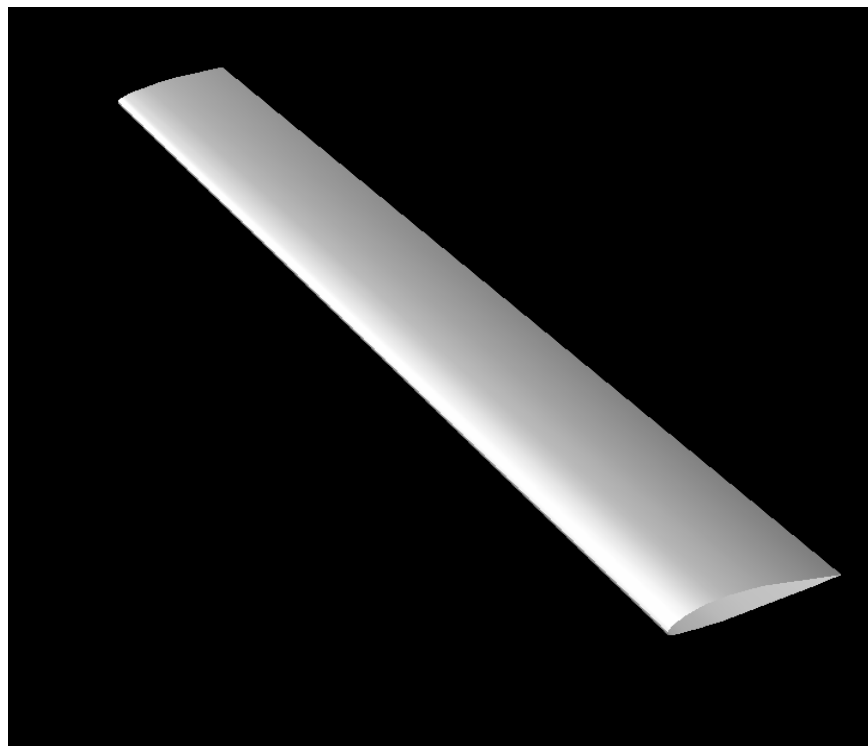


Figure 7.66 AAA-AML Wing Geometry

A second way of defining the geometry in AML is by using the TechnoSoft Wing Editor (Figure 7.67) by starting the AMSketcher.

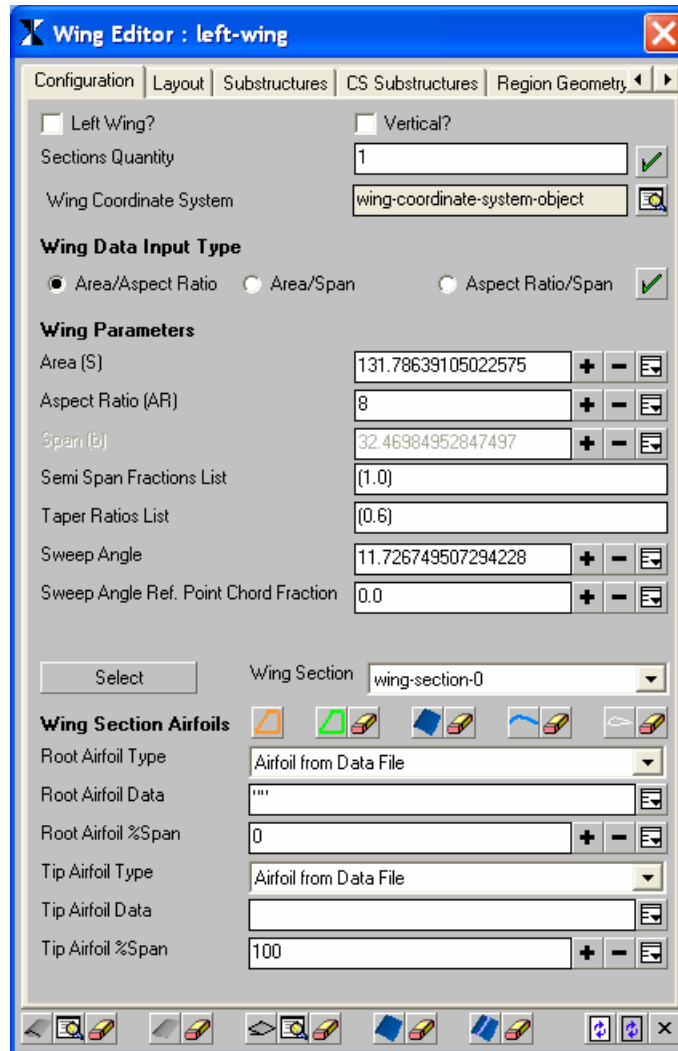


Figure 7.67 AML Wing Editor

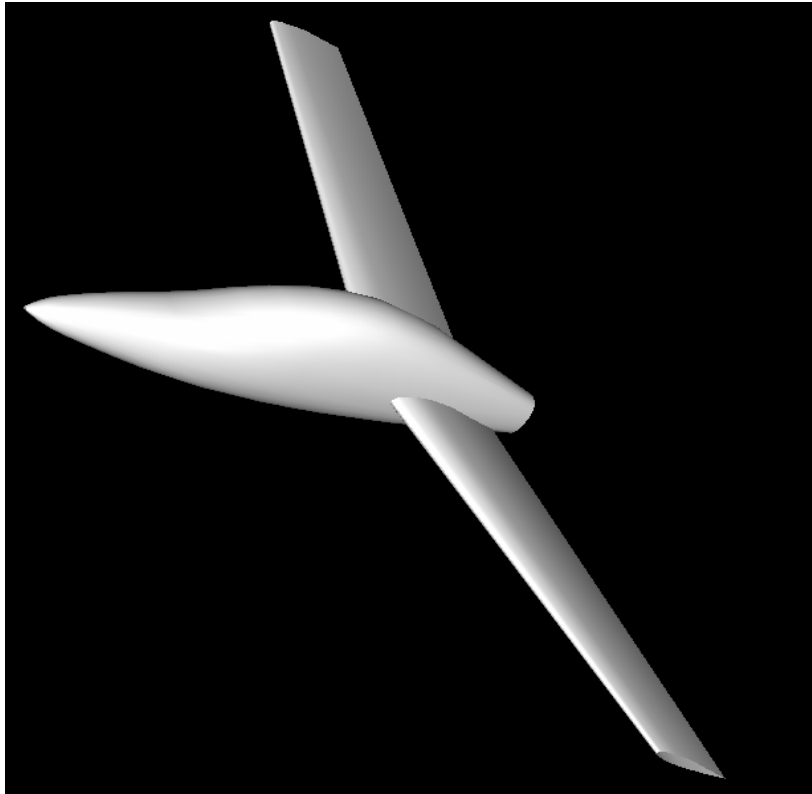


Figure 7.69 Fuselage-Wing Geometry

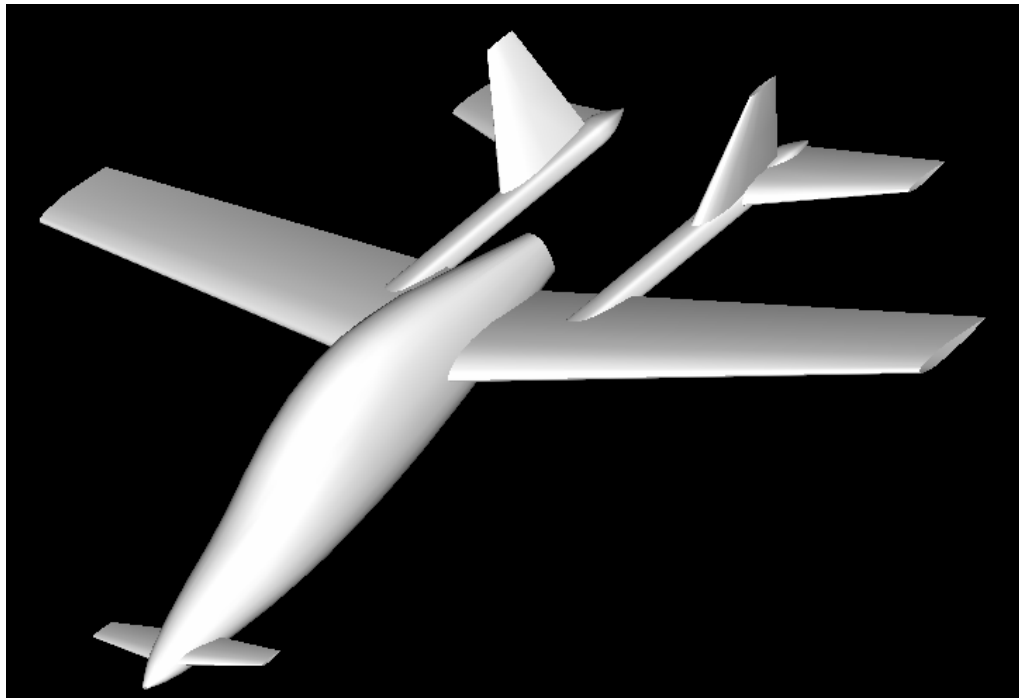


Figure 7.70 LSA 3D Geometry

7.2.3 Feedback on Use of AAA-AML for Design

Although AAA-AML is currently in the prototype phase, it is a very useful tool for sizing the airplane. All methods match AAA. A major advantage is the visual feedback of the geometry, which prevents embarrassing errors such as horizontal tail surfaces not physically attached to the rest of the airplane. Currently AAA-AML must be run side-by-side with AAA because no help system exists yet and AAA help is used for typical values of many parameters. A much more rapid calculation is performed than in AAA. Changing a parameter in a mission segment will cause immediate update of all parameters that depend on it. This is currently impossible in AAA, because the way AAA is designed. This will increase efficiency and will allow for more rapid iterations and/or more design choices.

The user-interface requires more work. An initial flow-chart user interface has been designed. Currently no units are shown and no engineering symbols are used.

8 Conclusions and Recommendations

This work resulted in the third generation of Advanced Aircraft Analysis (AAA) software, currently in release 3.1, which is now used by 279 manufacturers and universities in 45 countries with over 1000 licenses. The number of installations is an indication of its acceptance as a standard for a preliminary design tool.

The development of AAA-AML, a knowledge-based conceptual and preliminary design system, showed it is possible to integrate early conceptual and preliminary design steps with a system designed for detailed design. All knowledge (from AAA) is captured in the form of methods in an object-oriented fashion. Use of dll's (Dynamic Link Libraries) for the methods lowers debugging time and facilitates updates between two disparate software architectures. Combining methods from AAA with the AML architecture reduces the need for data exchange between multiple programs and thus cuts back in time and number of errors. Visual feedback of the 3D geometry at the early design stage will speed up the design process and prevent input errors.

Automatic recalculation and regeneration of the 3D geometry speeds up the design work significantly as opposed to the way calculations are performed in the Advanced Aircraft Analysis software.

Significant savings in design time have been proven at DARcorporation: a job using the second generation of AAA that took approximately 200 person-hours to complete, can now be performed in less than 40 hours using the third generation of AAA. It also resulted in less geometry errors. More design iterations can be performed in the same time-frame.

It is recommended to make the following additions and changes to AAA-AML:

1. Add units, both British and SI.
2. Add a help system.
3. Add an intuitive User Interface.
4. Add tools for cross-section definition of bodies.
5. Link the maximum lift coefficient calculations for flap sizing and clean wing to the performance sizing module, so that maximum lift coefficients are determined to satisfy the performance requirements.
6. Link Class I drag polar to the weight sizing module to check and update lift-to-drag ratios.
7. Integrate Class II weight iteration.

Before expanding the functionality, it is recommended to first concentrate on a user-interface and further linking of the different classes. Currently most of the Class II drag functionality is a direct copy from AAA, where each class in each flight segment contains properties such as flight speed and altitude. These properties are not linked

to the parent, so speed and altitude are not inherited from its parent class. This means speed and altitude must be entered in each class individually, which is cause for errors.

A continuation of development of this system is recommended where AML programmers will work side-by-side with AAA developers to replace AML code with more AAA dll's to lower maintenance costs and to keep development in sink with new AAA development.

9 References

1. Roskam, J.; *Airplane Design Part I: Preliminary Sizing of Airplanes*; DARcorporation, Lawrence, Kansas, 1989.
2. Roskam, J.; *Airplane Design Part II: Preliminary Configuration Design and Integration of the Propulsion System*; DARcorporation, Lawrence, Kansas, 1989.
3. Roskam, J.; *Airplane Design Part III: Layout Design of Cockpit, Fuselage, Wing and Empennage: Cutaways and Inboard Profiles*; DARcorporation, Lawrence, Kansas, 1989.
4. Roskam, J.; *Airplane Design Part IV: Layout Design of Landing Gear and Systems*; DARcorporation, Lawrence, Kansas, 1989.
5. Roskam, J.; *Airplane Design Part V: Component Weight Estimation*; DARcorporation, Lawrence, Kansas, 1989.
6. Roskam, J.; *Airplane Design Part VI: Preliminary Calculation of Aerodynamic, Thrust and Power Characteristics*; DARcorporation, Lawrence, Kansas, 1989.
7. Roskam, J.; *Airplane Design Part VII: Determination of Stability, Control and Performance Characteristics: FAR and Military Requirements*; DARcorporation, Lawrence, Kansas, 1989.
8. Roskam, J.; *Airplane Design Part VIII VIII: Airplane Cost Estimation and Optimization: Design Development Manufacturing and Operating*; DARcorporation, Lawrence, Kansas, 1990.
9. Roskam, J.; *Airplane Flight Dynamics and Automatic Flight Controls, Part I*; DARcorporation, Lawrence, Kansas, 1996.
10. Roskam, J.; *Airplane Flight Dynamics and Automatic Flight Controls, Part II*; DARcorporation, Lawrence, Kansas, 1996.
11. Roskam, J., Lan, C.T.; *Airplane Aerodynamics and Performance*; DARcorporation, 1997.
12. Malaek, S.M.B.; *Development of a System of Interactive Computer Programs for Airplane Conceptual Design and Advanced Airplane Analysis*; Ph.D. Dissertation, The University of Kansas, 1989.
13. Wood, K.D.; *Aerospace Vehicle Design*; Johnson Publishing, 1966.
14. Nicolai, L.M.; *Fundamentals of Aircraft Design*; Mets, Inc, 1975.
15. Torenbeek, E.; *Synthesis of Subsonic Airplane Design*; Springer (Kluwer), 1982.

16. Anemaat, W.A.J.; Computer Aided Performance Prediction for Airplane Design Version 2.0 Appendix B, p. 120-124, Delft University of Technology, Faculty of Aerospace Engineering, Report LR-488, June 1986.
17. Hale, F.J.; *Introduction to Aircraft Performance, Selection and Design*; Cambridge, 1984.
18. Heinemann; *Aircraft Design*; Nautical & Aviation Publishing, 1985.
19. Hollman, M.; *Modern Aircraft Design*; Hollman, 1989.
20. Thomas, F.; *Fundamentals of Sailplane Design*; College Park Press, 1993.
21. Crawford, D.R.; *A Practical Guide to Airplane Performance and Design*; Crawford, 1994.
22. Huenecke, K.; *Modern Combat Aircraft Design*; Naval Institute Press, 1994.
23. Hiscocks, R.D.; *Design of Light Aircraft*; Hiscocks, 1995.
24. Stinton, D.; *Design of the Aeroplane*; Oxford Blackwell Science, 1995.
25. Stinton, D.; *Design of the Airplane*; Oxford Blackwell Science, 1995.
26. Crawford, D.R.; *Airplane Design*; Crawford, 1997.
27. Anderson, J.; *Aircraft Performance and Design*; McGraw-Hill, 1999.
28. Fielding, J.P.; *Introduction to Aircraft Design*; Cambridge, 1999.
29. Jenkinson, L.R.; *Civil Jet Aircraft Design*; AIAA/Butterworth-Heinemann, 1999.
30. Whitford, R.; *Fundamentals of Fighter Design*; Crowood Press, 2000.
31. Raymer, D.; *Simplified Aircraft Design for Homebuilders*; Design Dimension Press, 2002.
32. Corke, T.C.; *Design of Aircraft*; Prentice Hall, 2003.
33. Jenkinson, L.R., Marchman, J.F.; *Aircraft Design Projects for Engineering Students*; AIAA/Butterworth-Heinemann, 2003.
34. Brandt, S.A., Stiles, R.J., Bertin, J.J., Whitford, R.; *Introduction to Aeronautics; A Design Perspective*; AIAA, 2004.
35. Raymer, D.; *Aircraft Design: A Conceptual Approach*; AIAA, 2006.
36. Jan Roskam, Seyyed Malaek; Automated Aircraft Design Configuration Design and Analysis; SAE 891072; General, Corporate and Regional Aviation Meeting and Exposition, Wichita, KS, April 11-13, 1989.
37. J. Roskam, S. Malaek, W. Anemaat, D. Gerren; Advanced Aircraft Analysis: A Powerful, User Friendly Framework for Airplane Preliminary Design and Analysis; AIAA Techfest XVI, Wichita, KS, Nov 2-4, 1989 and NASA/USRA Winter Conference, Long Beach, CA, Nov 6-7, 1989.

38. J. Roskam, S.M. Malaek, W. Anemaat; AAA (Advanced Aircraft Analysis): A User-Friendly Approach To Preliminary Aircraft Design; ICAS-90-2.10.2; The University of Kansas, Lawrence, KS, 1990.
39. Jan Roskam, William Anemaat; An Easy Way to Analyze Longitudinal and Lateral-Directional Trim Problems with AEO or OEI;1993 AIAA Techfest, Airport Ramada Inn, Wichita, KS, Nov 12-13, 1993.
40. Jan Roskam, William Anemaat; An Easy Way to Analyze Longitudinal and Lateral-Directional Trim Problems with AEO or OEI; SAE 941143; Aerospace Atlantic Conference and Exposition, Dayton, OH, April 18-22, 1994.
41. William A. Anemaat; G.A.-CAD, A Personal Computer Aided Design System for General Aviation Aircraft Configurations; SAE 951158; General, Corporate and Regional Aviation Meeting and Exposition, Wichita, KS, May 3-5, 1995.
42. Jan Roskam, William Anemaat; General Aviation Aircraft Design Methodology in a PC Environment; SAE 965520; 1996 World Aviation Congress, Anaheim, CA, Oct 21-24, 1996
43. William A. Anemaat, Kurt L. Schueler, C. Todd Kofford; General Aviation Airplane Design Tools for PC's; SAE 971473; General, Corporate and Regional Aviation Meeting and Exposition, Wichita, KS, April 29-May 1, 1997.
44. James Locke, Kurt L. Schueler, William A. Anemaat; General Aviation Preliminary Structural Design in a Personal Computer Environment; SAE 971501; General, Corporate & Regional Aviation Meeting & Exposition, Wichita, KS, April 29-May 1, 1997.
45. Timothy D. Olson; Aircraft Design Tools for PC's; SAE 971474; General, Corporate & Regional Aviation Meeting & Exposition, Wichita, KS, April 29-May 1, 1997.
46. Kurt L. Schueler, Steven J. Smith; Advanced Aircraft Analysis: A Powerful, User Friendly Framework for Airplane Preliminary Design and Analysis; SAE 951161; General, Corporate and Regional Aviation Meeting and Exposition, Wichita, KS, May 3-5, 1995.
47. Roy A. Liming; *Mathematics for Computer Graphics*; Aero Publishers Inc. ISBN 0-8168-6751-8; 1981.
48. William M. Newman, Robert F. Sproull; *Principles of Interactive Computer Graphics*; McGraw-Hill ISBN 0-07-046338-7; 1983.

49. Tom Lyche, Larry L. Schumaker Editors; *Mathematical Methods in Computer Aided Geometric Design*; Academic Press ISBN 0-12-460515-X; 1989.
50. James Foley, Andries van Dam, Steven Feiner, John Hughes; *Computer Graphics Principles and Practice*; Addison Wesley ISBN 0-201-12110-7; 1990.
51. Gerald Farin; *Curves and Surfaces for Computer Aided Geometric Design*; Academic Press ISBN 0-12-249051-7; 1990.
52. Ibrahim Zeid; *CAD/CAM Theory and Practice*; McGraw-Hill ISBN 0-07-072857-7; 1991
53. Robert C. Beach; *An Introduction to the Curves and Surfaces of Computer-Aided Design*; Van Nostrand Reinhold ISBN 0-442-00503-2; 1991.
54. Alan Watt; *3D Computer Graphics*; Addison Wesley ISBN 0-201-63186-5; 1993.
55. M.E. Mortenson; *Mathematics for Computer Graphics Applications*; Industrial Press ISBN 0-8311-3111-X; 1999.
56. Philip J. Schreiner, David H. Eberly; *Geometric Tools for Computer Graphics*; Morgan Kaufmann Publishers ISBN 1-55860-594-0; 2003.
57. Samuel R. Buss; *3-D Computer Graphics A Mathematical Introduction with OpenGL*; Cambridge University Press ISBN 0-521-82103-7; 2003.
58. Ibrahim Zeid; *Mastering CAD/CAM*; McGraw-Hill ISBN 0-07-266845-7; 2005.
59. Jeffrey V. Zweber, Hane Kabis, William W. Follett, Narayan Ramabadran; Towards an Integrated Modeling Environment for Hypersonic Vehicle Design and Synthesis; AIAA 2002-5172; AIAA/AAAF 11th International Space Planes and Hypersonic Systems and Technology, September 29-4 October, 2002, Orleans, France.
60. Adaptive Modeling Language Reference Manual, Version 4.17, Technosoft Inc., Cincinnati, OH, 2006.
61. William A. Anemaat, Balaji Kaushik, Richard D. Hale, Narayanan Ramabadran; A Knowledge-Based Design Framework for Aircraft Conceptual and Preliminary Design; SAE 2006-01-2403; SAE 2006 General Aviation Technology Conference & Exhibition, Wichita, KS Aug 30-31, 2006
62. V.M. Vasey-Glandon and R.D. Hale; "Knowledge Driven Composite Design Optimization Process and System," U.S. patent 5,984,511 issued 16 November, 1999, U.S. Patent 6,341,261 issued 22 January, 2002, and International patent EP 1 050 396 B1 issued 6 August, 2003.

63. R.D. Hale and V.M. Vasey-Glandon; "PACKS: An Affordable Knowledge-Driven Composite Design for Manufacturing Process." SAMPE 2001, May 6-10, 2001, Long Beach CA.
64. V.M. Vasey-Glandon and R.D. Hale; "PACKS (Parametric Composite Knowledge System): An Affordable Structural Definition Process for Composites", 41st AIAA/ASME/ASCE/AHS/ASC Structures, Structural Dynamics and Materials Conference, Atlanta, GA, 3-6 April, 2000.
65. A.P. Harper; Engineering Designer, Jan/Feb. 1999.
66. V. Mukhopadhyay, S-Y. Hsu, B.H. Mason, D.W. Sleight, H. Kamhawi, J.L. Dahl; Adaptive Modeling, Engineering Analysis and Design of Advanced Aerospace Vehicles; AIAA 2006-2182; 47th AIAA/ASME/ASCE/AHS/ASC Structures, Structural Dynamics, and Materials Conference, 1-4 May, 2006, Newport, Rhode Island.
67. Jorgen Dahl, Stephen Hill, Adel Chemaly; AMRaven: Adaptive Modeling Rapid Air Vehicle Engineering; SAE 2006-01-2402; SAE 2006 General Aviation Technology Conference & Exhibition, Wichita, KS Aug 30-31, 2006.
68. S.A. Coons, B. Herzog; Surfaces for Computer-Aided Aircraft Design; AIAA 67-895; AIAA 4th Annual Meeting and Technical Display, Anaheim, California/October 23-27, 1967.
69. Daniel P. Raymer; A Computer-Aided Aircraft Configuration Development System; AIAA 79-0064; 17th Aerospace Sciences Meeting, New Orleans, LA/January 15-17, 1979.
70. Antonio L. Elias; Computer-Aided Engineering: The AI Connection; Astronautics & Aeronautics, July/Aug 1983.
71. L.R. Jenkinson, D. Simons; A Computer Program For Assisting In The Preliminary Design Of Twin-Engined Propeller-Driven General Aviation Aircraft; Canadian Aeronautics and Space Journal, Vol. 30, No. 3, Sept 1984.
72. J. Alsina, J. Fielding, A. Morris; Progress Towards an Aircraft Design Expert System; Computer Applications in Aircraft Design and Operation, T. Murthy, J. Fielding, Eds., Springer-Verlag, Berlin, 1987.
73. Mark A. Kolb; A Flexible Computer Aid for Conceptual Design Based on Constraint Propagation and Component-Modeling; AIAA-88-4427; AHS and ASEE, Aircraft Design, Systems and Operations Meeting, Atlanta, GA, Sept 7-9, 1988.

74. I. Kroo, M. Takai; A Quasi-Procedural, Knowledge-Based System for Aircraft Design; AIAA-88-4428; AIAA/AHS/ASEE Aircraft Design, Systems and Operations Conference, Atlanta, GA, Sept 7-9, 1988.
75. Carl W. Dawson; 1993: A Vision of the Design Computer; AIAA-88-4451; AIAA/AHS/ASEE Aircraft Design, Systems and Operations Conference, Atlanta, GA, Sept 7-9, 1988.
76. David W. Hall, J. Edward Rogan; Design of High Altitude, Long Endurance Aircraft using a Computer Programming Language for Design Specifications; AIAA-88-4429; AIAA/AHS/ASEE Aircraft Design, Systems and Operations Conference, Atlanta, GA, Sept 7-9, 1988.
77. S.G. Wampler, A. Myklebust, S. Jayaram, P. Gelhausen; Improving Aircraft Conceptual Design - a Phigs Interactive Graphics Interface for ACSYNT; AIAA-88-4481; AIAA/AHS/ASEE Aircraft Design, Systems and Operations Conference, Atlanta, GA, Sept 7-9, 1988.
78. Bonnie L. Anderson; First Step Toward Integrating the Design Process; AIAA-88-4403; AIAA/AHS/ASEE Aircraft Design, Systems and Operations Conference, Atlanta, GA, Sept 7-9, 1988.
79. A. Bolukbasi, D. Furey, A. Goodworth; Application of Expert Systems to CAD/CAE; AIAA-89-2085; AIAA/AHS/ASEE Aircraft Design, Systems and Operations Conference, Seattle, WA, July 31 - Aug 2, 1989.
80. C. Bil; ADAS: A Design System for Aircraft Configuration Development; AIAA-89-2131; AIAA/AHS/ASEE Aircraft Design, Systems and Operations Conference, Seattle, WA, July 31 - Aug 2, 1989.
81. J. Gee; The Role of Interfaces in Design Integration; AIAA-89-2133; AIAA/AHS/ASEE Aircraft Design, Systems and Operations Conference, Seattle, WA, July 31 - Aug 2, 1989.
82. D.J. Paisley, J.R. Blystone, G.R. Wichmann; The Aerodynamic Assistant; AIAA 89-3132-CP; 7th AIAA Computers in Aerospace Conference, Monterey, CA, Oct 3-5, 1989.
83. C. Haberland, W. Fenske, O. Dranz, R. Stoer; Computer-Aided Conceptual Aircraft Configuration Development by an Integrated Optimization Approach; ICAS-90-2.6R; Institut für Luft- und Raumfahrt, Technische Universität Berlin.
84. I.M. Kroo; An Interactive System for Aircraft Design and Optimization; AIAA 92-1190; 1992 Aerospace Design Conference, February 3-6, 1992, Irvine, CA.

85. M. J. Buckley, K. W. Fertig, and D. E. Smith ;Design Sheet: An Environment for Facilitating Flexible Trade Studies During Conceptual Design; AIAA 92-1191;1992 Aerospace Design Conference, February 3-6, 1992, Irvine, CA.
86. Mark A. Kolb; Constraint-Based Component-Modeling for Knowledge-Based Design; AIAA 92-1192;1992 Aerospace Design Conference, February 3-6, 1992, Irvine, CA.
87. S. Jayaram, A. Myklebust; ACSYNT - A Standards-Based System for Parametric Computer Aided Conceptual Design of Aircraft; AIAA-92-1268; 1992 Aerospace Design Conference, February 3-6, 1992, Irvine, CA.
88. U. Jayaram, A. Myklebust, P. Gelhausen; Extracting Dimensional Geometric Parameters from B-Spline Surface Models of Aircraft; AIAA 92-4283; AIAA Aircraft Design Systems Meeting, Hilton Head, SC, Aug 24-26, 1992.
89. April Gilliam; Vehicles Knowledge-Based Design Environment; Journal of Spacecraft and Rockets, Vol 30, No.3, May-June 1993.
90. Daniel P. Raymer; Aircraft Aerodynamics Analysis on a Personal Computer (Using RDS Aircraft Design Software);SAE 932530;Aerotech '93, Costa Mesa, CA, Sept 27-30, 1993.
91. W.H. Mason, T.K. Arledge; ACSYNT Aerodynamic Estimation - An Examination and Validation for Use in Conceptual Design; AIAA-93-0973; AIAA/AHS/ASEE Aerospace Design Conference, Feb 16-19, 1993/Irvine, CA.
92. Arvid Myklebust, Paul Gelhausen; Improving Aircraft Conceptual Design Tools - New Enhancements to ACSYNT; AIAA-93-3970; AIAA Aircraft Design, Systems and Operations Meeting, Monterey, Aug 11-13, 1993.
93. Francisco Rivera, Jr., Sankar Jayaram; An Object-Oriented Method for the Definition of Mission Profiles for Aircraft Design; AIAA 94-0867;32nd Aerospace Sciences Meeting and Exhibit, January 10-13, 1994/Reno, NV.
94. Scott Angster, Sankar Jayaram; An Object-Oriented, Knowledge-Based Approach to Multi-Disciplinary Parametric Design; AIAA 95-0323; 33rd Aerospace Sciences Meeting and Exhibit, January 9-12, 1995/Reno, NV.
95. Robert E. Smith, Malcolm I.G. Bloor, Michael J. Wilson, Almuttil M. Thomas; Rapid Airplane Parametric Input Design (RAPID); AIAA 95-1687; Proceedings of 12th AIAA Computational Fluid Dynamics Conference, San Diego, CA, June 1995.

96. Paul A. Gelhausen, Mark D. Moore, James R. Gloude-mans; Overview of ACSYNT for Light Aircraft Design; SAE 951159; General, Corporate and Regional Aviation Meeting and Exposition, Wichita, KS, May 3-5, 1995.
97. Daniel P. Raymer; RDS Professional: Aircraft Design on a Personal Computer; SAE 951160; General, Corporate and Regional Aviation Meeting and Exposition, Wichita, KS, May 3-5, 1995.
98. James R. Gloude-mans, Paul C. Davis, Paul A. Gelhausen; A Rapid Geometry Modeler for Conceptual Aircraft; AIAA-96-0052; 34th Aerospace Science Meeting and Exhibit, Reno, NV Jan. 15-18, 1996.
99. D.B. Landrum, Eric G. Woodfin; Will It Fly' A Computer-based Aircraft Design Tool; AIAA 96-0160; 34th Aerospace Science Meeting and Exhibit, Reno, NV Jan. 15-18, 1996.
100. Max Blair, Greg Reich; A Demonstration of CAD/CAM/CAE in a Fully Associative Aerospace Design Environment; AIAA 96-1630; 37th AIAA/ASME/ASCE/AHS/ASC Structural Dynamics, and Materials Conference and Exhibit, Salt Lake City, UT Apr 15-17, 1996.
101. C. Wayne Mastin, Robert E. Smith, Ideen Sadrehaghighi, Michael R. Wiese; Geometric Model for a Parametric Study of the Blended-Wing-Body Airplane; AIAA 96-2416; 14th AIAA Applied Aerodynamics Conference, New Orleans, LA, June 17-20, 1996.
102. Jamshid A. Samareh; Use of CAD Geometry in MDO; AIAA 96-3991; 6th AIAA/USAF/NASA/ISSMO Symposium on Multidisciplinary Analysis and Optimization, Sept 4-6, 1996, Bellevue, WA.
103. Sonny Chai, W.H. Mason; Landing Gear Integration in Aircraft Conceptual Design; AIAA-96-4038; 6th AIAA/USAF/NASA/ISSMO Symposium on Multidisciplinary Analysis and Optimization, Sept 4-6, 1996, Bellevue, WA.
104. Robert E. Smith, Yvette Cordero, Wayne Mastin; Conceptual Airplane Design with Automatic Surface Generation; SAE 965517; 1996 World Aviation Congress, Anaheim, CA, Oct 21-24, 1996.
105. Randy W. Kaul, Kamran Rokhsaz; A Comparative Analysis of the Boeing 727-100 Using Three Advanced Design Methods; SAE 965518; 1996 World Aviation Congress, Anaheim, CA, Oct 21-24, 1996.
106. Daniel P. Raymer; An Update on RDS-Professional; SAE 965567; 1996 World Aviation Congress, Los Angeles, CA, Oct 21-24, 1996.

107. Brett Malone, Arvid Myklebust; ACSYNT, Commercialization Success; SAE 965568; 1996 World Aviation Congress, Los Angeles, CA, Oct 21-24, 1996.
108. Daniel P. Raymer; Aircraft Design Optimization on a Personal Computer; SAE 965609; 1996 World Aviation Congress, Los Angeles, CA, Oct 21-24, 1996.
109. Ilan Kroo; Multidisciplinary Optimization Application in Preliminary Design; AIAA 97-1408; 38th AIAA/ASME/ASCE/AHS/ASC Structures, Structural Dynamics and Materials Conference April 7-10, 1997, Kissimmee, Florida.
110. Matthew S. Schmidt, Chris Paulson; CAD Embedded CAE Tools for Aircraft Designers as Applied to Landing Gear; AIAA 97-3793; AIAA Modeling and Simulation Technologies Conference, New Orleans, LA, Aug 11-13, 1997.
111. Shahab Hasan; "Web-ACSYNT": Conceptual-Level Aircraft Systems Analysis on the Internet; SAE 975509; 1997 World Aviation Congress, Anaheim, CA, Oct 13-16, 1997.
112. William A. Anemaat, Kurt L. Schueler; Airplane Configuration Layout Design Using Object-Oriented Methods; SAE 975510; 1997 World Aviation Congress, Anaheim, CA, Oct 13-16, 1997.
113. R.K. Pant, J.P. Fielding, J. Snow; CRISTO: A code for Integrated Synthesis and Trajectory Optimization of Commuter and Regional Aircraft; SAE 975542; 1997 World Aviation Congress, Anaheim, CA, Oct 13-16, 1997.
114. William A. Anemaat; AGDA: Airplane Geometry Design Assistant; SAE 985508; 1998 World Aviation Congress, Anaheim, CA, Sept 28-30, 1998.
115. David C. Fliegel, Thomas P. Dickens, Andrew P. Winn; Experience with a Geometry Programming Language for CFD Applications; SAE 985572; 1998 World Aviation Conference, Anaheim, CA, Sept 28-30, 1998.
116. P. Raj; Aircraft Design in the 21st Century: Implications for Design Methods (invited); AIAA 98-2895; 29th AIAA Fluid Dynamics Conference, Albuquerque, New Mexico, June 15-18, 1998.
117. Z.W. Zhu, Y.Y. Chan; A New Genetic Algorithm for Aerodynamic Design Based on "Geometric Concept"; AIAA 98-2900; 29th AIAA Fluid Dynamics Conference, Albuquerque, New Mexico, June 15-18, 1998.
118. D.W. Way, J.R. Olds; SCORES: Developing an Object-Oriented Rocket Propulsion Analysis Tool; AIAA 98-3227; 34th AIAA/ASME/SAE/ASEE Joint Propulsion Conference & Exhibit.

119. Joseph J. Totah, Dr. David J. Kinney; Simulating Conceptual and Developmental Aircraft; AIAA 98-4161; AIAA Modeling and Simulation Technologies Conference and Exhibit, Boston, MA, Aug 10-12, 1998.
120. Max Blair; Enabling Conceptual Design in a Technology Driven Environment; AIAA 98-4741; 7th AIAA/USAF/NASA/ISSMO Symposium on Multidisciplinary Analysis and Optimization, 2-4 Sept. 1998, St. Louis, MO.
121. D.W.E. Rentema, F.W. Jansen, E. Torenbeek; The Application of AI and Geometric Modelling Techniques in Conceptual Aircraft Design; AIAA 98-4824; 7th AIAA/USAF/NASA/ISSMO Symposium on Multidisciplinary Analysis and Optimization, 2-4 Sept. 1998, St. Louis, MO.
122. Daniel Tejtel, Dimitri N. Mavris, Mark Hale; Conceptual Aircraft Design Environment: Case Study Evaluation of Computing Architecture Technologies; AIAA 98-4844; 7th AIAA/USAF/NASA/ISSMO Symposium on Multidisciplinary Analysis and Optimization, 2-4 Sept. 1998, St. Louis, MO.
123. Gregory L. Roth, William A. Crossley; Commercial Transport Aircraft Conceptual Design Using a Genetic Algorithm Based Approach; AIAA 98-4934; 7th AIAA/USAF/NASA/ISSMO Symposium on Multidisciplinary Analysis and Optimization, 2-4 Sept. 1998, St. Louis, MO.
124. Richard M. Wood, Steven X.S. Bauer; A Discussion of Knowledge Based Design; AIAA 98-4944; 7th AIAA/USAF/NASA/ISSMO Symposium on Multidisciplinary Analysis and Optimization, 2-4 Sept. 1998, St. Louis, MO.
125. J.M. Scott, J.R. Olds; Transforming Aerodynamic Datasets into Parametric Equations for use in Multi-disciplinary Design Optimization; AIAA 98-5208; 1998 Defense and Civil Space Conference and Exhibit, October 28-30, 1998, Huntsville, AL.
126. Cao LingJun, Ang Haisong; Conceptual/Preliminary Aircraft Design Using Genetic Algorithm and Fuzzy Mathematics; AIAA 99-0113; 37th AIAA Aerospace Sciences Meeting and Exhibit, January 11-14, 1999/Reno, NV.
127. J.C. Trapp, H. Sobiecky; Interactive Parametric Geometric Design; AIAA 99-0829; 37th AIAA Aerospace Sciences Meeting and Exhibit, January 11-14, 1999/Reno, NV
128. Hakan Yusan, Stephan Rudolph; On Systematic Knowledge Integration in the Conceptual Design Phase of Airships; AIAA 99-3909; 13th AIAA Lighter-than-Air Systems Technology Conference, Norfolk, VA, June 28-July 1, 1999.

129. Joseph J. Totah, Dr. David J. Kinney, John T. Kaneshige, Shane Agabon; An Integrated Vehicle Modeling Environment; AIAA 99-4106; AIAA Atmospheric Flight Mechanics Conference and Exhibit. 9-11 August 1999, Portland, OR.
130. Mark A. Hale, Dimitri N. Mavris, Dennis L. Carter; The Implementation of a Conceptual Aerospace Systems Design and Analysis Toolkit; SAE 1999-01-5639; 1999 World Aviation Congress, San Francisco, CA, Oct 19-21, 1999.
131. Graham S. Rhodes; The NextGRADE Prototype GUI for Intelligent Synthesis Environments; AIAA-99-1362; AIAA/ASME/ASCE/AHS/ASC Structures, Structural Dynamics, and Materials Conference and Exhibit, 40th, St. Louis, MO, Apr. 12-15, 1999.
132. J.L. Walsh, J.C. Townsend, A.O. Salas, J.A. Samareh, V. Mukhopadhyay, J.F. Barthelemy; Multidisciplinary High-Fidelity Analysis and Optimization of Aerospace Vehicles, Part I: Formulation; AIAA 2000-0418; 38th Aerospace Science Meeting and Exhibit, 10-13 January 2000/ Reno, NV.
133. J.F. Gundlach IV, P.A. Tétrault, F. Gern, A. Nagshineh-Pour, A. Ko, J.A. Schetz, W.H. Mason, R. Kapania, B. Grossman, R.T. Haftka; Multidisciplinary Design Optimization of a Strut-Braced Wing; AIAA 2000-0420; 38th Aerospace Science Meeting and Exhibit, 10-13 January 2000/ Reno, NV.
134. Jérôme Lépine, Jean-Yves Trépanier, Francois Pépin; Wing Aerodynamic Design Using an Optimized NURBS Geometrical Representation; AIAA 2000-0669; 38th Aerospace Science Meeting and Exhibit, 10-13 January 2000/ Reno, NV.
135. Max Blair, Alicia Hartong; Multidisciplinary Design Tools for Affordability; AIAA 2000-1378; 41th AIAA/ASME/ASCE/AHS/ASC, Structures, Structural Dynamics and Materials Conference April 3-6, 2000, Atlanta, Georgia.
136. Axel Schumacher, Roland Hierold; Parameterized CAD-Models for Multidisciplinary Optimization Processes; AIAA 2000-4912; 8th AIAA/USAF/NASA/ISSMO Symposium on Multidisciplinary Analysis and Optimization, 6-8 Sept. 2000, Long Beach, CA.
137. Ruben E. Perez, Joon Chung, Kamran Behdinan; Aircraft Conceptual Design using Genetic Algorithms; AIAA 2000-4938; 8th AIAA/USAF/NASA/ISSMO Symposium on Multidisciplinary Analysis and Optimization, 6-8 Sept. 2000, Long Beach, CA.

138. Daniel P. Raymer; Vehicle Scaling Laws for Multidisciplinary Optimization (Preliminary Report); AIAA 2001-0532; 39th AIAA Aerospace Sciences Meeting & Exhibit 8-11 January 2001 / Reno. NV.
139. Ruben E. Perez, Kamran Behdinan; Advanced Business Jet Conceptual Design and Cost Optimization Using a Genetic Algorithm Approach; AIAA 2001-4316; AIAA Atmospheric Flight Mechanics Conference and Exhibit. 6-9 August 2001, Montreal, Canada.
140. Ralph L. Carmichael; Algorithm for Calculating Coordinates of Cambered NACA Airfoils at Specific Chord Locations; AIAA 2001-5235; 1st AIAA Aerospace Technology, Integration & Operations Forum, 16-17 October, 2001, Los Angeles, CA.
141. Daniel P. Raymer; Vehicle Scaling Laws for Multidisciplinary Optimization: Use of Net Design Volume to Improve Optimization Realism; AIAA 2001-5246; 1st AIAA Aerospace Technology, Integration & Operations Forum, 16-17 October, 2001, Los Angeles, CA.
142. William A. Crossley, Eric T. Martin, David W. Fanjoy; A Multiobjective Investigation of 50-Seat Commuter Aircraft Using a Genetic Algorithm; AIAA 2001-5247; 1st AIAA Aerospace Technology, Integration & Operations Forum, 16-17 October, 2001, Los Angeles, CA
143. Richard M. Wood, Steven X.S. Bauer; Discussion of Knowledge-Based Design; Journal of Aircraft, Vol. 39, No 6, November-December 2002;
144. F. Schieck, N. Deligiannidis, T. Gottmann; A Flexible, Open-Structured Computer Based Approach for Aircraft Conceptual Design Optimisation; AIAA 2002-0593; 40th AIAA Aerospace Sciences Meeting, 14-17 January, 2002/Reno, NV.
145. T.L. Benyo; Project Integration Architecture (PIA) and Computational Analysis Programming Interface (CAPRI) for Accessing Geometry Data from CAD Files; AIAA 2002-0750; 40th AIAA Aerospace Sciences Meeting, 14-17 January, 2002/Reno, NV.
146. W.J. Vankan, M. Laban; A Spinware Based Computational Design Engine for Integrated Multi-Disciplinary Aircraft Design; AIAA 2002-5445; 9th AIAA/ISSMO Symposium on Multidisciplinary Analysis and Optimization. 4-6 September 2002, Atlanta, Georgia.

147. G. La Rocca, L. Krakkers, M.J.L. van Tooren; Development of an ICAD Generative Model for Blended Body Aircraft Design; AIAA 2002-5447; 9th AIAA/ISSMO Symposium on Multidisciplinary Analysis and Optimization. 4-6 September 2002, Atlanta, Georgia.
148. Risheng Lin, Abdollah A. Afjeh; An Extensible, Interchangeable and Sharable Database Model for Improving Multidisciplinary Aircraft Design; AIAA 2002-5613; 9th AIAA/ISSMO Symposium on Multidisciplinary Analysis and Optimization. 4-6 September 2002, Atlanta, Georgia.
149. J. Brent Staubach; Multidisciplinary Design Optimization, MDO, the Next Frontier of CAD/CAE in the Design of Aircraft Propulsion Systems; AIAA 2003-2803; AIAA/ICAS International Air and Space Symposium and Exposition: The Next 100 Y, 14-17 July 2003, Dayton, Ohio.
150. Juan J. Alonso, Joaquim R.R.A. Martins, James J. Reuther, Robert Haimes, Curran A. Crawford; High-Fidelity Aero Structural Design Using a Parametric CAD-Based Model; AIAA 2003-3429; 16th AIAA Computational Fluid Dynamics Conference. 23-26 June 2003, Orlando, Florida.
151. Holger Pfaender, Daniel DeLaurentis, Dimitri N. Mavris; An Object Oriented Approach for Conceptual Design Exploration of UAV-Based System-of Systems; AIAA 2003-6521; 2nd AIAA "Unmanned Unlimited" Systems, Technologies, and Operations - Aerospace 15-18 September 2003, San Diego, California.
152. Thomas A. Ozoroski, Kyle G. Mas, Andrew S. Hahn; A PC-Based Design and Analysis System for Lighter-Than-Air Unmanned Vehicles; AIAA 2003-6566; 2nd AIAA "Unmanned Unlimited" Systems, Technologies, and Operations - Aerospace 15-18 September 2003, San Diego, California.
153. Kevin G. Bowcutt; A Perspective on Future of Aerospace Vehicle Design; AIAA 2003-6957; 12th AIAA International Space Plane and Hypersonic Systems and Technologies, 15-19 December 2003, Norfolk, Virginia.
154. Satwiksai Seshasai, Amar Gupta; Knowledge-Based Approach to Facilitate Engineering Design; Journal of Spacecraft and Rockets, Vol 41, No.1, January-February 2004.
155. Marian Nemec, Michael J. Aftosmis, Thomas H. Pulliam; CAD-Based Aerodynamic Design of Complex Configurations Using a Cartesian Method;

- AIAA 2004-113; 42nd AIAA Aerospace Sciences Meeting, January 5-8, 2004/Reno, NV.
156. Curran A. Crawford, Robert Haimes; Synthesizing an MDO Architecture in CAD; AIAA 2004-281; 42nd AIAA Aerospace Sciences Meeting, January 5-8, 2004/Reno, NV.
 157. Nicholas Borer, Dimitri N. Mavris; Formulation of a Multi-Mission Sizing Methodology for Competing Configurations; AIAA 2004-0535; 42nd AIAA Aerospace Sciences Meeting, January 5-8, 2004/Reno, NV.
 158. John J. Doherty, Stephen C. McParlin; Generic Process for Air Vehicle Concept Design and Assessment; AIAA 2004-895; 42nd AIAA Aerospace Sciences Meeting, January 5-8, 2004/Reno, NV.
 159. Greg Mocko, Jitesh H. Panchal, Marco Gero Fernandez, Russell Peak, Farrokh Mistree; Towards Reusable Knowledge-Based Idealizations for Rapid Design and Analysis; AIAA 2004-2009; 45th AIAA/ASME/ASCE/AHS/ASC Structures Dynamics & Materials Conference 19-22 April 2004, Palm Springs, California.
 160. C. Cerulli, P.B. Meijer, M.J.L. van Tooren; Parametric Modeling of Aircraft Families for Load Calculation Support; AIAA 2004-2019; 45th AIAA/ASME/ASCE/AHS/ASC Structures Dynamics & Materials Conference 19-22 April 2004, Palm Springs, California
 161. Zhijie Lu, Eun-Suk Yang, Daniel A. DeLaurentis, and Dimitri N. Mavris; Formulation and Test of an Object-Oriented Approach to Aircraft Sizing; AIAA 2004-4302; 10th AIAA/ISSMO Multidisciplinary Analysis and Optimization Conference. 30 August - 1 September 2004, Albany, New York.
 162. Ted A. Manning, Peter J. Cage, Jennie M. Nguyen, Robert Haimes; ComGeom2: A Geometry Tool for Multidisciplinary Analysis and Data Sharing; AIAA 2004-4303; 10th AIAA/ISSMO Multidisciplinary Analysis and Optimization Conference. 30 August - 1 September 2004, Albany, New York.
 163. Nicolas Antoine, Ian Kroo, Karen Willcox, Garret Barter; A Framework for Aircraft Conceptual Design and Environmental Performance Studies; AIAA 2004-4314; 10th AIAA/ISSMO Multidisciplinary Analysis and Optimization Conference. 30 August - 1 September 2004, Albany, New York.
 164. Hu Liu, Gang Lin Wang, Xin Lai Lu, Zhe Wu; Preliminary Investigation of Integrated Multidisciplinary Optimization in Aircraft Conceptual Design; AIAA

- 2004-4319; 10th AIAA/ISSMO Multidisciplinary Analysis and Optimization Conference. 30 August - 1 September 2004, Albany, New York.
165. Atherton Carty, Clifton Davies; Fusion of Aircraft Synthesis and Computer Aided Design; AIAA 2004-4433; 10th AIAA/ISSMO Multidisciplinary Analysis and Optimization Conference. 30 August - 1 September 2004, Albany, New York.
166. Ruben E. Perez, Hugh H.T. Liu, Kamran Behdinan; Evaluation of Multidisciplinary Optimization Approaches for Aircraft Conceptual Design; AIAA 2004-4537; 10th AIAA/ISSMO Multidisciplinary Analysis and Optimization Conference. 30 August - 1 September 2004, Albany, New York.
167. Xinyu Zhang, Arvid Myklebust, Paul Gelhausen; A Geometric Modeler for the Conceptual Design of Ducted Fan UAVs; AIAA 2004-6538; AIAA 3rd "Unmanned Unlimited" Technical Conference, Workshop and Exhibit, 20-23 September 2004, Chicago, Illinois.
168. Risheng Lin, Abdollah A. Afjeh; An XML-Based Integrated Database Model for Multidisciplinary Aircraft Design; Journal of Aerospace Computing, and Communication, Vol. 1, March 2004.
169. Daniel M. Fudge, David W. Zingg, Robert Haimes; A CAD-Free and a CAD-Based Geometry Control System for Aerodynamic Shape Optimization; AIAA 2005-451; 43rd AIAA Aerospace Sciences Meeting and Exhibit. 10-13 January 2005, Reno, Nevada.
170. M.J.L. van Tooren, M. Nawijn, J.P.T.J. Berends, E.J. Schut; Aircraft Design Support Using Knowledge Engineering and Optimisation Techniques; AIAA 2005-2205; 46th AIAA/ASME/ASCE/AHS/ASC Structures Dynamics & Materials Conference.
171. B. Greschner, C. Yu, S. Zheng, M. Zhuang, Z.J. Wang, F. Thiele; Knowledge Based Airfoil Aerodynamic and Aeroacoustic Design; AIAA 2005-2968; 11th AIAA/CEAS Aeroacoustics Conference (26 the AIAA Aeroacoustics Conference) 23-25 May 2005, Monterey, California.
172. Daniel J. Neufeld, Joon Chung; Unmanned Aerial Vehicle Conceptual Design Using a Genetic Algorithm and Data Mining; AIAA 2005-7051; Infotech@Aerospace, 26-29 September 2005, Arlington, Virginia.

173. Adras Sobeter, Andy J. Keane, James Scanlan, Neil W. Bressloff; Conceptual Design of Airframes Using a Generic Geometry Service; AIAA 2005-7079; Infotech@Aerospace, 26-29 September 2005, Arlington, Virginia.
174. Bernd Chudoba, Xiao Huang; Development of a Dedicated Aerospace Vehicle Conceptual Design Knowledge-Based System; AIAA 2006-225; 44th AIAA Aerospace Sciences Meeting and Exhibit. 9-12 January 2006, Reno, Nevada.
175. M.J.L. van Tooren, E.J. Schut, J.P.T.J. Berends; Design "Feasilisation" using Knowledge Based Engineering and Optimization Techniques; AIAA 2006-731; 44th AIAA Aerospace Sciences Meeting and Exhibit. 9-12 January 2006, Reno, Nevada.
176. David L. Rodriguez, Peter Sturdza; A Rapid Geometry Engine for Preliminary Aircraft Design; AIAA 2006-929; 44th AIAA Aerospace Sciences Meeting and Exhibit. 9-12 January 2006, Reno, Nevada.
177. Mathias Wintzer, Peter Sturdza, Ilan Kroo; Conceptual Design of Conventional and Oblique Wing Configurations for Small Supersonic Aircraft; AIAA 2006-930; 44th AIAA Aerospace Sciences Meeting and Exhibit. 9-12 January 2006, Reno, Nevada.
178. M. Nawijn, M.J.L. van Tooren, J.P.T.J. Berends, P. Arendsen; Automated Finite Element Analysis in a Knowledge Based Engineering Environment; AIAA 2006-947; 44th AIAA Aerospace Sciences Meeting and Exhibit. 9-12 January 2006, Reno, Nevada.
179. Bernd Chudoba; Managerial Implications of Generic Flight Vehicle Design Synthesis; AIAA 2006-1178; 44th AIAA Aerospace Sciences Meeting and Exhibit. 9-12 January 2006, Reno, Nevada.
180. J.P.T.J. Berends, M.J.L. van Tooren; An Agent System Co-operating as a Design Build Team in a Multidisciplinary Design Environment; AIAA 2006-1482; 44th AIAA Aerospace Sciences Meeting and Exhibit. 9-12 January 2006, Reno, Nevada.
181. Hu Liu, Gang Lin Wang, Xin Lai Lu, Zhe Wu; Case-Based Reasoning for Developing Initial Aircraft Concepts; AIAA 2006-1487; 44th AIAA Aerospace Sciences Meeting and Exhibit. 9-12 January 2006, Reno, Nevada.
182. Hugh C. Briggs; Knowledge Management In The Engineering Design Environment; AIAA 2006-2238; 47th AIAA/ASME/ASCE/AHS/ASC

- Structures, Structural Dynamics, and Materials Conference, 1-4 May, 2006, Newport, Rhode Island.
183. Bil, C.; *Development and Application of a Computer-Based System for Conceptual Aircraft Design*. Delft University Press 1988.
 184. Middel, J.; *Development of a Computer Assisted Toolbox for Aerodynamic Design of Aircraft at Subcritical Conditions with Application to Three-Surface and Canard Aircraft*. Delft University Press 1992.
 185. SBIR 93-1 Phase I, 1994, Subtopic title: General Aviation Aircraft Configurations. Project title: A Personal Computer Aided Design System for General Aviation Aircraft Configurations. Contract Number: NAS1-20172 Issued by NASA Langley Research Center.
 186. SBIR 93-1 Phase II, 1995, Subtopic title: General Aviation Aircraft Configurations. Project title: A Personal Computer Aided Design System for General Aviation Aircraft Configurations. Contract Number: NAS1-20415 Issued by NASA Langley Research Center.
 187. Gloudemans, J.R., Vehicle Sketch Pad Documentation VSP 1.0. NASA Langley 2006.
 188. Borland Software Corporation, Borland Delphi Professional Version 6.0 (Build 6.240) Update Pack 2, 1983-2001.
 189. Taylor, J.W.R.; Jane's All the World's Aircraft. Issues used 1980-2003.
 190. Mantis Bug Tracking System; Version 1.0.6, 2005.
 191. Kitplanes Magazine; Aviation Publishing Group, LLC. December Issues 2002-2005.
 192. McGhee R. J., Beasley W. D., Wind-Tunnel Results for a Modified 17-Percent-Thick Low-Speed Airfoil Section, NASA TP 1919.
 193. DARcorporation, Advanced Aircraft Analysis Version 3.1 User's Manual, 2006.
 194. Chung-Lie Wang; Best Least Square Approximation by Minimum Property of Fourier Expansions; Theory of Approximation; With Applications; Proceedings of a Conference Conducted by The University of Calgary and The University of Regina, at The University of Calgary, Alberta, Canada, August 11-13, 1975. Academic Press, Inc. 1976.

195. William H. Press, Brian P. Flanery, Saul A. Teukolsky, William T. Vetterling; *Numerical Recipes in Pascal. The Art of Scientific Computing*. Cambridge University Press 1992.
196. W.A.J. Anemaat; A Computer-Aided Preliminary Design Methodology for Horizontal Tailplanes and Canards. MS-thesis, Delft University of Technology, Department of Aerospace Engineering, May 1987 (In Dutch).

Appendix A. Airplane Mission Specifications

A.1 Mission Specification for a Twin Engine Propeller Driven Airplane

Payload: 6 passengers at 175 lbs each (this includes the pilot) and 20 lbs total baggage

Range: 1,000 nm with max. payload. Reserves equal to 25% of required mission fuel

Altitude: 10,000ft (for the design range)

Cruise Speed: 250 kts at 75% power at 10,000ft

Climb: 10 minutes to 10,000ft at maximum take-off weight

Take-off and

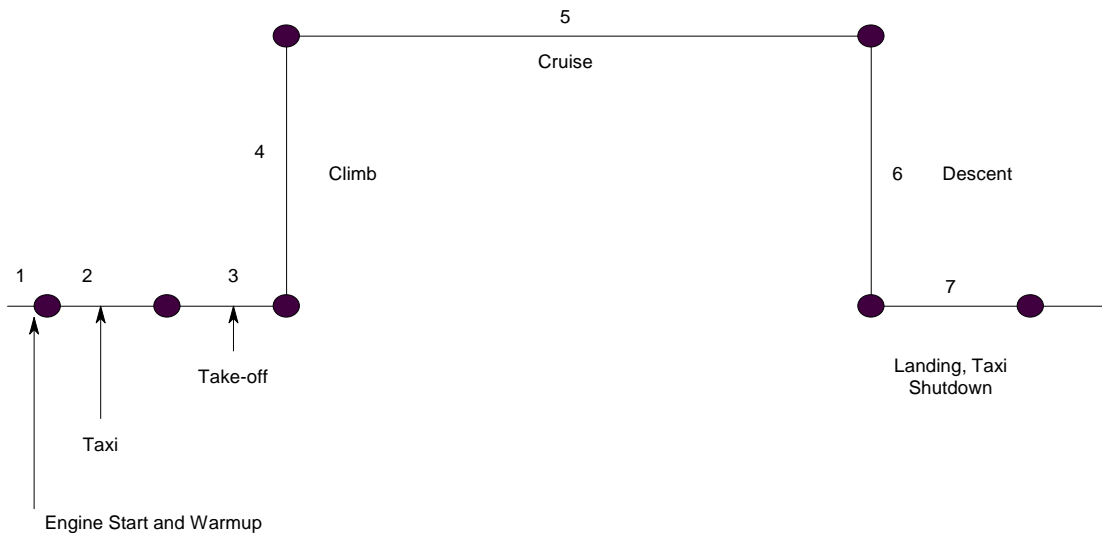
Landing: 1,500ft ground run at sea-level, std. day. Landing performance at 95% Take-off weight

Powerplants: Piston/propeller

Pressurization: None

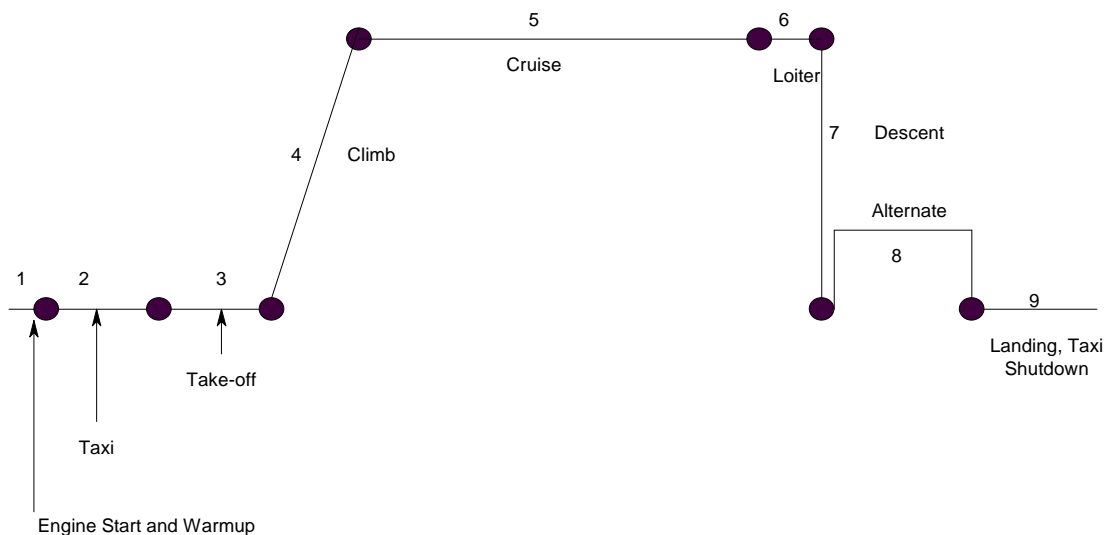
Certification: FAR 23

Mission Profile:



A.2 Mission Specification for a Jet Transport

Payload:	150 passengers at 175 lbs each and 30 lbs of baggage each
Crew:	Two pilots and three cabin attendants at 175 lbs each and 30 lbs baggage each
Range:	1,500 nm, followed by 1 hour loiter, followed by a 100 nm flight alternate
Altitude:	35,000ft (for the design range)
Cruise Speed:	$M = 0.82$ at 10,000ft
Climb:	Direct climb to 35,000ft at max. take-off weight is desired
Take-off and Landing:	FAR 25 field length, 5,000 ft at an altitude of 5,000ft and a 95 deg F day. Landing performance at 95% Take-off weight.
Powerplants:	Two Turbofans
Pressurization:	5,000 ft cabin at 35,000 ft
Certification:	FAR 25
Mission Profile:	



A.3 Mission Specification for a Fighter

Payload: 20x500 lbs bombs, carried externally and 2,000 lbs of ammunition for the GAU-81A multi-barrel cannon. The cannon weight of 4,000 lb is part of the empty weight.

Crew: One pilot (200 lbs)

Range and

Altitude: see mission profile. No reserves

Cruise Speed: 400 kts at sea level, with external load.

450 kts at sea level, clean

$M = 0.8$ at 40,000 ft at maximum take-off weight

$M = 0.85$ at 40,000 ft, clean

Climb: Direct climb to 40,000ft at max. take-off weight in 8 minutes is desired

Climb rate on one engine, at max. take-off weight should exceed 500 fpm on a 95 deg F day.

Take-off and

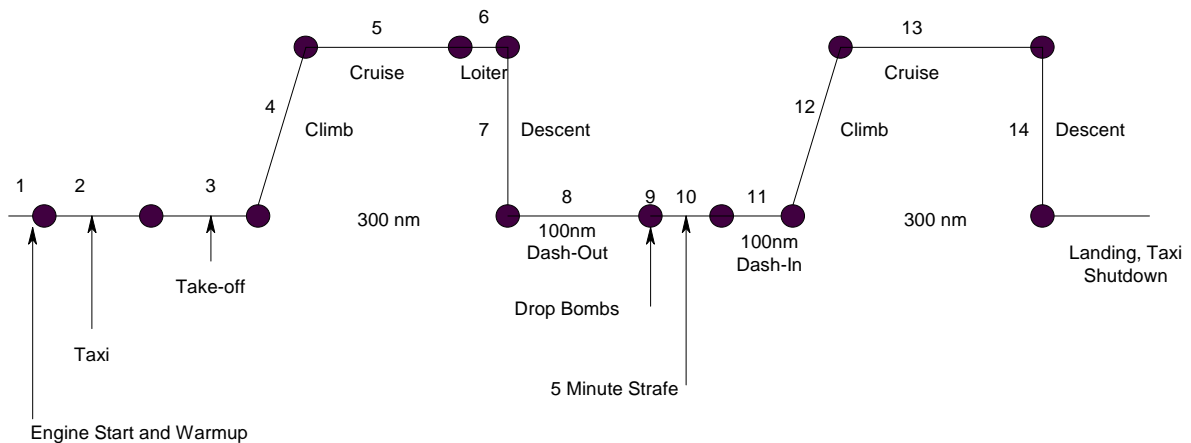
Landing: ground run of less than 2,400 ft at sea-level and a 95 deg F day.

Powerplants: Two Turbofans

Pressurization: 5,000 ft cockpit at 50,000 ft

Certification: Military

Mission Profile:



Appendix B. Advanced Aircraft Analysis 3.1 Module Description

B.1 Weight Module

B.1.1 Weight Sizing

The purpose of the Weight Sizing submodule is to rapidly estimate the following weight components and/or sensitivity coefficients:

- Take-off weight, W_{TO}
- Empty weight, W_E
- Fuel weight, W_F
- Sensitivity of take-off weight to aerodynamic, propulsion and mission parameters

These parameters are estimated on the basis of the following input:

- A mission specification
- Statistical relations between empty weight and take-off weight of existing airplanes

The weight sizing module contains a plot feature which displays the weight iteration process. The methods are based on Chapter 2, Sections 2.1 to 2.5 and Section 2.7 of Airplane Design Part I (Ref. 1).

Methods are included to establish a statistical relationship between empty weight and take-off weight for any type of airplane.

Different ranges can be plotted for varying payload.

B.1.2 Class I Weight

The purpose of this module is to estimate airplane component weights and to determine whether or not the center of gravity of the airplane is within the desirable range for different loading and unloading scenarios. The methods are based on Chapter 10 of Airplane Design Part II (Ref. 2), and Chapter 2 of Airplane Design Part V (Ref. 5).

This module also contains the moments of inertia calculation, based on Chapter 3 of Airplane Design Part V (Ref. 5). This option allows the user to estimate the moments of inertia of the airplane with the radii of gyration method. The radii of gyration may be calculated from the moment of inertial data. The user can provide the data or the preloaded data base can be used. The user has the option to select data from comparable airplanes. By selecting a category, a choice can be made between several available airplanes appearing in a table. Because the Class I inertia estimation is based on the selected aircraft, the user should choose the most comparable aircraft.

B.1.3 Class II Weight

The purpose of this module is to present a Class II method for estimating airplane component weights. The Class II estimation methods used in this module are based on those described in Airplane Design Part V. These methods employ empirical equations, which relate component weights to airplane design characteristics. In the Class II weight estimate module, the weight estimation methods are identified as follows:

- Cessna method
- USAF method
- General Dynamics (GD) method
- Torenbeek method

Because airplane component weight modeling in the software is a function of take-off weight, the Class II weight estimation is an iterative process.

Detailed moments of inertia based on component weights and component inertias can be calculated.

Total center of gravity and empty weight center of gravity are calculated. Forward and aft center of gravity are determined based on minimum and maximum weights of passengers, fuel, baggage, cargo, weapons etc.

B.1.4 Component Center of Gravity

This option allows the user to calculate the airplane center of gravity by entering weight components and their locations in a preformatted table. Tables are available for structure weight, fixed equipment weight, powerplant weight and total weight. Center of gravity of wing, canard, horizontal tail, V-Tail , tailbooms, nacelles and fuel tanks are calculated

B.2 Aerodynamics Module

B.2.1 Lift

The Lift submodule can be used for estimating the lifting characteristics of airplane lifting surfaces and high lift devices. Maximum lift coefficients for airfoils and wing, horizontal tail, vertical tail, v-tail and canard are calculated. The methods are based on Chapter 7 of Airplane Design Part II (Ref. 2). The methodology used to determine the lifting surface spanwise lift distribution is based on lifting line theory.

The function of the flaps submodule is to determine the type and size of high lift devices needed to meet the maximum lift requirement for take-off and landing conditions. The user can select the flap type from plain flap, split flap, single slotted flap, double-slotted flap, fowler flap and triple slotted flaps. Flaps can be sized or flap lift can be calculated for a given flap configuration. Drooped ailerons are accounted for. The methods are based on Chapter 7 of Airplane Design Part II (Ref. 2).

Ground effects on airplane lift are based on the methods in Chapter 8 of Airplane Design Part VI (Ref. 6).

Lift as function of angle of attack, elevator (canardvator, ruddervator) and horizontal tail (canard, v-tail) incidence can be calculated.

The lift coefficient at zero-angle-of-attack can be used to determine the lift coefficients, downwash angle, and upwash angle at zero airplane angle of attack, and the zero lift angle of attack. This module includes flap effects. The flap maximum lift coefficient can be plotted as function of flap deflection and flap chord ratio. The methods are described in Chapter 8 of Airplane Design Part VI (Ref. 6).

Further, the effect of body width on lift curve slope may also be calculated.

Propeller power effects (prop wash) are accounted for.

B.2.2 Class I Drag Polars

The Class I Drag submodule can be used for a first estimate of the airplane drag. The Class I Drag module has the following seven options:

- flaps in take-off configuration with gear down
- flaps in take-off configuration with gear up
- no flap deflection and gear up
- flaps in landing configuration with gear up
- flaps in landing configuration with gear down
- one engine inoperative configuration
- current airplane flight condition

The program will check to see if the airplane has retractable or fixed landing gear. All drag polars may be displayed at once: Gear Up, Gear Down, Flaps Up, Flaps Down, One Engine Inoperative and Current Condition. The methodology used to calculate the drag polar can be found in Chapter 3 of Airplane Design Part I (Ref. 1). The Class I Drag module relates the total airplane lift coefficient to the total airplane drag coefficient by a parabolic drag polar equation.

An iteration is built-in to calculate take-off weight based on L/D derived from the Class I drag polar.

B.2.3 Class II Drag Polars

The purpose of the Class II Drag submodule is to supply a Class II method for predicting drag polars of airplanes during the preliminary design phase. A detailed drag polar can be calculated for the subsonic, transonic and supersonic flow regimes.

The following drag calculations can be performed:

- wing drag coefficient
- horizontal tail drag coefficient
- vertical tail drag coefficient
- v-tail drag coefficient
- canard drag coefficient
- fuselage drag coefficient

- nacelle drag coefficient
- trailing edge flap drag coefficient
- leading edge flap drag coefficient
- gear drag coefficient
- canopy drag coefficient
- windshield drag coefficient
- floats drag coefficient
- stores drag coefficient
- trim drag coefficient
- spoiler drag coefficient
- miscellaneous drag coefficient
- pylon drag coefficient
- drag coefficient due to windmilling
- total aircraft drag coefficients

The program will account for fuselage base area change as a function of inoperative engines. Changes in nacelle drag are also accounted for due to inoperative engines. Dihedral is accounted for in the wetted areas of lifting surfaces.

The methods are based on Chapter 4 of Airplane Design Part VI (Ref. 6).

The drag coefficient can be plotted as a function of lift coefficient, Mach number, flap deflection and as a component build-up. Drag can also be plotted as a function of angle-of-attack for an untrimmed airplane. The drag can be approximated with a trendline.

B.2.4 Moment

The Moment submodule calculates the spanwise moment distribution on the wing, horizontal tail, vertical tail and canard. The ground effects on airplane moment are also determined. Methods are based on Airplane Design Part VI (Ref. 6).

Moment as function of angle of attack, elevator (canardvator) and horizontal tail (canard) incidence can be calculated.

This pitching moment at zero-angle-of-attack submodule can be used to determine the zero lift airplane pitching moment coefficients, and pitching moment coefficients at zero airplane angle of attack. This module includes flap effects. To account for each airplane component, the pitching moment coefficient components are calculated separately. The user can estimate the zero lift pitching moment coefficient, the effect of trailing and leading edge flaps on lift and pitching moment coefficients. The methods are described in Chapter 8 of Airplane Design Part VI (Ref. 6).

B.2.5 Aerodynamic Center

The Aerodynamic Center submodule can be used to calculate aerodynamic center locations of individual airplane components, and the aerodynamic center shift due to components. The aerodynamic center methods described are found in Airplane Design Part VI (Ref. 6).

The aerodynamic center and shift can be calculated for the following components:

- fuselage
- wing
- horizontal tail
- vertical tail
- v-tail
- canard
- nacelles
- floats
- stores
- tailbooms
- total airplane

B.2.6 Power Effects

The purpose of the Power Effects module is to calculate the effects of the operating propeller aerodynamic properties of the airplane. The effects of power are calculated for the following parameters:

- horizontal tail downwash angle
- v-tail downwash angle
- dynamic pressure ratio
- lift and pitching moment coefficients
- drag due to power

Power Effects can be applied to both single and multi-engine propeller driven aircraft.

B.2.7 Ground Effects

The Ground Effects module predicts the change in wing-fuselage lift coefficient, pitching moment coefficient and horizontal tail downwash angle due to the close proximity of the aircraft to the ground.

B.2.8 Dynamic Pressure Ratio

The Dynamic Pressure Ratio module allows the user to predict the horizontal tail, V-tail and vertical tail dynamic pressure ratio as a variation of angle of attack. The wake effects are also accounted for in these calculations.

B.3 Performance Module

B.3.1 Performance Sizing

The purpose of the Performance Sizing module is to allow for a rapid estimation of those airplane design parameters, which have a major impact on airplane performance. Airplanes are usually required to meet performance objectives in different categories depending on the mission profile. Meeting these performance objectives normally results in the determination of a range of values for:

- wing loading (W/S)
- thrust loading (T/W) or power loading (W/P)
- airplane maximum lift coefficients

The variables listed above are plotted in the form of a performance-matching plot. These plots depend on the type of airplane, the applicable specification and the applicable regulation(s). With the help of such a plot, the combination of the highest possible wing loading and the smallest possible thrust (or highest power) loading, which meets all performance requirements, can be determined. The methodology used for performance sizing can be found in Airplane Design Part I (Ref. 1).

B.3.2 Performance Analysis

The purpose of the Analysis submodule is to provide the user with Class II analysis methods for predicting the performance characteristics of an airplane. The methodology used to analyze the performance characteristics can be found in

Chapter 5 of Airplane Design Part VII (Ref. 7) and Airplane Aerodynamics and Performance (Ref. 11).

The performance characteristics consist of:

- Stall speed
- Dive and Descent
- Take-off distance
- Climb
- Cruise
- Maneuver
- Glide
- Landing Distance

The engine performance data such as thrust or power can be entered as function of speed.

B.4 Geometry Module

The purpose of the geometry module is to help the user determine the geometry of the fuselage, wing, horizontal tail, vertical tail, v-tail and canard and calculate related parameters. The methodology used to calculate the airplane component geometries is described in Airplane Design Part II (Ref. 2). Two-dimensional geometry can be defined for straight and cranked lifting surfaces. For the horizontal tail, vertical tail, v-tail and canard the volume coefficient method is available in the Stability & Control module.

The fuselage module shows all cross-sections of the fuselage and is used to determine fuselage camber, inclination angles of each segment and cross-sectional area distribution.

The control surfaces on each lifting surface can be plotted. The chord length at a specified surface chord station can be determined.

Fuel volume in the wing is calculated using Class I and Class II methods. Fuel in cranked wings is accounted for.

The airplane geometry can be exported to CAD programs that use AeroPack (Concepts Unlimited and Concepts 3D).

The lateral tip-over option allows the user to calculate the lateral angle between the airplane center of gravity and the landing gear. This angle is useful in determining the risk of lateral tip-over on the ground.

The pitch angle allows the user to calculate the angle between the landing gear rotation point and the tail, thus determining the probability of a tail strike on rotation.

All geometric parameters may be scaled, for instance to make a wind tunnel model.

B.5 Propulsion Module

In this module the installed power and thrust of airplanes can be calculated. In addition to the installed power/thrust estimation, this module also provides options for inlet and nozzle sizing, estimation of inlet pressure recovery. Power extraction is also accounted for. Calculations in this module are based on the methodologies outlined in Chapter 6 of Airplane Design Part VI (Ref. 6).

The methods are valid for piston engines, jet engines, turboprop and propfan engines. Installed thrust or power can be calculated from uninstalled engine performance.

B.6 Stability & Control Module

B.6.1 Stability & Control Derivatives

The purpose of the Derivatives submodule is to compute the non-dimensional aerodynamic stability and control derivatives for a rigid airplane in a given flight condition (i.e., for a given weight, altitude, and speed and c.g location). The derivatives module consists of longitudinal stability derivatives, lateral-directional stability derivatives, longitudinal control derivatives and lateral-directional control derivatives. The derivatives can be calculated for tail aft, canard and three-surface configurations.

For longitudinal stability derivatives the following options are available:

- steady state lift, drag, moment and thrust coefficients
- speed derivatives
- angle-of-attack derivatives
- rate of angle-of-attack derivatives
- pitch rate derivatives

For lateral-directional stability derivatives the following options are available:

- angle-of-sideslip derivatives
- rate of angle-of-sideslip derivatives
- roll rate derivatives
- yaw rate derivatives

For longitudinal control derivatives the following options are available:

- stabilizer control derivatives
- elevator control derivatives
- ruddervator control derivatives
- canard control derivatives
- canardvator control derivatives
- elevon control derivatives
- elevator tab control derivatives
- ruddervator tab control derivatives
- canardvator tab control derivatives
- elevon tab-control derivatives

For lateral-directional control derivatives the following options are available:

- aileron derivatives
- spoiler derivatives
- differential stabilizer derivatives
- rudder derivatives
- rudder tab derivatives
- aileron tab derivatives

B.6.2 Hingement Derivatives

The hingement submodule is used to determine the hingement coefficient derivatives of the elevator, rudder, aileron, canardvator, elevator tab, rudder tab, aileron tab and canardvator tab. The control surfaces can have unshielded, fully shielded and partially shielded horn balances. The methodology for the hingement calculations is found in Airplane Design Part VI (Ref. 6).

B.6.3 Class I Stability and Control/Empennage Sizing Analysis

The methodology used to analyze the Stability and Control characteristics can be found in Chapter 11 of Airplane Design Part II (Ref. 2). This module includes longitudinal stability and empennage sizing, directional stability and empennage sizing and minimum control speed with one engine inoperative stability/empennage sizing.

For Inputs are simplified and choice is given between geometric volume coefficient or volume coefficient based on C.G. and A.C.

B.6.4 Class II Stability and Control/Empennage Sizing Analysis

The methodology used to analyze the longitudinal and lateral-directional trim characteristics can be found in Chapter 5 of Flight Dynamics Part I (Ref. 9).

The Class II methods consist of trim diagram, longitudinal trim and lateral-directional trim. The elevator stick (or control wheel) forces, aileron stick (or control wheel)

forces and rudder pedal forces can be calculated. The trim diagram determines control deflections and angles of attack for different center of gravity locations to trim the airplane longitudinally. Trim diagrams include propeller power effects.

Other important stability and control characteristics such as take-off rotation and a variety of dynamic stability considerations are calculated that are not covered by the Class I method.

B.7 Dynamics Module

B.7.1 Dynamics

The purpose of the dynamics module is to help the user analyze the open loop dynamic characteristics of the airplane in a given flight condition. The methodology used to analyze open loop dynamic characteristics can be found in Airplane Flight Dynamics Part I (Ref. 9).

Dynamics is divided into estimation of the longitudinal and lateral-directional dynamic characteristics. Airplane transfer functions are determined. Flying qualities are checked against civil and military requirements. The effect of roll-pitch yaw coupling effect on the dynamic analysis is also determined. Sensitivity of various stability and control derivatives on flying qualities is also established. Phugoid and short period are determined. Spiral, Dutch roll and roll performance are investigated.

The Routh-Hurwitz stability requirements are calculated.

B.7.2 Control

The purpose of the Control module is to help the user analyze single and double loop feedback control systems of the airplane. If the open loop dynamic characteristics of the airplane are known, root locus analyses may be performed in the S-plane. The control analysis submodule can also be used to analyze a system open loop transfer

function in the frequency domain (Bode diagram). The methodology used to analyze feedback control systems can be found in Airplane Flight Dynamics Part II (Ref. 10).

The transfer functions can be selected from the standard airplane transfer functions or defined by the user. If the longitudinal and lateral-directional stability derivatives of the airplane are known, the user may use the Dynamics module prior to using the Control analysis module to generate the longitudinal and lateral-directional dynamic transfer functions of the airplane. These transfer functions are transferred into the Control analysis module, and can only be generated in the Dynamics module.

The transfer functions are:

- Speed-to-Elevator
- Angle-of-Attack-to-Elevator
- Pitch-Angle-to-Elevator
- Speed-to-Ruddervator
- Angle-of-Attack-to-Ruddervator
- Pitch-Angle-to-Ruddervator
- Speed-to-Stabilizer
- Angle-of-Attack-to-V-Tail
- Pitch-Angle-to-V-Tail
- Speed-to-Elevon
- Angle-of-Attack-to-Elevon
- Pitch-Angle-to-Elevon
- Speed-to-Canardvator
- Angle-of-Attack-to-Canardvator
- Pitch-Angle-to-Canardvator
- Human Pilot
- Sideslip-Angle-to-Aileron
- Bank-Angle-to-Aileron
- Heading-Angle-to-Aileron
- Sideslip-Angle-to-Rudder

- Angle-of-Attack-to-Stabilizer
- Pitch-Angle-to-Canardvator
- Bank-Angle-to-Rudder
- Pitch-Angle-to-Stabilizer
- Speed-to-Canard
- Heading-Angle-to-Rudder
- Speed-to-V-Tail
- Angle-of-Attack-to-Canard
- Defined by the user

The following control systems can be analyzed:

- single loop feedback
- double loop control systems with the inner loop gain in the forward path
- double loop control systems with the inner loop gain in the feedback path
- gyro tilt angle effect

The human pilot calculation can be used to estimate a human pilot transfer function for use in the open loop control system analysis. The human pilot module can be used to model pilots of differing abilities, reaction times and physical fitness. This module can even be used to show the dangers of a drunken pilot in the loop. The methodology used to analyze a human pilot transfer function can be found in Chapter 10 of Airplane Flight Dynamics Part II (Ref. 10).

B.8 Loads Module

The purpose of this module is to estimate loads placed on airplane components and to determine important information for structural design and sizing. The Loads module consists of two submodules: V-n Diagram and Structural Loads. The purpose of the V-n Diagram submodule is to determine load factors and their corresponding speeds. The purpose of the Structural Loads submodule is to calculate the internal forces and moments in the structural components of an airplane. Use of the Loads module options will be described in the following sections.

B.8.1 V-n Diagram

In this submodule, velocity vs. load factor (V-n) diagrams can be constructed for the following types of airplanes: FAR 23 certified, FAR 25 certified and MIL-A-8861(ASG) certified airplanes.

B.8.2 Structural Loads

In this submodule the total internal loads for each structural component can be calculated in any combination that the user desires.

The following options are available to calculate the loads acting on a structural component:

- structural loads on the fuselage
- structural loads on the wing
- structural loads on the horizontal tail
- structural loads on the canard
- structural loads on the vertical tail
- estimation of the accelerations and rates acting on the airplane. Before the total internal loads for any structural component can be calculated, the linear accelerations, angular accelerations and angular rates must be calculated using this option

B.9 Structures Module

B.9.1 Class I Sizing

The purpose of this module is to estimate the size and weight of the structural components. This is done using material properties and the results of the calculation of the total internal loads for the component from the loads module.

B.9.2 Materials

In this submodule material properties that are not listed in the available materials table may be added and have their characteristics defined. These materials will be added to the user defined category of the available materials table.

B.10 Cost Analysis Module

The purpose of this module is to estimate various costs of airplane design programs. The estimation methods are presented in such a manner that they can be applied to civil and military airplanes of all types. The cost escalation factor (CEF) used in this module accounts for inflation up to June 2006. The various cost definitions and cost estimation methods used for this module are as discussed in Chapter 1 through 7 of Airplane Design Part VIII (Ref. 8).

After invoking the cost module, seven options are displayed:

- **AMPR Weight** For estimation of the Aeronautical Manufacturers Planning Report (AMPR) weight. This weight parameter is needed for estimation of the various costs in an airplane program.
- **R.D.T.E. Cost** For estimation of the research, development, test and evaluation cost.
- **Prototype Cost** For estimation of the cost of development, manufacturing and flight testing of the prototypes. This submodule is to be used only for those airplane programs that are not intended for eventual production.
- **Acquisition Cost** For estimation of the manufacturing and acquisition costs. The difference between these costs is the profit made by the manufacturer.

- Operating Cost (military) For estimation of the military airplane operating costs.
- Operating Cost (civil) For estimation of the civil airplane operating costs.
- Life Cycle Cost For estimation of the life cycle cost of an airplane program.
The life cycle cost is defined as the sum of R.D.T.E. cost, acquisition cost, operating cost and disposal cost
- Price Data For estimation of the engine price, propeller price and airplane price as well as a rapid method for estimating prices of future designs.

B.11 Atmosphere

The purpose of the Atmosphere module is to calculate the properties of the standard atmosphere at a given altitude and temperature offset. Air density, pressure, temperature, speed of sound and acceleration of gravity are calculated as a function of altitude. For a given speed the Mach number is calculated.

B.12 Flight Condition

The purpose of the Flight Condition window is to set and define each flight condition to be included in the analysis. An airplane project can have one or more flight conditions defined. All parameters depending on speed, weight, flap deflection and center of gravity can be stored separately per flight condition. Flight conditions can be edited, moved, copied and deleted from the project.

Appendix C. Theory and history of CAD and Computer Graphics

Abstracts of books and papers related to CAD and Computer Graphics are given in chronological order. Abstracts are literal copies from the references, unless indicated otherwise by the initials WA.

1981 Roy A. Liming Mathematics for Computer Graphics Ref. 47

One of the earlier (first print 1979) books describing computer graphics in detail. Dr. Liming's book addresses the fundamental mathematics for graphic systems. It describes intersections, transformations and geometric projection. It uses aerospace examples.

1983 William M. Newman Principles of Interactive Computer Ref. 48
Robert F. Sproull Graphics

This book describes the basics of computer graphics similar to Foley and van Dam. It is one of the first books describing computer graphics (first print 1973). It shows detailed mathematics of transformations and displaying graphics on computer displays.

1989 Tom Lyche Mathematical Methods in Computer Aided Ref. 49
Larry L. Schumaker Geometric Design
Editors

This book is an edited collection of papers focusing on curve and surface methods for computer aided geometry design. The volume contains survey papers as well as full-length research papers. The mathematical objects discussed include univariate and

multivariate splines, algebraic curves, rational curves and surfaces, Bézier curves and surfaces, and finite elements.

1990 James Foley Computer Graphics Principles and Ref. 50
Andries van Dam Practice
Steven Feiner
John Hughes

Another classic textbook is Foley and van Dam. The authors provide a unique combination of current concepts and practical applications. The important algorithms in 2D and 3D graphics are detailed for easy implementation. There is also a thorough presentation of the mathematical principles of geometric transformations and viewing.

In this book, the authors explore multiple perspectives on the field of computer graphics: the user's, the application programmer's, the package implementor's, and the hardware designer's. For example, the issues of user-centered design are addressed in three chapters on interaction techniques, dialogue design, and user interface software. Hardware concerns are examined in a chapter, contributed by Steven Molnar and Henry Fuchs, on advanced architectures for real-time, high-performance graphics.

The topic coverage includes:

- Programming with SRGP, a simple but powerful raster graphics package that combines features of Apple's QuickDraw and MIT X-Window System's graphics library.
- Hierarchical, geometric modeling using SPHIGS, a simplified dialect of the 3D graphics standard PHIGS.
- Raster graphics hardware and software, including both basic and advanced algorithms for scan converting and clipping lines, polygons, conics, spline curves, and text.
- Image synthesis, including visible-surface determination, illumination and shading models, image manipulation, and anti-aliasing.

modeling. Part III describes graphics concepts such as transformations. Part IV deals with interactive tools to manipulate the geometry.

1991 Robert C. Beach An Introduction to the Curves and Ref. 53
 Surfaces of Computer-Aided Design

This book provides a foundation in mathematics for curves and surfaces used in computer graphics. FORTRAN programs are given as examples. Fundamentals of conics, quadratics and B-splines are discussed. Transformations, parametric representation of curves and surfaces, Coons surfaces, Bézier and B-spline curves and surfaces, and rational parametric curves are discussed. This book describes more of the mathematical background needed as compared to other books on the same topic.

1993 Alan Watt 3D Computer Graphics Ref. 54

This book brings together the techniques required to produce realistic images of three-dimensional solids. Topics are modeling and representation, viewing systems, parametric representation and scientific visualization. It includes algorithms in Pascal.

1999 Michael E. Mortenson Mathematics for Computer Graphics Ref. 55
 Applications

This book introduces the mathematics that is the foundation of many of today's most advanced computer graphics applications, including CAD/CAM and geometric modeling. Subject areas are: vectors, matrices, symmetry, transformations, Bézier curves, surfaces, and computer graphics display geometry.

2003 Philip J. Schreiner Geometric Tools for Computer Graphics Ref. 56
David H. Eberly

This book describes the building blocks and solutions to building primitives, distance calculation, approximation, decomposition, intersection determination, separation etc. It describes all the detailed mathematics related to 2D and 3D graphics programming. This book is primarily a reference guide.

2003 Samuel R. Buss 3-D Computer Graphics A Mathematical Ref. 57
Introduction with OpenGL

This book is an introduction to 3D computer graphics with particular emphasis on fundamentals and the mathematics underlying computer graphics. It includes descriptions on how to use the cross-platform OpenGL programming environment. It includes transformations and viewing, lighting and shading models, interpolation and averaging, Bézier curves and B-splines.

2005 Ibrahim Zeid Mastering CAD/CAM Ref. 58

This is the follow-on book to Zeid (WA). It contains a more modern handling of CAD/CAM systems and software. It includes feature based modeling, parametrics, NURBS (Non-uniform Rational B-Splines), collaborative design, PDM (Product Data Management) and PLM (Product Lifecycle Management).

Appendix D: Theory and History of Airplane Design Tools and Systems

Abstracts of papers related to airplane design tools, geometry definition, knowledge based design, artificial intelligence in airplane design are given in chronological order. Abstracts are literal copies from the references, unless indicated otherwise by the initials WA.

1967	S.A. Coons B. Herzog	Surfaces for Computer-Aided Aircraft Design	Ref. 68
------	-------------------------	--	---------

A simple but general way is described to define free-form surfaces such as airplane fuselages, wings, fillets, ducts, and other shapes by means of man-machine graphical interaction with a computer. In the past, much attention has been directed toward fitting mathematical functions to surfaces already defined by a mesh of points. The present discussion will center around the philosophy that in the preliminary phase of shape description the computer's aid should be enlisted at the very beginning, and that in this way the results of preliminary surface design become the first "master dimensions" of the airplane directly, without the necessity of refairing or other subsequent treatment. Furthermore, the computer data structure for the description of shape also serves as the skeleton upon which other associated data can be hung, such as velocity fields, pressures, temperatures, forces, and other physical quantities that arise in connection with analytical and design procedures.

1979	Daniel P. Raymer	A Computer-Aided Aircraft Configuration Development System	Ref. 69
------	------------------	---	---------

A minicomputer based program for the initial configuration development of aircraft concepts is described. The traditional procedures for configuration development are reviewed to establish requirements for the computer-aided system. The computer-aided procedures are demonstrated with an illustrative example beginning with initial sizing data and proceeding through a first concept, analysis, iteration, and successive

increases in the complexity level of the design, leading to computer generated loft lines, production layouts, and N.C. programming. Additional discussion addresses the requirements for minicomputer implementation, data base manipulation, and use by designers with no prior computer experience.

1983 Antonio L. Elias Computer-Aided Engineering: The AI Ref. 70
Connection

AI Techniques have penetrated the aerospace designer's world, and the proper industrial setting should accelerate both AI-related research and practical use of a Computer-Aided Preliminary Design System. The article describes MIT's Paper Airplane system

1984 L.R. Jenkinson A Computer Program For Assisting In The Ref. 71
D. Simons Preliminary Design Of Twin-Engined
Propeller-Driven General Aviation Aircraft

A computer program has been developed to analyze General Aviation, Twin-Engined, Propeller-driven aircraft (GATEP program). This program assumes that the initial systems study with the basic requirements has been completed. The more detailed project design phase is to be performed. The program allows to compare individual designs and includes parametric studies.

1987 J. Alsina Progress Towards an Aircraft Design Ref. 72
J. Fielding Expert System
A. Morris

The aim of this paper is to describe a two pass approach at developing an expert system for aircraft design. The initial steps, on which the rest of the design depends, are outlined. The first pass involved the creation of a wing design program which is described together with its implementation. In the second pass an aircraft

configuration program was attempted and the main details of the resulting output are described and the sources and types of knowledge identified. Based on this, the extensions to the system developed in the first phase are enumerated.

1988 Mark A. Kolb A Flexible Computer Aid for Conceptual Design Based on Constraint Propagation and Component-Modeling Ref. 73

Originally, computer programs for engineering design focused on detailed geometric design. Later, computer programs for algorithmically performing the preliminary design of certain well-defined classes of objects became commonplace. However, due to the need for extreme flexibility, it appears unlikely that conventional programming techniques will prove fruitful in developing computer aids for engineering conceptual design. The use of symbolic processing techniques, such as object-oriented programming and constraint propagation, facilitates such flexibility. Object-oriented programming allow programs, to be organized around the objects and behavior to be simulated, rather than around fixed) sequences of function- and subroutine-calls. Constraint propagation allows declarative statements to be understood as designating mathematical relationships among all the variables of the equation, rather than as uni-directional assignment to the variable on the left-hand side of the equation. This paper describes Rubber Airplane, a computer program which combines these techniques with a component-based database of design knowledge to form a prototype computer aid for conceptual design. The additional level of organizational structure obtained by arranging the design information in terms of design components provides greater convenience to the user, and results in a database which is easier both to maintain and to extend.

1988 I. Kroo, M. Takai A Quasi-Procedural, Knowledge-Based System for Aircraft Design Ref. 74

This paper deals with the development of a program for aircraft design, combining a rule-based advice and warning system with an extensible set of analysis routines in an

unconventional architecture. The system consists of several procedural modules for calculation of aircraft aerodynamics, structures, propulsion, and operating costs, which, when executed in the appropriate order, permit computation of desired results. Unlike conventional programs, the subroutines and order of execution are selected during the computation, based on the required results and on the currently available results. Unlike non-procedural programming languages, however, the modules are procedural, allowing the programmer the flexibility to include either short definitions or complex local procedures. This structure is encapsulated in an executive routine with a highly-interactive, event-driven, graphical interface and expert system. The rule-based system is used to assist the user in selecting intelligent design solutions and appropriate analysis procedures. This paper discusses the structure of the program, some of the difficulties encountered in its development, and its potential applications.

1988 Carl W. Dawson 1993: A Vision of the Design Computer Ref. 75

The ability to interconnect different computer systems and to share data and processing power has been made possible by the implementation of various standards. The power of new and emerging hardware and software technologies will have profound impact on the way new applications are developed and how an organization will use computer resources within the next five years.

1988 David W. Hall Design of High Altitude, Long Endurance Ref. 76
J. Edward Rogan Aircraft using a Computer Programming
Language for Design Specifications

In recent years, increasing attention has been given in the aerospace Industry to integration of aircraft design disciplines. This approach has been applied theoretically to sailplane design and to solar powered high altitude long endurance (HALE) aircraft design. More recently, it has been applied to the design of microwave powered aircraft. These studies describe attempts to arrive at integrated

designs of one class of aircraft using then-existing state-of-the-art computer capabilities. No attempt was made in any of these cases, though, to use new programming techniques derived from Artificial Intelligence (AI) research to develop more flexible systems for the conceptual design of HALE aircraft.

The purpose of this study was to investigate the feasibility of developing a general parametric sizing capability for micro-computers using integrated design methodology implementing an existing HALE methodology as a test case. The methodology described here incorporates some detailed calculations, many qualitative rules-of-thumb and constraints which are not easily quantified except by the accumulation of design experience. In this regard, the resultant software which will be developed in future efforts will be a knowledge-based system for the conceptual design of HALE aircraft.

1988	S.G. Wampler	Improving Aircraft Conceptual Design - a	Ref. 77
	A. Myklebust	Phigs Interactive Graphics Interface for	
	S. Jayaram	ACSYNT	
	P. Gelhausen		

Conceptual or preliminary design of aircraft is a demanding and sometimes tedious task. Creativity during the design process can be severely hampered by typical aircraft design codes due to slow batch turn-around times, delays caused by reduction of the data to meaningful results and lack of overall visual output of the aircraft model.

A computer-aided design (CAD) interface has been created for a well-known aircraft conceptual design code called ACSYNT (AirCraft SYNThesis). This interface permits the execution and control of the design process via interactive graphics menus and, by visual inspection of data and aircraft model shaded images, allows rapid evaluation of design configurations. This CAD interface was coded entirely with the new 3-D graphics standard, PHIGS (Programmers Hierarchical Interactive Graphics System). The CAD interface along with ACSYNT (called ACSYNT/VPI) is designed to be used on the new generation of high-speed imaging workstations. The

design and development of ACSYNT/VPL along with some preliminary results are discussed in this paper. The approach used in modeling, data storage and rendering is also described. The combination of a high-speed workstation engine to execute ACSYNT together with a high-speed rendering engine to display the results should give suitable feedback rates to promote truly interactive design.

1988 Bonnie L. Anderson First Step Toward Integrating the Design Ref. 78
Process

Preliminary aircraft designs are laid out by configuration design engineers. Designers refine these first estimates based on detailed analyses. Manually drawn designs are time consuming to iterate, and traditional computer aided design (CAD) methods simplify drawing changes; they do not ease the initial geometry construction.

A configuration layout system has been developed at Douglas Aircraft Company that reduces the construction and iteration times by specifically addressing configuration layout problems. The system parametrically defines parts of standard commercial aircraft for preliminary design. The interactive computer graphics system allows the designers to create and iterate their designs by automating repetitive tasks. The system supports analyses groups with a partially automated method to access standard geometry from completed designs. Configuration Layout significantly reduces the hours needed to obtain both the overall arrangement and the details of major components for conventional aircraft.

1989 Jan Roskam Automated Aircraft Design Configuration Ref. 36
Seyyed Malaek Design and Analysis

The University of Kansas, Flight Research Laboratory is developing an interactive, user-friendly computer program to perform preliminary design and analysis functions for fixed wing airplanes. This paper presents a discussion of the current status of this program. Use of the program is illustrated with an example application to an advanced stealth bomber.

1989	A. Bolukbasi D. Furey A. Goodworth	Application of Expert Systems to CAD/CAE	Ref. 79
------	--	---	---------

This paper presents a prototype rule-based Expert System developed to supplement a traditional CAD system for preliminary design of composite parts. The system uses an object-oriented methodology to model each of the components (objects) in the part. Each object represents the expertise inherent to itself in terms of rules. Rules describe both the individual characteristics of an object, such as methods used for calculating edge-distance, number of plies required, and failure criteria, and also the relationships and constraints that the object must maintain with other objects in the part. The system is very user friendly and is fully integrated with the production CAD system. The designs developed can be immediately imported into the CAD system for review, refinements, and merging into existing drawings.

1989	C. Bil	ADAS: A Design System for Aircraft Configuration Development	Ref. 80
------	--------	---	---------

This paper gives a description of the Aircraft Design and Analysis System (ADAS). ADAS has been developed to assess the potential of computer-tools in improving aircraft configuration development and design optimization. Automatic parameter sensitivity analysis and multivariate optimization are optional. Only standard and routine tasks have been automated to allow for user initiative and to retain a sufficient level of flexibility and general applicability of the system. Recent improvements relative to the initial pilot-version of ADAS will be highlighted. As an example, ADAS has been applied to a typical design optimization problem based on a hypothetical design specification of a short-haul passenger jet transport.

1989 J. Gee

The Role of Interfaces in Design
Integration

Ref. 81

Despite the prevalence of computer-aided design and analysis tools, the typical design cycle is far from automated. The problem can be largely attributed to the heterogeneous nature of the software tools. At Douglas Aircraft Company, a demand-driven interface links a preliminary geometric CAD model and an analysis program to accomplish the task of extracting and transforming information from the model and furnishing it to the analysis program. The interface represents an approach to integrating the design cycle that does not compromise the specificity of any of the design or analysis tools and that strongly fosters modularity. This paper discusses some of the key characteristics of Douglas' Configuration Geometry Data Base-Computer Aided Sizing and Evaluation (CGDB-CASE) interface and projects those characteristics into the future.

1989 D.J. Paisley

The Aerodynamic Assistant

Ref. 82

J.R. Blystone

G.R. Wichmann

The preliminary design of aircraft is a creative process that requires many iterations to develop a satisfactory solution given the constraints of the design requirements. The time required to develop a design using traditional methods precludes the examination of many alternatives, limiting the potential for achieving an optimal design. Existing software aid the process, but do not take advantage of advancing technologies to optimize the productivity of the designer.

The objective of the Aerodynamic Assistant program is to provide the conceptual designer with a tool that integrates the existing methodologies into a single homogeneous environment. It will provide rapid geometry feedback, expert advice, interfaces to detailed analysis tools, and a database management system to relieve the designer of data management chores.

1990	J. Roskam S.M. Malaek W. Anemaat	AAA (Advanced Aircraft Analysis): A User-Friendly Approach To Preliminary Aircraft Design	Ref. 38
------	--	---	---------

The paper demonstrates the utility of a user-friendly code developed for preliminary aircraft designers and for aircraft design students to rapidly evolve a new airplane design. The code applies to civil and military airplanes: all applicable performance and flying quality regulations have been 'built-in'. This provides the designer with instant appraisal about the status of his design relative to these regulations. Important features of the program are: 1) a common database, 2) built-in help files for theory and for design decision making and 3) report quality graphics for display of design results and trade studies.

1990	C. Haberland W. Fenske O. Dranz R. Stoer	Computer-Aided Conceptual Aircraft Configuration Development by an Integrated Optimization Approach	Ref. 83
------	---	---	---------

The objective of the conceptual design phase is the development of the aircraft configuration which is most efficient for a given specification. To numerically assist this procedure a CAE-system is presented which, as main attributes, handles arbitrary analysis and synthesis methods as modules in a method library, applies an always consistent and complete computer internal modeling of geometry and performance, and controls the design processing through a design management system as a central user interface. To point out the potential of this open program architecture, and, in particular, the modeling approach chosen an aerodynamic analysis of complete aircraft configurations is discussed. Furthermore, it can be shown that paralleling the multivariate optimization with the design synthesis leads to a more efficient strategy than the conventional successive procedure. With this integrated optimization approach a comparative concept evaluation can be performed.

1992 I.M. Kroo An Interactive System for Aircraft Design and Optimization Ref. 84

A system for aircraft design utilizing a unique analysis architecture, graphical interface, and suite of numerical optimization methods is described in this paper. The non-procedural architecture provides extensibility and efficiency not possible with conventional programming techniques. The interface for analysis and optimization, developed for use with this method, is described and its application to example problems is discussed.

1992 M. J. Buckley Design Sheet: An Environment for Facilitating Flexible Trade Studies During Conceptual Design Ref. 85
K. W. Fertig
D. E. Smith

This paper summarizes the capabilities of Design Sheet, a software program that facilitates trade studies during conceptual design. Design Sheet permits the designer to build a model for use in conceptual design by entering a set of algebraic equations in a very flexible form. The designer can then use Design Sheet to easily change the set of independent variables in the algebraic model, and to rapidly perform trade studies, optimization, and sensitivity analyses. The basic mathematics and algorithms used in Design Sheet are outlined. The functionality of Design Sheet is illustrated first with a simple example, and then with a more complex example involving initial aircraft sizing. For realistic conceptual design problems, it is argued that Design Sheet provides the capability to perform trade studies with significantly increased flexibility and efficiency.

1992 Mark A. Kolb Constraint-Based Component-Modeling for Knowledge-Based Design Ref. 86

The earliest computer programs for engineering design focused on detailed geometric design. Subsequently, computer programs for algorithmically performing the preliminary design of specific types of devices became commonplace. However, due

to the need for extreme flexibility, it appears unlikely that conventional programming techniques will prove fruitful in developing computer aids for engineering conceptual design. Symbolic processing techniques, such as constraint propagation and object-oriented programming, can facilitate such flexibility. This research has concentrated on applying these techniques to the development of a general-purpose computer aid for engineering conceptual design. Object-oriented programming techniques are utilized to implement a user-extensible database of design components. The mathematical relationships which model the geometry and physics of these components are managed via constraint propagation. To supplement this component-based hierarchy, special-purpose data structures are provided for describing component interactions and supporting state-dependent parameters. Three sample aerospace design problems have been implemented using the prototype design tool. The additional level of organizational structure obtained by representing design knowledge in terms of components is observed to provide greater convenience to the program user, and to result in a database of engineering information which is easier both to maintain and to extend.

1992	S. Jayaram	ACSynt - A Standards-Based System for	Ref. 87
	A. Myklebust	Parametric Computer Aided Conceptual	
		Design of Aircraft	

A group of eight U. S. aerospace companies together with several NASA and NAVY centers, led by NASA Ames Systems Analysis Branch, and Virginia Tech's CAD Laboratory agreed, through the assistance of American Technology Initiative, in 1990 to form the ACSynt Institute. The Institute is supported by a Joint Sponsored Research Agreement to continue the research and development in computer aided conceptual design of aircraft initiated by NASA Ames Research Center and Virginia Tech's CAD Laboratory. The result of this collaboration, a feature-based, parametric computer aided aircraft conceptual design code called ACSynt, is described in this paper. The code is based on analysis routines begun at NASA Ames in the early '70's. ACSynt's CAD system is based entirely on the ISO standard PHIGS and is graphics-device independent. The code includes a highly interactive graphical user interface, automatically generated Hermite and B-Spline surface models and shaded

image displays. Numerous features to enhance aircraft conceptual design are described.

1992	U. Jayaram A. Myklebust P. Gelhausen	Extracting Dimensional Geometric Parameters from B-Spline Surface Models of Aircraft	Ref. 92
------	--	--	---------

In an integrated design environment, the common thread between the different design stages is usually the geometric model of the object. However, the requirements for the geometric definition of the design are usually different at each stage. For example, geometric dimensional parameters (e.g. length, radius, etc.) are frequently used in the conceptual design stage whereas a surface model is often the form of geometry definition in the preliminary design stage. Frequently, the necessary design parameters are not transferred between different systems or design stages. Only the surface description remains. Also, if a surface is locally, interactively modified, the corresponding dimensional parameters may not be correct. The transformation of data between these different stages is crucial for the success of an integrated design environment. An acute need for this capability has been expressed by industry, especially the aerospace industry. The research presented in this paper creates methods to automatically obtain dimensional geometric parameters from the non-uniform B-spline surface description of an object. This study represents the first comprehensive treatment of this problem. These methods have been implemented successfully in the aircraft design software, ACSYNT, a computer-aided design system for conceptual aircraft design created at NASA-Ames and Virginia Tech. The methods created and implemented in this research are also of significance to general-purpose design.

1993	April Gilliam	Vehicles Knowledge-Based Design Environment	Ref. 89
------	---------------	--	---------

The Vehicles design environment is a knowledge-based system that assists designers in studying tradeoffs, evaluating alternative designs, and identifying design drivers.

The environment is composed of 1) analysis tools, such as parametric analysis and what-if analysis 2) subsystem sizing and performance models; a historical data base (of satellites that have already been built); and 4) an extensible architecture in which new models, tools, and design concepts may be added. We have found that building in both for the designer to explore a variety of space system design solutions as well as for the software developers to continually enhance Vehicles' capabilities is essential. The analysis tools, which have been very well received by the design community, include the capability to study parametric sensitivities, trace the derivation of results, and compare multiple design concepts. An integrated design environment, one that offers a variety of analysis and information handling tools, gives the designers the ability to view a design from different perspectives and across functional, organizational, and other boundaries.

1993	Daniel P. Raymer	Aircraft Aerodynamics Analysis on a Personal Computer (Using RDS Aircraft Design Software)	Ref. 90
------	------------------	--	---------

This paper discusses the creation of the aerodynamic analysis module of a PC-based aircraft design program called RDS, using the time-honored aerodynamic methods found in classical textbooks and the USAF DATCOM. Using this program, reasonably realistic aerodynamic results can be calculated in less than an hour given the geometric inputs which define an aircraft, such as component wetted areas, wing geometry, and cross-section areas. Aerodynamics analysis in RDS includes parasite drag (subsonic and supersonic), drag due to lift, lift curve slope, and maximum lift. Comparisons to T-38 data show good results.

1993	W.H. Mason T.K. Arledge	ACSYNT Aerodynamic Estimation - An Examination and Validation for Use in Conceptual Design	Ref. 91
------	----------------------------	--	---------

The aerodynamic prediction methodology available in ACSYNT is examined through comparison with aircraft data for a variety of classes of configurations. The predic-

tions are a synthesis of the best empirical procedures currently available. The paper presents selected results obtained from the comparison, and shows how the basic capability can be enhanced by user supplied adjustments to represent changes in technology levels when considering advanced aircraft designs. The predictions and basis for adjustments are described for a supersonic cruise vehicle (the XB-70), a large subsonic transport, and a typical fighter.

1993	Arvid Myklebust	Improving Aircraft Conceptual Design	Ref. 92
	Paul Gelhausen	Tools - New Enhancements to ACSYNT	

The continued improvement of aircraft computer-aided conceptual design tools depends on several factors. Among the most important is the ability to add numerous associated analysis and synthesis functions while still retaining the tools' speed and flexibility and the ability to maintain such large tools in a rapidly changing hardware and software environment. This paper presents an approach designed to assure the manageable growth of large parametric feature-based computer-aided aircraft conceptual design tools based on experience with ACSYNT (AirCraft SYNThesis).

A new approach to the design and subsequent modifications of graphical user interfaces (GUI) is described. This approach has the capabilities of X and Motif yet allows full use of the 3D ISO graphics standard (PHIGS) and *is* truly object-oriented, relying on C++. The resulting GUI builder is designed for extensibility and maintainability. New modules for ACSYNT based on this object-oriented GUI builder are mission specification, output data graphing, parametric component library, rule-based fuselage design, and an NEPP (NASA Engine Performance Program, a.k.a. NEPP) module.

New extensions to ACSYNT analysis functions are described. Among them are a new geometry-coupled aerodynamics module, rapid infra-red signature analysis, engine analysis with NEPP, and internal/external afterbody drag. To further enhance maintainability, an extensive validated test case library is under development.

1993 Jan Roskam An Easy Way to Analyze Longitudinal and Ref. 39
William Anemaat Lateral-Directional Trim Problems with
AEO or OEI

A user-friendly method for analyzing longitudinal and lateral-directional trim problems for airplanes with all engines operating (AEO) and with one engine inoperative (OEI) is presented. The method allows for rapid evaluation of various critical handling quality parameters, such as stick force per 'g' and stick force versus speed gradients. In addition, the effect of failures in trim systems on cockpit control forces and on control surface and/or tab deflections can be assessed. Also, the method can be used for sizing of tab control systems, downsprings, bobweights and interconnect springs. Finally, elevator hingemoment derivatives for rather arbitrary aerodynamic balance configurations can be quickly estimated.

1994 Francisco Rivera, Jr. An Object-Oriented Method for the Ref. 93
Sankar Jayaram Definition of Mission Profiles for Aircraft
Design

A mission profile is a detailed description of an aircraft's flight path and its in-flight activities. It is a vital aspect of the conceptual design of an aircraft. Although the analysis of the trajectory or mission of an aircraft is treated in great depth by a number of conceptual design software systems, a general methodology for defining the mission profile does not exist. This paper presents a new method for organizing the data and methods related to the definition of the mission profile for an aircraft. An object-oriented method is used to define the overall mission profile as a set of classes. The user interface methods which will provide the aircraft designer with tools to interactively define the mission profile are encapsulated within these classes. An object-oriented design provides this method with a high degree of extendibility. The encapsulation and inheritance features allow new types of phases and other mission data and methods to be simply "plugged" into an existing system. New classes can be defined with specific methods built into them to tailor the system to the needs of any existing conceptual aircraft design system. An implementation of this new method is also presented in this paper. The implementation provides the user

with a Motif-like interface which is based on the ISO standard for 3D graphics, PHIGS. This implementation has been integrated with the aircraft design software, ACSYNT (AirCRAFT SYNThesis). This integration and use of these methods with ACSYNT are also discussed.

1994	Jan Roskam William Anemaat	An Easy Way to Analyze Longitudinal and Lateral-Directional Trim Problems with AEO or OEI	Ref. 40
------	-------------------------------	---	---------

A user-friendly method for analyzing longitudinal and lateral-directional trim problems for airplanes with all engines operating (AEO) and with one engine inoperative (OEI) is presented. The method allows for rapid evaluation of various critical handling quality parameters, such as stick force per 'g' and stick force versus speed gradients. In addition, the effect of failures in trim systems on cockpit control forces and on control surface and/or tab deflections can be assessed. Also, the method can be used for sizing of tab control systems, downsprings, bobweights and interconnect springs. Finally, elevator hingemoment derivatives for rather arbitrary aerodynamic balance configurations can be quickly estimated.

1995	William Anemaat	G.A.-CAD, A Personal Computer Aided Design System for General Aviation Aircraft Configurations	Ref. 41
------	-----------------	--	---------

A personal computer based preliminary design system for General Aviation aircraft demonstrates a practical method to design and analyze general aviation aircraft configurations. The program provides a powerful framework to support the non-unique process of aircraft preliminary design. The system will allow design engineers to rapidly evolve an aircraft configuration from weight sizing through detailed performance calculations, while working within regulatory constraints. The program is designed to reduce the preliminary design phase cost and to bring advanced design methods to businesses which normally do not have the computational and/or modern design/analysis capability.

1995	Scott Angster Sankar Jayaram	An Object-Oriented, Knowledge-Based Approach to Multi-Disciplinary Parametric Design	Ref. 94
------	---------------------------------	--	---------

The use of computers in the area of design and manufacturing is commonplace in industry. Many companies are turning to custom designed in-house software to surpass the competition. A growing number are developing knowledge-based systems to capture the knowledge and expertise of employees before they retire. The use of traditional artificial intelligence languages can be cumbersome to engineers who are usually familiar with traditional languages such as FORTRAN and C. The use of expert systems shells can often hinder the customization of an expert system due to limitations of the shell. An alternative approach to these methods is the use of an object-oriented framework that facilitates the creation of customized expert systems. This framework, called the Expert Consultation Environment (ECE), alleviates the programming problems of expert system development and allows the engineer to concentrate on knowledge acquisition. This paper gives an overview of the ECE, as well as a description of a prototype implementation of the an ECE framework. A test case for the parametric, multi-disciplinary, conceptual design of aircraft is also described.

1995	Robert E. Smith Malcolm I.G. Bloor Michael J. Wilson Almuttil M. Thomas	Rapid Airplane Parametric Input Design (RAPID)	Ref. 95
------	--	---	---------

An efficient methodology is presented for defining a class of airplane configurations. Inclusive in this definition are surface grids, volume grids, and grid sensitivity. A small set of design parameters and grid control parameters govern the process. The general airplane configuration has wing, fuselage, vertical tail, horizontal tail, and canard components. The wing, tail, and canard components are manifested by solving a fourth-order partial differential equation subject to Dirichlet and Neumann boundary conditions. The design variables are incorporated into the boundary conditions, and the solution is expressed as a Fourier series. The fuselage has circular

cross section, and the radius is an algebraic function of four design parameters and an independent computational variable. Volume grids are obtained through an application of the Control Point Form method. Grid sensitivity is obtained by applying the automatic differentiation precompiler ADIFOR to software for the grid generation. The computed surface grids, volume grids, and sensitivity derivatives are suitable for a wide range of Computational Fluid Dynamics simulation and configuration optimizations.

1995	Paul A. Gelhausen	Overview of ACSYNT for Light Aircraft	Ref. 96
	Mark D. Moore	Design	
	James R. Gloudemans		

The focus of the 5 year long ACSYNT Institute has been to greatly increase the capability of the aircraft synthesis computer program, ACSYNT. The key improvements have followed from the advanced geometric modeling and display technology of current workstations. The higher fidelity model enables more accurate and general aerodynamic propulsion and weight computations with less reliance on regression methods and estimations. This paper focuses on the improvements that can enhance the state of the art in general aviation aircraft synthesis.

1995	Daniel P. Raymer	RDS Professional: Aircraft Design on a Personal Computer	Ref. 97
------	------------------	---	---------

RDS-Professional is a sophisticated yet friendly PC-based aircraft design and analysis system developed for the conceptual design of new aircraft and the initial analysis of derivatives and alternate missions. RDS-Professional is suitable for use by aircraft designers in industry, government, and academia for conceptual trade studies, technology evaluations, and preliminary performance predictions. This paper provides an overview of RDS-Professional and illustrates its usage for design of a general aviation aircraft.

1995	Kurt L. Schueler Steven J. Smith	Advanced Aircraft Analysis: A Powerful, User Friendly Framework for Airplane Preliminary Design and Analysis	Ref. 46
------	-------------------------------------	--	---------

The Advanced Aircraft Analysis software package (AAA) is a UNIX workstation based program for the preliminary design and analysis of airplanes. The program began as a research project at the University of Kansas Center for Research with the intent of creating a user-friendly framework for the unique, iterative process of airplane preliminary design. Marketing of AAA began in 1991 and it is now in use throughout the world by industry and academia. Further development of AAA is driven by user feedback and new methods as they become available.

AAA combines various methods of design and analysis of airplanes into one application completely controlled by a computer mouse. No prior knowledge of computers or operating systems is required to use AAA. The program leads the user through a path of choices to a point where data can be entered and processed. The structure of the program allows the user to make any calculation at any time given the proper input data. This paper discusses the methods and design process upon which AAA is based. In addition, example input and output data and graphs are presented.

1996	James R. Gloudemans Paul C. Davis Paul A. Gelhausen	A Rapid Geometry Modeler for Conceptual Aircraft	Ref. 98
------	---	---	---------

A new, highly interactive, parameter-based aircraft modeler has been developed for use in conceptual design. The Rapid Aircraft Modeler (RAM) was developed to generate detailed 3D geometric models quickly and easily. The models allow a visual inspection of the geometry parameters used in the conceptual aircraft design and optimization process. Fast and accurate geometry modeling also allows the designer to use more complex analysis methods earlier in the design process and reduces reliance on empiricism in conceptual design.

1996	D.B. Landrum Eric G. Woodfin	'Will It Fly' A Computer-based Aircraft Design Tool	Ref. 99
------	---------------------------------	--	---------

This paper summarizes a project to develop a user-friendly, yet technically correct, computer application for aircraft design and performance prediction. The result of this endeavor is a beta version of 'Will It Fly?', a Microsoft Visual Basic-based application that integrates wing design, engine selection, and payload requirements to meet specific aircraft mission requirements. The program is targeted toward college-level sophomore engineering students and provides the technical framework needed to successfully teach elementary aerodynamics and aircraft design. This paper describes the program's architecture and the philosophy behind its layout. Although written for the college level, potential modifications to the program are discussed which would result in an educational version suitable for middle- and high-school students. Development of this secondary-level version would be beneficial to the future of science education by exposing these students to the design process.

1996	Max Blair Greg Reich	A Demonstration of CAD/CAM/CAE in a Fully Associative Aerospace Design Environment	Ref. 100
------	-------------------------	--	----------

A vision is put forth in which CAD/CAM/CAE are integrated with Full Associativity in a Virtual Design Environment. Some elements of this vision are presented with an interactive demonstration. Intended audiences are CAD product developers, so they can see how their product is being used, aerospace vehicle designers, to provide an overview of one approach in the use of full associativity in an aerospace design environment, and aerospace analysts, to provide a perspective on how to better integrate their products and techniques into a powerful design environment. After a description of a virtual design process with feedforward and feedback, experience with the development of fully associative geometry for a blended wing and fuselage is presented. An example of total integration of fully associative geometry with aerospace structural optimization is given. The CAD/CAM software Pro/ENGINEER, is used as the basis for this work.

1996	C. Wayne Mastin Robert E. Smith Ideen Sadrehaghighi Michael R. Wiese	Geometric Model for a Parametric Study of the Blended-Wing-Body Airplane	Ref. 101
------	---	---	----------

A parametric model is presented for the blended wing-body airplane, one concept being proposed for the next generation of large subsonic transports. The model is defined in terms of a small set of parameters which facilitates analysis and optimization during the conceptual design process. The model is generated from a preliminary CAD geometry. From this geometry, airfoil cross sections are cut at selected locations and fitted with analytic curves. The airfoils are then used as boundaries for surfaces defined as the solution of partial differential equations. Both the airfoil curves and the surfaces are generated with free parameters selected to give a good representation of the original geometry. The original surface is compared with the parametric model, and solutions of the Euler equations for compressible flow are computed for both geometries. The parametric model is a good approximation of the CAD model and the computed solutions are qualitatively similar. An optimal NURBS approximation is constructed and can be used by a CAD model for further refinement or modification of the original geometry.

1996	Jamshid A. Samareh	Use of CAD Geometry in MDO	Ref. 102
------	--------------------	----------------------------	----------

The purpose of this paper is to discuss the use of Computer-Aided Design (CAD) geometry in a Multi-Disciplinary Design Optimization (MDO) environment. Two techniques are presented to facilitate the use of CAD geometry by different disciplines, such as Computational Fluid Dynamics (CFD) and Computational Structural Mechanics (CSM). One method is to transfer the load from a CFD grid to a CSM grid. The second method is to update the CAD geometry for CSM deflection.

1996	Sonny Chai W.H. Mason	Landing Gear Integration in Aircraft Conceptual Design	Ref. 103
------	--------------------------	---	----------

Landing gear integration is one of the more fundamental aspects of aircraft design. The design and integration process encompasses numerous engineering disciplines, e.g., structures, weights, runway design, and economics. Although the design process is well-documented, it appears not to have been automated for uses in multidisciplinary design optimization (MDO) procedures. The process remains a key responsibility of the configuration designer. This paper describes the development of an MDO-capable design methodology focused on providing the conceptual designer with tools to help automate the disciplinary analyses, e.g., geometry, kinematics, flotation, and weight. The procedures are described and illustrated by application to a notional large subsonic transport aircraft, illustrating the methods and design issues.

1996	Robert E. Smith Yvette Cordero Wayne Mastin	Conceptual Airplane Design with Automatic Surface Generation	Ref. 104
------	---	---	----------

A methodology and software to automatically define airplane configurations is presented. The general airplane configuration has wing, fuselage, vertical tail, horizontal tail, canard, pylon, and engine nacelle components. The wing, tail, canard, and pylon components are manifested by solving a fourth order partial differential equation subject to Dirichlet and Neumann boundary conditions. The design variables are incorporated into the boundary conditions, and the solution is expressed as a Fourier series. The fuselage and nacelles are described with analytic equations. The methodology is called Rapid Airplane Parametric Input Design (RAPID), and both batch and interactive software based on the technique are described. Examples of high-speed civil transport configurations and subsonic transport configurations are presented.

1996 Randy W. Kaul A Comparative Analysis of the Boeing 727- Ref. 105
Kamran Rokhsaz 100 Using Three Advanced Design
Methods

A comparative analysis has been performed on the Boeing 727-100 using three conceptual design codes. These programs were: The Aircraft Synthesis Program, ACSYNT, Advanced Aircraft Analysis, AAA, and RDS-Student. The objective of this study was to investigate differences in the conceptual design methodologies of these three programs.

All three codes showed reasonable prediction of drag in the subsonic flow regime. However all three programs had difficulty predicting transonic drag rise characteristics. The principal cause was the inability to accurately predict the critical drag rise Mach number. Difficulties in estimating the shape of the drag rise curve, relative to the critical Mach number, also contributed to the errors in drag prediction. AAA and RDS-Student gave reasonable predictions of maximum lift coefficient. ACSYNT could not model the triple-slotted flap system on the 727-100.

The three codes showed a consistent trend towards under-prediction of empty weight. The best empty weight predictions were seen in the propulsion group. The largest variations between predicted and actual weight were seen in the fixed equipment group. The wing structural weight prediction was also an area of concern.

Performance analyses suffered from the accumulation of errors in the other analysis modules of all three codes. Prediction methods in the geometry, aerodynamics, propulsion, weights and high lift modules need to be calibrated to a reference configuration of similar characteristics before performance can be reliably predicted.

1996 Jan Roskam General Aviation Aircraft Design Ref. 42
William Anemaat Methodology in a PC Environment

A personal computer based preliminary design system for aircraft demonstrates a practical method to design and analyze any aircraft configuration. The program

provides a powerful framework to support the non-unique process of aircraft preliminary design. The system will allow design engineers to rapidly evolve an aircraft configuration from weight sizing through detailed performance calculations, while working within regulatory constraints. The program is designed to reduce the preliminary design phase cost and to bring advanced design methods to small businesses and universities.

1996 Daniel P. Raymer An Update on RDS-Professional Ref. 106

RDS-Professional is a conceptual aircraft design and analysis system developed for operation on a personal computer. Based on the methods in the AIAA textbook 'Aircraft Design: A Conceptual Approach', *RDS* features a 3-D *CAD* module for design layout, and has analysis modules for aerodynamics, weights, propulsion, and cost. *RDS* includes capabilities for aircraft sizing, mission analysis, and performance analysis including takeoff, landing, rate of climb, P_s , f_s , turn rate, and acceleration. *RDS* also provides graphical output for drag polars, L/D ratio, thrust curves, flight envelope, and range parameter, and features both traditional carpet plot optimization and a multivariable design optimizer. Comparative studies indicate that *RDS-Professional* produces results within the usual accuracy for conceptual design efforts.

1996 Brett Malone ACSYNT, Commercialization Success Ref. 107
Arvid Myklebust

This paper chronicles the events of the ACSYNT software development project, the formation of the ACSYNT Institute, and the commercialization effort leading to a corporate entity, Phoenix Integration, Inc. Through the cooperation of government, industrial and academic concerns, a unique, focused research and development effort was organized for the development of software tools to aid in the conceptual design of aircraft. The goals of this jointly-sponsored effort were to provide a standard, consistent, generic environment in which aircraft conceptual modeling and analysis could take place. The ACSYNT Institute provided a climate that was conducive to

common R&D goals, formation of nonproprietary solutions and joint research efforts between government and industry. The resulting R&D direction, associated technology, and energized market provided the right ingredients for a commercialization effort. Phoenix Integration, Inc. is the result of a seven year, \$3M effort to provide unique software technology to a focused design engineering market.

1996 Daniel P. Raymer Aircraft Design Optimization on a Personal Computer Ref. 108

A PC-based program module was developed to simultaneously optimize an aircraft for thrust-to-weight ratio, wing loading & aspect ratio, sweep, taper ratio, and thickness ratio, in the presence of performance constraints, to a selected weight or cost measure-of-merit. A simple yet robust optimization scheme was employed, relying on the ever-increasing power of personal computers to permit exhaustive searching by a simple gradient method rather than using some more-sophisticated but more complex and perhaps less-robust optimization strategy. Results indicate the program works, within the limitations of the classical analysis methods used.

1997 Ilan Kroo Multidisciplinary Optimization Application in Preliminary Design Ref. 109

Multidisciplinary design optimization (MDO) has played an important role in aircraft preliminary design for 30 years, yet it is far from a mature field. This paper discusses the increasingly widespread use of MDO for aircraft design, describing the evolution of computational tools and strategies, and summarizing some current research directions. The objective of this review is not to provide a comprehensive survey of MDO methods and applications, but rather to highlight some interesting aspects that suggest how this field is developing.

In the aerospace community the perception of quality no longer relates to only whether the product performs to specification. The perception now includes whether or not the hardware was produced “on-time and on-cost”. To live up to the expanding expectations and maintain a competitive stance, design cycles times have to be reduced to maintain sound control on program costs and schedules. As the continuous change occurs, traditional analytical approaches are being scrutinized for streamlined efficiency. When shown to be antiquated, new approaches are adopted to rise to the challenge. A major challenge has been to transform old paradigms into new paradigms. Once such change has been to remove the barriers between disciplines and form product development teams to encourage cross-pollination of engineering activities. As part of the natural evolution of the teams, CAE tools have to become embedded within the CAD environment. This embedding of tools tremendously reduces duplication of effort, redundant data bases, amount of coordination, and thereby program costs.

The foundation of the paper being presented here is the application of CAD embedded CAE tools. The “new paradigm” that will be demonstrated by this paper is the Simulation Driven Design (SDD) environment. The application example that will be used is a landing gear exposed to the following environments: variable speed drop test and retraction. The CAD tool that will be applied is CATIA. CATIA provides a solid modeling environment for designing components and mechanical assemblies. The CAE tools that will be applied are CATDADS, PolyFEM and EASY5. CATDADS is a tool that is used to predict the behavior of mechanical assemblies. The equations of motion are automatically formed and solved. Positions, velocities, accelerations and reaction loads are predicted for all components in the assembly. PolyFEM is a finite element analysis package that includes interfaces to CAD products, an automatic mesher, and a p-type finite element solver. EASY5 is a control design tool which distinguishes itself from other tools on the market by its hydraulics libraries. The CAD/CAE tools are used in conjunction to achieve the desired “total system prototype” prior to any physical devices being constructed.

1997 William A. Anemaat General Aviation Airplane Design Tools for Ref. 43
Kurt L. Schueler PC's
C. Todd Kofford

DARcorporation is developing an interactive, user-friendly computer program to perform preliminary design and analysis functions for fixed wing general aviation airplanes. The system allows design engineers to rapidly evolve an aircraft configuration from weight sizing through detailed performance calculations, while working within regulatory constraints. This paper shows the main features of the newly developed user interface for general aviation airplane design in a windows based environment. The ease of use will bring computer aided design methods to people previously not exposed to these methods because of the high amount of difficult computer knowledge needed.

1997 Timothy D. Olson Aircraft Design Tools for PC's Ref. 45

Recent technology advancements in hardware and software has allowed the emergence of the PC as a cost effective aircraft design/analysis platform. Software packages such as CSI-CADD, Vellum Solids, and AeroPack provide "Lockheed" class modeling tools for a wide variety of design projects. Modeling tools for airfoils, wings, and polyconic surfaces are discussed as well as data extraction methods for wetted areas, volumes, centroids, area curves, obscuration plots, meshing, and custom interfaces to design analysis programs such as GA-CAD.

1997 James Locke General Aviation Preliminary Structural Ref. 44
Kurt L. Schueler Design in a Personal Computer
William A. Anemaat Environment

A personal computer based preliminary structural design system has been developed for general aviation aircraft. Structural design is coupled with other elements of the preliminary design process to provide a unique and powerful framework for the

1997	R.K. Pant J.P. Fielding J. Snow	CRISTO: A code for Integrated Synthesis and Trajectory Optimization of Commuter and Regional Aircraft	Ref. 113
------	---------------------------------------	---	----------

His paper describes a computer code for conceptual design of mission optimized twin-turboprop Commuter or Regional aircraft. Optimum configurations and flight profiles of such aircraft are determined by coupling this code to an optimization code based on Simulated Annealing. As an example, minimum DOC configurations were determined for 50-seat Regional Aircraft for operation over three stage lengths. The DOC per seat-nm and DOC per trip of the optimum aircraft were found to be comparable or significantly (8 to 17%) lower than the corresponding values for five contemporary 40 to 50 seater aircraft for short stage lengths.

1998	William A. Anemaat	AGDA: Airplane Geometry Design Assistant	Ref. 114
------	--------------------	---	----------

DARcorporation developed an interactive, user-friendly windows based computer program to perform preliminary design and analysis functions for fixed wing airplanes. This paper shows the development of AGDA: Airplane Geometry Design Assistant, a program used to facilitate the geometric data transfer between analysis and CAD software.

One major problem with the use of standard CAD programs is how to recognize different parts of the airplane in the analysis programs. Most routines need certain geometric parameters of the airplane e.g. wing span, fuselage length etc. An easier and user-friendlier method is to use an interface program between the analysis and the standard (commercially available) drafting program, which takes away the drawing instructions. In this way the user can concentrate on making the drawing without having to worry about how the program wants the different parts drawn.

1998 David C. Fliegel Experience with a Geometry Programming Ref. 115
Thomas P. Dickens Language for CFD Applications
Andrew P. Winn

The Boeing Aero Grid and Paneling System (AGPS) is a programming language with built-in geometry features. Accessible through either a graphical user interface (GUI) or through a command line, AGPS can be used by operators with different levels of experience.

Distributed with AGPS are approximately 300,000 lines of macros, or command files, which automate many engineering design and analysis tasks. Most command files were developed to produce inputs to engineering analysis codes such as A502 and TRANAIR. In many cases, command files have been grouped together in AGPS “packages,” which offer users simple menu pick and dialog options to automate entire engineering processes.

1998 P. Raj Aircraft Design in the 21st Century: Ref. 116
Implications for Design Methods (invited)

In this paper, a perspective is presented on the challenges that aircraft industry in general, and military aircraft industry in particular, is facing as we enter the 21st century. To the “higher, faster, farther” doctrine, that dominated airplane evolution in the 20th century, “affordable” has been added. The defense industrial sector and the U.S. Department of Defense have undertaken several initiatives to tackle the affordability challenge. Some of the key initiatives, such as lean aircraft initiative and simulation based acquisition, are highlighted to provide a context in which aircraft design will have to be carried out in the years to come. The principal goal of these initiatives is to reduce life cycle cost while maintaining technological superiority. Since aircraft design has a disproportionately large impact on life cycle cost, the traditional design practices are undergoing a significant change. The integrated product and process development concept is driving this change. New design practices have profound implications for methods needed to support them. Dramatic improvements in the effectiveness of the design methods are needed to

enable design of high quality aircraft at affordable cost. Relevant issues are examined in depth from a computational fluid dynamics perspective.

1998	Z.W. Zhu	A New Genetic Algorithm for Aerodynamic	Ref. 117
	Y.Y. Chan	Design Based on "Geometric Concept"	

A new Genetic Algorithm based on a “Geometric Concept” - Geometric Genetic Algorithm (GGA) is proposed. Without the binary coding required by a Standard Genetic Algorithm (SGA), the application of GGA to design variables is straightforward. Furthermore, the reproduction strategy is designed to improve the GGA’s robustness and efficiency. The numerical results confirm that GGA works well for model problems showing improvements in not only convergence but also accuracy. The new method is successfully applied to aerodynamic designs for transonic airfoils with drag reduction.

1998	D.W. Way	SCORES: Developing an Object-Oriented	Ref. 118
	J.R. Olds	Rocket Propulsion Analysis Tool	

SCORES (SpaceCraft Object-oriented Rocket Engine Simulation) is an analysis tool being developed for conceptual-level spacecraft and launch vehicle design. Written in C++, SCORES provides rocket thrust and Isp for propulsion system trade studies. Common gateway interface scripts, written in Perl, provide an interface with the World Wide Web. The design parameters used in SCORES are mixture ratio, chamber pressure, throat area, and expansion ratio, making SCORES effective in multidisciplinary design optimization. This paper describes the current status in the development of SCORES, compares chemical equilibrium results against accepted equilibrium codes STANJAN and CEA, compares engine thrust and Isp predictions against available engine data for nine rocket engines, and discusses areas for future work. SCORES accurately predicts equilibrium mole fractions and adiabatic flame temperature over a wide range of operating conditions within 0.5%. Uncorrected errors of less than 10% within SCORES engine thrust and specific impulse calculations are within acceptable tolerances for use in conceptual-level Subscripts

design. Statistically correcting the performance predictions reduces these errors appreciably and act provides the designer with additional information, the confidence interval of the calculations.

1998 Joseph J. Totah Simulating Conceptual and Developmental Ref. 119
Dr. David J. Kinney Aircraft

This paper presents results of a new capability to perform real-time simulation of conceptual and developmental aircraft. The objective is to seamlessly perform real-time simulation of arbitrary aircraft configurations whose geometric, inertial, and aerodynamic characteristics are either specified or estimated using conceptual design software, and then flown with a pre-existing flight control architecture that does not require gain scheduling or redesign. This new capability is first examined by comparing design estimates with known characteristics of an existing aircraft. The results correlate well with known inertial and closed-loop dynamic characteristics, however limitations are noted in the estimates of the aerodynamics. Another aircraft examined is that of a concept designed to fly on the surface of Mars. Although correlation data does not exist for this aircraft, the results indicated the conceptual Mars aircraft exhibits well behaved closed-loop dynamic characteristics with some coupling noted in the directional axis that may be attributed to spiral instability. These results represent a first step towards the completion of an integrated tool to simulate conceptual and developmental aircraft.

1998 Max Blair Enabling Conceptual Design in a Ref. 120
Technology Driven Environment

A proven general purpose design modeling environment has been adapted to facilitate technology insertion in the aerospace design process. The vision, which is demonstrated here, is one of a series of steps toward the goal of developing high fidelity design trades between cost and performance at the highest level.

Two factors make this work innovative. First, we are using an advanced design modeling environment with dependency tracking, demand-driven calculations and run-time object creation. Secondly, we explore how this computer software innovation can be used to tightly integrate design scenarios with technology-driven vehicle designs.

The design scenario involves multiple sorties taken from a suite of segmented trajectories and a suite of vehicle concepts. Once a sortie-object has been formulated with a combination of a trajectory object and a vehicle object, the equations of motion are integrated to assess the fuel consumed. Any point in the trajectory can be selected to examine maneuver load requirements and the relative position of other sorties or targets in the scenario. Subsequently, the vehicle can be resized or redesigned to meet the maneuver loads and mission requirements.

1998	D.W.E. Rentema F.W. Jansen E. Torenbeek	The Application of AI and Geometric Modelling Techniques in Conceptual Aircraft Design	Ref. 121
------	---	--	----------

This paper describes the setup of AIDA, a computer tool that support the designer during the first phases of aircraft design. This conceptual phase begins with the specifications and finishes with one or more feasible concepts. An aircraft concept includes the configuration and some sizing parameters.

The structure of AIDA is based on observations of the conceptual design process and some theoretical design aspects. Several Artificial Intelligence techniques are implemented to deal with the qualitative character of this process, such as Case-Based Reasoning and Rule-Based Reasoning. These reasoning techniques enable the use of experience, which is implicitly available in existing aircraft, and the execution of parameter studies for a wide variety of design specifications. The concept is geometrically modeled with feature-based techniques in order to automatically visualize it.

These reasoning and modeling techniques are implemented in separate modules. This modular setup of the AIDA system allows for separate developments. The focus is on the cooperation of the modules.

1998	Daniel Tejtel	Conceptual Aircraft Design Environment:	Ref. 122
	Dimitri N. Marvis	Case Study Evaluation of Computing	
	Mark Hale	Architecture Technologies	

Designers need to use a variety of different codes in order to solve today's complex design problems; codes which must all be made to work together. Tools can be developed which facilitate the integration of these varied codes, so that they can be used together to solve a single problem. Using a computational architecture, a procedure has been set up which allows for a complete aerodynamic analysis of a High Speed Civil Transport. The computer architecture serves as a framework within which any number of diverse codes can be linked; data can be exchanged, stored, and otherwise managed; and decisions regarding the design of a vehicle can be made. The use of a computational tool called a Process Element as the method of code implementation allows for the basic analysis procedure to be easily modified and added to and to be used with higher-level, probabilistic-based design methods. By means of the High Speed Civil Transport aerodynamic analysis example problem described in this paper, the key features of the computational architecture, as well as its capabilities and limitations, are examined and evaluated.

1998	Gregory L. Roth	Commercial Transport Aircraft Conceptual	Ref. 123
	William A. Crossley	Design Using a Genetic Algorithm Based	
		Approach	

Fixed-wing aircraft design is a complex engineering problem, yet the conceptual phase of design is often limited in the number of design variables examined. Further, to begin the design process, many decisions about an aircraft's configuration are based upon qualitative choices of the designer(s). The use of a genetic algorithm (GA) can assist in aircraft conceptual design by reducing the number of qualitative

decisions made during the design process while increasing the number of design variables taken into consideration. The genetic algorithm is a search method based on the patterns of natural selection and reproduction common to biological populations. Since the GA operates as a non-calculus based method, discrete and continuous design variables can be handled with equal ease. This paper describes a hybrid approach with the implementation of a GA as a less-biased, automated approach to conceptual aircraft design and the application of CONMIN, a calculus-based method of feasible directions, to refine the results obtained with the GA. Civilian transport class aircraft are the current focus. The resulting optimization-analysis code is used to generate potential conceptual designs for a specified mission. Results from these design efforts are discussed with insight into the use of GA's for conceptual aircraft design.

1998 Richard M. Wood A Discussion of Knowledge Based Design Ref. 124
Steven X.S. Bauer

A discussion of knowledge and Knowledge-Based design as related to the design of aircraft is presented. The paper discusses the perceived problem with existing design studies and introduces the concepts of design and knowledge for a Knowledge-Based design system. A review of several Knowledge-Based design activities is provided. A Virtual Reality, Knowledge-Based system is proposed and reviewed. The feasibility of Virtual Reality to improve the efficiency and effectiveness of aerodynamic and multidisciplinary design, evaluation, and analysis of aircraft through the coupling of virtual reality technology and a Knowledge-Based design system is also reviewed. The final section of the paper discusses future directions for design and the role of Knowledge-Based design.

1998	J.M. Scott J.R. Olds	Transforming Aerodynamic Datasets into Parametric Equations for use in Multi- disciplinary Design Optimization	Ref. 125
------	-------------------------	--	----------

This paper presents a method of transforming aerodynamic datasets generated in Aerodynamic Preliminary Analysis System (APAS) into parametric equations which may subsequently be used in a multidisciplinary design optimization (MDO) environment for analyzing aerospace vehicles.

APAS is an analysis code which allows the user to create a simple geometric model of a vehicle and then calculate the aerodynamic force coefficients of lift, drag, and pitching moment over a wide range of flight conditions. As such, APAS is a very useful tool for conceptual level vehicle designs since it allows the force coefficients for a given design to be calculated relatively quickly and easily.

However, APAS suffers from an outdated user interface and, because it is tedious to generate a new dataset during each design iteration, it is quite difficult to integrate into an MDO framework. Hence the desire for a method of transforming the APAS output into a more usable form.

The approach taken and described in this paper involves the use of regression analysis techniques and response surface methodology to accomplish the data transformation with two goals in mind. The first goal was to develop a parametric model for calculating the aerodynamic coefficients for a single unique geometry. The second goal was to extend this model to capture

1999	Cao LingJun Ang Haisong	Conceptual/Preliminary Aircraft Design Using Genetic Algorithm and Fuzzy Mathematics	Ref. 126
------	----------------------------	--	----------

The abstract has been edited for English. Calculation methods used are based on Nicolai.

The paper describes a new method for conceptual/preliminary aircraft design. A genetic algorithm is applied to the design process. A coding method that converts a design scheme to a genetic individual is developed. So a design scheme is represented by a chromosome. Thus, using genetic operators, the best design scheme is obtained through an optimization procedure.

Genetic optimization is combined with fuzzy mathematics during the design process. Fuzzy mathematics is applied to the optimization process in two ways:

Firstly, a unique method of calculating the fitness value of design schemes is developed. Common design tools, such as Approximate Group Weights Method, Energy-Maneuverability Method, are used for design analysis. The Weighted Values of these design tools are calculated. The results of design analysis are used to build the fuzzy system model and judgment matrix. The judgment results are applied to obtain the fitness value of design schemes based on common design analysis.

Secondly, Fuzzy Judgment including Tier upon Tier Analysis is used for generating individuals of the initial population. Based on the Fuzzy Judgment, every individual of the initial population generated has a relatively high Arrange Value. Thus, the initial population is pre-optimized and the average fitness value of initial population is better than that using mere genetic algorithms.

Numerical experiments show that the efficiency of genetic optimization is increased after applying Tier upon Tier Analysis into the design procedure. A design case is included in this paper, and the results are deemed satisfactory. A software package has been developed based on the methods introduced above.

1999 J.C. Trapp
H. Sobiecky

Interactive Parametric Geometric Design Ref. 127

Mathematically accurate shape generation for aerospace applications needs to keep up with progress in CFD and production tools. One reason is the present lack of good and powerful tools for the geometric definition of airframes. Standard CAD tools may

be used, but they do not support the design of aircraft in a problem-oriented way. Based on well established and tested parametric algorithms a new design tool will be presented which offers the possibility to define configurations in an object-oriented manner. Interactive control makes the tool easy to use. It may be used as a preprocessor for any kind of CAD program to build wind tunnel models or to define the net topology needed for numerical simulation. Furthermore it will fit perfectly in an automatic optimization environment due to the parametric definitions of the geometry. This paper covers a description of the underlying geometric algorithms, the software design and the usage of the new tool.

1999	Hakan Yusan Stephan Rudolph	On Systematic Knowledge Integration in the Conceptual Design Phase of Airships	Ref. 128
------	--------------------------------	---	----------

At any instant during the conceptual design phase, all available knowledge about the design needs to be systematically integrated, processed and analyzed to generate a consistent design parameter set. Systematic computer support is therefore a useful tool in airship design to process analytical equations representing different aspects of partial design models. A constraint management approach is well suited for such a task, because the constraints in form of analytical equations may be gradually added, deleted or modified throughout the conceptual design phase.

A graph theoretical approach is implemented to put the conceptual design equations automatically into a solution order and to identify the couplings between the partial design models. This automatic (re-)configuration of design equations adds new flexibility to the conceptual design phase. The key graph algorithms of the approach are demonstrated first using a system of simple equations. The approach is applied secondly to a typical conceptual airship design problem by exchanging different partial conceptual airship design models. Several limitations and advantages of the approach are also identified.

1999	Joseph J. Totah Dr. David J. Kinney John T. Kaneshige Shane Agabon	An Integrated Vehicle Modeling Environment	Ref. 129
------	---	---	----------

This paper describes an Integrated Vehicle Modeling Environment for estimating aircraft geometric, inertial, and aerodynamic characteristics, and for interfacing with a high fidelity, workstation based flight simulation architecture. The goals in developing this environment are to aid in the design of next generation intelligent flight control technologies, conduct research in advanced vehicle interface concepts for autonomous and semi-autonomous applications, and provide a value-added capability to the conceptual design and aircraft synthesis process. Results are presented for three aircraft by comparing estimates generated by the Integrated Vehicle Modeling Environment with known characteristics of each vehicle under consideration. The three aircraft are a mid-sized, twin-engine commercial transport concept, a modified F-15 with moveable canards attached to the airframe, and a small, single-engine, uninhabited aerial vehicle. Estimated physical properties and dynamic characteristics are correlated with those known for each aircraft over a large portion of the flight envelope of interest. The results show significant improvement in estimating vehicle aerodynamic characteristics using an improved vortex lattice code, and represent the completion of a critical step toward meeting the stated goals for developing this modeling environment.

1999	Mark A. Hale Dimitri N. Mavris Dennis L. Carter	The Implementation of a Conceptual Aerospace Systems Design and Analysis Toolkit	Ref. 130
------	---	--	----------

The Conceptual Aerospace Systems Design and Analysis Toolkit (CASDAT) provides a baseline assessment capability for the Air Force Research Laboratory. The historical development of CASDAT is of benefit to the design research community because considerable effort was expended in the classification of the analysis tools. Its implementation proves to also be of importance because of the definition of assessment use cases. As a result, CASDAT is compatible with accepted analysis

2000	J.L. Walsh	Multidisciplinary High-Fidelity Analysis and	Ref. 132
	J.C. Townsend	Optimization of Aerospace Vehicles, Part I:	
	A.O. Salas	Formulation	
	J.A. Samareh		
	V. Mukhopadhyay		
	J.F. Barthelemy		

An objective of the High Performance Computing and Communication Program at the NASA Langley Research Center is to demonstrate multidisciplinary shape and sizing optimization of a complete aerospace vehicle configuration by using high-fidelity, finite element structural analysis and computational fluid dynamics aerodynamic analysis in a distributed, heterogeneous computing environment that includes high performance parallel computing. A software system has been designed and implemented to integrate a set of existing discipline analysis codes, some of them computationally intensive, into a distributed computational environment for the design of a high speed civil transport configuration. The paper describes the engineering aspects of formulating the optimization by integrating these analysis codes and associated interface codes into the system. The discipline codes are integrated by using the Java programming language and a Common Object Request Broker Architecture (CORBA) compliant software product. A companion paper presents currently available results.

2000	J.F. Gundlach IV P.A. Tétrault F. Gern A. Nagshineh-Pour A. Ko J.A. Schetz W.H. Mason R. Kapania B. Grossman R.T. Haftka	Multidisciplinary Design Optimization of a Strut-Braced Wing	Ref. 133
------	---	---	----------

Recent transonic airliner designs have generally converged upon a common cantilever low-wing configuration. It is unlikely that further large strides in performance are possible without a significant departure from the present design paradigm. One such alternative configuration is the strut-braced wing, which uses a strut for wing bending load alleviation, allowing increased aspect ratio and reduced wing thickness to increase the lift to drag ratio. The thinner wing has less transonic wave drag, permitting the wing to unsweep for increased areas of natural laminar flow and further structural weight savings. High aerodynamic efficiency translates into smaller, quieter, less expensive engines with lower noise pollution. A Multidisciplinary Design Optimization (MDO) approach is essential to understand the full potential of this synergistic configuration due to the strong interdependency of structures, aerodynamics and propulsion. NASA defined a need for a 325-passenger transport capable of flying 7500 nautical miles at Mach 0.85 for a 2010 service entry date. Lockheed Martin Aeronautical Systems (LMAS), as Virginia Tech's industry partner, placed great emphasis on realistic constraints, projected technology levels, manufacturing and certification issues. Numerous design challenges specific to the strut-braced wing became apparent through the interactions with LMAS.

2000	Jérôme Lépine Jean-Yves Trépanier Francois Pépin	Wing Aerodynamic Design Using an Optimized NURBS Geometrical Representation	Ref. 134
------	--	---	----------

The success of an aerodynamic wing design process is highly influenced by the wing geometric representation and parameterization. In practice, the geometric representation and parameterization used has a direct impact on the number of design variables and on the smoothness of the profile. The goal of the present paper is to investigate the performance of an optimized non-uniform rational B-spline (NURBS) geometrical representation for wing aerodynamic design. The NURBS representation significantly reduces the number of design variables needed to define a wing profile geometry and at the same time ensures good smoothness properties. This methodology results in a faster design process compared with common geometric representations. Examples of aerodynamic optimization for two and three dimensional cases are given, illustrating the efficiency of this method for wing design.

2000	Max Blair Alicia Hartong	Multidisciplinary Design Tools for Affordability	Ref. 135
------	-----------------------------	---	----------

A proven general purpose design modeling environment has been adapted to address affordability issues at the design synthesis level with the integration of Geometric Modeling and Activity-Based Cost Modeling.

Two factors make this work innovative. First, we are using an advanced design modeling environment with dependency tracking, demand-driven calculations and run-time object creation. Secondly, we explore ways this computer software innovation can be used to tightly integrate geometric modeling with activity-based cost modeling.

The example focuses on the synthesis of a hot structures solution for a high speed lifting surface.

2000	Axel Schumacher Roland Hierold	Parameterized CAD-Models for Multidisciplinary Optimization Processes	Ref. 136
------	-----------------------------------	--	----------

This paper describes the use of parameterized CAD-models for the shape optimization in the multidisciplinary design process. The idea is the implementation of an efficient CAD-system and an efficient finite-element-pre-processor in the shape optimization loop. The optimization system coordinates the different programs and selects applicable finite-element-codes (e.g. different codes for static analysis and crash). The number of the geometric parameters of a CAD-model is very high, so that the definition of key parameters as design variables is necessary. The application examples are primarily automotive parts.

2000	Ruben E. Perez Joon Chung Kamran Behdinan	Aircraft Conceptual Design using Genetic Algorithms	Ref. 137
------	---	--	----------

Aircraft design is a complex multidisciplinary process to determine aircraft configuration variables that satisfy a set of mission requirements. It is very hard for aircraft designers to foresee the consequences of changing certain variables. Furthermore, conventional optimization processes are limited by the type and number of parameters used, resulting in sub-optimal designs. The objective of this research is to test the functionality and implementation of a multidisciplinary aircraft conceptual design optimization method using an adaptive genetic algorithm (GA), as a feasible alternative to the existing sizing and optimization methods. To illustrate the approach the algorithm is used to optimize a medium range commercial aircraft, with takeoff weight as an optimization goal, subjected to constraints in performance and geometric parameters. Adaptive and traditional formulations for the handling of constraints by the GA are tested and compared. Results show the ability of the adaptive GA to unbiased search through the design space of aircraft conceptual designs, leading to more viable aircraft configurations than the traditional GA approach at reduced timeframes, with a lower cost than current aircraft design optimization procedures.

2001 Daniel P. Raymer Vehicle Scaling Laws for Multidisciplinary Ref. 138
Optimization (Preliminary Report)

This paper reports on progress towards definition of a set of vehicle scaling laws suitable for use in multidisciplinary design optimization (MDO) programs intended for use in aircraft conceptual and preliminary design. These are intended to provide factors and methodologies for adjusting the analysis inputs as a baseline aircraft design is parametrically changed during optimization. To the greatest extent possible, “real world” effects are being considered. This research is also attempting to define selection criteria and suitable candidates for design variables, constraints, and measures of merit.

This research is a company-funded initiative of Conceptual Research Corporation and is being done in cooperation with the Swedish Royal Institute of Technology (KTH). Results of this effort are being applied to the RDS-Professional aircraft design software and should be suitable for use by MDO researchers and code developers in the field of aircraft conceptual design optimization.

2001 Ruben E. Perez Advanced Business Jet Conceptual Ref. 139
Kamran Behdinan Design and Cost Optimization Using a
Genetic Algorithm Approach

The present challenge of the business and regional aircraft markets is to obtain a high-performance aircraft with a premium on passenger comfort at a very low price. With the maturity of the high subsonic aircraft markets, a significant increase in performance efficiency had been obtained, but the main challenge still lies in the tradeoffs between the possible obtained performance and aircrafts cost. This research discusses the application of a Genetic Algorithm (GA) in conceptual design and optimization to obtain the optimum external configuration for a long range, eight passenger business aircraft to meet the above objectives. Operating Cost of the aircraft is considered as the objective function to be minimized, and constraints are imposed in performance and geometric parameters based on the given aircraft requirements. Continuous and discrete aircraft variables are defined within the GA

including items that are not precisely known until well into the design process such as structural components, avionics, systems, equipment, landing gear, routing, and access provisions. Therefore, NDV can be used to assure that a design layout has a credible geometry such that the design, when finalized, will contain all required components without requiring excessively tight packaging, which can lead to fabrication and maintenance difficulties. Furthermore, NDV assessment can be used as a constraint in MDO optimization to help improve the design realism of the resulting optimized configuration.

This effort is part of an ongoing project to define a set of vehicle scaling laws suitable for use in multidisciplinary design optimization (MDO) programs intended for use in aircraft conceptual and preliminary design. This research is a company-funded initiative of Conceptual Research Corporation and is being done in cooperation with the Swedish Royal Institute of Technology (KTH). Results of this effort are being applied to the RDS-Professional aircraft design software and should be suitable for use by MDO researchers and code developers in the field of aircraft conceptual design optimization.

2001	William A. Crossley Eric T. Martin David W. Fanjoy	A Multi-objective Investigation of 50-Seat Commuter Aircraft Using a Genetic Algorithm	Ref. 142
------	--	--	----------

Aircraft conceptual design is a complex, multidisciplinary process. Often many decisions about the aircraft concept are made early on based on qualitative information subject to an engineer's experience and personal preferences. A genetic algorithm (GA) seeks to reduce the number of qualitative decisions required and increase the number of design variables that can be considered. Genetic algorithms are search methods based on the patterns of natural selection seen in biological populations. Because the GA is not a calculus based method, continuous, discrete, and integer design variables can be easily in a single run of the code. This feature allows the GA to combine concept selection with aircraft sizing. Multi-objective genetic algorithms can generate a large number of designs that approximate the

Pareto-optimal set in a single run of the code. A multi-objective GA is applied to a 50-seat commuter aircraft design problem.

2002 Richard M. Wood Discussion of Knowledge-Based Design Ref. 143
Steven X.S. Bauer

A discussion of knowledge and knowledge-based design, as related to the design of aircraft, is presented. A review of several knowledge-based design activities conducted at NASA Langley Research Center is provided, and a framework for a knowledge-based design capability is proposed and reviewed. The use of information technology to improve the efficiency and effectiveness of aerodynamic and multidisciplinary design, evaluation, and analysis of aircraft through the coupling of these technologies and knowledge-based design is reviewed. The final section of the paper discusses future directions for design and the role of knowledge-based design.

2002 F. Schieck A Flexible, Open-Structured Computer Ref. 144
N. Deligiannidis Based Approach for Aircraft Conceptual
T. Gottmann Design Optimisation

In the early design stages of a new aircraft, there is a strong need to broaden the knowledge base about the evolving aircraft project, allowing a profound analysis of the presented solutions and of the design driving requirements. With the presented methodology, a tool is provided to help increase and improve that needed information. The developed program system is open-structured, allowing the design engineer maximum flexibility in a first step-by-step analysis, before switching to the automated scaling and optimization modes. By exchanging few particular modules of the entire program system, the tool is applicable to a broad scale of different aircraft types. In an extended requirement model, performance requirements are represented along with other operational requirements. An aircraft model is introduced in sufficient detail for conceptual design considerations. The step-by-step analysis functions are presented. The computer-aided scaling methodology is explained, which, controlled by an optimization module, automatically resizes the aircraft model

until it satisfies the requirements in an optimum solution regarding a selectable figure of merit. Typical results obtained at the end of the scaling are discussed together with knowledge gained along the process, and an example is given.

2002	T.L. Benyo	Project Integration Architecture (PIA) and Computational Analysis Programming Interface (CAPRI) for Accessing Geometry Data from CAD Files	Ref. 145
------	------------	---	----------

Integration of a supersonic inlet simulation with a computer aided design (CAD) system is demonstrated. The integration is performed using the Project Integration Architecture (PIA). PIA provides a common environment for wrapping many types of applications. Accessing geometry data from CAD files is accomplished by incorporating appropriate function calls from the Computational Analysis Programming Interface (CAPRI). CAPRI is a CAD vendor neutral programming interface that aids in acquiring geometry data directly from CAD files. The benefits of wrapping a supersonic inlet simulation into PIA using CAPRI are; direct access of geometry data, accurate capture of geometry data, automatic conversion of data units, CAD vendor neutral operation, and on-line interactive history capture. This paper describes the PIA and the CAPRI wrapper, and details the supersonic inlet simulation demonstration.

2002	Jeffrey V. Zweber Hanee Kabis William W. Follett Narayan Ramabadran	Towards an Integrated Modeling Environment for Hypersonic Vehicle Design and Synthesis	Ref. 59
------	--	--	---------

The US Air Force Research Laboratory, along with its contractor partners, is developing an integrated modeling environment for the conceptual and preliminary-level design and synthesis of airbreathing, hypersonic vehicles. This effort is built on the team's successful prototype of a similar environment for rocket-powered space access vehicles. The modeling environment under development will begin by

developing a 3-4 level deep hierarchy of objects that represent a hypersonic vehicle. Initially, these objects will contain only conceptual-level representations of the geometry and mass properties of the vehicle and its components. This initial information will be used with a vehicle synthesis routine to develop an initial conceptual design. This is typically called the “as drawn” design. The second step in the design process is an initial analysis of the aerodynamic and propulsive characteristics of the vehicle. These analyses will be conducted in the environment and the geometric model that was developed in the initial hierarchy of objects will be of sufficient fidelity to support these analyses. Next, the mass properties, aerodynamic and propulsion analysis results will be used by a trajectory simulation code, also integrated into the environment, to determine if the initial vehicle design will meet the mission performance requirements. Finally, the results of the trajectory simulation will be used to iteratively resize the vehicle until the mission requirements are satisfied. The above process depicts what is known as the closure process, that is, matching the required vehicle propellant fraction for a given mission to the available vehicle propellant fraction. The purpose of the integrated modeling environment is to streamline this closure process. Additionally, this paper describes the modeling environment used for this effort, lessons learned from the development of the environment for rocket-powered vehicles, and the next steps planned to expand the capabilities of the integrated modeling environment.

2002	W.J. Vankan	A Spinware Based Computational Design	Ref. 146
	M. Laban	Engine for Integrated Multi-Disciplinary	
		Aircraft Design	

This paper deals with the software architecture and the global functionality of the Computational Design Engine (CDE) that is developed in the MOB project. This CDE comprises a multidisciplinary set of tools for design, analysis and optimization of blended wing body aircraft. Automatic design evaluation processes, involving complex sequences of analysis computations and data exchange, are available to the user. To guide the user through the complex structure of software tools and data, a user oriented framework, based on the SPINeware middleware system, has been built on top of the functional level implementation of the CDE.

2002	G. La Rocca L. Krakera M.J.L. van Tooren	Development of an ICAD Generative Model for Blended Body Aircraft Design	Ref. 147
------	--	---	----------

Aim of the EC sponsored project ‘Multidisciplinary Design and Optimization of Blended Wing-Bodies’ is the development and application of a fully integrated Computer Design Engine (CDE). TU Delft contributed to the project with the development of a Blended Wing-Body Multi-Model Generator, which is able to supply geometries and data to the analysis software, either commercial of the shelf (COTS) or tailor made, used by the various disciplinary groups in the project team (aerodynamics, structures, stability and control etc.). A full parametric definition of the aircraft has been implemented in the KTI ICAD environment. The ICAD Multi-Model Generator (or Generative Model) holds the ‘knowledge’ of the Blended Wing Body aircraft, such that consistent models can be generated, at different levels of fidelity, suitable for the various disciplines involved in the CDE. A large range of aircraft variants can be generated, just editing the values of the aircraft parameters, which are all collected in one single input file. The optimizer can change the parameters value within the optimization loop, without the need for user interactive sessions. The generative model can be run in batch mode, even from remote sites.

2002	Risheng Lin Abdollah A. Afjeh	An Extensible, Interchangeable and Sharable Database Model for Improving Multidisciplinary Aircraft Design	Ref. 148
------	----------------------------------	--	----------

Advances in computer capacity and speed together with increasing demands on efficiency of aircraft design process have intensified the use of simulation-based analysis tools to explore design alternatives both at the component and system levels. High fidelity engineering simulation, typically needed for aircraft design, will require extensive computational resources and database support for the purposes of design optimization as many disciplines are necessarily involved. Even relatively simplified models require exchange of large amounts of data among various disciplinary analyses. Crucial to an efficient aircraft simulation-based design therefore is a robust data modeling methodology for both recording the information and providing data

transfer readily and reliably. To meet this goal, data modeling issues involved in the aircraft multidisciplinary design are first analyzed in this study. Next, an XML-based, extensible data object model for multidisciplinary aircraft design is constructed and implemented. The implementation of the model through aircraft databinding allows the design applications to access and manipulate any disciplinary data with a lightweight and easy-to-use API. In addition, language independent representation of aircraft disciplinary data in the model fosters interoperability amongst heterogeneous systems thereby facilitating data sharing and exchange between various design tools and systems.

2003 J. Brent Staubach Multidisciplinary Design Optimization, Ref. 149
MDO, the Next Frontier of CAD/CAE in the
Design of Aircraft Propulsion Systems

Systematic exploration of the design space has been a hallmark of the aerospace industry since the Wright brothers first designed the Wright Flyer 100 years ago. During the first half century of flight the exploration of the design space was primarily driven by hand drawings, hand calculations, and extensive experimental testing. With the advent of modern digital computers 50 years ago there has been a continuous shift to computer based “virtual” design and testing. Today, it is routine to use 3dimensional numerical physics models to predict the behavior of jet engines that are fully defined with 3-dimensional CAD models. Design engineers can iteratively manipulate the shape and configuration of their products, numerically test them, and move through a “virtual” design space to find improved designs. Computing power has grown to the point where automated navigation through this virtual design space is now possible and becoming practical. Multidisciplinary Design Optimization, MDO, based on Computer Aided Optimization, CAO, is the next frontier of the CAD/CAE revolution. Over the next quarter century MDO will enable the automatic and systematic exploration of full engine systems subject to multiple high fidelity physical phenomena. This paper outlines the promise and challenges of realizing MDO in the design of gas turbine aircraft propulsion systems.

2003 Juan J. Alonso High-Fidelity Aero Structural Design Using Ref. 150
Joaquim R.R.A. Martins a Parametric CAD-Based Model
James J. Reuther
Robert Haimes
Curran A. Crawford

This paper presents two major additions to our high-fidelity aero-structural design environment. Our framework uses high-fidelity descriptions for both the flow around the aircraft (Euler and Navier-Stokes) and for the structural displacements and stresses (a full finite-element model) and relies on a coupled-adjoint sensitivity analysis procedure to enable the simultaneous design of the shape of the aircraft and its underlying structure to satisfy the measure of performance of interest. The first of these additions is a direct interface to a parametric CAD model that we call AEROSURF and that is based on the CAPRI Application Programming Interface (API). This CAD interface is meant to facilitate designs involving complex geometries where multiple surface intersections change as the design proceeds and are complicated to compute. In addition, the surface geometry information provided by this CAD-based parametric solid model is used as the common geometry description from which both the aerodynamic model and the structural representation are derived. The second portion of this work involves the use of the Finite Element Analysis Program (FEAP) for the structural analyses and optimizations. FEAP is a full-purpose finite element solver for structural models which has been adapted to work within our aero-structural framework. In addition, it is meant to represent the state-of-the-art in finite element modeling and it is used in this work to provide realistic aero-structural optimization costs for structural models of sizes typical in aircraft design applications. The capabilities of these two major additions are presented and discussed. The parametric CAD-based geometry engine, AEROSURF, is used in aerodynamic shape optimization and its performance is compared with our standard, in-house, geometry model. The FEAP structural model is used in optimizations using our previous version of AEROSURF (developed in-house) and is shown to provide realistic results with detailed structural models.

2003	Holger Pfaender Daniel DeLaurentis Dimitri N. Mavris	An Object Oriented Approach for Conceptual Design Exploration of UAV- Based System-of Systems	Ref. 151
------	--	---	----------

The exploration of an integrated system of UAVs involves the concurrent design of systems (e.g. vehicles), networks, and operational plan. The complexity of the resulting design space even at the conceptual level can easily become unmanageable and finding preferred regions of the combined design space that are not simply a sub-optimal collection of individually optimized entities is a difficult task. Abstraction of the system, therefore, is required and achieved by using an object oriented approach for modeling the integrated system. Implementing this approach enhances the ability to efficiently search the combined system-of-systems design space. This approach is tested on a UAV-based package delivery architecture, examining tradeoffs between vehicle performance and the network topology for the economic viability of a notional service provider. The object oriented implementation is found to provide superior modeling flexibility compared to previous approaches.

2003	Thomas A. Ozoroski Kyle G. Mas Andrew S. Hahn	A PC-Based Design and Analysis System for Lighter-Than-Air Unmanned Vehicles	Ref. 152
------	---	---	----------

The Airship Design and Analysis Code (ADAC) was developed using Visual Basic and Microsoft Excel. ADAC was specifically designed to assess the feasibility of long endurance LTA vehicles required to perform station keeping missions at altitudes between 52,000 and 72,000 feet. The methods used in ADAC are presented including explanations of some innovative concepts that separate ADAC from previous codes. Examples include a direct calculation of the minimum required solar array area, and a method to account for a super-pressure buoyancy factor. In addition, ADAC allows a design technique which decouples power and endurance which results in smaller vehicles for given mission requirements. ADAC was validated for low altitude vehicles and also was compared to other design concepts previously developed for similar missions. ADAC was used with wind speed profile data to identify an optimal operating altitude near 18.9 km (62,000 ft) for the

Portland, Maine location. Depending on the wind data input, airship volumes between 20,000 and 70,000 m³ were required for 1000 kg payloads using regenerative fuel cells.

2003 Kevin G. Bowcutt A Perspective on Future of Aerospace Ref. 153
Vehicle Design

Hypersonic vehicles are, by necessity, highly integrated flying machines. They are also subject to inherently high uncertainties in both performance and economics. Combined, these characteristics render conventional design practices inadequate for developing hypersonic vehicles. As advanced analysis algorithms enable more sophisticated design tools, and computer speed continues to grow exponentially, systems will be designed in an ever more integrated fashion to wring the most out of robustness, performance and economics. For hypersonic systems in particular, adequate performance and economic viability is unlikely without first developing and using improved, integrated design methods. Hypersonic vehicles are therefore representative of systems requiring an integrated design approach, and will be used to illustrate future trends in design practice. A vision for the future of system design is presented and status is given for some aspects of progress being made toward achieving this vision.

2004 Satwiksai Seshasai Knowledge-Based Approach to Facilitate Ref. 154
Amar Gupta Engineering Design

A knowledge-based approach is presented to facilitate the engineering design process relating to spacecraft. The degree of collaboration across temporal and spatial boundaries plays a major role in determining the aggregate time and cost involved in each instance of spacecraft design. A major aspect of such collaboration is the issue of communications: the ability to capture the detailed needs of every stakeholder in the process, as well as rationale for the major design decisions. The approach described provides a framework for facilitating the decision making process in engineering design, by eliciting and capturing the goals and requirements of every

stakeholder in the design process through utility and expense functions. An interactive system has been designed that incorporates a four-faceted knowledge-based framework of knowledge acquisition, knowledge discovery, knowledge management, and knowledge dissemination. We describe the combination of the multi-attribute interview software tool MIST and Space Systems Policy Architecture and Research Consortium (SSPARCy) paradigms to develop an evolving knowledge repository that enables one to perform crucial applications whose success is today contingent on geographical proximity. The proposed knowledge-based approach can be readily adopted to facilitate other applications that involve sustained collaboration across geographic and corporate boundaries.

2004	Marian Nemec Michael J. Aftosmis Thomas H. Pulliam	CAD-Based Aerodynamic Design of Complex Configurations Using a Cartesian Method	Ref. 155
------	--	---	----------

A modular framework for aerodynamic optimization of complex geometries is developed. By working directly with a parametric CAD system, complex-geometry models are modified and tessellated in an automatic fashion. The use of a component-based Cartesian method significantly reduces the demands on the CAD system, and also provides for robust and efficient flow field analysis. The optimization is controlled using either a genetic or quasi-Newton algorithm. Parallel efficiency of the framework is maintained even when subject to limited CAD resources by dynamically re-allocating the processors of the flow solver. Overall, the resulting framework can explore designs incorporating large shape modifications and changes in topology.

2004	Curran A. Crawford Robert Haimes	Synthesizing an MDO Architecture in CAD	Ref. 156
------	-------------------------------------	---	----------

This paper presents an approach to multidisciplinary design optimization (MDO) that uses computer aided design (CAD) as both a way to integrate computational tools and as a novel way of formulating the optimization problem. CAD typically forms the

final step in a design process, as a repository of the final design and a precursor to manufacturing. The present methodology moves the CAD model instantiation to the beginning of the design process, where it forms the common base for all follow-on analyses and other engineering tasks. The proper methods for constructing the model and software to use the model for analysis are presented. Using this approach, a large reduction in the duplication of effort is achieved, together with the ability to arrive at physical solutions to the design problem incorporating knowledge acquired from previous projects. The use of a single CAD definition greatly enhances MDO tasks by maintaining consistency between models and providing a visualization tool. A validation of this approach is also presented, applied to the design of a wind turbine for power production.

2004	Nicholas Borer Dimitri N. Mavris	Formulation of a Multi-Mission Sizing Methodology for Competing Configurations	Ref. 157
------	-------------------------------------	---	----------

The creation of long design cycle time vehicles such as aircraft often shrouds the true requirements the vehicle will face in its operational life. The requirements that seem to dominate decisions early in the design may be obsolete by the time the vehicle reaches the operational stage. Other, formerly less stringent or less important requirements may come to the forefront and present challenges to a product already near production, resulting in high cost to change or diminished performance. This problem is compounded in the design of multi-mission aircraft, as the attributes of one mission that dominates decisions made today may not in the future. Furthermore, the design team may have several system configurations in mind at the early stages of multi-role vehicle design, and one configuration that appears attractive may ultimately not be in the face of evolving requirements. This paper presents a method that makes use of surrogate, reduced-order models to increase computational efficiency coupled with probabilistic techniques to account for uncertainty in the requirements parameters. This method can ultimately be used to help a design team select a representative set of requirements for the design of multi-mission aircraft. It also provides for assistance in selecting the overall vehicle configuration that can best meet these requirements. This process is partially illustrated on a notional multi-role fighter designed to replace three legacy aircraft.

2004	John J. Doherty Stephen C. McParlin	Generic Process for Air Vehicle Concept Design and Assessment	Ref. 158
------	--	--	----------

In recent years, the UK Ministry of Defence (MOD) has funded development, by QinetiQ and its predecessor organizations, of processes and tools to assess the performance of air vehicles, with the objective of maintaining status as an intelligent customer for a variety of air vehicle types. During this period, Operational Requirements have been evolving, requiring increased flexibility and the capability to produce accurate performance data for novel air vehicle concepts, including those which are not adequately represented by existing semi-empirical methods and databases. In order to explain the assessment process that has been developed, an example manned aircraft application is described. The component parts of the assessment process, and the underlying techniques and technologies are also described. Finally, indications are given of possible future directions.

2004	Greg Mocko Jitesh H. Panchal Marco Gero Fernandez Russell Peak Farrokh Mistree	Towards Reusable Knowledge-Based Idealizations for Rapid Design and Analysis	Ref. 159
------	--	--	----------

Design and analysis are two key aspects of the product development process, which is iterative by nature and requires knowledge from several different domains. For example, designers devise product specifications based on required functions, whereas, analysis experts analyze the behavior of the resulting product using various models to verify that the design meets required functions. Should analysis results indicate unacceptable behavior, the design is sent back to designers for modification, resulting in an often costly, iterative loop between design and analysis that repeats itself throughout the product development process. Significant cost and time savings can be achieved by reducing this iteration between designers and analysts. In this paper, we present a knowledge-based framework for integrating design and analysis activities, aimed at reducing the associated iterations. Specific research issues presented in this paper include developing a knowledge-based repository of analysis

models and a means for extracting appropriate models from the repository. The concept of a design model hyperspace is proposed for storing analysis models in a hierarchical fashion, based on idealization levels. The associations between design and analysis models are captured using flexible associativities between them. The knowledge-based framework is presented in the context of multifunctional design of Linear Cellular Alloys (LCAs).

2004	C. Cerulli	Parametric Modeling of Aircraft Families	Ref. 160
	P.B. Meijer	for Load Calculation Support	
	M.J.L. van Tooren		

In the present work, a knowledge-based parametric Multi Model Generator (MMG) for reproducing a conventional aircraft family is presented. The intent is to introduce the MMG into a dedicated Design and Engineering Engine (DEE) for performing load calculation in the preliminary design phase. For this purpose the MMG has to be capable to supply different models of the same product, i.e. structure, mass and aerodynamic models, to feed a set of analysis tools. The generated models are extracted from a Knowledge Based Engineering (KBE) product tree, which is capable to hold the knowledge of the complete aircraft product. The definition of the aircraft is fully parametric, so that consistent models for the different disciplines can be generated for a large variety of aircraft configurations by variation of a single input file. The present work is mainly focused on the description of the structural model extracted from the MMG. The aircraft is modeled as an assembly of components, which in turn are built up as an assembly of so-called High-Level Primitives. The wing trunk primitive, presented in previous works, is used for reproducing all the lifting components; the fuselage trunk is presented as a new primitive used to reproduce the fuselage and engine nacelles. A flow diagram for the complete DEE is presented to show the position of the MMG in the load calculation process.

2004	Zhijie Lu Eun-Suk Yang Daniel A. DeLaurentis Dimitri N. Mavris	Formulation and Test of an Object- Oriented Approach to Aircraft Sizing	Ref. 161
------	---	--	----------

Although aircraft sizing is a critical element in the conceptual and preliminary design phases, state-of-practice aircraft sizing computer programs seldom provide the flexibility needed to size revolutionary concept vehicles and to perform variable fidelity disciplinary analysis. Revolutionary concepts are future air vehicles that look, behave, and operate fundamentally differently than those in current and past experience. In order to address this problem and extend the state-of-the-art, this paper presents a new, object-oriented aircraft sizing framework. The framework builds upon recent developments mainly in the areas of multidisciplinary analysis and object-oriented programming. Domain and analysis scalabilities are achieved in this framework by modeling the building blocks of an aircraft sizing environment (e.g. mission profile and contributing disciplinary analysis tools) as objects. Further, sizing algorithms for particular revolutionary concepts being developed can be easily integrated with the proposed approach. Example applications utilizing this new sizing framework are provided in this paper for validation and test purposes.

2004	Ted A. Manning Peter J. Cage Jennie M. Nguyen Robert Haimes	ComGeom2: A Geometry Tool for Multidisciplinary Analysis and Data Sharing	Ref. 162
------	--	---	----------

ComGeom2, a new geometry tool for multidisciplinary data analysis and data sharing, was developed. Serving common computational geometry, including boundary regions, ComGeom2 helps ensure greater geometric consistency during the analysis of complex systems, such as aerospace vehicles. ComGeom2 implements a combination of technologies that together enhance the management of parametric geometry: ComGeom2 automates geometry through CAPRI, a programming interface for controlling CAD geometry; it makes use of an extensible component template library, permitting one to model systems of unlimited variety; and it employs the

Launch Vehicle Language (LVL), a subsystem database that simplifies and standardizes system configuration and parameter specification. ComGeom2's end product is an accurate, watertight surface discretization of the overall geometry for use in computational analysis. The surface mesh contains, in each element, boundary region and component labels for use in boundary condition tagging. ComGeom2 is presented in the context of launch vehicle systems.

2004	Nicolas Antoine Ilan Kroo Karen Willcox Garret Barter	A Framework for Aircraft Conceptual Design and Environmental Performance Studies	Ref. 163
------	--	--	----------

Although aircraft environmental impact has been a concern since the beginning of commercial aviation, continuous growth in passenger traffic and increasing public awareness make aircraft noise and emissions critical considerations in the design of future aircraft. This research explores the feasibility of including environmental performance as an optimization objective at the aircraft conceptual design stage, allowing a quantitative analysis of the trade-offs between environmental performance and operating cost. A program for aircraft design and optimization was developed, using a multi-objective genetic algorithm to determine optimal aircraft configurations and to estimate the sensitivities between the conflicting objectives of low noise, low emissions, and operating costs. The design tool is based on a new application integration framework incorporating a detailed noise prediction code, engine simulator, and aircraft analysis and optimization modules. This paper describes the framework and design approach, including initial results that illustrate environmental performance trades and explore the feasibility of very low-noise and low-emissions designs that could dramatically decrease the environmental impact of commercial aviation.

2004	Hu Liu Gang Lin Wang Xin Lai Lu Zhe Wu	Preliminary Investigation of Integrated Multidisciplinary Optimization in Aircraft Conceptual Design	Ref. 164
------	---	--	----------

In aircraft conceptual design, optimizing initial concepts is a vital task and can be well enhanced through proper application of MDO. Integrated MDO presented in this paper aims at exploiting the advantages of integrating three kinds of software tools: specific design systems that can generate initial concepts conveniently, frameworks supporting MDO that supply abundant design exploration techniques, third-party numerical codes that compensate deficiency of empirical methods for discipline analyses. Based on a design system developed by the authors, basic measures for integrating involved tools were proposed and implemented. The preliminary investigation also concerned strategies for improving the efficiency of optimization and the way of avoiding mutual interference between components during optimization. To exemplify the usage of integrated MDO and validate the effectiveness of proposed methods, an imaginary fighter aircraft was optimized with three different optimization tasks, and the final optimum was determined through further analyses of the results.

2004	Atherton Carty Clifton Davies	Fusion of Aircraft Synthesis and Computer Aided Design	Ref. 165
------	----------------------------------	---	----------

For the benefits of an integrated MDA environment to have a tangible effect on real world aircraft design, a robust integration of those tools used to conduct analysis and those used to develop a design from a geometric standpoint is required. Each must draw upon the strengths of the other in order to mitigate its own weaknesses and fortify the system as a whole. If the fusion of these technologies does not occur, the potential gains of a true MDD environment will likely go unrealized, not because these gains are unattainable, but because analysis does not fully participate the design cycle. Integration of these processes presents the opportunity to strike a balance between the world of MDA and MDD, thus enabling true MDO.

2004	Ruben E. Perez Hugh H.T. Liu Kamran Behdinan	Evaluation of Multidisciplinary Optimization Approaches for Aircraft Conceptual Design	Ref. 166
------	--	---	----------

This paper presents the evaluation of different MDO architectures using an extended set of metrics, which take into consideration optimization and formulation structure characteristics. Demonstrative comparisons are made for analytic and supersonic business jet conceptual design examples. Results show the promising features of the proposed evaluation metrics to define a standardized guideline when dealing with multidisciplinary optimization formulations which can be applied to aircraft conceptual design problems.

2004	Xinyu Zhang Arvid Myklebust Paul Gelhausen	A Geometric Modeler for the Conceptual Design of Ducted Fan UAVs	Ref. 167
------	--	---	----------

A rapid, parametric, geometric modeler, PAGE (Parametric Aircraft Geometry Engine), has been developed for the conceptual design of ducted fan vertical takeoff and landing, unmanned air vehicles (VTOL UAV). The motivation for developing this modeler is the demand for a convenient and rapid tool for the geometric definition of UAV airframes. Conceptual/preliminary design multidisciplinary optimization codes require parametric geometric models that are less detailed than those produced by traditional CAD systems. Traditional CAD systems are time consuming and not suitable in the conceptual/preliminary design stage. Software is available which provides parametric, geometric modeling for the conceptual design of fixed-wing aircraft. This tool builds on lessons from the fixed-wing tools in that it has increased flexibility required for the development of VTOL UAV concepts incorporating ducted fans. This paper describes the design and usage of the software.

2004	Risheng Lin Abdollah A. Afjeh	An XML-Based Integrated Database Model for Multidisciplinary Aircraft Design	Ref. 168
------	----------------------------------	---	----------

Advances in computer capacity and speed, together with increasing demands on efficiency of aircraft design process, have intensified the use of simulation-based analysis tools to explore design alternatives both at the component and system levels. High fidelity engineering simulations, typically needed for aircraft design, will require extensive computational resources and database support for the purpose of design optimization, as many disciplines are necessarily involved. Even relatively simplified models require exchange of large amounts of data among various disciplinary analyses. Crucial to an efficient aircraft simulation-based design, therefore, is a robust data modeling methodology for both recording the information and exchanging data efficiently and reliably. To meet this goal, data modeling issues involved in the aircraft multidisciplinary design are first examined in this study. Development and implementation of an XML-based, extensible data object model suitable for multidisciplinary aircraft design is then discussed. The model, which incorporates aircraft databinding and aircraft persistence engine, allows the design applications to access, manipulate and manage any disciplinary data with a lightweight and easy-to-use API. In addition, language independent representation of aircraft disciplinary data in the model fosters interoperability amongst heterogeneous systems, thereby facilitating data sharing and exchanging between various design tools and systems.

2005	Daniel M. Fudge David W. Zingg Robert Haimes	A CAD-Free and a CAD-Based Geometry Control System for Aerodynamic Shape Optimization	Ref. 169
------	--	---	----------

The performance of an aerodynamic shape optimization routine is greatly dependent on its geometry control system. This system must accurately parameterize the initial geometry and generate a flexible set of design variables for the optimization cycle. It must also generate new instances of the geometry based on the changes to the design variables dictated by the optimization routine. In response to changes in the geometry, it is also desirable to generate a new surface grid with the same topology as

the original grid. This new surface grid can be used to perturb the associated volume grid. This paper presents two geometry control systems, a CAD-free system, and a CATIA V5 CAD-based system. The two systems provide practical tools for aerodynamic optimization. They also provide a basis for comparing CAD-free and CAD-based systems and understanding additional issues that need to be addressed in order to develop reliable optimization systems.

2005	M.J.L. van Tooren	Aircraft Design Support Using Knowledge	Ref. 170
	M. Nawijn	Engineering and Optimisation Techniques	
	J.P.T.J. Berends		
	E.J. Schut		

Multi-disciplinary optimization of aircraft is normally restricted to a solution domain defined by a selection of design variables. Optimization theory however makes a distinction between design variables and design parameters. For aircraft design problems, variables specify limited differences within an aircraft configuration while parameters relate to complex variations within a configuration and inter-type differences, i.e. differences in configuration. During an optimization, parameters are normally fixed and the optimization is limited to finding a combination of values for the design variables that will minimize or maximize an objective function like weight or range. The mathematics required to optimize at a higher level and support the choice between different concepts are not available nor are product models that allow variation between configurations during the optimization process. In this paper the latter problem is addressed and the use of Knowledge Engineering for parametric modeling of aircraft is discussed. It will be shown that a proper combination of object oriented programming, rule based instantiation of objects and a geometry engine allows parametric modeling in the optimization sense. The principle and implementation of High Level Primitives (HLPs), i.e. functional building blocks, in a so-called Multi-Model Generator (MMG) is shown to be a proper approach to the problem of parametric modeling of complex products. It will also be shown how these parametric models can be used and initialized in so-called Design and Engineering Engines (DEEs). A DEE facilitates initiation of design parameters and variables, instantiates HLPs and creates Multiple Models to support the required

multi-disciplinary view on the system as required in multi-disciplinary analysis and optimization. The DEE offers a framework for design decisions in the conceptual design phase. An example of a DEE implementation is shown. The Initiator component of the DEE estimates the starting values for parameters and variables and is an optimizer by itself. An example is given for the initiator component in a sample DEE for composite aircraft tails.

2005	B. Greschner	Knowledge Based Airfoil Aerodynamic and	Ref. 171
	C. Yu	Aero-acoustic Design	
	S. Zheng		
	M. Zhuang		
	Z.J. Wang		
	F. Thiele		

A systematic investigation of the unsteady flows around a series of NACA airfoils is carried out. The main objective is to conduct manual design case studies on the connections between an airfoil shape characteristics and its aerodynamic and aero-acoustic performance. The approach employs the unsteady CFD flow simulations in the near field of an airfoil and the FW-H integral method for the far field noise prediction. The work focuses on analyzing the aerodynamic and aero-acoustic performance of an airfoil and examining the sensitivities of the objective functions to various weighting factors. The results include identifying the optimum symmetric and asymmetric airfoils among the airfoils and suggesting the possible optimum airfoil characteristics. The results can be used to guide the selections of the geometric parameters and constraints in a fully automated aerodynamic and aero-acoustic optimization.

2005	Daniel J. Neufeld Joon Chung	Unmanned Aerial Vehicle Conceptual Design Using a Genetic Algorithm and Data Mining	Ref. 172
------	---------------------------------	---	----------

Aircraft design is a complex process involving multiple co-dependent design variables and many design decisions. For commercial aircraft design, this difficulty is offset somewhat by the wealth of knowledge available. Observing existing designs has provided useful empirical relationships and insights for the designer to apply yielding a relatively well defined problem. The wide variety of configuration possibilities, mission profiles, and the relative lack of historical data leave the problem of unmanned aerial vehicle (UAV) design less defined. The purpose of this research was to develop a robust optimization package for UAV design using data mining to aid configuration decisions and to develop empirical relationships applicable to a wide variety of mission profiles. An optimization software package was developed using a Genetic Algorithm (GA) and Data Mining. The algorithm proved successful in carrying out the preliminary design phase of a number of test cases similar to existing UAVs. Designs produced by the algorithm promise improved performance and reduced development time. Future work will introduce high fidelity analysis to the framework developed in this research.

2005	Adras Sobeter Andy J. Keane James Scanlan Neil W. Bressloff	Conceptual Design of Airframes Using a Generic Geometry Service	Ref. 173
------	--	--	----------

With the increased freedom in layout selection possible when designing an Unmanned Air Vehicle (UAV) concept (compared, for example, to the relatively constrained and mature world of commercial airliner design), comes the significant challenge of building a geometry engine that will provide the variety of airframe models demanded by the highly global nature of the design search. In order to enable multidisciplinary trade-off studies, both an external surface and an internal structure are required –a single, generic model is used to supply these, in the form of a parametric geometry residing in a commercial CAD tool. In addition to discussing

the challenges of offering a truly flexible geometry service, the UAV-specific issues of the initial sizing of the model are discussed. A wealth of statistical data provides one of the traditional handholds for this step in manned aircraft conceptual design – the applicability of such statistical approaches to their unmanned counterparts is discussed.

2006	Bernd Chudoba, Xiao Huang	Development of a Dedicated Aerospace Vehicle Conceptual Design Knowledge- Based System	Ref. 174
------	------------------------------	--	----------

What has to be avoided most is that when knowledge stops evolving, it turns into opinion or dogma. This statement challenges rebuttal which immediately can be counter-acted by asking: How many truly capable aerospace vehicle design knowledge-based systems can be found to take advantage of design data, information, experience, and knowledge of past and present aerospace projects easily available at the fingertips? A major inconsistency can be observed in the ability to design advanced aerospace vehicles with respect to design knowledge required and design knowledge available. Advanced and especially ‘novel’ vehicle design is, as a fact, characterized by permanent lack of knowledge available at the conceptual design stage. As implied by novelty, design knowledge available naturally lags behind design knowledge required. The degree of this discrepancy is a measure for the design risks involved. As a consequence, the ability to perform efficient multi-disciplinary design is quickly becoming a lost skill without persistent knowledge-maintenance. A wide range of technical solutions for a multitude of problems have been assessed and demonstrated in aeronautical history. Unfortunately, much of that knowledge is either ignored for a variety of reasons or it has been simply forgotten. Some of today’s conventional and unconventional flight vehicle design proposals would appear less risky or radical, if an up-to-date vehicle design knowledge-based system would be available to the practicing engineer and project lead. As a result, a striking discrepancy has to be accepted between ‘what can be done’ to ‘what could be done’. This paper outlines the research strategy adopted at the AVD Laboratory towards the development of a dedicated aerospace vehicle conceptual design knowledge-based system (KBS). This apparent ‘white space’ is readily confirmed

having provided a perspective on the original contribution the research makes to aerospace science and engineering. An approach towards the construction of a dedicated conceptual design KBS is presented, placing strong emphasis on a systematic and thorough knowledge utilization process. The researchers are confident that not only is the study distinctive and different from previous research, but that it is worth doing.

2006	M.J.L. van Tooren E.J. Schut J.P.T.J. Berends	Design "Feasilisation" using Knowledge Based Engineering and Optimization Techniques	Ref. 175
------	---	--	----------

The Multi-Disciplinary Design process can be supported by partial automation of analysis and optimization steps. Design and Engineering Engines (DEEs) are a useful concept to structure this automation. Within the DEE a product is parametrically defined using Knowledge Based Engineering. This parametric model needs to be initiated. This is done by simulating the heuristic methods normally used by designers to estimate the first values for the parameters and variables describing their designs. The initiation of values for structural parameters and variables is elaborated for a sample composite panel structure. It is shown that the Initiator part of the DEE concept can be implemented using optimization with schematic models as a mimic of the designers work.

2006	David L. Rodriguez Peter Sturdza	A Rapid Geometry Engine for Preliminary Aircraft Design	Ref. 176
------	-------------------------------------	--	----------

A rapid geometry engine (RAGE) has been developed to allow for preliminary design analysis without labor-intensive CAD support. The geometry tool builds complex aircraft configurations using a component-based approach. Basic algorithms for creating the primary components are presented and discussed. Examples of many widely varying geometry models are shown. A select geometry model is analyzed with several aerodynamic analysis methods ranging in fidelity to further demonstrate

the versatility of the geometry tool. Example uses of the tool in optimization problems are also presented. Future plans for the geometry engine are also discussed.

2006	Mathias Wintzer Peter Sturdza Ilan Kroo	Conceptual Design of Conventional and Oblique Wing Configurations for Small Supersonic Aircraft	Ref. 177
------	---	---	----------

A design process that included high and low fidelity modeling integrated through Kriging-based fits of the high fidelity results was developed and demonstrated on conventional and oblique wing designs. Additional design variables are required when higher fidelity models are introduced, and rather than suboptimize the design (for example using additional design variables to minimize drag), the Kriging models allowed the additional degrees of freedom to be included in the fully integrated model at acceptable cost. Although the basic conceptual design method was not designed to accommodate oblique wings, the use of response surface models allowed such designs to be included with little modification of the design code. The method generated reasonable conventional designs, although at Mach 1.6, the range and field length constraints are critical and the field length chosen here is arguably acceptable. The oblique wing designs show little advantage in cruise performance at this design speed, but the low speed performance is exceptional and leads to an interesting design concept. Relative advantages of the oblique wing increase as field length requirements are tightened and as the required cruise Mach number is reduced.

2006	M. Nawijn M.J.L. van Tooren J.P.T.J. Berends P. Arendsen	Automated Finite Element Analysis in a Knowledge Based Engineering Environment	Ref. 178
------	---	--	----------

Efficient use of finite element based analysis in a knowledge based automated design environment requires the solution of two problems. First, it must be ensured that for every instantiation of a parametric product model, the geometry is segmented (discretized) in such a way that proper element connectivity can be assured. Second,

since changes in product variables (dimensional changes) and changes in product parameters (configuration changes) will lead to changes in the mesh topology, the product attributes (e.g. material and supports) must be linked to the product geometry and not to element meshing. This paper shows that the segmentation process normally carried out by FEM experts manually, can be implemented with Knowledge Based Engineering (KBE). As a result it is guaranteed that the geometry associated to any instantiation of the product model is properly segmented and the connectivity issue is handled in a robust way. This paper shows that the dependency of the FEM model definition on the underlying mesh can be solved by adding information and/or knowledge to the geometric data from the KBE tool. In a traditional CAD based design environment, the knowledge generated in the geometric design stage is inaccessible to the FEM pre-processing process due to the fact that data transfer formats are incapable of capturing this knowledge. It is shown that in a KBE environment information/knowledge stored in the product model can be extracted and made accessible. Finally, it is shown by an elaborate example of a rudder design case that the combination of properly segmented geometry and the knowledge extracted from the product model together with a newly developed, Python based Knowledge Based Engineering Finite Element Analysis tool allows for the flexible incorporation of automated FEM analysis in a multi-disciplinary design environment.

2006 Bernd Chudoba

Managerial Implications of Generic Flight
Vehicle Design Synthesis

Ref. 179

When defining a new product like an aircraft, space access vehicle or space mission, the Advanced Projects Group evaluates the available design space and compares it with the design space required to accomplish the specified mission. As with any product development process, the general life-cycle characteristics are established first during the conceptual design (CD) phase, clearly before a design proposal can be released to the follow-on design phases such as preliminary design (PD), detail design (DD), flight test (FT), and finally operation and disposal. As a rule of thumb, it can be assumed that around 80% of the flight vehicle configuration and mission tandem are determined during the CD phase alone, which is the key phase where the initial brainstorming has to take place. Clearly, it is the responsibility of the CD team to

simulate the entire life-cycle of the project from ‘cradle to grave’ where the focus is on correctness rather accuracy in order to identify the design space and offer an overall proof of design convergence. Currently, the important primary aerospace vehicle and mission design decisions at CD level are still made using extremely simple analysis and heuristics. A reason for this scenario is the difficulty in synthesizing the range of individual design disciplines for both, classical and novel aerospace vehicle conceptual designs, in more than an ad-hoc fashion. Although the CD segment is seen as the most important step in the product development phase due to its pre-defining function, it is the least well understood part of the entire product evolution process due to its level of abstraction. This paper presents the roadmap towards the next generation of aerospace lifecycle synthesis systems, a software and management process capable to immediately calculate cost and time implications while simultaneously linking design, manufacturing, testing, and operation. A historical review of how design has been accomplished until today is presented. The design approaches are categorized and the characteristics of today’s state-of-the-art design synthesis systems are discussed. A specification for the new class of intelligent generic design synthesis systems is presented capable of satisfying the demands imposed by the new breed of high-performance aircraft, space access vehicles, space missions, and others. Finally, the development status of the next generation Aerospace Vehicle Design Synthesis (AVDS-PrADO) simulation-based acquisition environment is presented.

2006	J.P.T.J. Berends M.J.L. van Tooren	An Agent System Co-operating as a Design Build Team in a Multidisciplinary Design Environment	Ref. 180
------	---------------------------------------	---	----------

The Multi-Disciplinary Design and Optimization process of products can be supported by automation of analysis and optimization steps. Design and Engineering Engines (DEEs) are a useful concept to structure this automation. Within the DEE, a product is parametrically defined using Knowledge Based Engineering. The analysis of a particular product instantiation is performed by discipline analysis tools. These analysis tools are owned by Specialists in their design domain and these Specialists combined form a traditional human Design and Build Team (DBT). The discipline

tools themselves can participate as team members in the virtual DBT by the help of agents. These agents are responsible for the agent-agent, agent-tool and agent-actor communications. Tools and Agents, together with human actors form a hybrid DBT which is capable of solving MDO problems. Four functions are identified within the framework knowing resource management, resource interfacing, process execution support and information flow control functions. The framework is verified against a real-world MDO design problem.

2006	Hu Liu Gang Lin Wang Xin Lai Lu Zhe Wu	Case-Based Reasoning for Developing Initial Aircraft Concepts	Ref. 181
------	---	--	----------

To make use of the knowledge and experience embedded in previous aircraft concepts, as well as improve the quality and efficiency of design by using existed information, application of case-based reasoning has been investigated. In this paper, an adapted flow of applying this technique is firstly presented according to the process of conceptual design, and the traditional methods for two tasks in this flow, i.e., case representation and retrieval, have been improved. Considering the complexity of aircraft and dynamic increase of information during conceptual design, a hierarchy model was proposed to represent a concept as aggregation of sources, groups, segments and attributes. Based on this model, a hierarchy nearest-neighbor method and a method called distance criterion for calculating group similarity were proposed to retrieve the “best-matching” case. These methods have been implemented in a design system and an example is presented to validate their effectiveness.

2006	V. Mukhopadhyay	Adaptive Modeling, Engineering Analysis	Ref. 66
	S-Y. Hsu	and Design of Advanced Aerospace	
	B.H. Mason	Vehicles	
	D.W. Sleight		
	H. Kamhawi		
	J.L. Dahl		

This paper describes initial progress towards the development and enhancement of a set of software tools for rapid adaptive modeling, and conceptual design of advanced aerospace vehicle concepts. With demanding structural and aerodynamic performance requirements, these high fidelity geometry based modeling tools are essential for rapid and accurate engineering analysis at the early concept development stage. This adaptive modeling tool was used for generating vehicle parametric geometry, outer mold line and detailed internal structural layout of wing, fuselage, skin, spars, ribs, control surfaces, frames, bulkheads, floors, etc., that facilitated rapid finite element analysis, sizing study and weight optimization. The high quality outer mold line enabled rapid aerodynamic analysis in order to provide reliable design data at critical flight conditions. Example application for structural design of a conventional aircraft and a high altitude long endurance vehicle configuration are presented. This work was performed under the Conceptual Design Shop sub-project within the Efficient Aerodynamic Shape and Integration project, under the former Vehicle Systems Program. The project objective was to design and assess unconventional atmospheric vehicle concepts efficiently and confidently. The implementation may also dramatically facilitate physics-based systems analysis for the NASA Fundamental Aeronautics Mission. In addition to providing technology for design and development of unconventional aircraft, the techniques for generation of accurate geometry and internal sub-structure and the automated interface with the high fidelity analysis codes could also be applied towards the design of vehicles for the NASA Exploration and Space Science Mission projects.

The Aerospace and Defense industry is experiencing an increasing loss of knowledge through workforce reductions associated with business consolidation and retirement of senior personnel. Significant effort is being placed on process definition as part of ISO certification and, more recently, CMMI certification. The process knowledge in these efforts represents the simplest of engineering knowledge and many organizations are trying to get senior engineers to write more significant guidelines, best practices and design manuals.

A new generation of design software, known as Product Lifecycle Management systems, has many mechanisms for capturing and deploying a wider variety of engineering knowledge than simple process definitions. These hold the promise of significant improvements through reuse of prior designs, codification of practices in workflows, and placement of detailed how-tos at the point of application.

TechnoSoft has developed and released an air vehicle design engineering environment in collaboration with AFRL, NASA and major aerospace industries. The Adaptive Modeling Rapid Air Vehicle Engineering (AMRaven) environment is a generative modeling environment enabling the integrated design and analysis of air vehicles. AMRaven is built on the AML object-oriented framework incorporating a custom design environment with a suite of modeling features that support the rapid design and configuration of air vehicles. The generation of detailed analysis models for coupled aerodynamic and structural analysis is fully automated.

Unique to the AMRaven framework is a feature-based design environment that incorporates a set of custom components such as pods, wings, and control surfaces for outer mold line (OML) design and spars, ribs, and bulkheads for substructure layout.

AMRaven integrates design and analysis process automation within a common environment to facilitate the engineering process and the assessment of technology variables and their impact on vehicle performance.

This paper describes the underlying general framework, the AMRaven design environment, aerodynamic and structural analysis capabilities, and a number of other modules.

2006	William A. Anemaat Balaji Kaushik Richard D. Hale Narayanan Ramabadran	A Knowledge-Based Design Framework for Aircraft Conceptual and Preliminary Design	Ref. 61
------	---	---	---------

Experience has shown that process and system level thinking enables significant reductions in design cycle time by avoiding technically correct but irrelevant calculations. Irrelevance often arises when the correct analysis is performed at the wrong stage in the product definition. Current iterative approaches to engineering design require considerable duplication of effort, much of which comes from modeling multiple design abstractions for varied levels and types of analyses. To ensure that appropriate domain knowledge is available at the appropriate time, skills and experience with tools that enable more robust trade studies for increasingly detailed design with inputs from increasingly diverse disciplines are required.

Vehicle-focused efforts have broad appeal for attracting high quality, diverse students and facilitate strategic alignment of teaching and research. Towards this end, industry, government, and academic partners have teamed to develop a knowledge-based engineering framework complete with a generative multidisciplinary modeling and analysis environment supporting air vehicle synthesis called AMRaven. AMRaven supports process design automation and integrates design exploration and optimization across multiple disciplines. The framework facilitates rapid vehicle development integrating feature-based 3D geometric modeling, 3D parametric meshing, analysis (aerodynamics, propulsion, trajectory, weight estimation, etc.), and simulation. This paper discusses specifically how the tool is used for conceptual and

preliminary design and analysis of airplanes, the concepts of which are based on Advanced Aircraft Analysis (AAA) tools. DARcorporation developed this powerful framework to support the iterative and non-unique process of aircraft conceptual and preliminary design.

The system architecture is managed using an object-oriented modeling language called AML (Adaptive Modeling Language), developed and marketed by TechnoSoft, Inc. AML emphasizes the decomposition of engineering problems into classified objects, and strongly supports the most powerful feature of object-oriented modeling – the ability to construct a class hierarchy in which complex classes inherit properties from simpler classes. This is the same mechanism that powers human understanding: the ability to make abstractions and then build upon them to create more complex concepts. AML is a mature, commercially-available architecture containing many of the objects necessary for developing integrated design, analysis, and manufacturing tools. AML automatically builds and manages networks of dependencies between objects, so that when an object changes all dependent objects are automatically updated. AAA allows students and preliminary design engineers to rapidly evolve an aircraft configuration from early weight sizing through open loop and closed loop dynamic stability and sensitivity analysis, while working within regulatory and cost constraints. The program is specifically designed to assist in the design learning process while reserving that individual creative judgment which is essential to the process of airplane design. The University of Kansas is incorporating these emerging tools across the engineering undergraduate curriculum, while enhancing their capabilities and disseminating these enhancements. Student learning will be enhanced to include situated knowledge gained through meaningful connections between courses and experiential learning on common projects supporting the research enterprise.

Appendix E. Description of Functions and Procedures in Dynamic Link Libraries

Dynamic Link Libraries (dll) are used to define most of the methods used in AAA-AML. The functions and procedures are written in Borland Delphi 6 (Ref. 188) a Pascal-based development environment. Functions and procedures developed for the Advanced Aircraft Analysis software (see Chapter 5) are modified so that they can be used in a dll. To turn a function or procedure in a valid dll call the following modifications are necessary:

1. Add stdcall; to the end of the call
2. add the function call to the exports list at the end of the dll file
3. The dll program must start with the word: library.
4. Translate the enumerated data type into integers by using the ordinal value

The following types are used to be compatible with the AML language:

double	double precision, 5.0×10^{-324} .. 1.7×10^{308} , 15-16 significant digits, 8 bytes
integer	signed 32-bit, -2147483648..2147483647
boolean	true or false

The following dll's have been developed:

1. AeroCoef.dll
2. DragCoefficient.dll
3. WeightSizing.dll
4. Atmosphere.dll
5. FuselageDrag.dll
6. WeightII.dll

The following dll's have also been developed but have not been tested in AAA-AML and methods are not described in Chapter 6. The methods have been tested in the third generation AAA:

7. GroundEffect.dll (based on methods in Ref. 6)
8. BetaDot.dll (based on methods in Ref. 6)
9. LatDirStabFigures.dll (based on methods in Ref. 6)
10. Hingement.dll (based on methods in Ref. 6)

In AML the function must first be declared as a foreign function with:

```
define-foreign-function
```

The following function declaration in Delphi is also shown in AML:

Delphi:

```
function FuselageZeroLiftDragSubsonic(  
  ExitAirflow : boolean;  
  H : double;  
  dT : double;  
  Mach : double;  
  S : double;  
  Lf : double;  
  Sbase : double;  
  Sfus : double;  
  SwetFus : double;  
  SwetLam : double;  
  K : double;  
  XtransLf : double;  
  KInstallDrag : double) : double;
```

AML:

```
(define-foreign-function (FuselageZeroLiftDragSubsonic  
  (:name "FuselageZeroLiftDragSubsonic")  
  (:return-type :double)  
  )  
  
  (exit-airflow :int)  
  (h :double)  
  (dT :double)  
  (Mach :double)  
  (S :double)  
  (iF :double)  
  (sBase :double)  
  (SFus :double)  
  (sWetFus :double)  
  (sWetLam :double)  
  (k :double)  
  (xtransLf :double)  
  (kInstalldrag :double)  
  )
```

The following sections describe all functions and procedures with their input and output parameters. It is recommended using these descriptions in conjunction with Refs. 1-11 and 15 and 16.

E.1 AeroCoef.dll

function ChordLength(Cr,Ct,Eta : double) : double;

Description

Calculate chord length for straight tapered wing

Input

Cr.....root chord

Ct.....tip chord

Etaspanwise station [fraction]

Output

ChordLengthlocal chord length

function ThicknessRatio(tcr,tct,Lambda,Eta : double) : double;

Description

Calculate thickness ratio for straight tapered wing at eta

Input

tcrroot chord thickness ratio

tct.....tip chord thickness ratio

Lambdataper ratio

Etaspanwise station [fraction]

Output

ThicknessRatio.....local chord thickness ratio

unit of output [%, fraction] is the same of the units of the Input [%, fraction]

function ThicknessRatioBar(tcr,tct,Lambda: double) : double;

Description

Calculate thickness ratio for straight tapered wing at MGC location

Input

tcrroot chord thickness ratio

tct.....tip chord thickness ratio

Lambdataper ratio

Output

ThicknessRatioBarthickness ratio of a straight tapered wing at MGC location;
unit of output [%, fraction] is the same of the units of the
Input [%, fraction]

function CLAlphaNacelle(wnac,lnac : double) : double;

Description

Nacelle lift curve slope depending on width, wnac and length, lnac

Input

wnacnacelle width

lnacnacelle length

Output

CLAlphaNacellenacelle lift curve slope in 1/rad

**procedure QbarRatio(Xapexw,CR,Cbar,Zcr4w,Xach,Zach,iw,alpha,epsh,
CDow : double; var DelZwake,ZhWake,Eta : double);**

Description

Dynamic pressure ratio calculation based on Roskam Airplane Design Part VI
p. 269-270, Z-coordinates are positive up

Input

XapexwX-location of the wing apex

function DelAlphaEps(Sweep,AR,Lambda : double) : double;

Description

Roskam Airplane Design Part VI Fig.8.41 Effect of Linear Twist on Wing Angle of Attack for Zero Lift

Input

Sweep.....quarter-chord sweep angle [deg]

AR.....aspect ratio

Lambdataper ratio

Output

DelAlphaEps ratio of change in wing zero-lift angle-of-attack to linear twist angle

function AlphaZeroMachRatio(M,Sweep,toverc : double) : double;

Description

Part VI Fig.8.42 Mach Number Correction for Zero-Lift Angle of Attack of Cambered Airfoils. Linear extrapolation for $t/c > 16$

Input

M.....Mach number

Sweep.....quarter-chord sweep angle [deg]

toverc.....thickness ratio [%]

Output

AlphaZeroMachRatioratio of cambered airfoil zero-lift angle-of-attack at a given Mach number to that same variable at Mach 0.3

**function AlphaZero(Mach,alpha0sec,TwistAngle,tc,Sweep,AR,Lambda : double)
: double;**

Description

Roskam Airplane Design Part VI eq.8.21 calculation of zero lift angle of attack of a lifting surface

Input

MachMach number
alpha0sec.....airfoil zero-lift angle-of-attack [deg]
TwistAngle.....twist angle [deg]
tc.....thickness ratio [%]
Sweep.....quarter-chord sweep angle [deg]
AR.....aspect ratio
Lambdataper ratio

Output

AlphaZerolifting surface zero-lift angle-of-attack [deg]

procedure DiederichFactors(F : double; var C1,C2,C3 : double);

Description

Torenbeek Synthesis of Subsonic Airplane Design: calculation of lifting line factors

Input

FDiederich's factor, $2.0 * \pi * AR / (c_{l\alpha} * \cos(Sweep * \pi / 180.0))$

Output

C1first intermediate calculation coefficient for lift distribution
C2.....second intermediate calculation coefficient for lift distribution
C3.....third intermediate calculation coefficient for lift distribution

function fLiftDistribution(Eta,SweepB : double) : double;

Description

Torenbeek Synthesis of Subsonic Airplane Design: Calculation of the lift distribution parameter f

Input

Etanon-dimensional semispan station [fraction]

SweepBeffective quarter-chord sweep angle in compressible flow [deg]

Output

fLiftDistributionDiederich's lift distribution factor

function CaprimeOverC(df,CfOverC : double) : double;

Description

Torenbeek Synthesis of Subsonic Airplane Design Fig G-7 : extended chord definition and typical values. C' for single slotted flap used for the C'_a of a double slotted flap

Input

dfflap deflection [deg]

CfOverCflap chord ratio [fraction]

Output

CaprimeOverCchord increment due to flap to original chord ratio

**function dcl2DPlainFlap(RootTc,TipTc,cla2D0,Lambda,EtaIn,EtaOut,CfC,df :
double) : double;**

Description

Calculation of airfoil lift increase due to plain flap extension for zero angle of attack

Input

RootTc.....root airfoil thickness ratio [fraction]

TipTc.....tip airfoil thickness ratio [fraction]

cla2D0.....airfoil lift curve slope at low Mach number

Lambdataper ratio
EtaIninboard flap station [fraction]
EtaOutoutboard flap station [fraction]
CfCflap chord ratio [fraction]
dfflap deflection [deg]

Output

dcl2DPlainFlapairfoil lift increase due to plain flap deflection

function dcl2DSplitFlap(cia2D0,CfC,Mach,df : double) : double;

Description

Calculation of the airfoil lift increase due to split flap extension for zero angle of attack

Input

cia2D0airfoil lift curve slope at low Mach number
CfCflap chord ratio [fraction]
MachMach number
dfflap deflection [deg]

Output

dcl2DSplitFlapairfoil lift increase due to split flap deflection

function dcl2DSingleSlottedFlap(cia2D0,CfC,Mach,df : double) : double;

Description

Calculation of the airfoil lift increase due to single slotted flap extension for zero angle of attack

Input

cia2D0airfoil lift curve slope at low Mach number
CfCflap chord ratio [fraction]
MachMach number
dfflap deflection [deg]

Output

dcl2DSingleSlottedFlapairfoil lift increase due to single slotted flap deflection

function dcl2DDoubleSlottedFlap(PhiTEUpper,df2,C1C,C2C,CfC,df : double) : double;

Description

Calculation of the airfoil lift increase due to double slotted flap extension for zero angle of attack

Input

PhiTEUpper ...airfoil upper surface trailing edge angle, $\arctan((10(y_{90}-y_{100})/c)$ [deg]
df2aft flap deflection angle relative to the forward flap [deg]
C1Cforward flap chord ratio [fraction]
C2Caft flap chord ratio [fraction]
CfCtotal flap chord ratio [fraction]
dftotal flap deflection [deg]

Output

dcl2DDoubleSlottedFlap.....airfoil lift increase due to double slotted flap deflection

function Alfa0One(claR,claT,Sweep4,AR,S,Lambda,Mach : double) : double;

Description

Torenbeek Synthesis of Subsonic Airplane Design: calculation of alfa_0_1 from (E-16) and (E-17)

Input

claRroot chord airfoil lift curve slope [1/rad]
claTtip chord airfoil lift curve slope [1/rad]
Sweep4half-chord sweep angle [deg]
ARaspect ratio
Slifting surface area
Lambdataper ratio
MachMach number

Output

Alfa0One.....aerodynamic twist factor

**function AlphaZeroSurface(Mach,alpha0R,alpha0T,GeoTwist,clAlphaR,
clAlphaT,tcR,tcT,Sweep4,AR,S,Lambda : double) : double;**

Description

Calculation of zero lift angle of attack of a lifting surface with airfoil variation

Input

MachMach number
alpha0Rroot airfoil zero-lift angle-of-attack
alpha0Ttip airfoil zero-lift angle-of-attack
GeoTwist.....geometric twist angle
clAlphaRroot airfoil lift curve slope
clAlphaTtip airfoil lift curve slope
tcRroot chord thickness ratio [%]
tcTtip chord thickness ratio [%]
Sweep4quarter-chord sweep angle [deg]
ARaspect ratio
Slifting surface area
Lambdataper ratio

Output

AlphaZeroSurfacezero-lift angle-of-attack of a lifting surface [deg]

function FlapSpanKb(EtaInboard,EtaOutboard,Lambda : double) : double;

Description

Roskam Airplane Design Part VI Fig.8.52 Effect of Taper Ratio and Flap Span on K_b

Input

EtaInboard.....inboard flap station [fraction]
EtaOutboardoutboard flap station [fraction]
Lambdataper ratio [fraction]

Output

FlapSpanKb.....flap-span factor

function AlphaDeltaSingleSlotted(df,CfOverC : double) : double;

Description

Roskam Airplane Design Part VI Fig.8.17 Lift Effectiveness of a Single Slotted Flap

Input

dfflap deflection [deg]

CfOverCflap chord ratio [fraction]

Output

AlphaDeltaSingleSlotted.....lift effectiveness of a single slotted flap

function AlphaDeltaTripleSlotted(df,CfOverC : double) : double;

Description

Torenbeek Synthesis of Subsonic Airplane Design Fig.G-7 Triple Slotted Flap

Input

dfflap deflection [deg]

CfOverCflap chord ratio [fraction]

Output

AlphaDeltaTripleSlotted.....lift effectiveness of triple slotted flaps

function EtaIslottedFlaps(Phi,CiOverC : double) : double;

Description

Roskam Airplane Design Part VI Fig 8.20 Lift Effectiveness for Slotted Flaps

Input

Phiflap deflection [deg]

CiOverCflap chord ratio of the ith-segment flap [fraction]

Output

EtaiSlottedFlapsempirical lift efficiency factor of the ith-segment flap of a double slotted flaps

function LiftEffectiveness(CiOverC : double) : double;

Description

Roskam Airplane Design Part VI Fig.8.21 Lift Effectiveness for Trailing Edge Flaps

Input

CiOverCflap chord ratio of the ith-segment flap [fraction]

Output

LiftEffectivenesslift effectiveness of the ith-segment flap of a double slotted flaps

function TripleSlottedEffectiveness(df : double) : double;

Description

Torenbeek Synthesis of Subsonic Airplane Design Fig.G-6 Lift Effectiveness for Triple Slotted Flaps

Input

dfflap deflection [deg]

Output

TripleSlottedEffectivenessflap effectiveness factor

function EtatDoubleSlotted(df1,df2 : double) : double;

Description

Roskam Airplane Design Part VI Fig.8.22 Correction Factor for Aft Flap

Input

df1deflection angle of the forward flap [deg]

df2deflection angle of the aft flap [deg]

Output

EtaDoubleSlottedaft flap correction factor

function AlphaDeltaSplitFlap(df,CfOverC : double) : double;

Description

Roskam Airplane Design Part VI Fig.8.24 Lift Effectiveness of a Split Flap

Input

dfflap deflection [deg]

CfOverCflap chord ratio [fraction]

Output

AlphaDeltaSplitFlaplift effectiveness of a split flap

function CprimeOverC(df,CfOverC : double) : double;

Description

Torenbeek Synthesis of Subsonic Airplane Design: Fig G-7 : The extended chord definition and typical values

Input

dfflap deflection [deg]

CfOverCflap chord ratio [fraction]

Output

CprimeOverCflap-extended to flap-retracted wing chord ratio

function dcl2DTripleSlottedFlap(c_la2D0,C_fC,Mach,df : double) : double;

Description

Calculation of the airfoil lift increase due to triple slotted flap extension for zero angle of attack

Input

c_la2D0airfoil lift curve slope at low Mach number

C_fCflap chord ratio [fraction]

MachMach number

dfflap deflection [deg]

Output

dcl2DTripleSlottedFlap.....airfoil lift increase due to triple slotted flap deflection

function dcl2DFowlerFlap(c_la2D0,C_fC,Mach,df : double) : double;

Description

Calculation of the airfoil lift increase due to fowler flap extension for zero angle of attack

Input

c_la2D0airfoil lift curve slope at low Mach number

C_fCflap chord ratio [fraction]

MachMach number

dfflap deflection [deg]

Output

dcl2DFowlerFlapairfoil lift increase due to fowler flap deflection

**function DeltaCLWingFlapZeroAlpha(CLaw,cla2D0,AR,Lambda,EtaIn,EtaOut,
CfC,Mach,df : double) : double;**

Description

Calculation of the wing lift increase due to flap extension for zero wing angle of attack

Input

CLawclean-wing lift curve slope
cla2D0airfoil lift curve slope at low Mach number
ARaspect ratio
Lambdataper ratio
EtaInflap inboard station [fraction]
EtaOutflap outboard station [fraction]
CfCflap chord ratio [fraction]
MachMach number
dfflap deflection [deg]

Output

DeltaCLWingFlapZeroAlphawing lift increase due to flap deflection

**function CLalphaWingFlap(CLaw,Lambda,EtaIn,EtaOut,CfC,df : double) :
double;**

Description

Calculation of the wing lift curve slope due to flap extension Roskam Airplane Design Part VI eq. 8.28, $CL_{\alpha f} = K \cdot CL_{\alpha}$

Input

CLawclean wing lift curve slope
Lambdataper ratio
EtaInflap inboard station [fraction]
EtaOutflap outboard station [fraction]
CfCflap chord ratio
dfflap deflection [deg]

Output

CLAlphaWingFlap.....wing lift curve slope with flap deflected

function OswaldFactor(AR,Lambda : double) : double;

Description

Calculation of the Oswald span efficiency factor from Fig.3.2 of Roskam :
Methods for Estimating Stability and Control Derivatives of Conventional Subsonic
Airplanes

Input

AR.....aspect ratio

Lambdataper ratio

Output

OswaldFactorOswald's span efficiency factor

function ForceBreakMach(tc,AR,Sweep2 : double) : double;

Description

Datcom Fig 4.1.3.2-53b Transonic Sweep Correction for Force-Break Mach Number

Input

tc.....thickness ratio [%]

AR.....aspect ratio

Sweep2.....half-chord sweep angle [deg]

Output

ForceBreakMach.....force-break Mach number

function CLAlphaRatioForceBreak(tc,AR : double) : double;

Description

Datcom Fig 4.1.3.2-54a Correction to Lift-Curve Slope for Force-Break Mach Number

Input

tc.....thickness ratio [%]

AR.....aspect ratio

Output

CLAlphaRatioForceBreakforce-break to theoretical wing lift curve slope ratio

function aOverCTrans(tc,AR : double) : double;

Description

Datcom Fig. 4.1.3.2-54b Chart for Determining Lift Curve Slope at Ma

Input

tc.....thickness ratio [%]

AR.....aspect ratio

Output

aOverCTransratio of reduction in wing lift curve slope at M_a to wing lift curve slope at force-break Mach number

**function CLAlphaSubs(Mach,AR,cla2D,Sweep4,Lambda,Gap3D : double) :
double;**

Description

Roskam Airplane Design Part VI eq.8.22 Calculation of Subsonic Lift Curve Slope for a Lifting Surface

Input

MachMach number

AR.....aspect ratio
cla2D.....airfoil lift curve slope
Sweep4.....quarter-chord sweep angle [rad]
Lambdataper ratio
Gap3D.....lifting surface gap correction factor

Output
CLAlphaSubssubsonic lifting surface lift curve slope

**function CLAlphaTrans(Mach,AR,cla2D,Sweep4,Lambda,Gap3D,tc : double) :
double;**

Description

Datcom 3.1.3.2 Calculation of Transonic Lift Curve Slope for a Lifting Surface

Input

MachMach number
AR.....aspect ratio
cla2D.....airfoil lift curve slope
Sweep4.....quarter-chord sweep angle [rad]
Lambdataper ratio
Gap3D.....lifting surface gap factor
tc.....thickness ratio [%]

Output

CLAlphaTrans.....transonic lifting surface lift curve slope

**function CLAlphaLiftSurface(Mach,AR,cla2D,Sweep4,Lambda,Gap3D,tc :
double) : double;**

Description

Roskam Airplane Design Part VI eq.8.22 Calculation of Lift Curve Slope for a
Lifting Surface

Input

MachMach number
AR.....aspect ratio

cla2Dairfoil lift curve slope
Sweep4quarter-chord sweep angle [rad]
Lambdataper ratio
Gap3Dlifting surface gap correction factor
tc.....thickness ratio

Output

CLAlphaLiftSurfacelift curve slope of the lifting surface

**function DownWashGradient(A,CLaWM,CLaW0,Sweep,Lambda,hH,IH,b :
double) : double;**

Description

Roskam Airplane Design Part VI eq.845-8.48 Calculation of downwash at the horizontal tail

Input

A.....wing aspect ratio
CLaWMwing lift curve slope
CLaW0.....wing lift curve slope at low Mach number
Sweep.....quarter-chord sweep angle [rad]
Lambdataper ratio
hH.....vertical distance between the wing and horizontal tail
IH.....horizontal distance between mean geometric chord quarter-chord
points of the wing and the horizontal tail
b.....span

Output

DownWashGradient.....downwash gradient at horizontal tail

function UpwashGradient(Xbarac,A : double) : double;

Description

Roskam Airplane Design Part VI Fig.8.67 : Wing Upwash Gradient
Calculation of the upwash at point Xbarac due to the wing

Input

Xbaracdistance forward of root quarter-chord point in root chords

A.....aspect ratio

Output

UpwashGradientupwash gradient in front of wing

function NACCrAftSweep(LESweep,Mach,A,Lambda : double) : double;

Description

Roskam Airplane Design Part VI Fig 8.100 Effect of Aspect Ratio, Sweep Angle and Taper Ratio on Wing Aerodynamic Center. Subsonic; linear extrapolation for $Atan^{LE} < 1$ and $Atan^{LE} > 6$

Input

LESweepleading edge sweep angle [rad]

MachMach number

A.....aspect ratio

Lambdataper ratio

Output

NACCrAftSweepwing aerodynamic center location from wing apex in terms of root chord

function NACCr(LESweep,Mach,A,Lambda : double) : double;

Description

Aerodynamic center as function of root chord

Input

LESweepleading edge sweep angle [rad]

MachMach number

A.....aspect ratio

Lambdataper ratio

Output

NACCraerodynamic center in terms of root chord

**procedure clAlphaSectional(OpclAlphaSectional,OpRootclAlpha,OpTipclAlpha,
OpTaperRatio : TOpCode);**

Description

Calculate sectional clAlpha from root and tip clAlpha

Input

OpclAlphaSectionalvalue of airfoil lift curve slope in database

OpRootclAlphavalue of root airfoil lift curve slope in database

OpTipclAlphavalue of tip airfoil lift curve slope in database

OpTaperRatio.....value of taper ratio in database

Output

clAlphaSectionalairfoil lift curve slope

function K_WB(Diameter,Span : double) : double;

Description

Datcom Fig 4.3.1.2-10 Lift Ratio Slender Body Theory

Input

Diameter.....maximum fuselage diameter at wing-fuselage intersection

Span.....span of the lifting surface

Output

K_WBratio of the wing lift in the presence of the body to the wing-alone lift

function K_BW(Diameter,Span : double) : double;

Description

Datcom Fig 4.3.2-10 Lift Ratio Slender Body Theory

Input

Diameter.....maximum fuselage diameter at wing-fuselage intersection

Span.....span of the lifting surface

Output

K_BWratio of body lift in the presence of the wing to the wing-alone lift

function DeltaDownwashFlapFactor(hhoverb : double) : double;

Description

Roskam Airplane Design Part VI Fig. 8.70 Incremental Downwash Angle at the Horizontal Tail due to Flaps

Input

hhoverbratio of horizontal tail height (relative to wing) to wing semispan

Output

DeltaDownwashFlapFactor.....factor to calculate incremental downwash angle
at the horizontal tail due to flaps

**function LiftCoefficient(Alpha,AlphaZero,AlphaStar,AlphaCLMax,AlphaStall,
CLAlpha,CLmax,CLStall : double) : double;**

Description

Calculates the lift coefficient for a given angle of attack; between AlphaStar and AlphaCLmax a conic is used; between AlphaCLmax and AlphaStall a conic is used

Input

Alpha.....angle-of-attack [deg]
AlphaZerozero-lift angle-of-attack [deg]
AlphaStarangle-of-attack limit for linear lift region [deg]
AlphaCLMax .angle-of-attack for maximum lift coefficient [deg]
AlphaStallangle-of-attack for stall lift coefficient [deg]
CLAlpha.....lift curve slope [1/rad]
CLmax.....maximum lift coefficient
CLStallstall lift coefficient

Output

LiftCoefficient lift coefficient

**function AspectRatioEff(r1,LambdaV,Av,Sv,Sh,Zfch,Xcv,Zapexv,Zach : double)
: double;**

Description

Roskam Airplane Design Part VI, pp 386-390 Calculation of effective aspect ratio of a single vertical tail

Input

r1fuselage depth in region of vertical tail ($=2r_1$)
LambdaV.....vertical tail taper ratio
Av.....vertical tail aspect ratio
Svvertical tail area
Shhorizontal tail area
Zfch.....fuselage centerline in region of horizontal tail
Xcvrelative positions of the horizontal and vertical tails
Zapexv.....vertical tail Z-apex

Zach.....horizontal tail Z-location of aerodynamic center

Output

AspectRatioEff.....vertical tail effective aspect ratio

function AvfAv(bv,r1,LambdaV : double) : double;

Description

Roskam Airplane Design Part VI Fig.10.14 Ratio of Vertical Tail Aspect Ratio in Presence of Fuselage to that of an Isolated Tail

Input

bv.....vertical tail effective span
r1fuselage depth in region of vertical tail ($=2r_1$)
LambdaV.....vertical tail taper ratio

Output

AvfAvratio of vertical tail aspect ratio in presence of fuselage to that of isolated tail

function AvhfAvf(Zhbv,Xcv : double) : double;

Description

Roskam Airplane Design Part VI Fig.10.15 Ratio of Vertical Tail Aspect Ratio in Presence of Fuselage and Horizontal Tail to that in Presence of Fuselage Alone

Input

Zhbvhorizontal tail vertical location to vertical tail span ratio
Xcv.....relative positions of the horizontal and vertical tails

Output

AvhfAvfratio of vertical tail aspect ratio in presence of fuselage and horizontal tail to that in presence of fuselage alone

function Kvh(ShSv : double) : double;

Description

Roskam Airplane Design Part VI Fig.10.16 Factor which Accounts for Relative Size of Horizontal and Vertical Tail

Input

ShSvhorizontal tail to vertical tail area ratio

Output

Kvh.....factor which accounts for relative size of horizontal and vertical tail

function AspectRatioEffTwin(bvPrime,Av,Sv : double) : double;

Description

Roskam Airplane Design Part VI, pp 386-390 Calculation of effective aspect ratio of the twin vertical tail

Input

bvPrimespan of a twin vertical tail measured from the horizontal-vertical tails intersection to the tip of the vertical tail

Av.....vertical tail aspect ratio

Svvertical tail area

Output

AspectRatioEffTwineffective aspect ratio of a twin vertical tail

function AveffAvTwin(bv bv : double) : double;

Description

Roskam Airplane Design Part VI Fig.10.19 Effective Value of Vertical Tail Aspect Ratio used with Fig.10.18

Input

bv bvhorizontal tail vertical location for a twin vertical tail, measured from the top of vertical tail

Output

AveffAvTwineffective to geometric aspect ratio of a twin vertical tail

function CyBvRatio(r1bv,bhlf : double) : double;

Description

Roskam Airplane Design Part VI Fig.10.17 Wing-Fuselage-Horizontal Tail Interference on Sideforce due to Sideslip of Twin Vertical Tails

Input

r1bvfuselage depth at quarter chord point of vertical panels to vertical tail span ratio

bhlfhorizontal tail span to fuselage length ratio

Output

CyBvRatiowing-fuselage-horizontal-tail interference on side-force due to sideslip of twin vertical tails

function AlphaDeltaCLRatio(AR,CfC : double) : double;

Description

Roskam Airplane Design Part VI Fig.8.53 Effect of Aspect Ratio and Flap-Chord Ratio on the three-Dimensional Flap Effectiveness

Input

AR.....lifting surface aspect ratio

CfC.....flap chord ratio [fraction]

Output

AlphaDeltaCLRatiothree-dimensional flap effectiveness factor

function Kprime(CfOverC,DeltaF : double) : double;

Description

Roskam Airplane Design Part VI Fig.8.13 and part II Fig.8.13: Correction factor for Nonlinear Lift Behavior of Plain Flaps modeled with $K' \cdot df/60$, per CfC, linear interpolation and extrapolation in CfC

Input

CfOverC.....flap chord ratio [fraction]

DeltaF.....flap deflection [deg]

Output

Kprimecorrection factor for nonlinear lift behavior of plain flaps

function KDoublePrime(CfOverC,DeltaF : double) : double;

Description

Derivative to DeltaF of Kprime*DeltaF function

Input

CfOverC.....flap chord ratio [fraction]

DeltaF.....flap deflection [deg]

Output

KDoublePrimederivative of K' to flap deflection

function CIDeltaTheory(CfC,tc : double) : double;

Description

Roskam Airplane Design Part II Fig.7.5 and Roskam Airplane Design Part VI Fig.8.14 Lift Effectiveness of a Plain Flap

Input

CfC.....flap chord ratio [fraction]

tc.....thickness ratio [fraction]

Output

CIDeltaTheory.....theoretical lift effectiveness of a plain flap

function CIDeltaRatio(CfC,ClalphaRatio : double) : double;

Description

Roskam Airplane Design Part VI Fig.8.15 Correction Factor for Plain Flap Lift

Input

CfC.....flap chord ratio [fraction]

ClalphaRatiopredicted to theoretical ratio of airfoil lift curve slope

Output

ClDeltaRatiopredicted to theoretical ratio of two dimensional plain flap lift effectiveness

**function AlphaDelta(Mach,de,CeC,AR,cla2D0,RootTc,TipTc,EtaIn,EtaOut,
Lambda : double) : double;**

Description

Calculate section lift effectiveness parameter

Input

MachMach number
de.....elevator deflection [deg]
CeCelevator chord ratio [fraction]
AR.....aspect ratio
cla2D0.....airfoil lift curve slope at low Mach number
RootTc.....root airfoil thickness ratio [fraction]
TipTc.....tip airfoil thickness ratio [fraction]
EtaInnon-dimensional elevator inboard station [fraction]
EtaOutnon-dimensional elevator outboard station [fraction]
Lambdataper ratio

Output

AlphaDeltasection lift effectiveness parameter

function BetaCldeltaK(EtaIn,EtaOut,SweepBeta,BetaARwK : double) : double;

Description

Roskam Airplane Design Part VI Fig.10.46 Aileron Rolling Moment Parameter

Input

EtaInaileron inboard station [fraction]
EtaOutaileron outboard station [fraction]
SweepBeta.....effective quarter-chord sweep angle in compressible flow [deg]
BetaARwK.....aspect ratio and airfoil lift curve slope parameter

Output

BetaCldeltaK.....aileron rolling moment parameter

function RollParameter(EtaIn,EtaOut,SweepBeta,BetaARwK : double) : double;

Roskam Airplane Design Part VI Fig.10.46 Aileron Rolling Parameter

Input

EtaIn.....aileron inboard station [fraction]

EtaOut.....aileron outboard station [fraction]

SweepBeta.....effective quarter-chord sweep angle in compressible flow [deg]

BetaARwK.....aspect ratio and airfoil lift curve slope parameter

Output

RollParameteraileron rolling moment parameter

function KYawAileron(Eta,Aw,Lambda : double) : double;

Description

Roskam Airplane Design Part VI Fig.10.48 Correlation Constant for Yawing Moment due to Aileron Deflection. Linear extrapolation for $Aw < 3.0$

Input

Eta.....aileron station [fraction]

Aw.....wing aspect ratio

Lambda.....wing taper ratio

Output

KYawAileron.....correlation constant for yawing moment due to aileron deflection

**function CIDeltaA(M,clAlpha,AR,Lambda,Sweep4,EtaIn,EtaOut,RootTC,
TipTC,CaOverC,da : double) : double;**

Description

rolling moment coefficient derivative of two anti-symmetrically deflected ailerons

Input

M.....Mach number
clAlpha.....airfoil lift curve slope
AR.....aspect ratio
Lambdataper ratio
Sweep4.....quarter-chord sweep angle [deg]
EtaIn.....aileron inboard station [fraction]
EtaOut.....aileron outboard station [fraction]
RootTC.....root airfoil thickness ratio [fraction]
TipTC.....tip airfoil thickness ratio [fraction]
CaOverCaileron chord ratio [fraction]
da.....aileron deflection [deg]

Output

CIDeltaAaileron control power

function GapEffect2DLiftCurveSlope(xcgap,Gap : double) : double;

Description

Effect of control surface gap on lift curve slope

Input

xcgap.....gap location to local chord ratio
Gap.....gap size to local chord ratio

Output

GapEffect2DLiftCurveSlopegap correction for airfoil lift curve slope

function GapEffectLiftCurveSlope(AR,xcgap,Gap : double) : double;

Description

Effect of control surface gap on lift curve slope

Input

AR.....aspect ratio

xcgap.....gap location to local chord ratio

Gap.....gap size to local chord ratio

Output

GapEffectLiftCurveSlopegap correction for lifting surface lift curve slope

**function BalanceEffectControl(Balance : double; NoseShape : TNoseShape) :
double;**

Description

Effect of control surface balance on control effectiveness

Input

Balance.....ratio of the control surface area forward-of to that aft-of hingeline

NoseShape.....leading edge shape of the control surface

Output

BalanceEffectControl.....correction factor due to the size and type of control
surface balance

function CriticalMach(CL,Sweep4,AR,tc,dCmcr : double) : double;

Description

Critical Mach number of a lifting surface

Input

CLlift coefficient

Sweep4.....quarter-chord sweep angle [deg]

AR.....aspect ratio

tc.....thickness ratio [fraction]
dCmcr.....increment in critical Mach number due to aspect ratio variation

Output
CriticalMachcritical Mach number

function DebarDa1(Xi,Cf : double) : double;

Description
Roskam Airplane Design Part VI Fig.8.115 Effect of Fuselage (or Nacelle) segment
Location on Upwash Gradient, curve (1)

Input
Xi.....X-location of segment centroid
Cf.....Wing-Fuselage intersection chord length

Output
DebarDa1upwash gradient

function DebarDa2(DX5,Cf : double) : double;

Description
Roskam Airplane Design Part VI Fig.8.115 Effect of Fuselage (or Nacelle) segment
Location on Upwash Gradient, curve (2)

Input
DX5.....X-location of segment centroid directly in front of the wing
Cf.....Wing-Fuselage intersection chord length

Output
DebarDa1upwash gradient

E.2 DragCoefficient.dll

function FrictionCoef(Re,Mach : double) : double;

Description

Roskam Airplane Design Part VI Fig.4.3 Turbulent Mean Skin-Friction Coefficient

Input

ReReynolds number

MachMach number

Output

FrictionCoefskin-friction coefficient

function ThicknessRatio(tcr,tct,Lambda,Eta : double) : double;

Description

Calculate thickness ratio for straight tapered wing at eta

Input

tcrroot chord thickness ratio

tct.....tip chord thickness ratio

Lambdataper ratio

Etanon-dimensional semi-span station

Output

ThicknessRatio.....thickness ratio

(unit of output is the same as the unit of the inputs)

function Rwf(Reynolds,Mach : double) : double;

Description

Roskam Airplane Design Part VI Fig.4.1 Wing Fuselage Interference Factor

Input

ReynoldsReynolds number

MachMach number

Output

Rwf.....wing fuselage interference factor

function RLS(CosGam,Mach : double) : double;

Description

Roskam Airplane Design Part VI Fig.4.2 Lifting Surface Correcting Factor

Input

CosGam.....cosine of the locus that connects the local maximum thickness along
the span

MachMach number

Output

RLSlifting surface correction factor

function RECutoff(loverk,Mach : double) : double;

Description

Roskam Airplane Design Part VI Fig.4.77 Effect of Mach Number on the Relation
Between Cut-off Reynolds Number and Roughness

Input

loverkadmissible roughness (l/k) ; where

lreference length

k.....equivalent sand roughness

MachMach number

Output

RECutOffcutoff Reynolds number

function LESuction(RILER,A,Lambda,SweepLE,M : double) : double;

Description

Roskam Airplane Design Part VI Fig. 4.7 Leading Edge Suction Parameter

Input

RILERReynolds number of the leading edge radius

A.....aspect ratio

Lambdataper ratio

SweepLEleading edge sweep angle [rad]

M.....Mach number

Output

LESuctionleading edge suction parameter

function InducedDragFactor(BetaA,Sweep,Lambda : double) : double;

Description

Roskam Airplane Design Part VI Fig.4.9 Induced Drag Factor due to Linear Twist

Input

BetaABeta \times A ; where

BetaPrandtl-Glauert correction factor, $\sqrt{1-M^2}$

A.....aspect ratio

Sweepquarter chord sweep angle [deg]

Lambdataper ratio

Output

InducedDragFactorinduced drag factor due to linear twist

function ZeroLiftDragFactor(BetaA,Sweep,Lambda : double) : double;

Description

Roskam Airplane Design Part VI Fig.4.10: Zero-Lift Drag Factor due to Linear Twist

Input

BetaABeta \times A ; where

BetaPrandtl-Glauert correction factor, $\sqrt{1-M^2}$

A.....aspect ratio

Sweep.....quarter chord sweep angle [deg]

Lambdataper ratio

Output

ZeroLiftDragFactor.....zero-lift drag factor due to linear twist

**procedure ZeroLiftDragSubs(h,dT,Mach,A,Lambda,S,Sweep4,tcr,tct,Df,lf,
Lprime,k,XtransC : double;
var Swet,CDow : double; var Error : boolean);**

Description

Roskam Airplane Design Part VI section 4.2.1.1, calculate the subsonic zero-lift drag coefficient and wetted area of a lifting surface

Input

h.....altitude

dTtemperature increment relative to the standard temperature

MachMach number

A.....aspect ratio

Lambdataper ratio

Splanform area

Sweep4.....quarter-chord sweep angle [rad]

tcrroot chord thickness ratio [fraction]

tct.....tip chord thickness ratio [fraction]

Dffuselage diameter

lffuselage length

Lprime.....airfoil thickness location parameter

k.....equivalent sand roughness
XtransCX-location of flow transition to chord ratio [fraction]

Output

Swet.....wetted area
CDowzero-lift drag coefficient of the lifting surface
Errortrue if a calculation error occurs

**procedure LiftDragSubs(h,dT,Mach,A,Lambda,S,Sweep4,ILERC,
Twist,CLaw,CL : double; var CDLw : double);**

Description

Roskam Airplane Design Part VI Section 4.2.1.2, calculate the subsonic drag coefficient due to lift of a lifting surface

Input

h.....altitude
dTtemperature increment relative to the standard temperature
MachMach number
A.....aspect ratio
Lambdataper ratio
Splanform area
Sweep4.....quarter-chord sweep angle [rad]
ILERCleading edge radius to chord ratio [fraction]
Twisttwist angle [rad]
CLaw.....lift curve slope of the lifting surface [/rad]
CLlifting surface lift coefficient

Output

CDLw.....lift induced drag of the lifting surface

procedure WaveDrag(tc,A,M : double; var CDWave,CDgradient : double);

Description

Roskam Airplane Design Part VI Fig.4.11 Zero-Lift Wave Drag Coefficient and gradient at that point

Input

tc.....thickness ratio [fraction]

A.....aspect ratio

M.....Mach number

Output

CDWave.....wave drag coefficient

CDgradient.....local slope of the wave drag coefficient versus Mach number plot

function ZeroLiftWaveDrag(tc,A,M : double) : double;

Description

Roskam Airplane Design Part VI Fig.4.11 Zero-Lift Wave Drag Coefficient and gradient at that point

Input

tc.....thickness ratio

A.....aspect ratio

M.....Mach number

Output

ZeroLiftWaveDrag.....zero-lift wave drag coefficient

procedure WaveDragPeak(tc,A : double; var MCDpeak,CDpeak : double);

Description

Calculate the peak in the drag coefficient as function of mach for transonic region

Input

tc.....thickness ratio [fraction]

A.....aspect ratio

Output

MCDpeak.....transonic Mach number that corresponds to peak wave drag coefficient

CDpeakpeak wave drag coefficient in the transonic range

**procedure DragDivergence(tc,A : double; var MDD,MCD0,CDgradient :
double);**

Description

Calculate the Mach number for drag divergence (at $CD = 0.002$)

calculate the Mach number for $CD = 0$

Input

tc.....thickness ratio [fraction]

A.....aspect ratio

Output

MDDdrag divergence Mach number

MCD0Mach number at which the wave drag first started

CDgradient.....slope of the wave drag coefficient versus Mach number plot at MDD

function ZeroLiftWaveDragSweep(tc,A,M,Sweep,CDpeak : double) : double;

Description

Calculate the wave drag coefficient for wings with sweep

quadratic interpolation between $CD = 0.002$, $delCD = 0$ and $CDpeak,delCD = delCDpeak$

Input

tc.....thickness ratio [fraction]

A.....aspect ratio

M.....Mach number

Sweep.....sweep angle (Section 4.2.2.1, Roskam Airplane Design Part VI:
quarter-chord sweep) [rad]

CDpeakpeak wave drag coefficient in the transonic range

Output

ZeroLiftWaveDragSweepzero-lift wave drag coefficient of a swept wing

**procedure ZeroLiftDragTrans(h,dT,Mach,A,Lambda,S,Sweep4,tcr,tct,Df,lf,
Lprime,k,XtransC : double;var Swet,CDw :
double; var Error : boolean);**

Description

Calculate the transonic zero-lift drag coefficient of a lifting surface

Input

h.....altitude
dTtemperature increment relative to standard atmosphere
MachMach number
A.....aspect ratio
Lambdataper ratio
Splanform area
Sweep4.....quarter-chord sweep angle [rad]
tcrroot chord thickness ratio [fraction]
tct.....tip chord thickness ratio [fraction]
Dffuselage diameter at the lifting-surface-fuselage intersection
lffuselage length
Lprime.....airfoil thickness location parameter
k.....equivalent sand roughness
XtransCX-location of flow transition to chord ratio [fraction]

Output

Swet.....wetted area of the lifting surface
CDwtransonic drag coefficient of the lifting surface
Errortrue if a calculation error occurs

function TransLiftDrag(tc,A,M,Lambda,LEAngle : double) : double;

Description

Roskam Airplane Design Part VI Fig.4.13 Transonic Drag due to Lift
calculate C_D/C_L^2

Input

tc.....thickness ratio [fraction]
A.....aspect ratio
M.....Mach number
Lambdataper ratio [fraction]
LEAngle.....leading angle [rad]

Output

TransLiftDrag transonic drag coefficient due to lift

**procedure LiftDragTrans(h,dT,Mach,A,Lambda,S,Sweep4,tcr,tct,ILERC,
Twist,CLaw,CL : double;var CDLw : double);**

Description

Calculate the transonic drag coefficient due to lift of a lifting surface

Input

h.....altitude
dTtemperature increment relative to standard atmosphere
MachMach number
A.....aspect ratio
Lambdataper ratio
Splanform area
Sweep4.....quarter-chord sweep angle [rad]
tcrroot chord thickness ratio [fraction]
tct.....tip chord thickness ratio [fraction]
ILERCleading edge radius to chord ratio [fraction]
Twisttwist angle [rad]
CLaw.....lift curve slope of the lifting surface [/rad]
CLlifting surface lift coefficient

Output

CDLw.....transonic lift induced drag of the lifting surface

function SupersonicLiftDrag(RoundLE : boolean;M,bw,Crw : double) : double;

Description

Roskam Airplane Design Part VI fig 4.16 Supersonic Drag due to Lift

Input

RoundLE.....round leading edge

M.....Mach number

bw.....span

Crw.....root chord

Output

SupersonicLiftDrag.....supersonic drag coefficient due to lift

**procedure ZeroLiftDragSupers(h,dT,Mach,A,Lambda,S,Sweep4,tcr,tct,Df,
ILERC,k : double; var Swet,CDow : double);**

Description

Calculate the supersonic zero-lift drag coefficient and wetted area of a lifting surface

Input

h.....altitude

dT.....temperature increment relative to standard atmosphere

Mach.....Mach number

A.....aspect ratio

Lambda.....taper ratio

S.....planform area

Sweep4.....quarter chord sweep angle [rad]

tcr.....root chord thickness ratio [fraction]

tct.....tip chord thickness ratio [fraction]

Df.....fuselage diameter at the lifting-surface-fuselage intersection

ILERC.....leading edge radius to chord ratio [fraction]

k.....equivalent sand roughness

Output

Swet.....wetted area

CDowsupersonic zero-lift drag coefficient

procedure LiftDragSupers(Mach,A,Lambda,S,CL : double;var CDLw : double);

Description

Calculate the supersonic drag coefficient due to lift of a lifting surface

Input

MachMach number

A.....aspect ratio

Lambdataper ratio

Splanform area

CLlift coefficient

Output

CDLw.....supersonic drag coefficient due to lift

**procedure FuselageZeroLiftDragSubs(ExitAirflow : boolean;
h,dT,Mach,S,lf,Sbase,Sfus,SwetFus,SwetLam,k,XtransLf : double;
var CDofus : double);**

Description

Calculate the subsonic laminar flow zero-lift drag coefficient of a lifting body

Input

ExitAirflowengine nozzle coincide with fuselage base

h.....altitude

dTtemperature increment relative to standard atmosphere

MachMach number

Splanform area

lffuselage length

Sbasefuselage base area

Sfusfuselage frontal area

SwetFus.....fuselage wetted area

SwetLamlaminar flow portion of the fuselage wetted area
k.....equivalent sand roughness
XtransLfX-location of flow transition to fuselage length ratio [fraction]

Output

CDofussubsonic fuselage zero-lift drag coefficient

function CylinderDragRatio(lf,df : double) : double;

Description

Roskam Airplane Design Part VI Fig.4.19 Ratio of the Drag Coefficient of a Circular Cylinder of Finite Length to that of a Cylinder of Infinite Length

Input

lffuselage length
dffuselage diameter

Output

CylinderDragRatioRatio of the Drag Coefficient of a Circular Cylinder of Finite Length to that of a Cylinder of Infinite Length

function CylinderCrossFlowDrag(Mach,Alpha : double) : double;

Description

Roskam Airplane Design Part VI Fig.4.20 Steady State Cross-Flow Drag Coefficient for Two-Dimensional Circular Cylinders

Input

MachMach number
Alpha.....angle-of-attack [rad]

Output

CylinderCrossFlowDragSteady State Cross-Flow Drag Coefficient for Two-Dimensional Circular Cylinders

function BaseDragFairing(Mach,CDb,db,df : double) : double;

Description

Roskam Airplane Design Part VI Fig.4.21 Transonic Fairing for Fuselage Base Drag Coefficient

Input

MachMach number

CDbfuselage base drag coefficient at Mach 0.60

db.....fuselage base diameter

dfmaximum fuselage diameter

Output

BaseDragFairingtransonic fuselage base drag coefficient

function CDwParabolic(lf,df,Mach : double) : double;

Description

Roskam Airplane Design Part VI Fig.4.22 Wave Drag Coefficient for Parabolic Fuselages

Input

lffuselage length

dffuselage diameter

MachMach number

Output

CDwParabolic Wave Drag Coefficient for Parabolic Fuselages

**procedure FuselageZeroLiftDragTrans(ExitAirflow : boolean;
 h,dT,Mach,S,lf,Sbase,Sfus,SwetFus,k : double;
 var CDofus : double);**

Description

Calculate the transonic zero-lift drag coefficient of a lifting body

Input

ExitAirflowengine nozzle coincide with fuselage base
h.....altitude
dTtemperature increment relative to standard atmosphere
MachMach number
Sreference area (wing)
lffuselage length
Sbasefuselage base area
Sfusfuselage maximum frontal area
SwetFus.....fuselage wetted area
k.....equivalent sand roughness

Output

CDofustransonic zero-lift drag coefficient of a lifting body

function ParabolicBodyDrag(a,df,l,M : double) : double;

Description

Roskam Airplane Design Part VI Fig.4.24 Drag of Slender Forebodies or Afterbodies of Parabolic Profile

Input

a.....nose diameter of forebody or base diameter of afterbody
dfmaximum diameter of forebody or afterbody
llength of forebody or afterbody
M.....Mach number

Output

ParabolicBodyDrag.....drag of slender forebodies or aftbodies of parabolic profile

function ConicalBodyDrag(a,d,l,M : double) : double;

Description

Roskam Airplane Design Part VI Fig.4.25 Drag of Slender, Conical Forebodies and Aftbodies

Input

a.....nose diameter of forebody or base diameter of afterbody

d.....maximum diameter of forebody or afterbody

llength of forebody or afterbody

M.....Mach number

Output

ConicalBodyDragdrag of slender, conical forebodies and aftbodies

function ParabolicBodyInterferenceDrag(d,IN,IA,IC : double) : double;

Description

Roskam Airplane Design Part VI Fig.4.26 Interference Drag for Parabolic Bodies

Input

d.....body diameter

IN.....length of the forebody

IA.....length of the aftbody

IC.....length of the middlebody

Output

ParabolicBodyInterferenceDraginterference drag for parabolic bodies

function CDANCnoCenter(db,d,IN,IA : double) : double;

Description

Roskam Airplane Design Part VI Fig.4.27 Interference Drag of Truncated Aftbodies Behind Parabolic Forebody with no Constant Center section

Input

db.....base diameter of the body
d.....maximum diameter of the body
IN.....length of the forebody
IA.....length of the afterbody

Output

CDANCnoCenterinterference drag of truncated aftbodies behind parabolic forebody with no constant center section

function BaseDragNoBoattail(M : double) : double;

Description

Roskam Airplane Design Part VI Fig.4.28 Base Drag Coefficient for Bodies of Revolution with no Boattail

Input

M.....Mach number

Output

BaseDragNoBoattailbase drag coefficient for bodies of revolution with no boattail

function CpbConic(Mach,db,d,lA : double) : double;

Description

Roskam Airplane Design Part VI Fig.4.29 Base Pressure Coefficient for Conical Boattails

Input

MachMach number

db.....base diameter of the boattail

d.....maximum body diameter

lA.....length of the afterbody

Output

CpbConicbase pressure coefficient for conical boattails

function CpbOgive(Mach,db,d,lA : double) : double;

Description

Roskam Airplane Design Part VI Fig.4.29 Base Pressure Coefficient for Ogive Boattails (Datcom)

Input

MachMach number

db.....base diameter of the afterbody

d.....maximum body diameter

lA.....length of the afterbody

Output

CpbOgivebase pressure coefficient for ogive boattails


```
procedure FuselageZeroLiftDragSupers(h,dT,Mach,S,lf,Sbfus,Sfus,SwetFus,
lfore,afore,lafter,Shapefore, Shapeafter,k : double;
var CDofus : double);
```

Description

Calculate the supersonic zero-lift drag coefficient of a lifting body

Input

h.....altitude
dTtemperature increment relative to standard atmosphere
MachMach number
Sreference area (wing)
l_fbody length
S_{bfus}base area of the body
S_{fus}maximum frontal area of the body
S_{wetFus}.....wetted area of the body
l_{fore}length of the forebody
a_{fore}nose diameter of the forebody
l_{after}length of the aftbody
Shape_{fore}shape of the forebody
Shape_{after}shape of the aftbody
k.....equivalent sand roughness

Output

CDofussupersonic zero-lift drag coefficient of a lifting body

```
function DCdpPlain(CfC,df : double) : double;
```

Description

Roskam Airplane Design Part VI Fig.4.44 Profile Drag Increment: Plain Flaps

Input

CfCflap-chord to wing-chord ratio [fraction]
dfflap deflection [deg]

Output

DCdpPlain.....profile drag increment of plain flaps

function DCdpSplit(CfC,tc,df : double) : double;

Description

Roskam Airplane Design Part VI Fig.4.45 Profile Drag Increment: Split Flaps

Input

CfC.....flap-chord to wing-chord ratio [fraction]

tc.....thickness ratio [fraction]

df.....flap deflection [deg]

Output

DCdpSplitprofile drag increment of split flaps

function DCdpSingleSlotted(CfC,df : double) : double;

Description

Roskam Airplane Design Part VI Fig.4.46 Profile Drag Increment: Single Slotted Flaps

Input

CfC.....flap-chord to wing-chord ratio [fraction]

df.....flap deflection [deg]

Output

DCdpSingleSlottedprofile drag increment of single slotted flaps

function DCdpDoubleSlotted(CfC,df : double) : double;

Description

Roskam Airplane Design Part VI Fig.4.47 Profile Drag Increment: Double Slotted Flaps

Input

CfC.....flap-chord to wing-chord ratio [fraction]

df.....flap deflection [deg]

Output

DCdpDoubleSlotted.....profile drag increment of double slotted flaps

function DCdpFowler(CfC,df : double) : double;

Description

Roskam Airplane Design Part VI Fig.4.48 Profile Drag Increment: Fowler Flaps

Input

CfC.....flap-chord to wing-chord ratio [fraction]

df.....flap deflection [deg]

Output

DCdpFowler.....profile drag increment of fowler flaps

function KInducedDrag(AR,Etai,Etao : double) : double;

Description

Roskam Airplane Design Part VI Fig.4.52 -4.53: Induced Drag Factor for Interrupted Flaps

Input

AR.....aspect ratio

Etai.....inboard flap station [fraction]

Etao.....outboard flap station [fraction]

Output

KInducedDrag.....induced drag factor for interrupted flaps

function DCDCanopyConicalL1(L1R : double) : double;

Description

Roskam Airplane Design Part VI Fig.4.62 Effect of L1 on Canopy Drag: Conical Canopy

Input

L1Rcanopy forebody-length to canopy height (frontal-radius) ratio

Output

DCDCanopyConicalL1incremental canopy drag due to conical forebody length of canopy

function DCDCanopyStreamL1(L1R : double) : double;

Description

Roskam Airplane Design Part VI Fig.4.62 Effect of L1 on Canopy Drag : StreamLined Canopy

Input

L1Rcanopy forebody-length to canopy height (frontal-radius) ratio

Output

DCDCanopyStreamL1incremental canopy drag due to streamlined forebody length of canopy

function DCDCanopyConicalL3(L3R : double) : double;

Description

Roskam Airplane Design Part VI Fig.4.64 Effect of L3 on Canopy Drag : Conical Aft End

Input

L3Rcanopy aftbody-length to canopy height (frontal-radius) ratio

Output

DCDCanopyConicalL3.....incremental canopy drag due to conical aft-end length of canopy

function DCdpFowler(CfC,df : double) : double;

Description

Roskam Airplane Design Part VI Fig.4.48 Profile Drag Increment : Fowler Flaps

Input

CfC.....flap-chord to wing-chord ratio [fraction]

df.....flap deflection [deg]

Output

DCdpFowler.....profile drag increment of fowler flaps

function KInducedDrag(AR,Etai,Etao : double) : double;

Description

Roskam Airplane Design Part VI Fig.4.52 -4.53: Induced Drag Factor for Interrupted Flaps

Input

AR.....aspect ratio

Etai.....inboard flap station [fraction]

Etao.....outboard flap station [fraction]

Output

KInducedDrag.....induced drag factor for interrupted flaps

function DCDCanopyConicalL1(L1R : double) : double;

Description

Roskam Airplane Design Part VI Fig.4.62 Effect of L1 on Canopy Drag : Conical Canopy

Input

L1Rcanopy forebody-length to canopy height (frontal-radius) ratio

Output

DCDCanopyConicalL1incremental canopy drag due to conical forebody length of canopy

function DCDCanopyStreamL1(L1R : double) : double;

Description

Roskam Airplane Design Part VI Fig.4.62 Effect of L1 on Canopy Drag: StreamLined Canopy

Input

L1Rcanopy forebody-length to canopy height (frontal-radius) ratio

Output

DCDCanopyStreamL1incremental canopy drag due to streamlined forebody length of canopy

function DCDCanopyConicalL3(L3R : double) : double;

Description

Roskam Airplane Design Part VI Fig.4.64 Effect of L3 on Canopy Drag: Conical Aft End

Input

L3Rcanopy aftbody-length to canopy height (frontal-radius) ratio [fraction]

Output

DCDCanopyConicalL3.....incremental canopy drag due to conical aft-end length of canopy

function DCDCanopyStreamL3(L3R : double) : double;

Description

Roskam Airplane Design Part VI Fig.4.64 Effect of L3 on Canopy Drag : Streamlined Aft End

Input

L3Rcanopy aftbody-length to canopy height (frontal-radius) ratio [fraction]

Output

DCDCanopyStreamL3 incremental canopy drag due to streamlined aft-end length of canopy

function CDCanopy(Mach,L1R,L3R,Alfa,ForeShape,AftShape : double) : double;

Description

Calculation of canopy drag with Mach correction and influence of angle of attack

Input

MachMach number

L1Rcanopy forebody-length to canopy height (frontal-radius) ratio

L3Rcanopy aftbody-length to canopy height (frontal-radius) ratio

Alfaangle-of-attack [rad]

ForeShapeforebody shape of the canopy

AftShapeaftbody shape of the canopy

Output

CDCanopy.....canopy drag with Mach and angle-of-attack corrections

function CpbBody(Mach : double) : double;

Description

Roskam Airplane Design Part VI Fig.4.29 top line $d_b/d = 1.0$ used for nacelles and stores in supersonic flow regime, minus sign is omitted

Input

MachMach number

Output

CpbBodybase pressure coefficient

function DCDnacelleStraight(XL : double) : double;

Description

Roskam Airplane Design Part VI Fig.4.41a Wing-Nacelle Drag Interference Factor for straight wings (sweep < 5 deg)

Input

XLlongitudinal nacelle inlet location to wing chord ratio

Output

DCDnacelleStraightwing-nacelle drag interference factor for straight wings

function DCDnacelleSwept(XL,Mach : double) : double;

Description

Roskam Airplane Design Part VI Fig.4.41b Wing-Nacelle Drag Interference Factor for swept wings, Sweep > 5 deg

Input

XLlongitudinal nacelle inlet location to wing chord ratio

MachMach number

Output

DCDnacelleSwept.....wing-nacelle drag interference factor for swept wings

function FuselageNacelleDrag(tD,LiftCoef : double) : double;

Description

Roskam Airplane Design Part VI Fig.4.42 Fuselage-Nacelle Drag Interference -0.05 for the free nacelle

Input

tD.....nacelle lateral location to nacelle diameter ratio [fraction]
LiftCoef.....lift coefficient

Output

FuselageNacelleDragfuselage-nacelle drag interference drag factor

function PlainProfileDrag(CeC,EtaIn,EtaOut,Lambda,S,Sh,de,Sweep : double) : double;

Description

Roskam Airplane Design Part VI eq.4.84, calculation of profile drag due to deflection of a control surface

Input

CeCelevator chord ratio [fraction]
EtaIninboard station of the control surface [fraction]
EtaOutoutboard station of the control surface [fraction]
Lambdataper ratio
Sreference area (wing)
Shhorizontal tail area
de.....control surface deflection [deg]
Sweep.....quarter-chord sweep angle of the lifting surface [rad]

Output

PlainProfileDragprofile drag due to deflection of a control surface

**function CDwindMilling(Nout : integer; Mach,S,Sinl,Snoz,BPR : double) :
double;**

Description

Calculation of the drag due to Nout windmilling engines

for BPR = 0.0 the ratio of average flow velocity = 0.25

for BPR < 2.0 the ratio of average flow velocity = 0.42

for BPR > 2.0 the ratio of average flow velocity = 0.12 for the primary airflow

for BPR > 2.0 the ratio of average flow velocity = 0.92 for the fan airflow

Input

Nout.....number of outboard engines

MachMach number

Sreference area (wing)

Sinlinlet area

Snoz.....nozzle area

BPR.....by-pass ratio

Output

CDwindMilling.....engine windmilling drag coefficient

**function CDstoppedProp(Nout,Nstopped,np : integer;
Mach,h,dT,S,SHP,Dp : double) : double;**

Description

Calculation of the drag due to Nout windmilling engines and Nstopped stopped propellers

Input

Nout.....number of outboard engines

Nstoppednumber of stopped propellers

np.....number of blades per propeller

MachMach number

h.....altitude

dTtemperature increment relative to standard atmosphere

Sreference area (wing)

SHPmaximum rated shaft horsepower of the engine in the flight condition
being considered

Dp.....diameter of the propeller

Output

CDstoppedPropdrag due to windmilling engine(s) and stopped propeller(s)

E.3 WeightSizing.dll

```
procedure TakeoffWeightSizing(A,B,Mres,Mtfo,WpExpTotal,WfRefuel,  
    MffUncor,Wfcorr,Wto,WPL,Wcrew : double;  
    var TakeoffWeight,EmptyWeight : double;  
    var Error : integer);
```

Description

Calculate take-off weight and empty weight

Input

A.....regression coefficient A
B.....regression coefficient B
Mresreserve fuel fraction
Mtfo.....trapped fuel and oil fraction
WpExpTotal.....total expended payload [lb]
WfRefuel.....total refueled fuel weight [lb]
MffUncoruncorrected fuel fraction from equation [6-11]
Wfcorrfuel weight correction from equation [6-11] [lb]
Wto.....estimated take-off weight [lb]
WPLtotal payload weight [lb]
Wto.....total crew weight [lb]

Output

TakeoffWeighttake-off weight [lb]
EmptyWeightempty weight [lb]
Errorerror message number

- 3: Reserve fuel, fuel-fraction or trapped fuel and oil do not contain the right data.
- 4: IT IS NOT POSSIBLE TO FIND AN ANSWER with $B < 1$ and this combination input variables, there is no intersection between the curves
- 5: Estimated Take-off Weight is too high, or the combination of A, B and Mff gives a very high solution
- 7: Argument of log function less than or equal to zero
- 8: The second solution for the take-off weight 2×10^9
- 9: There is no solution for $B = 1$
- 16: There are two solutions for the take-off weight. The lowest weight is automatically selected.
- 18: The regression coefficient $B < 0.0$

E.4 Atmosphere.dll

```
procedure GetAtmosProperties(Altitude,DeltaT : double;  
                           var p,T,Rho,Delta,Sigma,Theta,a,g : double);
```

Description

Calculate all atmospheric properties

Input

Altitudealtitude [ft]

DeltaTtemperature offset [deg R]

Output

p.....pressure [lb/ft²]

Ttemperature [deg R]

Rho.....air density [slugs/ft³]

Delta.....pressure ratio (pressure at altitude/pressure a 0ft ISA)

Sigmadensity ratio (density at altitude/density a 0ft ISA)

Thetatemperature ratio (temperature at altitude/temperature a 0ft ISA)

a.....speed of sound [ft/s]

g.....acceleration of gravity [ft/s²]

```
function ReynoldsNumber(Altitude,DeltaTemp,Mach,CharLength : double) :  
double;
```

Description

Calculate Reynolds Number

Input

Altitudealtitude [ft]

DeltaTemp.....temperature offset [deg R]

MachMach Number

CharLengthcharacteristic length [ft]

Output

ReynoldsNumberReynolds Number

function GravityAcceleration(Altitude : double) : double;

Description

Calculate all acceleration of gravity

Input

Altitudealtitude [ft]

Output

GravityAcceleration.....acceleration of gravity [ft/s²]

function AirViscosity(Altitude,DeltaTemp : double) : double;

Description

Calculate kinematic viscosity

Input

Altitudealtitude [ft]

DeltaTemp.....temperature offset [deg R]

Output

AirViscositykinematic viscosity [ft²/s]

function SpeedOfSound(Altitude,DeltaTemp : double) : double;

Description

Calculate speed of sound

Input

Altitudealtitude [ft]

DeltaTemp.....temperature offset [deg R]

Output

SpeedOfSoundspeed of sound [ft/s]

function AirDensity(Altitude,DeltaTemp : double) : double;

Description

Calculate air density

Input

Altitudealtitude [ft]

DeltaTemp.....temperature offset [deg R]

Output

AirDensity.....air density [slugs/ft³]

function AirPressure(Altitude,DeltaTemp : double) : double;

Description

Calculate air pressure

Input

Altitudealtitude [ft]

DeltaTemp.....temperature offset [deg R]

Output

AirPressure.....pressure [lb/ft²]

function AirSigma(Altitude,DeltaTemp : double) : double;

Description

Calculate density ratio

Input

Altitudealtitude [ft]

DeltaTemp.....temperature offset [deg R]

Output

AirSigma.....density ratio (density at altitude/density a 0ft ISA)

E.5 FuselageDrag.dll

```
function FuselageLiftDragSubsonicTransonic(CL,Mach,CL_zero_Airplane,  
      CL_Alpha,Wing_Area,Fus_Base_Area,  
      Fus_Planform_Area,Fus_Length,Fus_Diam : double) : double;
```

Description

Calculate the fuselage subsonic or transonic drag coefficient due to lift

Input

CLairplane lift coefficient
MachMach number
CL_zero_Airplane.....Airplane zero angle of attack lift coefficient
CL_Alpha.....airplane lift curve slope [1/rad]
Wing_Area.....wing area [ft²]
Fus_Base_Areafuselage base area [ft²]
Fus_Planform_Area ...fuselage planform area [ft²]
Fus_Lengthfuselage length [ft]
Fus_Diam.....fuselage maximum diameter [ft]

Output

FuselageLiftDragSubsonicTransonic.....fuselage drag coefficient due to lift

```
function FuselageLiftDragSupersonic(CL,Mach,CL_zero_Airplane,CL_Alpha,  
      Wing_Area,Fus_Base_Area,Fus_Planform_Area,  
      Fus_Cross_Section_a,Fus_Cross_Section_b,  
      Fus_Cross_Section_w : double) : double;
```

Description

Calculate the fuselage supersonic drag coefficient due to lift

Input

CLairplane lift coefficient
MachMach number
CL_zero_Airplane.....Airplane zero angle of attack lift coefficient
CL_Alpha.....airplane lift curve slope [1/rad]
Wing_Area.....wing area [ft²]

Fus_Base_Areafuselage base area [ft²]
 Fus_Planform_Areafuselage planform area [ft²]
 Fus_Cross_Section_a....fuselage cross-section parameter a [ft]
 Fus_Cross_Section_b....fuselage cross-section parameter b [ft]
 Fus_Cross_Section_w...fuselage cross-section parameter w [ft]

Output

FuselageLiftDragSupersonic.....fuselage drag coefficient due to lift

**function FuselageZeroLiftDragSubsonic(ExitAirflow : boolean;
 h,dT,Mach,S,lf,Sbase,Sfus,SwetFus,SwetLam,k,
 XtransLf,KInstallDrag : double) : double;**

Description

Calculate the subsonic zero-lift drag coefficient of a fuselage

Input

ExitAirflowengine nozzle coincide with fuselage base
 h.....altitude [ft]
 dTtemperature increment relative to standard atmosphere [deg R]
 MachMach number
 Splanform area [ft²]
 lffuselage length [ft]
 Sbasefuselage base area [ft²]
 Sfusfuselage frontal area [ft²]
 SwetFus.....fuselage wetted area [ft²]
 SwetLamlaminar flow portion of the fuselage wetted area
 k.....equivalent sand roughness
 XtransLfX-location of flow transition to fuselage length ratio [fraction]
 KInstallDrag...installation losses factor

Output

FuselageZeroLiftDragSubsonicsubsonic fuselage zero-lift drag coefficient

**function FuselageZeroLiftDragTransonic(ExitAirflow : boolean;
h,dT,Mach,S,lf,Sbase,Sfus,SwetFus,k,
KInstallDrag : double) : double;**

Description

Calculate the transonic zero-lift drag coefficient of a fuselage

Input

ExitAirflowengine nozzle coincide with fuselage base

h.....altitude [ft]

dTtemperature increment relative to standard atmosphere [deg R]

MachMach number

Splanform area [ft²]

lffuselage length [ft]

Sbasefuselage base area [ft²]

Sfusfuselage frontal area [ft²]

SwetFus.....fuselage wetted area [ft²]

k.....equivalent sand roughness

KInstallDrag...installation losses factor

Output

FuselageZeroLiftDragTransonic.....transonic fuselage zero-lift drag coefficient

**function FuselageZeroLiftDragSupersonic(h,dT,Mach,S,lf,Sbfus,Sfus,SwetFus,
l_fore,a_fore,l_after,Shape_fore, Shape_after,k,
KInstallDrag : double) : double;**

Description

Calculate the supersonic zero-lift drag coefficient of a fuselage

Input

h.....altitude

dTtemperature increment relative to standard atmosphere

MachMach number

Sreference area (wing)

lfbody length

Sbfusbase area of the body

Sfusmaximum frontal area of the body
 SwetFus.....wetted area of the body
 l_forelength of the forebody
 a_forenose diameter of the forebody
 l_afterlength of the aftbody
 Shape_foreshape of the forebody
 Shape_aftershape of the aftbody
 k.....equivalent sand roughness
 KInstallDrag...installation losses factor

Output

FuselageZeroLiftDragSupersonic ...supersonic zero-lift drag coefficient of a fuselage

**function WingLiftDragSubsonic(h,dT,Mach,A,Lambda,S,Sweep4,ILERC,
 Twist,wing_root_cl_alpha,wing_tip_cl_alpha,CLw,
 GapW : double) : double;**

Description

Roskam Airplane Design Part VI Section 4.2.1.2, calculate the subsonic drag coefficient due to lift of a lifting surface

Input

h.....altitude
 dTtemperature increment relative to the standard temperature
 MachMach number
 A.....aspect ratio
 Lambdataper ratio
 Splanform area
 Sweep4.....quarter-chord sweep angle [rad]
 ILERCleading edge radius to chord ratio [fraction]
 Twisttwist angle [rad]
 wing_root_cl_alpha....root airfoil lift curve slope [1/rad]
 wing_tip_cl_alpha.....tip airfoil lift curve slope [1/rad]
 CLw.....lifting surface lift coefficient
 GapWgap factor

Output

WingLiftDragSubsoniclift induced drag of the lifting surface

**function WingLiftDragTransonic(h,dT,Mach,A,Lambda,S,Sweep4,tcr,tct,
ILERC,Twist,wing_root_cl_alpha,wing_tip_cl_alpha,CLw,
GapW : double) : double;**

Description

Calculate the transonic drag coefficient due to lift of a lifting surface

Input

h.....altitude
dTtemperature increment relative to standard atmosphere
MachMach number
A.....aspect ratio
Lambdataper ratio
Splanform area
Sweep4.....quarter-chord sweep angle [rad]
tcrroot chord thickness ratio [fraction]
tct.....tip chord thickness ratio [fraction]
ILERCleading edge radius to chord ratio [fraction]
Twisttwist angle [rad]
wing_root_cl_alpha....root airfoil lift curve slope [1/rad]
wing_tip_cl_alpha.....tip airfoil lift curve slope [1/rad]
CLw.....lifting surface lift coefficient
GapWgap factor

Output

WingLiftDragTransonic.....transonic lift induced drag of the lifting surface

**function VertTailLiftDragSubsonic(h,dT,Mach,A,Lambda,S,Sweep4,ILERC,
Twist,root_cl_alpha,tip_cl_alpha,Cy,
Gap : double) : double;**

Description

Roskam Airplane Design Part VI Section 4.2.1.2, calculate the subsonic drag coefficient due to lift of a vertical tail

Input

h.....altitude
dTtemperature increment relative to the standard temperature
MachMach number
A.....aspect ratio
Lambdataper ratio
Splanform area
Sweep4.....quarter-chord sweep angle [rad]
ILERCleading edge radius to chord ratio [fraction]
Twisttwist angle [rad]
root_cl_alpha.....root airfoil lift curve slope [1/rad]
tip_cl_alpha.....tip airfoil lift curve slope [1/rad]
Cyvertical tail sideforce coefficient
Gap.....gap factor

Output

VertTailLiftDragSubsonicsideforce induced drag of the vertical tail

**function VertTailLiftDragTransonic(h,dT,Mach,A,Lambda,S,Sweep4,tcr,tct,
ILERC,Twist,root_cl_alpha,tip_cl_alpha,Cy,
Gap : double) : double;**

Description

Calculate the transonic drag coefficient due to sideforce of a vertical tail

Input

h.....altitude
dTtemperature increment relative to standard atmosphere

MachMach number
 A.....aspect ratio
 Lambdataper ratio
 Splanform area
 Sweep4.....quarter-chord sweep angle [rad]
 tcrroot chord thickness ratio [fraction]
 tct.....tip chord thickness ratio [fraction]
 ILERCleading edge radius to chord ratio [fraction]
 Twisttwist angle [rad]
 root_cl_alpha.....root airfoil lift curve slope [1/rad]
 tip_cl_alpha.....tip airfoil lift curve slope [1/rad]
 Cyvertical tail sideforce coefficient
 Gap.....gap factor

Output

VertTailLiftDragTransonictransonic sideforce induced drag of the vertical tail

**function FlapLiftDrag(CLWingClean,WingAlphazeroClean,
 wing_root_cl_alpha,wing_tip_cl_alpha,AR,Lambda,
 Sweep4,GapW,EtaIn,EtaOut,CfC,Mach,
 df,tcr,tct,PhiTEUpper,df2,C1C,C2C : double;
 TEFlap : integer) : double;**

Description

Calculation of the drag due to flap

Input

CLWingCleanwing clean lift coefficient
 WingAlphazeroClean.wing clean zero lift angle of attack [deg]
 wing_root_cl_alpha....root airfoil lift curve slope [1/rad]
 wing_tip_cl_alpha.....tip airfoil lift curve slope [1/rad]
 ARaspect ratio
 Lambdataper ratio
 Sweep4.....quarter-chord sweep angle [rad]
 GapWgap factor
 EtaIn.....flap inboard station [fraction]

EtaOutflap outboard station [fraction]
 CfCflap chord ratio [fraction]
 MachMach number
 dfflap deflection [deg]
 tcrroot chord thickness ratio
 tct.....tip chord thickness ratio
 PhiTEUpperairfoil upper surface trailing edge angle, $\arctan((10(y_{90}-y_{100})/c)$ [deg]
 df2aft flap deflection angle relative to the forward flap [deg]
 C1Cforward flap chord ratio [fraction]
 C2Caft flap chord ratio [fraction]
 TEFlap.....type of flap

Output

FlapLiftDragflap drag due to flap deflection

**function LEdeviceDrag(CDzerowing,Lambda,Sweep4,EtaIn,EtaOut,
 CfC : double) : double;**

Description

Calculation of the drag due to leading edge flap

Input

CDzerowingwing clean drag coefficient
 WingAlphazeroClean.wing clean zero lift angle of attack [deg]
 Lambdataper ratio
 Sweep4.....quarter-chord sweep angle [rad]
 EtaInflap inboard station [fraction]
 EtaOutflap outboard station [fraction]
 CfCflap chord ratio [fraction]

Output

LEdeviceDragleading edge flap drag coefficient

E.6 WeightII.dll

function KsSuper(DeltaM : double) : double;

Description

Torenbeek (Ref. 15) Figure 4-12, Calculation of Ks for Supercharged engines to estimate dry weight of reciprocating engines

Input

DeltaMpressure ratio [in.Hg/(lb/ft²)]

function KsTurbo (DeltaM : double) : double;

Description

Torenbeek (Ref. 15) Figure 4-12, Calculation of Ks for Supercharged engines to estimate dry weight of reciprocating engines

Input

DeltaMpressure ratio [in.Hg/(lb/ft²)]

E.7 GroundEffect.dll

For input and output parameters used in the listed figures, see Roskam Airplane Design Part VI (Ref. 6). Same variables and units as the figures are used.

function TrailingVortexFtv(hb2,DeltaXb2 : double) : double;

Description

Roskam Airplane Design Part VI Figure 8.73, Factor Due to Image Trailing Vortices

function ImageVortexLLo(hcr,CLcosSweep : double) : double;

Description

Roskam Airplane Design Part VI Figure 8.74 Part VI. Parameter Accounting for Ground Effect on Lift due to Bound Vortices

function FlapGroundEffectDelDelCL(hcr,FlapSpan : double; Flap : integer) : double;

Description

Roskam Airplane Design Part VI Figure 8.76 Effect of Flap Deflection on the Ground Influence on Lift

function CirculationBg(hc,CLwb : double) : double;

Description

Roskam Airplane Design Part VI Figure 8.79 Parameter Accounting for Variation in Circulation with Lift and Height above Ground

function bprimeb(Lambda,AR : double) : double;

Description

Roskam Airplane Design Part VI Figure 8.123 Effective Span in the Presence of the Ground

function bfprimebw(bfoverb : double) : double;

Description

Roskam Airplane Design Part VI Figure 8.124 Effective Wing Span in Presence of the Ground

**function DeltaAlpha(Alpha,hagl,CL,b,Sweep4,Cr,MGCw,AR,Xapexw,Xcg,
Zcr4w,Zcg,iw,CLalphaWF,DCLalphaWFpower,ni,no,df :
double; Flap : integer) : double;**

Description

Increment in airplane angle of attack due to ground effect

Input

Alpha.....angle of attack in deg
hagl.....height above the ground in ft
CLlift coefficient
b.....wing span
Sweep4.....quarter chord sweep in deg
Cr.....wing root chord in ft
MGCw.....wing mean geometric chord in ft
AR.....wing aspect ratio
XapexWwing X-apex
Xcg.....c.g. X-location in ft
Zcr4wwing root quarter chord z-location
Zcgz-location of C.G.
iw.....wing incidence in deg
CLalphaWF.....CLalpha wing fuselage
DCLalphaWFpower...increase in CLalpha wing fuselage due to power effects
niflap inboard station in %

no.....flap outboard station in %
dfflap deflection in deg
Flapflap type

Output

DeltaAlphaincrement in airplane angle of attack in deg

**procedure IterateCLground(Alpha,hagl,CLoge,CLAlpha,b,Sweep4,Cr,MGCw,
AR,Xapexw,Xcg,Zcr4w,Zcg,iw,CLalphaWF,
DCLalphaWFpower,ni,no,df : double; Flap : integer;
var CL : double; var Error : boolean);**

Description

Calculate CL in ground effect for a given angle of attack Alpha

Input

Alpha.....angle of attack in deg
hagl.....height above the ground in ft
CLoge.....Zero angle of attack lift coefficient in ground effect
CLAlpha.....airplane lift curve slope in 1/rad
b.....wing span
Sweep4.....quarter chord sweep in deg
Cr.....wing root chord in ft
MGCw.....wing mean geometric chord in ft
AR.....wing aspect ratio
XapexWwing X-apex
Xcg.....c.g. X-location in ft
Zcr4wwing root quarter chord z-location
Zcgz-location of C.G.
iw.....wing incidence in deg
CLalphaWF.....CLAlpha wing fuselage
DCLalphaWFpower...increase in CLAlpha wing fuselage due to power effects
niflap inboard station in %
no.....flap outboard station in %
dfflap deflection in deg
Flapflap type

Output

CLairplane lift coefficient

Errortrue if a calculation error occurs

E.8 BetaDot.dll

For input and output parameters used in the listed figures, see Roskam Airplane Design Part VI (Ref. 6). Same variables and units as the figures are used.

function SidewashAlpha (Zvb2,A,SweepLE,Lambda,Mach : double) : double;

Description

Roskam Airplane Design Part VI Figure 10.30 sidewash contribution due to angle of attack. Linear interpolation between leading edge angle and Mach number.

Input

Zvb2 $Z_v/(b/2)$
A.....Aspect ratio
SweepLE.....leading edge sweep angle [deg]
Lambdataper ratio
MachMach number

Output

SidewashDihedralwing dihedral sidewash parameter

function SidewashDihedral(Zvb2,A,SweepLE,Mach : double) : double;

Description

Roskam Airplane Design Part VI Figure 10.31 sidewash contribution due to wing dihedral. Linear interpolation between leading edge angle and Mach number.

Input

Zvb2 $Z_v/(b/2)$
A.....Aspect ratio
SweepLE.....leading edge sweep angle [deg]
MachMach number

Output

SidewashDihedralwing dihedral sidewash parameter

function SidewashTwist (Zvb2,A,SweepLE,Lambda,Mach : double) : double;

Description

Roskam Airplane Design Part VI Figure 10.32 sidewash contribution due to wing twist. Linear interpolation between leading edge angle and Mach number.

Input

Zvb2 $Z_v/(b/2)$
A.....Aspect ratio
SweepLE.....leading edge sweep angle [deg]
Lambdataper ratio
MachMach number

Output

SidewashTwistwing twist sidewash parameter

**function SidewashFuselage(HighWing : boolean;
Zvb2,A,SweepLE,Lambda,Mach,Dfb : double) : double;**

Description

Roskam Airplane Design Part VI Figure 10.33 sidewash contribution due to body influence. Linear interpolation between leading edge angle and Mach number, quadratic interpolation between D_f/b .

Input

HighWing.....true for high wing, false for low wing
Zvb2 $Z_v/(b/2)$
A.....Aspect ratio
SweepLE.....leading edge sweep angle [deg]
Lambdataper ratio
MachMach number
DfbFuselage diameter/wing span

Output

SidewashFuselageFuselage sidewash parameter

E.9 LatDirStabFigures.dll

For input and output parameters see Roskam Airplane Design Part VI (Ref. 6)

```
procedure CyBvTwinVertTail(S,bvPrime,Av,Sv,PhiTE,r1,yvTwin,lf : double;  
var CyBv,AvEff : double);
```

Description

Roskam Airplane Design Part VI pp.389-391, calculation of sideslip derivative C_{y_beta} for twin vertical tails

Input

Swing area [ft²]
bvPrimedistance from horizontal tail to vertical tail tip (See Ref. 6 Fig.10.18)
Avvertical tail aspect ratio
Svvertical tail area [ft²]
PhiTEairfoil trailing edge angle [deg]
r1fuselage dept in region of vertical tail [ft]
yvTwinspanwise distance between two vertical tail panels [ft]
fffuselage length [ft]

Output

CyBvvertical tail sideforce gradient due to sideslip [1/rad]
AvEffvertical tail effective aspect ratio

```
function SidewashGradient(AR,S,Sweep4,Sv,zw,zf,nv : double) : double;
```

Description

Roskam Airplane Design Part VI eq. (10.31)

Input

ARwing aspect ratio
Swing area [ft²]
Sweep4quarter chord sweep [rad]
Svvertical tail area [ft²]

zwvertical distance between fuselage center line and wing root
quarter point [ft]
zffuselage height at wing root [ft]
nv.....vertical tail dynamic pressure ratio

Output

SidewashGradientsidewash gradient

**function CyBvSingleVertTail(A,S,Sweep4,Av,Sv,r1,zw,
zf,CLav : double) : double;**

Description

Roskam Airplane Design Part VI pp.389-391, calculation of sideslip derivative
C_{y_beta} for single vertical tail

A.....wing aspect ratio
Swing area [ft²]
Sweep4.....quarter chord sweep [rad]
Av.....vertical tail aspect ratio
Svvertical tail area [ft²]
r1fuselage dept in region of vertical tail [ft]
zwvertical distance between fuselage center line and wing root quarter
point [ft]
zffuselage height at wing root [ft]
CLav.....vertical tail lift curve slope [1/rad]

Output

CyBvSingleVertTail ..vertical tail sideforce gradient due to sideslip [1/rad]

function KNWingFuselage(XMLf,LfSsbS,H1H2,Hwf : double) : double;

Description

Roskam Airplane Design Part VI Fig.10.28 Factor Accounting for Wing-Fuselage
Interference with Directional Stability.

function CIBetaWing(Sweep2,AR,Lambda : double) : double;

Description

Roskam Airplane Design Part VI Fig.10.20 Wing Sweep Contribution to Rolling Moment due to Sideslip. Sweep2 in deg

function SweepCompressibility(MCosSweep2,ACosSweep2 : double) : double;

Description

Roskam Airplane Design Part VI Fig.10.21 Compressibility Correction to Wing Sweep.

function FusCorrectionFactor(LfB,ACosSweep2 : double) : double;

Description

Roskam Airplane Design Part VI Fig.10.22 Fuselage Correction Factor.

function CIBetaWingAR(AR,Lambda : double) : double;

Description

Roskam Airplane Design Part VI Fig.10.23 Wing Aspect Ratio Contribution to Rolling Moment due to Sideslip.

function CIBetaDihedral(AR,Sweep2,Lambda : double) : double;

Description

Roskam Airplane Design Part VI Fig.10.24 Wing Geometric Dihedral Contribution to Rolling Moment due to Sideslip

function DihedralCompressibility(MCosSweep2,ACosSweep2 : double) : double;

Description

Roskam Airplane Design Part VI Fig.10.25 Compressibility Correction to Wing Dihedral.

function ClBetaWingTwist(AR,Lambda : double) : double;

Description

Roskam Airplane Design Part VI Fig.10.26 Contribution of Wing Twist to Rolling Moment due to Sideslip

function KReynoldsFuselage(RN : double) : double;

Description

Roskam Airplane Design Part VI Fig.10.29 Effect of Fuselage Reynolds Number on Wing-Fuselage Directional Stability.

**function RollDampingParameter(Sweep4,BetaARkappa,
Lambda : double) : double;**

Description

Roskam Airplane Design Part VI Fig.10.35 Roll Damping Parameter.

function DragRollDampingParameter(AR,Sweep4 : double) : double;

Description

Roskam Airplane Design Part VI Fig.10.36 Drag-due-to-Lift Roll Damping Parameter.

function CnpWingTwist(AR,Lambda : double) : double;

Description

Roskam Airplane Design Part VI Fig.10.37 Effect of Wing Twist on Cnp.

function CnpFlapDeflection(AR,Lambda,bfoverb : double) : double;

Description

Roskam Airplane Design Part VI fig.10.38 Effect of Symmetrical Flap Deflection on Cnp.

function ClrWing(AR,Lambda,Sweep4 : double) : double;

Description

Roskam Airplane Design Part VI Fig.10.41 Wing Rolling Moment due to Yaw Rate Derivative: Lifting Effect.

function ClrWingTwist(AR,Lambda : double) : double;

Description

Roskam Airplane Design Part VI Fig.10.42 Effect of Wing Twist on Clr.

function ClrFlap(EtaFlap,Lambda,AR : double) : double;

Description

Roskam Airplane Design Part VI fig.10.43 Effect of Symmetric Flap Deflection on Clr

function CnrWingLift(AR,Sweep4,XoverC,Lambda : double) : double;

Description

Roskam Airplane Design Part VI Fig.10.44 Wing Yaw Damping Derivative: Lifting Effect.

function CnrWingDrag(AR,Sweep4,XoverC : double) : double;

Description

Roskam Airplane Design Part VI Fig.10.45 Wing Yaw Damping Derivative: Drag Effect.

E.10 HingeMoment.dll

For input and output parameters see Roskam Airplane Design Part VI (Ref. 6)

function chaPrimeTheory(ToverC,CfoverC : double) : double;

Description

Roskam Airplane Design Part VI Figure 10.63 b

Theoretical rate of change of hinge moment with angle of attack for a two dimensional airfoil in inviscid incompressible flow

function chaPrimeRatio(CfoverC,a1ratio : double) : double;

Description

Roskam Airplane Design Part VI Figure 10.63 a

Ratio of rate of change of hinge moments with angle of attack for a two dimensional airfoil in inviscid incompressible flow

function clalphaRatio(tanTauover2,logR,Xtransition : double) : double;

Description

Roskam Airplane Design Part VI Figure 10.64

Effect of Airfoil Thickness and Trailing Edge Angle on Lift Curve Slope

function claTheory(ToverC,PhiTe : double) : double;

Description

Roskam Airplane Design Part VI Figure 10.64

Theoretical lift curve slope of an airfoil

PhiTE in deg

Effect of Airfoil Thickness and Trailing Edge Angle on Lift Curve Slope

function chAlpha2D(ToverC,PhiTE,CfoverC,Re,Xtransition : double) : double;

Description

Roskam Airplane Design Part VI eq. (10.129)

Calculate the rate of change of hinge moment coefficient with angle of attack for a plain control in incompressible two-dimensional flow

function chaBalanced(cha,Cb,Cf,ToverCf : double; Shape : TNoseShape) : double;

Description

Roskam Airplane Design Part VI Figure 10.65a

Calculate the rate of change of hinge moment coefficient with angle of attack for a balanced control in incompressible two-dimensional flow

function Kalpha(eta : double) : double;

Description

Roskam Airplane Design Part VI Figure 10.77

Three-Dimensional Correction Factor for the Control Surface Hingemoment Derivative due to Angle of Attack for effect of control surface span

function Kdelta(eta : double) : double;

Description

Roskam Airplane Design Part VI Figure 10.78

Three-Dimensional Correction Factor for the Control Surface Hingemoment Derivative due to Control Surface Deflection for effect of control surface span

procedure HingeFactors(A,clAlpha,CfoverC : double; var F1,F2 : double);

Description

Roskam Airplane Design Part VI Figure 10.77 a

Conversion factors to hinge moment coefficients for finite aspect ratio

function FactorF3(CfoverC,Balance : double) : double;

Description

Roskam Airplane Design Part VI Figure 10.77 c

Conversion factor F3 to hinge moment coefficients for finite aspect ratio

function K1Hinge(Eta,Lambda : double; WingShape : TipShapeType) : double;

Description

K1, ratio of induced angle of attack at any section to induced angle of attack

function chdPrimeTheory(ToverC,CfoverC : double) : double;

Description

Roskam Airplane Design Part VI Figure 10.69 b

Theoretical rate of change of hinge moment with control deflection for a two dimensional airfoil in inviscid incompressible flow

function chdPrimeRatio(CfoverC,cldPrimeRatio : double) : double;

Description

Roskam Airplane Design Part VI Figure 10.69 b

Ratio of rate of change of hinge moments with control deflection for a two dimensional airfoil in inviscid incompressible flow

function ChDelta2D(ToverC,PhiTE,CfoverC,Re,Xtransition : double) : double;

Description

Roskam Airplane Design Part VI eq. 10.134 - 10.135

Calculate the rate of change of hinge moment coefficient with control deflection for a plain control in incompressible two-dimensional flow

function chdBalanced(chd,Cb,Cf,ToverCf,ToverC : double; Shape : TNoseShape) : double;

Description

Roskam Airplane Design Part VI Figure 10.71

Calculate the rate of change of hinge moment coefficient with angle of attack for a balanced control in incompressible two-dimensional flow

function DchdShieldedHorn(CfoverC,ToverC,AHB : double; BluntNose : boolean) : double;

Description

Effect of horn balance on hinge moment coefficient for shielded horns

function DchdUnShieldedHorn(ToverC,AHB : double) : double;

Description

Effect of horn balance on hinge moment coefficient due to control deflection for unshielded horns

function DchaUnShieldedHorn(ToverC,AHB : double) : double;

Description

Effect of horn balance on hinge moment coefficient due to angle of attack for unshielded horns

Appendix F. Least-Squares Method to Digitize Figures

This Appendix describes the numerical methods used to digitize the figures used in AAA and AAA-AML. A separate program has been developed that can be used to digitize curves depending on one, two or three independent variables. The methods are based on Refs. 194-196.

F.1 One Independent Variable

For one independent variable a polynomial equation can be fitted through the data.

The maximum order is the number of points – 1. The equation is as follows:

$$y = \sum_{i=0}^{power} p_i a^i \quad (F-1)$$

with

a independent variable

y dependent variable

power degree of the polynomial equation

F.2 Two Independent Variables

For two independent variables polynomial equations can be fitted through the data to fit a surface. The equation is as follows:

$$y = \sum_{i=0}^{power} \sum_{j=0}^i p_{j+0.5i(i+1)} a^{i-j} b^j \quad (F-2)$$

with

- a first independent variable
- b second independent variable
- y dependent variable
- power degree of the polynomial equation

F.3 Three Independent Variables

For three independent variables polynomial equations can be fitted through the data to fit a surface. The equation is as follows:

$$y = \sum_{m=0}^{power} \sum_{n=0}^m \sum_{k=0}^n p_i a^{m-n} b^{n-k} c^k \quad (F-3)$$

$$with \ i = \frac{m}{6} (m^2 + 3m + 2) + \frac{n(n+1)}{2} + k + 1$$

- a first independent variable
- b second independent variable
- c third independent variable
- y dependent variable
- power degree of the polynomial equation

F.4 Digitizing Methods

The coefficients of the different polynomials are solved by using a least-squares method. A figure is read-off for a set of points on the x-axis and a corresponding value is read-off for the y-axis. The unknown coefficients, p , from equations (F-1)-(F-3) are stored in a vector \underline{x} . The vector \underline{b} contains the function values of the read-off charts (y-values). A matrix A is constructed by obtaining the read-off independent variables (x-axis values, a in equation F-1). Each row contains the independent variable to the power of the column location as follows:

$$A = \begin{pmatrix} 1 & a_1 & a_1^2 & \dots & a_1^m \\ 1 & a_2 & a_2^2 & \dots & a_2^m \\ \vdots & & & & \vdots \\ \vdots & & & & \vdots \\ 1 & a_n & a_n^2 & \dots & a_n^m \end{pmatrix} \quad (\text{F-4})$$

The problem can now be written as a set of linear equations as follows:

$$A\underline{x} = \underline{b} \quad (\text{F-5})$$

The least-squares method now states that to solve the $n \times m$ system of equation (F-5) in a least-squares sense is equivalent to solving the $m \times m$ system:

$$A^T A \underline{x} = A^T \underline{b} \quad (\text{F-6})$$

Equation (F-6) is solved as follows:

1. Determine the vectors \underline{c}_j and \underline{a}_j^* from:

$$\underline{a}_j^* = \frac{\underline{c}_j}{\|\underline{c}_j\|} \quad , \quad j = 1, 2, \dots \quad (\text{F-7})$$

with:

$$\underline{c}_1 = \underline{a}_1 \quad (\text{F-8})$$

$$\underline{c}_{j+1} = \underline{a}_{j+1} - \sum_{k=1}^j \langle \underline{a}_{j+1}, \underline{a}_k^* \rangle \underline{a}_k^* \quad , \quad j = 1, 2, \dots \quad (\text{F-9})$$

where \underline{a}_j is the j-th column of matrix A.

$\| \quad \|$ is the notation for the norm of the vector

$\langle _ , _ \rangle$ is the notation for scalar product of two vectors

2. Determine the vector \underline{x} from:

$$x_n = \frac{\langle \underline{b}, \underline{c}_n \rangle}{\|\underline{c}_n\|^2} \quad (\text{F-10})$$

$$x_{n-j} = \frac{\left\langle \underline{b} - \sum_{k=n-j+1}^n x_k \underline{a}_k, \underline{c}_{n-j} \right\rangle}{\|\underline{c}_{n-j}\|^2} \quad , \quad \text{for } j = 1, \dots, n-1 \quad (\text{F-11})$$

This method is straight forward to solve the coefficients p of equation (F-1). For (F-2) and (F-3) each curve is digitized independently with the above methods. Then for the system with 2 independent variables a curve is fitted through each set of coefficients p for each curve with the same methods as listed above. For three independent variables, that process is repeated again by fitting polynomials through the coefficients for two independent variables.

The methods are implemented in a computer program with a user-interface to enter the read-off values. A plotting procedure is available to check the final results. The program can either automatically set the order of each polynomial based on required accuracy or a specific order can be preset by the user.